CHARACTERIZATION OF THE CHROMOSOMAL AMINOGLYCOSIDE 6'-*N*-ACETYLTRANSFERASE FROM *ENTEROCOCCUS FAECIUM*

By

KARI-ANN DRAKER, B.SC.

A Thesis

Submitted to the School of Graduate Studies

in Partial Fulfillment of the Requirements

for the Degree

Doctor of Philosophy

McMaster University

STUDIES ON THE AMINOGLYCOSIDE MODIFYING ENZYME AAC(6')-Ii

DOCTOR OF PHILOSOPHY (2003) McMaster University
(Biochemistry) Hamilton, Ontario

TITLE: Characterization of the Chromosomal Aminoglycoside 6'-*N*-Acetyltransferase from *Enterococcus faecium*

AUTHOR: Kari-ann Draker, B.Sc. (McMaster University)

SUPERVISOR: Professor G.D. Wright

NUMBER OF PAGES: xviii, 212

Abstract

The clinical utility of aminoglycoside antibiotics is undermined by the action of bacterial modifying enzymes that inactivate these antimicrobial agents and confer drug resistance. Basic research on the aminoglycoside modifying enzymes has contributed to a greater understanding of the molecular mechanism of aminoglycoside detoxification by these proteins, information that is relevant to inhibitor studies and other approaches aimed at reversing bacterial aminoglycoside resistance *in vivo*. Described here is the characterization of AAC(6')-Ii, a chromosomally encoded aminoglycoside 6'-*N*-acetyltransferase from the Gram positive pathogen *Enterococcus faecium* and a member of the GCN5-related superfamily of acyltransferase enzymes.

Research on AAC(6')-Ii has focused on the kinetic and catalytic mechanism of aminoglycoside modification by this enzyme, in addition to inhibitor studies and investigations into a possible alternate role for this acetyltransferase *in vivo.* Using steady state-kinetic analysis of product and dead-end inhibition of protein activity, we have determined that AAC(6')-Ii follows a ternary complex, ordered bi-bi kinetic mechanism, with additional evidence supporting subunit cooperativity in the AAC(6')-Ii dimer. This work was complemented by studies that characterized substrate-induced conformational changes in AAC(6')-Ii, as well as analysis of solvent viscosity and isotope effects that identified the catalytic steps governing the steady-state rate of aminoglycoside inactivation. Together with the structural details of AAC(6')-Ii in complex with AcCoA, site-directed mutagenesis and related studies have also identified amino acid residues

important to the chemistry of drug acetylation as well as those involved in the binding of aminoglycoside substrates, providing us with a better understanding of the molecular mechanism of AAC(6')-Ii catalysis. Our results to date have been applied to numerous inhibitor studies, which have resulted in the identification of cationic peptides and semi-synthetic aminoglycosides that demonstrate potent inhibition of AAC(6')-Ii activity *in vitro*. Finally, the acetylation of *E. faecium* proteins by AAC(6')-Ii has been shown by both *in vitro* and *in vivo* analysis, complementing the structural and functional homology observed for this enzyme and protein acetyltransferases, in addition to supporting our hypothesis that AAC(6')-Ii may have an alternate function in the host bacteria. As a whole, these studies have extensively characterized the activity of AAC(6')-Ii, which is relevant to ongoing and future inhibitor studies and to an understanding of the similarities and differences among enzymes in the GCN5-related *N*-acetyltransferase superfamily.

Acknowledgements

First and foremost, I would like to thank my supervisor, Gerry Wright, for his financial and personal commitment to this project as well as his professional and positive attitude towards everyone in his lab. His ongoing support and willingness to explore new avenues of research kept me motivated and content throughout my graduate studies. My growth as a scientist and as an individual can largely be attributed to the positive working environment that Gerry maintains in his lab through his patience, understanding, and an objective outlook of the "big picture". I will truly miss being a part of the Wright lab.

I also wish to acknowledge my committee members, David Andrews, Eric Brown, and Paul Berti, whose attentiveness and interest in my project made a significant contribution to the overall progress of my work. Many thanks also go to Leanne Wybenga-Groot, David Burk, and Albert Berghuis for their collaborations and crystallographic studies on the AAC(6')-Ii protein. My sincerest thanks also go to past and present members of the Wright lab who always took the time to help me, especially Paul Thompson, Gary Marshall, Denis Daigle, John Neu, Geoff McKay, Greg Broadhead, Kalinka Koteva, and Linda Pulcins.

Finally, my commitment to graduate school would not have been possible without the support of my family and dearest friends. I am forever grateful to my parents, Pat and Mike, for their unconditional emotional and financial support over the past six years. For the many fond memories I have of my time at McMaster I thank my colleagues and friends Roman, Tejal, Sherry, Nadine, Kalinka, Nicole, JC, Ishac, and Tariq.

Table of Contents

List of Abbreviations

AAC	aminoglycoside acetyltransferase
AANAT	arylalkylamine *N*-acetyltransferase
AcCoA	acetyl-coenzyme A
ADP	adenosine diphosphate
AG	aminoglycoside
AME	aminoglycoside modifying enzyme
ANT	aminoglycoside nucleotidylyltransferase
APH	aminoglycoside phosphotransferase
ATP	adenosine triphosphate
BHI	brain heart infusion
CD	circular dichroism
CoA	coenzyme A
DTDP	4,4'-dithiodipyridine
DTT	dithiothreitol
EDP-I	energy-dependent phase I
EDP-II	energy-dependent phase II
EDTA	*N,N,N,* N'-ethylenediaminetetraacetic acid
GNAT	GCN5-related *N*-acetyltransferase
HAT	histone acetyltransferase
HEPES	*N*-(2-hydroxyethyl)piperazine-*N*'-2-ethanesulfonic acid
HSQC	heteronuclear single quantum coherence
IPTG	β-D-thiogalactopyranoside
ITC	isothermal titration calorimetry
LB	luria Bertani
MES	2-[N-morpholino]ethansulfonic acid
MIC	minimum inhibitory concentration
OD	optical density
PCR	polymerase chain reaction
PDB	protein data base
PEG	polyethylene glycol
PMSF	phenylmethylsulfonyl fluoride
PVDF	polyvinyldifluoride
SDS-PAGE	sodium dodecyl sulfate-polyacrylamide gel electrophoresis
TLC	thin layer chromatography
VRE	vancomycin resistant enterococci

List of Figures

Chapter 4

Chapter 5

Chapter 6

Chapter 7

List of Tables

Publications

1. DiGiammarino, E. L., K. Draker, G. D. Wright, and E. H. Serpersu (1998). Solution studies of isepamicin and conformational comparisons between isepamicin and butirosin A when bound to an aminoglycoside 6'-*N*-acetyltransferase determined by NMR spectroscopy. *Biochemistry* **37**:3638-44.

2. Wybenga-Groot, L. E., K. Draker, G. D. Wright, and A. M. Berghuis (1999). Crystal structure of an aminoglycoside 6'-N-acetyltransferase: defining the GCN5-related *N*-acetyltransferase superfamily fold. *Structure Fold Des.* **7**:497-507.

3. Sucheck, S. J., A. L. Wong, K. M. Koeller, D. D. Boehr, K. Draker, P. Sears, G. D. Wright, & C.-H. Wong (2000). Design of bifunctional antibiotics that target bacterial rRNA and inhibit resistance-causing enzymes. *J. Am. Chem. Soc.* **122**:5230-5231.

4. Boehr, D. D., K. Draker, K. Koteva, M. Bains, R. E. Hancock, and G. D. Wright (2003). Broad-spectrum peptide inhibitors of aminoglycoside antibiotic resistance enzymes. *Chem. Biol.* **10**:189-96.

5. Draker, K., D. D. Boehr, N. H. Elowe, T. J. Noga, and G. D. Wright (2003). Functional annotation of putative aminoglycoside antibiotic modifying proteins in *Mycobacterium tuberculosis* H37Rv. *J. Antibiotics* **56**:135-142.

6. Draker, K., D. B. Northrop, and G. D. Wright (2003). Kinetic mechanism of the GCN5-related chromosomal aminoglycoside acetyltransferase AAC(6')-Ii from *Enterococcus faecium*: evidence of dimer subunit cooperativity. *Biochemistry* **42**: 6565-6574.

7. Boehr, D. D., K. Draker, and G. D. Wright (2003). Aminoglycosides and aminocyclitols. Edited by R. G. Finch, D. Greenwood, S. R. Norrby, and R. J. Whitley. In *Antibiotic and chemotherapy. Anti-infective agents and their use in therapy.* Churchill Livingstone, UK. 155-184.

8. Draker, K. & G. D. Wright (2003). Molecular mechanism of the enterococcal aminoglycoside 6'-*N*-acetyltransferase AAC(6')-Ii: Role of GNAT-conserved residues in the chemistry of antibiotic inactivation. *Biochemistry*. In Press.

Chapter 1

Introduction

1.1 Discovery and Use of Antibiotics to Treat Bacterial Infections

The infectious nature of some microorganisms, including bacteria, was only beginning to be understood when Louis Pasteur presented his Germ Theory of Disease in 1878 (Pasteur & Lister, 1996). Complementing Pasteur's theory was the pioneering work of Joseph Lister on antiseptic techniques and Robert Koch's isolation of bacteria on solid media, which helped to revolutionize the field of early bacteriology (Levy, 1992a). These advances ultimately led to the use of antimicrobial agents to treat specific bacterial infections, such as the early use of synthetic sulfonamides in the treatment of haemolytic streptococcal infections in the 1930's (Greenwood, 2003). The famous discovery of penicillin by Alexander Fleming in 1929 was the first documented account of a natural product with antibacterial activity (Fleming, 1929), with the subsequent use (and overuse) of this antibiotic in the 1940s said to define the beginning of an antibiotic era (Greenwood, 2003).

For over 70 years, the use of antibiotics as well as synthetic and semisynthetic antimicrobials continues to be the fundamental treatment regimen for both Gram positive and Gram negative bacterial infections. The underlying effectiveness of these agents is due to their selective toxicity towards bacteria, targeting basic prokaryotic metabolic processes and cellular machinery that differ in eukaryotic cells. Currently, the vast number of antimicrobial agents available, estimated at over 100 in 1992 (Neu, 1992), interfere with such processes as bacterial cell wall synthesis, protein synthesis, nucleic acid metabolism and folic acid synthesis (Sefton, 2002). Table 1 provides a brief overview of current antimicrobial agents and their mechanism of action.

Table 1.1: Classes of antibacterial agents and their mode of action

Antimicrobial Target	Drug Class	Examples	Recent Reviews
Protein Synthesis			
30S Ribosomal subunit	**Aminoglycosides**	Gentamicin Tobramycin	Boehr *et al.*, 2003b
	Tetracyclines	Doxycycline Minocycline	Chopra & Roberts, 2001
50S Ribosomal subunit	**Macrolides**	Azithromycin Erythromycin	Blondeau, 2002
	Lincosamides	Clindamycin Lincomycin	Carrasco *et al.*, 2002
	Streptogramins	Pristinamycin Virginiamycin	Johnston *et al.*, 2002
Formation of 70S initiation complex	**Oxazolidinones**	Linezolid	Moellering, 2003
Cell Wall Synthesis			
Transpeptidases	**Cephalosporins**	Cefotaxime Ceftriaxone	Marshall & Blair, 1999
	Penicillins	Amoxicillin Carbenicillin	Wright, 1999a
Acyl-D-Ala-D-Ala of peptidoglycan	**Glycopeptides**	Vancomycin Teicoplanin	Allen & Nicas, 2003
Folate Biosynthesis			
Dihydrofolate reductase (DHFR)	**Diamino-pyrimidines**	Trimethoprim Trimetrexate	Fishman, 1998
Pteroate sythase	**Sulfonamides**	Sulfadiazine Sulfamethoxazole	Smith & Powell, 2000
DNA Replication & Transcription			
DNA Gyrase/ Topoisomerase IV	**Quinolones**	Ciprofloxacin Nalidixic acid	Schmitz *et al.*, 2002
RNA Polymerase	**Rifamycins**	Rifampicin Rifapentine	Khasnobis *et al.*, 2002
DNA strands	**Nitroimidazoles**	Metronidazole	Edwards, 1993
	Nitrofurans	Nitrofurazone	Guay, 2001

1.2 Bacterial Resistance to Antimicrobial Agents

Bacterial resistance to antimicrobial agents is an alarming and well known phenomenon, the result of a combination of the misuse and overuse of antimicrobials as well as the outstanding ability of bacteria to adapt under selective pressure. It is interesting to note that bacterial resistance was predicted by Alexander Fleming in the 1940s, even prior to the inevitable emergence of penicillin-resistant staphylococci after this antibiotic was misused and widely available without a doctor's prescription (Levy, 1992b). Since then, the use of various antimicrobials to combat bacterial infections has consistently been paralleled with the emergence of bacteria resistant to these compounds. In fact, bacterial resistance has been observed for all known classes of antimicrobial agents (Normark & Normark, 2002), even for the newest oxazolidinone drug linezolid (Tsiodras *et al.*, 2001; Herrero *et al.*, 2002; Rahim *et al.*, 2003). The impact of antimicrobial resistance on the clinical treatment of bacterial infections is therefore enormous, as recently discussed in several excellent reviews (Virk & Steckelberg, 2000; Normark & Normark, 2002; Sefton, 2002).

Bacteria utilize several mechanisms to resist the action of antimicrobials. Resistance can be broadly classified as intrinsic or acquired, with the latter having the greatest impact on the emergence of resistance in a clinical setting. Intrinsic resistance occurs in the absence of antimicrobial selective pressure and is predominately the result of some natural property of a bacterial species, an example being the resistance of mycoplasma to β-lactams due to the lack of peptidoglycan in their cell wall (Normark & Normark,

2002). In contrast, acquired bacterial resistance is the result of selective pressure after exposure to an antimicrobial, commonly occurring by acquisition of mobile genetic elements such as plasmids or transposons containing resistance genes, or by chromosomal mutations that confer bacterial resistance (Neu, 1992). The major mechanisms by which bacteria resist the action of antibiotics and other antimicrobials are summarized in Table 1.2;

Table 1.2: Major mechanisms of bacterial resistance to antimicrobial agents

Mechanism of Resistance	Examples	References
Drug inactivation • expression of modifying enzymes	**Aminoglycoside Modifying Enzymes** • *N-acetyltransferases* *O-phosphotransferases,* *O-nucleotidylyltransferases*	Wright, 1999b
	β-lactamases	Miller *et al.*, 2001
Alterations in drug target • mutation or target modification	**Quinolone Resistance** • mutation of DNA gyrase & topoisomerase IV	Hooper, 2002
	Macrolide Resistance • methylation of 23S rRNA	Blondeau, 2002
Target Bypass System • changes to metabolic pathway	**Diaminopyrimidine Resistance** • acquisition of altered DHFR enzyme	Huovinen *et al.*, 1995
Active efflux • drugs are extruded out of the cell by membrane proteins	**Tetracycline Resistance** • Tet H^+ antiporters	Chopra & Roberts, 2001
	Multi-Drug Resistance • ABC Transporters	Van Bambeke *et al.*, 2000
Altered Uptake • changes in cell permeability to drug	**Aminoglycoside Resistance** • OprH overexpression	Young *et al.*, 1992

1.3 The Aminoglycosides

1.3.1 Discovery and General Properties of the Aminoglycosides

The aminoglycosides (AGs) represent an important class of antimicrobial agents that have found use in the treatment of bacterial infections for over 50 years (Begg & Barclay, 1995). The first AG to be discovered was streptomycin in 1944, isolated from the producing organism *Streptomyces griseus* (Schatz *et al.*, 1944). This was followed by the identification of similar compounds also produced by *Streptomyces spp.*, such as neomycin, kanamycin and tobramycin, in addition to the gentamicins isolated from *Micromonospora* (Lortholary *et al.*, 1995). Table 1.3 lists common AGs, including natural and semisynthetic derivatives of this antibiotic class (Boehr *et al.*, 2003b).

Aminoglycosides are cationic molecules characterized by a central aminocyclitol ring, with two or more aminosugars attached (Figure 1.1). Further classification is based on the presence (or absence) of a 2-deoxystreptamine ring and the glycosyl linkages, which defines the three classes of aminoglycosides (Table 1.3 and Figure 1.1).

Table 1.3: Classes of aminoglycoside antimicrobials

Aminoglycosides With a 2-Deoxystreptamine Ring		Other Aminoglycosides
4,6-disubstituted	4,5-disubstituted	
Amikacin	Butirosin	Apramycin
Arbekacin	Lividomycin	Fortimicin
Dibekacin	Neomycins	Hygromycin
Gentamicins	Paromomycin	Spectinomycin
Isepamicin	Ribostamycin	Streptomycin
Kanamycins		
Netilmicin		
Sisomicin		
Tobramycin		

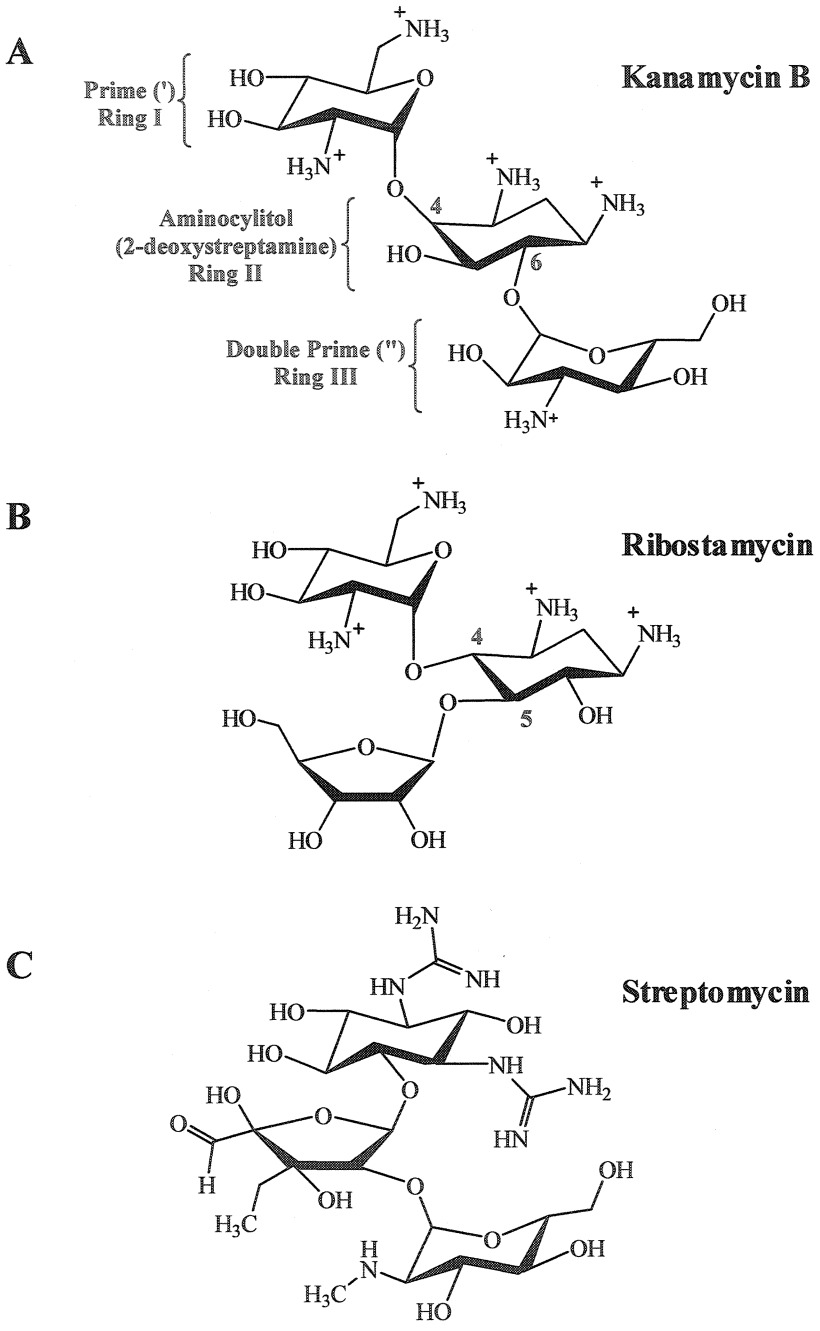

Figure 1.1: Representative structures of the three classes of aminoglycosides. Shown in **A** is the 4,6-disubstituted deoxystreptamine AG kanamycin B, with the prime, aminocyclitol, and double prime rings indicated. Ribostamycin, a 4,5-disubstituted 2-deoxystreptamine AG, is shown in **B**. AGs that do not contain a 2-deoxystreptamine ring make up the third class, such as streptomycin shown in **C**.

1.3.2 Aminoglycoside Uptake

AGs enter bacterial cells by a multi-step process involving three main phases. This process was initially characterized for streptomycin uptake by *Escherichia coli* and *Pseudomonas aeruginosa,* utilizing both susceptible and resistant strains of bacteria (Bryan & Van den Elzen, 1976). The first stage of AG uptake consists of the rapid adsorption of cationic AGs to the negatively charged surface of the bacterial outer membrane, occurring predominantly by reversible electrostatic interactions (Taber *et al.*, 1987). Subsequent steps are dependent upon electron transport, and are therefore termed energy-dependent phases (Bryan & Van den Elzen, 1976; Bryan & Kwan, 1983; Muir *et al.*, 1985). Energy-dependent phase I (EDP-I) is the second, rate-limiting step of AG uptake and involves the transport of AGs across the cell membrane, most likely by a facilitated transport mechanism that remains poorly understood (Taber *et al.*, 1987). EDP-II describes the last stage of drug uptake, characterized by the initial binding of AGs to the 30S subunit of the bacterial ribosome (Bryan & Kwan, 1983). This event has previously been shown to cause misreading and premature termination of nascent polypeptide chains without disruption of initiation complex formation (Melancon *et al.*, 1992; Mingeot-Leclercq *et al.*, 1999). Mistranslated proteins have been found to accumulate in the plasma membrane during the energy-dependent phases of AG uptake, causing membrane damage and efflux of cations and other cytoplasmic components out of the cell (Davis *et al.*, 1986; Busse *et al.*, 1992). These events are believed to play a role in the bactericidal action of AGs in addition to their inhibition of protein synthesis, as described in more detail in the following section.

1.3.3 Aminoglycoside Mode of Action

AGs fall into the class of antimicrobial agents that inhibit protein synthesis (Table 1.1), with their main target being the prokaryotic ribosome. More specifically, these drugs bind to the 16S rRNA A site of the 30S ribosomal subunit, shown initially by chemical footprinting studies (Moazed & Noller, 1987; Miyaguchi *et al.*, 1996; Recht *et al.*, 1996). Recent structural determinations of various AGs bound to the 30S ribosomal subunit or RNA oligonucleotides have also revealed the subtle differences in the mode of binding to the A site decoding region, shown by crystallographic studies with paromomycin, streptomycin, and spectinomycin (Carter *et al.*, 2000), as well as hygromycin (Brodersen *et al.*, 2000), and tobramycin (Vicens & Westhof, 2002). AG specificity for bacterial versus eukaryotic ribosomes has also been characterized, and is due to differences in the rRNA A site (Recht *et al.*, 1999).

In general, AG binding to the 30S ribosomal subunit disrupts protein synthesis in bacteria, causing the inhibition of translation initiation (Gale *et al.*, 1981) as well as the mistranslation and premature termination of nascent polypeptides (Davies *et al.*, 1965; Davies *et al.*, 1966; Davies & Davis, 1968; Lando *et al.*, 1973). These effects alone, however, do not explain the bactericidal action of AGs, as other antimicrobials that bind to the prokaryotic ribosome (see Table 1.1) are only bacteriostatic in nature (Lortholary *et al.*, 1995; Wright, 2002). The lethal activity of AGs appears to involve secondary effects on cell membrane integrity, with the incorporation of mistranslated proteins into the bacterial cell membrane and the subsequent formation of membrane channels believed to play a critical role (Lando *et al.*, 1973; Davis, 1987; Davis, 1988).

1.3.4 Clinical Use of Aminoglycosides

The AGs remain an important drug class used in the current treatment of serious Gram positive and Gram negative bacterial infections (Boehr *et al.*, 2003b). The major advantages of AG use are attributed to their potent bactericidal activity and concentration-dependent killing towards pathogenic enterococci, staphlococci, mycobacteria, gram negative bacilli and others (Gonzalez & Spencer, 1998; Edson & Terrell, 1999; Boehr *et al.*, 2003b). In addition, AGs are often co-administered with a cell wall active agent such as a β-lactam or glycopeptide to treat serious infections that result in endocarditis or sepsis (Boehr *et al.*, 2003b). Some AGs have even found other clinical uses, such as paromomycin in the treatment of parasitic infections (Davidson, 1998; Nyirjesy *et al.*, 1998). Table 1.4 provides examples of select aminoglycosides and their use in clinical treatment.

Table 1.4: Examples of aminoglycoside clinical use [a]

Aminoglycoside	Clinical Use
Gentamicin	Gram negative septicaemia Endocarditis
Neomycin	Topical treatment of skin infections Prophylaxis prior to surgery
Spectinomycin	Gonorrhea (single dose)
Streptomycin	*Mycobacterium tuberculosis* (tuberculosis)
Tobramycin	*Pseudomonas aeruginosa* (cystic fibrosis)

[a] The information in this table was gathered from Gonzolez & Spencer (1998), Edson & Terrel (1999), and Boehr *et al.* (2003b).

1.4 Mechanisms of AG Resistance

Similar to other antimicrobial agents, resistance to AGs was observed shortly after their introduction into clinical use, with the first cases of streptomycin resistance noted in the 1950s, followed by kanamycin, neomycin, and gentamicin resistance in the 1960s (Davies & Wright, 1997). Bacteria utilize several mechanisms to resist the action of AGs, including altered drug uptake, AG efflux, ribosomal modification, and AG inactivation.

1.4.1 Altered AG Uptake

Since AG uptake is an energy-dependent process (see section *1.3.2*), resistance can occur as a result of bacterial mutations that affect electron transport, a mechanism which has been observed in both Gram positive and Gram negative bacteria (Bryan & Van Den Elzen, 1977; Muir & Wallace, 1979; Miller *et al.*, 1980; Muir *et al.*, 1981; Taber *et al.*, 1981; Taber *et al.*, 1987). Variations in the outer membrane of some bacteria can also account for reductions in AG uptake, seen in *Burkholderia cepacia* (Moore & Hancock, 1986), *P. aeruginosa* mutants overexpressing OprH outer membrane protein (Young *et al.*, 1992), and mutants of *E. coli* with reduced levels of oligopeptide binding protein OppA (Kashiwagi *et al.*, 1998). In general, bacteria with altered AG uptake are not clinically relevant, as electron transport or cell membrane mutants are often not viable and do not arise as a result of AG exposure (Wright, 2002).

1.4.2 AG Efflux

Another form of resistance is the active efflux of AGs out of bacterial cells. Although this mechanism is also not regarded as clinically important, it does account for the intrinsic AG resistance observed in *Burkholderia pseudomallei* (Moore *et al.*, 1999)

and *P. aeruginosa* (Aires *et al.*, 1999; Li *et al.*, 2003). Additional multi-drug efflux pumps conferring AG resistance have also been characterized from other bacteria, including *Mycobacterium fortuitum* (Aínsa *et al.*, 1998) and *E. coli* (Edgar & Bibi, 1997). The emerging picture therefore appears to be that this mechanism may be intrinsic to many different bacteria (Van Bambeke *et al.*, 2000; Wright, 2002).

1.4.3 Ribosomal Modification and Drug Inactivation

The most clinically relevant mechanisms of AG resistance involve modification of the AG target, the bacterial ribosome, and by the production of AG modifying enzymes (AMEs) that inactivate this class of antimicrobials. In general, ribosomal modification is achieved through point mutations in ribosomal proteins or rRNA, as well as by methylation of rRNA (Wright, 2002). Streptomycin resistance in the pathogen *Mycobacterium tuberculosis,* for example, is predominantly the result of mutation of the *rpsL* gene coding for ribosomal protein S12, or mutation of the 16S rRNA *rrs* gene resulting in various base substitutions (Honore & Cole, 1994; Sreevatsan *et al.*, 1996). Methylation of 16S rRNA by ribosomal RNA methyltransferases is another form of target modification, but is predominantly found only as a self-protection mechanism in AG-producing bacteria (Thompson *et al.*, 1985; Beauclerk & Cundliffe, 1987; Skeggs *et al.*, 1987; Kelemen *et al.*, 1991; Kojic *et al.*, 1992). The biochemical basis for AG resistance by target modification is the disruption or decreased affinity of drug binding to the ribosome (Davies & Wright, 1997), a phenomenon also observed when AGs are modified (Llano-Sotelo *et al.*, 2002). The mechanism of AG inactivation by bacterial modifying enzymes is described in more detail in the following sections.

1.5 Aminoglycoside Modifying Enzymes

Of greatest clinical concern is AG resistance conferred by modifying proteins, which are commonly encoded on transferable plasmids and transposons for easy dissemination of the resistance genes to other strains, and even other species, of bacteria (Courvalin & Carlier, 1981; Shaw *et al.*, 1993). The AMEs are divided into three main classes based on the chemistry of drug modification, grouped as AG *O*-phosphotransferases (APHs), *O*-adenylyltransferases (ANTs), or *N*-acetyltransferases (AACs) (Table 1.5). AME nomenclature proposed by Shaw *et al.* (1993) is used to identify AMEs and also provides important details on modification activity. Using the AME AAC(6')-Ii as an example, the naming scheme indicates the class of modifying enzyme (AAC), followed by the regiospecificity of group transfer (6') and the resistance phenotype (I), designated with a roman numeral. A small case letter (i) is also used to signify a unique protein (Shaw *et al.*, 1993). This nomenclature has proved invaluable, especially considering the large number of AMEs (>50) that have been identified (Davies & Wright, 1997). Several excellent reviews have covered the topic of AMEs in detail (Davies, 1991; Shaw *et al.*, 1993; Bush & Miller, 1998; Wright, 1999b; Azucena & Mobashery, 2001; Smith & Baker, 2002). The following sections will therefore give only a brief overview for each of the APH and ANT class of enzymes, followed by a more in-depth review of the AAC protein class.

Table 1.5: Regiospecificity and examples of AG modification catalysed by the AMEs

Class of AME and typical modification reaction	Typical regiospecificities & AG substrates
Aminoglycoside N-Acetyltransferases (AACs) 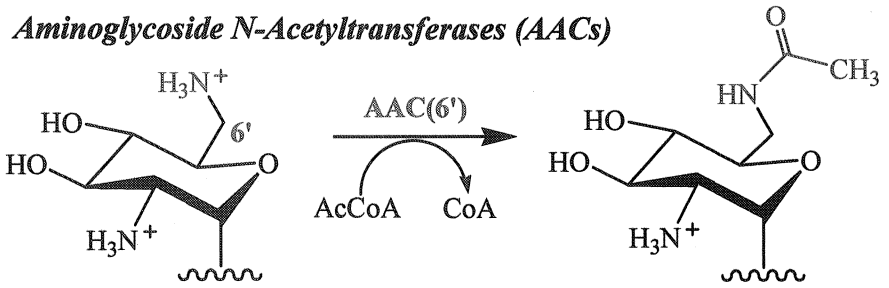	***2'*** gentamicin, tobramycin, netilimicin ***6'*** tobramycin, netilimicin, sisomicin ***1*** apramycin, paromomycin, ribostamycin ***3*** gentamicin, tobramycin, sisomicin
Aminoglycoside O-Phosphotransferases (APHs) 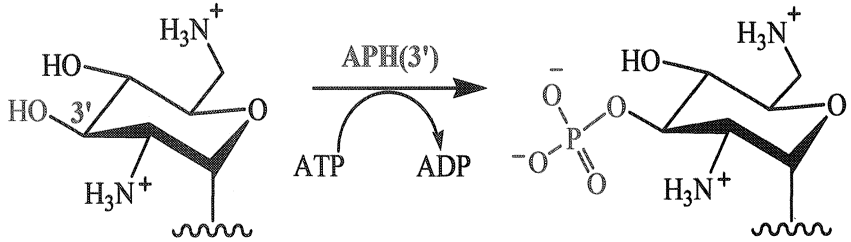	***3'*** kanamycin, neomycin, ribostamycin ***2"*** amikacin, gentamicin, tobramycin ***3"*** streptomycin ***4*** hygromycin ***6*** streptomycin ***9*** spectinomycin
Aminoglycoside O-Adenylyltransferases (ANTs) 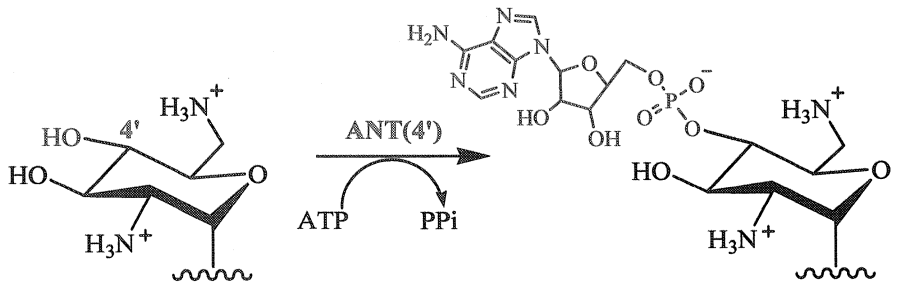	***4'*** amikacin, tobramycin, isepamicin ***2"*** gentamicin, tobramycin, kanamycin ***3"*** streptomycin, spectinomycin ***6*** streptomycin ***9*** spectinomycin

1.5.1 Aminoglycoside Phosphotransferases (APHs)

Phosphorylation of AGs is achieved through the activity of APH enzymes, which are ATP-dependent kinases that transfer the γ-phosphate of ATP to a free hydroxyl group, generating modified AG and ADP (Table 1.5). APHs represent the second largest group of AMEs, with varying regiospecificity for the 3', 5", and 2" hydroxyls on 2-deoxystreptamine-containing AGs, as well as the 4 & 7" positions on hygromycin, the 9 hydroxyl on spectinomycin, and the 3" & 6 positions on streptomycin (reviewed in Wright & Thompson, 1999). APH enzymes are present in pathogenic enterococci, staphylococci, and enterobacteriaceae, commonly encoded on resistance plasmids or transposons (Shaw *et al.*, 1993; Wright, 2002). Chromosomally encoded APH genes have also been identified, however, in AG producing bacteria and others (Wright & Thompson, 1999). From a clinical standpoint, the AG resistance conferred in Gram positive cocci by the phosphotransferase activity of the bifunctional AAC(6')-APH(2") enzyme is particularly disturbing, as it can inactivate virtually all 2-deoxystreptamine-containing AGs (Culebras & Martinez, 1999). Characterization of numerous APHs has contributed to a greater understanding of AG resistance conferred by these kinases (Wright & Thompson, 1999; Azucena & Mobashery, 2001; Smith & Baker, 2002). In particular, the crystal structure of APH(3')-IIIa reveals that this phosphotransferase is structurally homologous to eukaryotic protein kinases (Hon *et al.*, 1997), suggesting an evolutionary link and also complementing previous inhibitor studies (Daigle *et al.*, 1997).

1.5.2 Aminoglycoside Adenylyltransferases (ANTs)

ANTs catalyse the regiospecific transfer of an adenylyl group from ATP to an AG hydroxyl group, generating pyrophosphate (PPi) and modified drug (Table 1.5). Enzymes with regiospecificity for the 4'& 2" hydroxyls on 2-deoxystreptamine-containing AGs, the 6 & 3" positions on streptomycin, and the 9 & 3" hydroxyls on spectinomycin have been identified (Shaw *et al.*, 1993). The ANTs are currently the smallest group of AMEs, with less than 10 unique proteins identified to date (Wright, 2002). Similar to other AG inactivating enzymes, ANTs are encoded on resistance plasmids and transposons for easy dissemination of *ant(2")* and *ant(3")* genes among Gram negative bacteria and *ant(4')*, *ant(6)*, and *ant(9)* genes among Gram positive bacteria (Shaw *et al.*, 1993). The *ant(6')-Ib* gene from *Bacillus subtilis*, however, is encoded on the chromosome (Ohmiya *et al.*, 1989). AG modification by ANT(2") enzymes is of particular clinical relevance, as this activity confers resistance to the important AGs tobramycin and gentamicin in several Gram negative pathogens (Miller *et al.*, 1997). Characterization of ANT(2")-Ia from *E. coli* has provided valuable information regarding the mechanism of AG modification by this important subclass of ANTs (reviewed in (Wright, 2002)). Further insight has come from the structural determinations of ANT(4')-Ia from *S. aureus*, which represented the first reported crystal structures of any AME (Sakon *et al.*, 1993; Pedersen *et al.*, 1995). Interestingly, the overall fold of this enzyme showed high structural homology to eukaryotic DNA polymerases, which led to the recognition that ANTs are members of a larger nucleotidylyltransferase superfamily (Aravind & Koonin, 1999).

1.5.3 Aminoglycoside Acetyltransferases (AACs)

The AACs represent the largest group of AG inactivating enzymes, with over 48 unique enzymes identified from both Gram positive and Gram negative bacteria (see Table 1.6). These AMEs transfer the acetyl group from AcCoA to AG free amino groups predominantly, producing acetylated AG and CoA (Table 1.5). This family is grouped into AAC(1), AAC(3) AAC(2'), and AAC(6') enzymes, based on the regiospecificity of modification to 2-deoxystreptamine-containing AGs as well as fortimcin and apramycin (Shaw *et al.*, 1993). A current list of known AAC enzymes is included in Table 1.6.

Acetyl transfer to the aminocyclitol ring of AGs occurs by the action of AAC(1) and AAC(3) enzymes. Two AAC(1) enzymes have been identified to date, one conferring apramycin resistance in *E. coli* (Lovering *et al.*, 1987) and the other acetylating paromomycin in an actinomycete strain but oddly not conferring resistance to this drug (Sunada *et al.*, 1999). Both proteins are of little clinical relevance. In contrast, AAC(3) enzymes complicate the treatment of many bacterial infections due to their inactivation of tobramycin and gentamicin (Miller *et al.*, 1997; Wright, 2002). AAC(3)-I from *Serratia marcescens* was studied in detail in the 1970s by Northrop's group, revealing a broad AG substrate specificity for this AAC and the kinetic mechanism of acetyl transfer (Williams & Northrop, 1976, 1978a, 1978b). An inhibitory bisubstrate analog for this protein was also designed by this group (Williams & Northrop, 1979). More recent findings have come from the structural elucidation of AAC(3)-I in complex with CoA, the first AAC crystal structure to be reported (Wolf *et al.*, 1998).

Table 1.6: AAC family of enzymes

Enzyme	Host Bacteria	AG Resistance Profile[a]	Reference[b]
AAC(1)	*Escherichia coli*	Apr, Liv, Paro, Ribo	Lovering *et al.*, 1987
	Actinomycete strain	unknown	Sunada *et al.*, 1999
AAC(3)-I		Gent, Fort	
AAC(3)-I	*Serratia marcescens*		Javier Teran *et al.*, 1991
AAC(3)-Ib	*P. aeruginosa*		Schwocho *et al.*, 1995
AAC(3)-Ic	*P. aeruginosa*		Riccio *et al.*, 2003
AAC(3)-II		Gent, Tob, Dbk, Ntl, 2'Ntl, 6'Ntl, Siso	
AAC(3)-IIa	*Enterobacteriaceae*		Allmansberger *et al.*, 1985
AAC(3)-IIb[c]	*S. marcescens*		Rather *et al.*, 1992
AAC(3)-IIc	*E. coli*		Javier Teran *et al.*, 1991
AAC(3)-III		Gent, Tob, Dbk, Kan, 5-Epi, Siso, Neo, Paro, Liv	
AAC(3)-IIIa	*P. aeruginosa*		Vliegenthart *et al.*, 1991
AAC(3)-IIIb	*P. aeruginosa*		AAA25682
AAC(3)-IIIc	*P. aeruginosa*		AAA25683
AAC(3)-IVa	*E. coli*	Apr, Gent, Tob, Dbk, Ntl, 2'Ntl, 6'Ntl, Siso	Hedges & Shannon, 1984
AAC(3) *misc*			
AAC(3)-VIa	*Enterobacter cloacae*	Gent, 6'Ntl, Siso	Rather *et al.*, 1993a
AAC(3)-VII	*Streptomyces rimosus*	unknown	Lopez-Cabrera *et al.*, 1989
AAC(3)-VIII	*Streptomyces fradiae*	unknown	Salauze *et al.*, 1991
AAC(3)-IX	*Micromonospora chalcea*	unknown	Salauze *et al.*, 1991
AAC(3)-X	*S. griseus*	Gent, Kan, Dbk	Hotta *et al.*, 1988
AAC(2')-I		Gent, Tob, Dbk, Ntl, 2'Ntl, Siso	
AAC(2')-Ia	*Providencia stuartii*		Rather *et al.*, 1993b
AAC(2')-Ib	*Mycobacterium fortuitum*		Aínsa *et al.*, 1996
AAC(2')-Ic	*Mycobacterium tuberculosis*		Aínsa *et al.*, 1997
AAC(2')-Id	*Mycobacterium smegmatis*		Aínsa *et al.*, 1997
AAC(2')-Ie	*Mycobacterium leprae*		Cole *et al.*, 2001

Table 1.6: *continued*

Enzyme	Host Bacteria	AG Resistance Profile[a]	Reference[b]
AAC(6')-I		Tob, Dbk, Amk, 5-Epi Ntl, 2'Ntl, Siso	
AAC(6')-Ia	*Citrobacter diversus*		Tenover *et al.*, 1988
AAC(6')-Ib	*S. marcescens*		Tran van Nhieu & Collatz, 1987
AAC(6')-Ic	*S. marcescens*		Shaw *et al.*, 1992
AAC(6')-Id	*Klebsiella pneumoniae*		Schmidt *et al.*, 1988
AAC(6')-Ie	*Enterococcus faecalis*	& Fort	Ferretti *et al.*, 1986
AAC(6')-If	*Enterobacter cloacae*		Teran *et al.*, 1991
AAC(6')-Ig	*Acinetobacter haemolyticus*		Lambert *et al.*, 1993
AAC(6')-Ih	*Acinetobacter baumanni*		Lambert *et al.*, 1994
AAC(6')-Ii	*Enterococcus faecium*		Costa *et al.*, 1993
AAC(6')-Ij	*A. baumanni*		Lambert *et al.*, 1994
AAC(6')-Ik	*Acinetobacter sp.* CIP-A165		Rudant *et al.*, 1994
AAC(6')-Il	*Enterobacter aerogenes*		Bunny *et al.*, 1995
AAC(6')-Im	*Citrobacter freundii*		Hannecart-Pokorni *et al.*, 1997)
AAC(6')-In	*C. freundii*		Wu *et al.*, 1997
AAC(6')-Iq	*Klebsiella pneumoniae*		Centron & Roy, 1998
AAC(6')-Ir	*Acinetobacter* sp. 14		Rudant *et al.*, 1999
AAC(6')-Is	*Acinetobacter* sp. 15		Rudant *et al.*, 1999
AAC(6')-It	*Acinetobacter* sp. 16		Rudant *et al.*, 1999
AAC(6')-Iu	*Acinetobacter* sp. 17		Rudant *et al.*, 1999
AAC(6')-Iv	*Acinetobacter* sp. 631		Rudant *et al.*, 1999
AAC(6')-Iw	*Acinetobacter* sp. 640		Rudant *et al.*, 1999
AAC(6')-Ix	*Acinetobacter* sp. BM27222		Rudant *et al.*, 1999
AAC(6')-Iy	*Salmonella enterica*		Magnet *et al.*, 1999
AAC(6')-Iz	*Stenotrophomonas maltophilia*		Lambert *et al.*, 1999
AAC(6')-II		Gent, Tob, Dbk, 5-Epi Ntl, 2'Ntl, Siso	
AAC(6')-IIa	*P. aeruginosa*		Rather *et al.*, 1993a
AAC(6')-IIb	*Pseudomonas fluorescens*		AAA25680
AAC(6')-IIc	*P. aeruginosa*		AAD46626

[a] AG resistance profile refers to the *in vivo* resistance conferred by the enzyme which identifies the regiospecificity and AG resistance profile (information gathered fom Shaw *et al.* (1993)). The abbreviations used are; Gent, gentamicin; Tob, tobramycin; Dbk, dibekacin; Ntl, netilimicin; 2'Ntl, 2'-*N*-ethylnetilmicin; 6'Ntl, 6'-N-ethylnetilmicin; Siso, sisomicin; 5-Epi, 5-episisomicin; Fort, fortimicin; Apr, apramycin; Liv, lividomycin; Paro, paromomycin; Ribo, ribostamycin; Kan, kanamycin, Neo; neomycin.

[b] protein sequences that were submitted directly into the NCBI databank are referenced with the protein id.

[c] also referred to as AAC(3)-Vb (Shaw *et al.*, 1993)

Most remarkable about the AAC(3)-I fold was the striking structural homology it shared with the yeast histone acetyltransferase yHAT1 (Dutnall *et al.*, 1998), even in the absence of significant amino acid sequence homology. Based on their structures, these two enzymes became the first representative members of the GCN5 related *N*-acetyltransferase (GNAT) superfamily, a diverse group of prokaryotic and eukaryotic enzymes that share conserved structural motifs important for the binding of AcCoA (Neuwald & Landsman, 1997; Dyda *et al.*, 2000). Interestingly, the three dimensional structures of AAC(6')-Ii from *E. faecium* (Wybenga-Groot *et al.*, 1999) and AAC(2')-Ic from *M. tuberculosis* (Vetting *et al.*, 2002) reveal that these proteins are also GNAT members, suggesting that all AAC enzymes, regardless of regiospecificity, share a common structural fold. The GNAT superfamily is discussed in more detail in chapter 4 and has also been reviewed elsewhere (Dyda *et al.*, 2000).

The final two subclasses of AACs modify the primed ring of 2-deoxystreptamine-containing AGs. The AAC(2') group of enzymes is made up of 5 unique proteins that are chromosomally encoded in *Providencia* or *Mycobacterium* species (Table 1.6). Although these enzymes do not confer clinically relevant AG resistance, characterization of AAC(2")-Ia from *P. stuartii* (Payie *et al.*, 1995; Payie & Clarke, 1997) and AAC(2")-Ic from *M. tuberculosis* (Hegde *et al.*, 2002; Vetting *et al.*, 2002) have pointed to alternate functions for these proteins *in vivo*. In addition, the structural elucidation of AAC(2')-Ic in complex with CoA and various AG substrates has provided valuable information on the binding of AGs by this enzyme, with possible relevance to other AACs.

The AAC(6') subfamily of modifying enzymes is the largest of any AME subclass, with 27 unique enzymes (Table 1.6). The majority of these genes are encoded on transferable resistance plasmids and transposons, with exceptions including the chromosomally encoded *aac(6')-Ic*, *aac(6')-Ii*, *aac(6')-Iy*, and *aac(6')-Iz* genes, as well as the *aac(6')* genes identified from species of *Acinetobacter* (see Table 1.6). Clinically relevant resistance conferred by the activity of these *N*-acetyltransferases is almost exclusive to Gram negative bacteria, with the exception of AAC(6')-Ii activity in enterococci (Costa *et al.*, 1993) and AAC(6')-APH(2") activity in enterococci and staphylococci (Ferretti *et al.*, 1986). AG Modification by the bifunctional enzyme has been shown to account for almost half of the observed AG resistance in pathogenic *Staphlococcus aureus* and *E. faecalis* (Miller *et al.*, 1997). Similarly, the low-level intrinsic resistance conferred by AAC(6')-Ii complicates the clinical treatment of infections caused by *E. faecium* (Costa *et al.*, 1993).

All AAC(6')s have the capacity to acetylate clinically useful AGs, including amikacin in the case of the AAC(6')-I enzymes and gentamicin for the AAC(6')-II class (Shaw *et al.*, 1993). As a large group, these enzymes share between 10 to 15 % amino acid sequence homology (Shaw *et al.*, 1993), with sequence alignment of these proteins identifying several distinct subgroups of 6' *N*-acetylating enzymes, represented in Figure 1.2 by a phylogenetic tree. In particular, AAC(6')-Ii from *E. faecium* shares over 40% amino acid sequence homology with AAC(6')-Ia from *Citrobacter diversus* (Tenover *et al.*, 1988), AAC(6')-Il from *Citrobacter freundi* (Hannecart-Pokorni *et al.*, 1997), and AAC(6')-Iq from *Klebsiella pneumoniae* (Centron & Roy, 1998).

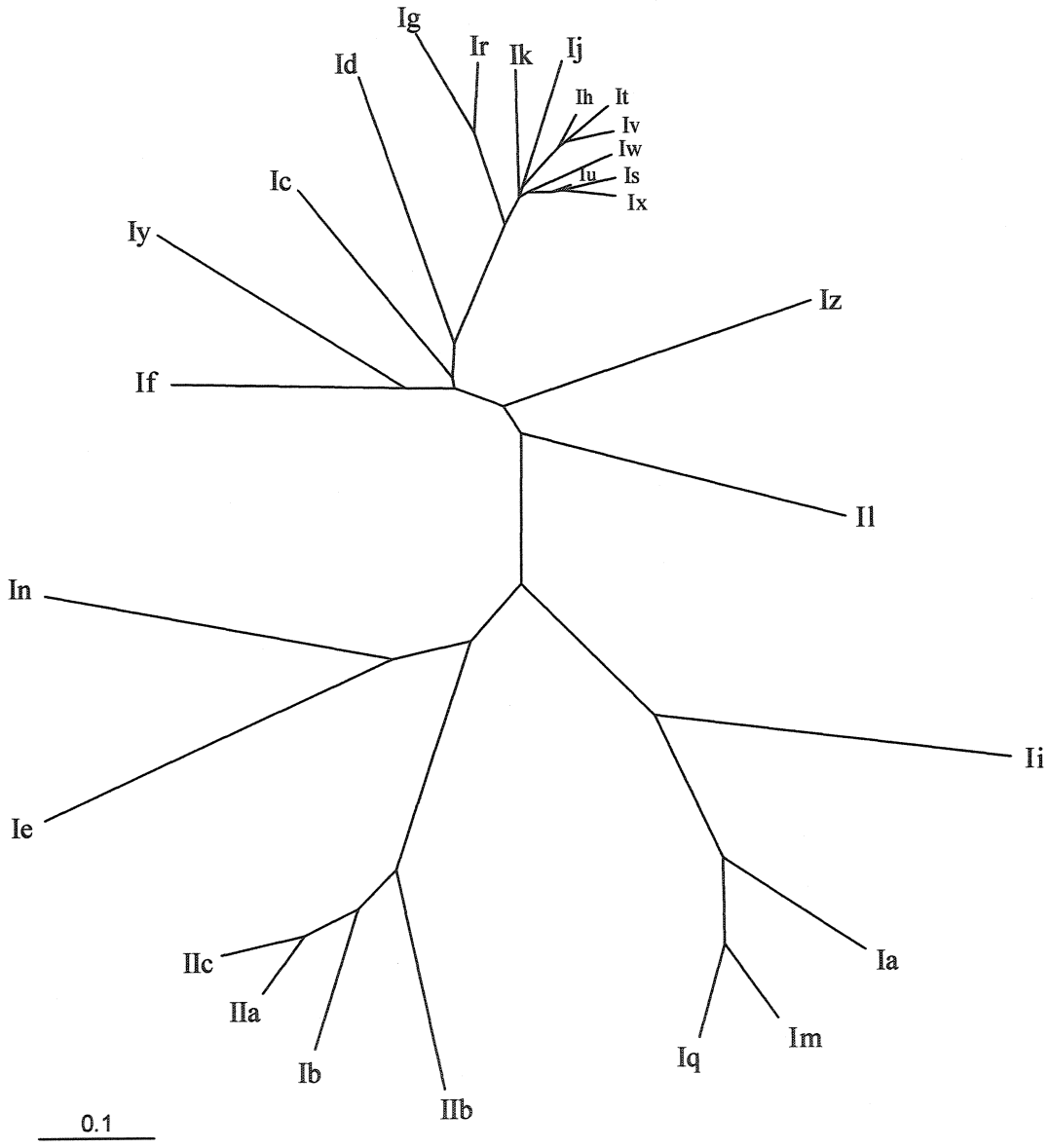

Figure 1.2: Phylogenetic relationships among the AAC(6') subfamily of enzymes. For simplicity, only the AG resistance profile (I or II) and the unique protein designation is shown. The host organisms and other details for each of the AAC(6') enzymes can be found in Table 1.6. Sequences were aligned using the program Clustal W (Thompson *et al.*, 1994). The unrooted phylogenetic tree was generated using TreeView (Page, 1996), with the branch scale at left signifying 0.1 nucleotide substitutions per site.

Studies on several AAC(6') proteins have helped to characterize the enzymatic activity of these AG resistance determinants. Research on AAC(6')-Iy from *Salmonella enterica* has characterized this enzyme and the mechanism by which the cryptic chromosomal gene is activated (Magnet *et al.*, 1999; Magnet *et al.*, 2001; Hegde *et al.*, 2002). Studies in our lab have concentrated on the bifunctional AAC(6')-APH(2') and AAC(6)-Ii enzymes from Gram positive cocci, with several published reports on their kinetic characterization (Wright & Ladak, 1997; Daigle *et al.*, 1999a; Daigle *et al.*, 1999b), structural determinations (Wybenga-Groot *et al.*, 1999), and inhibitor studies (Daigle *et al.*, 1997; Sucheck *et al.*, 2000; Boehr *et al.*, 2003a; Boehr *et al.*, 2003c). The following section will give a brief overview of what is known about AAC(6')-Ii, the enzyme that is the focus of the research described in this thesis.

1.6 AAC(6')-Ii From Enterococcus faecium

The chromosomal *aac(6')-Ii* gene was characterized in 1993 by Costa *et al.*, who first reported the sequence of the gene and the encoded acetyltransferase protein of ~ 21 kDa (Costa *et al.*, 1993). Insertional inactivation of the *aac(6')-Ii* gene confirmed that expression of the modifying enzyme was responsible for the low-level aminoglycoside resistance observed in *E. faecium* (Costa *et al.*, 1993). The AAC(6')-Ii enzyme was subsequently overexpressed in *E. coli* and successfully purified by a three step chromatography procedure, as shown in Figure 1.3A (Wright & Ladak, 1997). A robust continuous kinetic assay first described by Williams & Northrop (1978a) is used to monitor AAC(6')-Ii acetyl transfer activity in the steady-state (Figure 1.3B).

A.

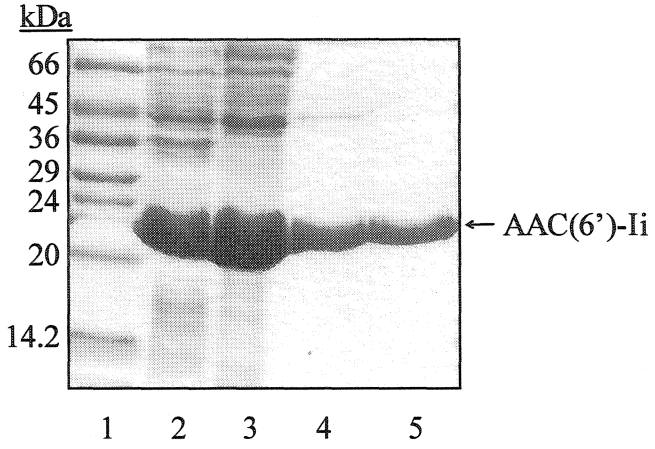

B.

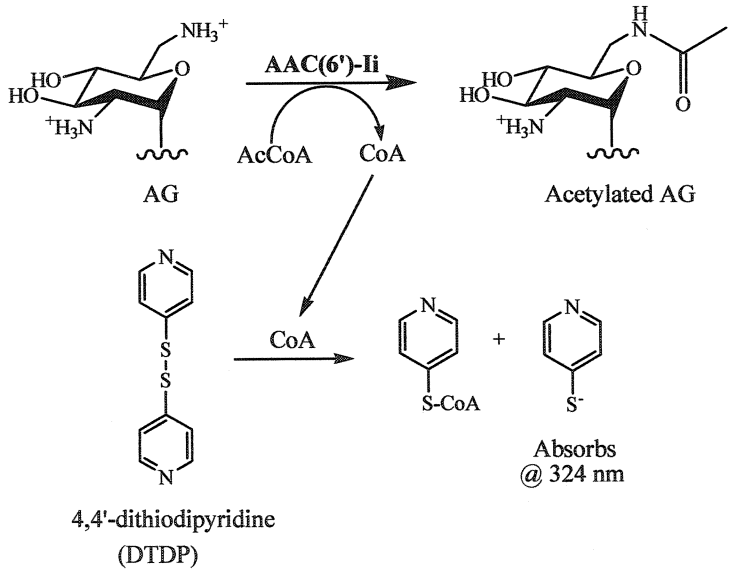

Figure 1.3: AAC(6')-Ii purification and spectrophotometric assay. Shown in **A.** is the purification of AAC(6')-Ii from *E. coli* overexpressing the 21 kDa protein. The SDS-20% polyacrylamide gel was stained with Coomassie blue. Lane 1, molecular mass standards; lane 2, unpurified cell lysate; lane 3, pooled fractions after anion exchange chromatography; lane 4, pooled fractions after gel filtration chromatography; lane 5, pure AAC(6)-Ii collected after affinity chromatography. See Wright & Ladak (1997) for additional purification details. **B.** Continuous spectrophotometric assay used to detect AAC(6')-Ii acetyl transfer activity. The assay involves the *in situ* titration of CoA product with DTDP, generating a thiolate species that absorbs at 324 nm.

Initial *in vitro* studies on purified AAC(6')-Ii revealed a stable enzyme that exists as a homodimer in solution and displays a broad AG substrate specificity and varying kinetic properties depending on the aminoglycoside substrate (Wright & Ladak, 1997). Different binding modes for the 4,5- and 4,6-disubstituted deoxystreptamine AGs were hypothesized based on steady-state kinetic analysis (Wright & Ladak, 1997) and further supported by NMR spectroscopy studies (DiGiammarino *et al.*, 1998). In addition, specificity constants were found to be fairly low ($k_{cat}/K_m \sim 10^4$ $M^{-1}s^{-1}$) and minimum inhibitory concentrations (MICs) were observed to be positively correlated to k_{cat}, the rate at saturating AG, and not k_{cat}/K_m, the rate at subsaturating AG, revealing a suboptimal level of AG detoxification by this AME (Wright & Ladak, 1997). These results, together with the chromosomal origin of the *aac(6')-Ii* gene, suggested that this protein may have another function in *E. faecium* besides aminoglycoside modification (Wright & Ladak, 1997).

The structural determination of AAC(6')-Ii in complex with AcCoA, solved by Wybenga-Groot *et al.* (1999), provided a great deal of information relevant to the binding of substrates by this protein and the mechanism of acetyl transfer. It also identified this enzyme as a member of the GNAT superfamily, which already included AAC(3')-I and the histone acetyltransferase yHAT based on the previously reported crystal structures (Dutnall *et al.*, 1998; Wolf *et al.*, 1998). Biochemical evidence gathered by myself (see chapter 7) also revealed that AAC(6')-Ii can acetylate eukaryotic H3/H4 histones and a number of small basic proteins, suggesting that certain members of the GNAT superfamily are both structural and functional homologs (Wybenga-Groot *et al.*, 1999).

The AAC(6')-Ii monomer has an obvious V-like structure, consisting of N- and C-terminal domains that diverge as a result of a GNAT-conserved β-bulge in β-strand 4 (Wybenga-Groot *et al.*, 1999). This separation forms a cleft-like region between the two domains and creates an AcCoA binding site, as shown in Figure 1.4. Interestingly, the majority of contacts made between the protein and AcCoA are made through interactions with the main chain backbone of the protein (Wybenga-Groot *et al.*, 1999). A negatively charged surface patch in active site proximity is also apparent from the structure and is believed to draw in the cationic AG substrate (Wybenga-Groot *et al.*, 1999). The structure of the AAC(6')-Ii dimer with bound CoA has also been recently reported (Burk *et al.*, 2003), with relevance to some of the research described in the chapters that follow.

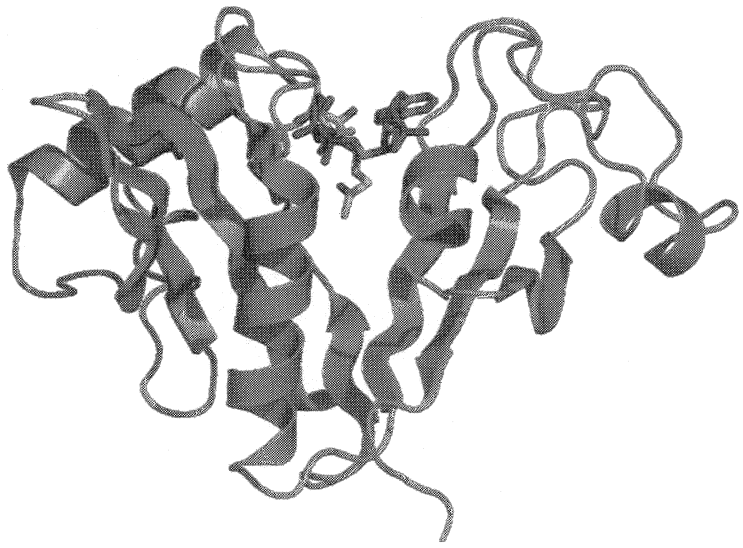

Figure 1.4: Structure of the AAC(6')-Ii monomer in complex with AcCoA (Wybenga-Groot *et al.*, 1999). As shown above, AcCoA is bound in the cleft-like region between the N-terminal (left) and C-terminal (right) domains of the monomer. This figure was generated using the pdb code 1b87 and PyMOL molecular graphics software (DeLano, 2002).

1.7 AAC(6')-Ii Research Described Here

This thesis describes the further characterization of the AAC(6')-Ii protein, which has entailed many different avenues of study. Chapter 2 summarizes research that was done to better understand the substrate-induced conformational changes observed for this enzyme, shown to be an essential part of acetyl transfer catalysis. The next chapter reports the kinetic mechanism of AAC(6')-Ii, which describes the order of substrate binding and formation of a ternary complex required for productive AG inactivation. Studies to further define the molecular mechanism of AAC(6')-Ii catalysis is then detailed in chapter 4, which describes the characterization of several GNAT-conserved residues and their potential role in AAC(6')-Ii acetyl transfer chemistry. Similarly, the chapter that follows investigates the role of several negatively charged amino acids in AG binding. Chapter 6 summarizes various inhibitor studies, including the characterization of several cationic peptides that were shown to inhibit AAC(6')-Ii as well as other AMEs. Finally, chapter 7 describes numerous studies performed with wild type and mutant strains of *E. faecium* in attempts to identify an alternate *in vivo* role for AAC(6')-Ii.

Overall, the research described here contributes to a greater understanding of the mechanism of AG modification by this resistance enzyme, with relevance to other AACs and even other important proteins that are part of the GNAT superfamily. A detailed and extensive understanding of the different classes of AMEs, achieved by studying the enzymology and mechanism behind AG inactivation, will no doubt lead to methods to ultimately overcome AG resistance.

1.8 References

Aínsa, J. A., M. C. Blokpoel, I. Otal, D. B. Young, K. A. De Smet, and C. Martin. (1998) Molecular cloning and characterization of Tap, a putative multidrug efflux pump present in *Mycobacterium fortuitum* and *Mycobacterium tuberculosis*. *J Bacteriol* 180: 5836-43.

Aínsa, J. A., C. Martin, B. Gicquel, and R. Gomez-Lus. (1996) Characterization of the chromosomal aminoglycoside 2'-*N*-acetyltransferase gene from *Mycobacterium fortuitum*. *Antimicrob Agents Chemother* 40: 2350-5.

Aínsa, J. A., E. Perez, V. Pelicic, F. X. Berthet, B. Gicquel, and C. Martin. (1997) Aminoglycoside 2'-*N*-acetyltransferase genes are universally present in mycobacteria: Characterization of the *aac(2')-Ic* gene from *Mycobacterium tuberculosis* and the *aac(2')-Id* gene from *Mycobacterium smegmatis*. *Mol Microbiol* 24: 431-41.

Aires, J. R., T. Kohler, H. Nikaido, and P. Plesiat. (1999) Involvement of an active efflux system in the natural resistance of *Pseudomonas aeruginosa* to aminoglycosides. *Antimicrob Agents Chemother* 43: 2624-8.

Allen, N. E. & T. I. Nicas. (2003) Mechanism of action of oritavancin and related glycopeptide antibiotics. *FEMS Microbiol Rev* 26: 511-32.

Allmansberger, R., B. Brau, and W. Piepersberg. (1985) Genes for gentamicin-(3)-*N*-acetyltransferases III and IV. Ii. Nucleotide sequences of three *aac(3)-III* genes and evolutionary aspects. *Mol Gen Genet* 198: 514-20.

Aravind, L. & E. V. Koonin. (1999) DNA polymerase beta-like nucleotidyltransferase superfamily: Identification of three new families, classification and evolutionary history. *Nucleic Acids Res* 27: 1609-18.

Azucena, E. & S. Mobashery. (2001) Aminoglycoside-modifying enzymes: Mechanisms of catalytic processes and inhibition. *Drug Resist Updat* 4: 106-17.

Beauclerk, A. A. & E. Cundliffe. (1987) Sites of action of two ribosomal RNA methylases responsible for resistance to aminoglycosides. *J Mol Biol* 193: 661-71.

Begg, E. J. & M. L. Barclay. (1995) Aminoglycosides-50 years on. *Br J Clin Pharmacol* 39: 597-603.

Blondeau, J. M. (2002) The evolution and role of macrolides in infectious diseases. *Expert Opin Pharmacother* 3: 1131-51.

Boehr, D. D., K. Draker, K. Koteva, M. Bains, R. E. Hancock, and G. D. Wright. (2003a) Broad-spectrum peptide inhibitors of aminoglycoside antibiotic resistance enzymes. *Chem Biol* 10: 189-96.

Boehr, D. D., K. Draker, and G. D. Wright, eds. (2003b). Aminoglycosides and aminocyclitols. Edited by R. G. Finch, D. Greenwood, S. R. Norrby and R. J. Whitley. In *Antibiotic and Chemotherapy. Anti-infective agents and their use in therapy*. UK: Churchill Livingstone.

Boehr, D. D., S. I. Jenkins, and G. D. Wright. (2003c) The molecular basis of the expansive substrate specificity of the antibiotic resistance enzyme aminoglycoside acetyltransferase-6'-aminoglycoside phosphotransferase-2". The role of Asp-99 as an active site base important for acetyl transfer. *J Biol Chem* 278: 12873-80.

Brodersen, D. E., W. M. Clemons, Jr., A. P. Carter, R. J. Morgan-Warren, B. T. Wimberly, and V. Ramakrishnan. (2000) The structural basis for the action of the antibiotics tetracycline, pactamycin, and hygromycin B on the 30S ribosomal subunit. *Cell* 103: 1143-54.

Bryan, L. E. & S. Kwan. (1983) Roles of ribosomal binding, membrane potential, and electron transport in bacterial uptake of streptomycin and gentamicin. *Antimicrob Agents Chemother* 23: 835-45.

Bryan, L. E. & H. M. Van den Elzen. (1976) Streptomycin accumulation in susceptible and resistant strains of *Escherichia coli* and *Pseudomonas aeruginosa*. *Antimicrob Agents Chemother* 9: 928-38.

Bryan, L. E. & H. M. Van Den Elzen. (1977) Effects of membrane-energy mutations and cations on streptomycin and gentamicin accumulation by bacteria: A model for entry of streptomycin and gentamicin in susceptible and resistant bacteria. *Antimicrob Agents Chemother* 12: 163-77.

Bunny, K. L., R. M. Hall, and H. W. Stokes. (1995) New mobile gene cassettes containing an aminoglycoside resistance gene, *aacA7*, and a chloramphenicol resistance gene, *catB3*, in an integron in pBWH301. *Antimicrob Agents Chemother* 39: 686-93.

Burk, D. L., N. Ghuman, L. E. Wybenga-Groot, and A. M. Berghuis. (2003) X-ray structure of the AAC(6')-Ii antibiotic resistance enzyme at 1.8 Å resolution; examination of oligomeric arrangements in GNAT superfamily members. *Protein Sci* 12: 426-37.

Bush, K. & G. H. Miller. (1998) Bacterial enzymatic resistance: Beta-lactamases and aminoglycoside-modifying enzymes. *Curr Opin Microbiol* 1: 509-15.

Busse, H. J., C. Wostmann, and E. P. Bakker. (1992) The bactericidal action of streptomycin: Membrane permeabilization caused by the insertion of mistranslated proteins into the cytoplasmic membrane of *Escherichia coli* and subsequent caging of the antibiotic inside the cells due to degradation of these proteins. *J Gen Microbiol* 138 (Pt 3): 551-61.

Carrasco, D. A., M. Vander Straten, and S. K. Tyring. (2002) A review of antibiotics in dermatology. *J Cutan Med Surg* 6: 128-50.

Carter, A. P., W. M. Clemons, D. E. Brodersen, R. J. Morgan-Warren, B. T. Wimberly, and V. Ramakrishnan. (2000) Functional insights from the structure of the 30S ribosomal subunit and its interactions with antibiotics. *Nature* 407: 340-8.

Centron, D. & P. H. Roy. (1998) Characterization of the 6'-*N*-aminoglycoside acetyltransferase gene *aac(6')-Iq* from the integron of a natural multiresistance plasmid. *Antimicrob Agents Chemother* 42: 1506-8.

Chopra, I. & M. Roberts. (2001) Tetracycline antibiotics: Mode of action, applications, molecular biology, and epidemiology of bacterial resistance. *Microbiol Mol Biol Rev* 65: 232-60 ; second page, table of contents.

Cole, S. T., K. Eiglmeier, J. Parkhill, K. D. James, N. R. Thomson, P. R. Wheeler, N. Honore, T. Garnier, C. Churcher, D. Harris, K. Mungall, D. Basham, D. Brown, T. Chillingworth, R. Connor, R. M. Davies, K. Devlin, S. Duthoy, T. Feltwell, A. Fraser, N. Hamlin, S. Holroyd, T. Hornsby, K. Jagels, C. Lacroix, J. Maclean, S. Moule, L. Murphy, K. Oliver, M. A. Quail, M. A. Rajandream, K. M. Rutherford, S. Rutter, K. Seeger, S. Simon, M. Simmonds, J. Skelton, R. Squares, S. Squares, K. Stevens, K. Taylor, S. Whitehead, J. R. Woodward, and B. G. Barrell. (2001) Massive gene decay in the leprosy bacillus. *Nature* 409: 1007-11.

Costa, Y., M. Galimand, R. Leclercq, J. Duval, and P. Courvalin. (1993) Characterization of the chromosomal *aac(6')-Ii* gene specific for *Enterococcus faecium*. *Antimicrob Agents Chemother* 37: 1896-903.

Courvalin, P. & C. Carlier. (1981) Resistance towards aminoglycoside-aminocyclitol antibiotics in bacteria. *J Antimicrob Chemother* 8 Suppl A: 57-69.

Culebras, E. & J. L. Martinez. (1999) Aminoglycoside resistance mediated by the bifunctional enzyme 6'-N-aminoglycoside acetyltransferase-2"-*O*-aminoglycoside phosphotransferase. *Front Biosci* 4: D1-8.

Daigle, D. M., D. W. Hughes, and G. D. Wright. (1999a) Prodigious substrate specificity of AAC(6')-APH(2"), an aminoglycoside antibiotic resistance determinant in enterococci and staphylococci. *Chem Biol* 6: 99-110.

Daigle, D. M., G. A. McKay, P. R. Thompson, and G. D. Wright. (1999b) Aminoglycoside antibiotic phosphotransferases are also serine protein kinases. *Chem Biol* 6: 11-8.

Daigle, D. M., G. A. McKay, and G. D. Wright. (1997) Inhibition of aminoglycoside antibiotic resistance enzymes by protein kinase inhibitors. *J Biol Chem* 272: 24755-8.

Davidson, R. N. (1998) Practical guide for the treatment of leishmaniasis. *Drugs* 56: 1009-18.

Davies, J. & B. D. Davis. (1968) Misreading of ribonucleic acid code words induced by aminoglycoside antibiotics. The effect of drug concentration. *J Biol Chem* 243: 3312-6.

Davies, J., L. Gorini, and B. D. Davis. (1965) Misreading of RNA codewords induced by aminoglycoside antibiotics. *Mol Pharmacol* 1: 93-106.

Davies, J., D. S. Jones, and H. G. Khorana. (1966) A further study of misreading of codons induced by streptomycin and neomycin using ribopolynucleotides containing two nucleotides in alternating sequence as templates. *J Mol Biol* 18: 48-57.

Davies, J. & G. D. Wright. (1997) Bacterial resistance to aminoglycoside antibiotics. *Trends Microbiol* 5: 234-40.

Davies, J.E. (1991) Aminoglycoside-aminocyclitol antibiotics and their modifying enzymes. In *Antibiotics in laboratory medicine*. V. Lorian,eds. Williams and Wilkins, Baltimore, Maryland. 691-713.

Davis, B. B. (1988) The lethal action of aminoglycosides. *J Antimicrob Chemother* 22: 1-3.

Davis, B. D. (1987) Mechanism of bactericidal action of aminoglycosides. *Microbiol Rev* 51: 341-50.

Davis, B. D., L. L. Chen, and P. C. Tai. (1986) Misread protein creates membrane channels: An essential step in the bactericidal action of aminoglycosides. *Proc Natl Acad Sci U S A* 83: 6164-8.

DeLano, W. L. The PyMOL molecular graphics system 0.82. DeLano Scientific, San Carlos, CA. USA.

DiGiammarino, E. L., K. A. Draker, G. D. Wright, and E. H. Serpersu. (1998) Solution studies of isepamicin and conformational comparisons between isepamicin and butirosin a when bound to an aminoglycoside 6'-*N*-acetyltransferase determined by NMR spectroscopy. *Biochemistry* 37: 3638-44.

Dutnall, R. N., S. T. Tafrov, R. Sternglanz, and V. Ramakrishnan. (1998) Structure of the histone acetyltransferase HAT1: A paradigm for the GCN5-related *N*-acetyltransferase superfamily. *Cell* 94: 427-438.

Dyda, F., D. C. Klein, and A. B. Hickman. (2000) GCN5-related *N*-acetyltransferases: A structural overview. *Annu Rev Biophys Biomol Struct* 29: 81-103.

Edgar, R. & E. Bibi. (1997) MdfA, an *Escherichia coli* multidrug resistance protein with an extraordinarily broad spectrum of drug recognition. *J Bacteriol* 179: 2274-80.

Edson, R. S. & C. L. Terrell. (1999) The aminoglycosides. *Mayo Clin Proc* 74: 519-28.

Edwards, D. I. (1993) Nitroimidazole drugs-action and resistance mechanisms. I. Mechanisms of action. *J Antimicrob Chemother* 31: 9-20.

Ferretti, J.J., K.S. Gilmore, and P. Courvalin. (1986) Nucleotide sequence analysis of the gene specifying the bifunctional 6'-aminoglycoside acetyltransferase 2"-aminoglycoside phosphotransferase enzyme in *Streptococcus faecalis* and identification and cloning of gene regions specifying the two activities. *J. Bacteriol.* 167: 631-638.

Fishman, J. A. (1998) Treatment of infection due to *Pneumocystis carinii*. *Antimicrob Agents Chemother* 42: 1309-14.

Fleming, A. (1929) On the bacterial action of cultures of a penicillium, with special reference to their use in the isolation of *B. Influenzae*. *Brit J Exp Path* 10: 226-236.

Gale, E. F., E. Cundliffe, P.E. Reynolds, M. H Richmond, and M. J. Waring. (1981). In *The Molecular Basis of Antibiotic Action*, eds. John Wiley and Sons, London. 418-439.

Gonzalez, L. S., 3rd & J. P. Spencer. (1998) Aminoglycosides: A practical review. *Am Fam Physician* 58: 1811-20.

Greenwood, D., ed. 2003. *Historical introduction.* Edited by R. G. Finch, D. Greenwood, S. R. Norrby and R. J. Whitley. In *Antibiotic and Chemotherapy. Anti-infective agents and their use in therapy.* UK: Churchill Livingstone.

Guay, D. R. (2001) An update on the role of nitrofurans in the management of urinary tract infections. *Drugs* 61: 353-64.

Hannecart-Pokorni, E., F. Depuydt, L. de wit, E. van Bossuyt, J. Content, and R. Vanhoof. (1997) Characterization of the 6'-*N*-aminoglycoside acetyltransferase gene *aac(6')-Im* [corrected] associated with a sulI-type integron. *Antimicrob Agents Chemother* 41: 314-8.

Hedges, R. W.&K. P. Shannon. (1984) Resistance to apramycin in *Escherichia coli* isolated from animals: Detection of a novel aminoglycoside-modifying enzyme. *J Gen Microbiol* 130 (Pt 3): 473-82.

Hegde, S. S., T. K. Dam, C. F. Brewer, and J. S. Blanchard. (2002) Thermodynamics of aminoglycoside and acyl-coenzyme A binding to the *Salmonella enterica* AAC(6')-Iy aminoglycoside *N*-acetyltransferase. *Biochemistry* 41: 7519-27.

Herrero, I. A., N. C. Issa, and R. Patel. (2002) Nosocomial spread of linezolid-resistant, vancomycin-resistant *Enterococcus faecium. N Engl J Med* 346: 867-9.

Hon, W. C., G. A. McKay, P. R. Thompson, R. M. Sweet, D. S. Yang, G. D. Wright, and A. M. Berghuis. (1997) Structure of an enzyme required for aminoglycoside antibiotic resistance reveals homology to eukaryotic protein kinases. *Cell* 89: 887-95.

Honore, N. & S. T. Cole. (1994) Streptomycin resistance in Mycobacteria. *Antimicrob Agents Chemother* 38: 238-42.

Hooper, D. C. (2002) Fluoroquinolone resistance among Gram-positive cocci. *Lancet Infect Dis* 2: 530-8.

Hotta, K., J. Ishikawa, M. Ichihara, H. Naganawa, and S. Mizuno. (1988) Mechanism of increased kanamycin-resistance generated by protoplast regeneration of *Streptomyces griseus*. I. Cloning of a gene segment directing a high level of an aminoglycoside 3-*N*-acetyltransferase activity. *J Antibiot (Tokyo)* 41: 94-103.

Huovinen, P., L. Sundstrom, G. Swedberg, and O. Skold. (1995) Trimethoprim and sulfonamide resistance. *Antimicrob Agents Chemother* 39: 279-89.

Javier Teran, F., M. Alvarez, J. E. Suarez, and M. C. Mendoza. (1991) Characterization of two aminoglycoside-(3)-*N*-acetyltransferase genes and assay as epidemiological probes. *J Antimicrob Chemother* 28: 333-46.

Johnston, N. J., T. A. Mukhtar, and G. D. Wright. (2002) Streptogramin antibiotics: Mode of action and resistance. *Curr Drug Targets* 3: 335-44.

Kashiwagi, K., M. H. Tsuhako, K. Sakata, T. Saisho, A. Igarashi, S. O. da Costa, and K. Igarashi. (1998) Relationship between spontaneous aminoglycoside resistance in *Escherichia coli* and a decrease in oligopeptide binding protein. *J Bacteriol* 180: 5484-8.

Kelemen, G. H., E. Cundliffe, and I. Financsek. (1991) Cloning and characterization of gentamicin-resistance genes from *Micromonospora purpurea* and *Micromonospora rosea. Gene* 98: 53-60.

Khasnobis, S., V. E. Escuyer, and D. Chatterjee. (2002) Emerging therapeutic targets in tuberculosis: Post-genomic era. *Expert Opin Ther Targets* 6: 21-40.

Kojic, M., L. Topisirovic, and B. Vasiljevic. (1992) Cloning and characterization of an aminoglycoside resistance determinant from *Micromonospora zionensis*. *J Bacteriol* 174: 7868-72.

Lambert, T., G. Gerbaud, and P. Courvalin. (1994) Characterization of the chromosomal *aac(6')-Ij* gene of Acinetobacter sp. 13 and the *aac(6')-Ih* plasmid gene of *Acinetobacter baumannii*. *Antimicrob Agents Chemother* 38: 1883-9.

Lambert, T., G. Gerbaud, M. Galimand, and P. Courvalin. (1993) Characterization of *Acinetobacter haemolyticus aac(6')-Ig* gene encoding an aminoglycoside 6'-*N*-acetyltransferase which modifies amikacin. *Antimicrob Agents Chemother* 37: 2093-100.

Lambert, T., M. C. Ploy, F. Denis, and P. Courvalin. (1999) Characterization of the chromosomal *aac(6')-Iz* gene of *Stenotrophomonas maltophilia*. *Antimicrob Agents Chemother* 43: 2366-71.

Lando, D., M. A. Cousin, and M. Privat de Garilhe. (1973) Misreading, a fundamental aspect of the mechanism of action of several aminoglycosides. *Biochemistry* 12: 4528-33.

Levy, S. B. (1992a) The disease and the cure. The microscopic world of bacteria and antibiotics. In *The Antibiotic Paradox. How miracle drugs are destroying the miracle.* Plenum Press, New York, USA. 13-51.

Levy, S. B. (1992b) From tragedy the antibiotic age is born. In *The Antibiotic Paradox. How miracle drugs are destroying the miracle.* Plenum Press, New York, USA. 1-12.

Li, X. Z., K. Poole, and H. Nikaido. (2003) Contributions of mexab-oprm and an emre homolog to intrinsic resistance of *Pseudomonas aeruginosa* to aminoglycosides and dyes. *Antimicrob Agents Chemother* 47: 27-33.

Llano-Sotelo, B., E. F. Azucena, L. P. Kotra, S. Mobashery, and C. S. Chow. (2002) Aminoglycosides modified by resistance enzymes display diminished binding to the bacterial ribosomal aminoacyl-tRNA site. *Chem Biol* 9: 455-63.

Lopez-Cabrera, M., J. A. Perez-Gonzalez, P. Heinzel, W. Piepersberg, and A. Jimenez. (1989) Isolation and nucleotide sequencing of an aminocyclitol acetyltransferase gene from *Streptomyces rimosus* forma paromomycinus. *J Bacteriol* 171: 321-8.

Lortholary, O., M. Tod, Y. Cohen, and O. Petitjean. (1995) Aminoglycosides. *Med Clin North Am* 79: 761-87.

Lovering, A. M., L. O. White, and D. S. Reeves. (1987) AAC(1): A new aminoglycoside-acetylating enzyme modifying the Cl aminogroup of apramycin. *J Antimicrob Chemother* 20: 803-13.

Magnet, S., P. Courvalin, and T. Lambert. (1999) Activation of the cryptic *aac(6')-Iy* aminoglycoside resistance gene of Salmonella by a chromosomal deletion generating a transcriptional fusion. *J Bacteriol* 181: 6650-5.

Magnet, S., T. Lambert, P. Courvalin, and J. S. Blanchard. (2001) Kinetic and mutagenic characterization of the chromosomally encoded *Salmonella enterica* AAC(6')-Iy aminoglycoside *N*-acetyltransferase. *Biochemistry* 40: 3700-9.

Marshall, W. F. & J. E. Blair. (1999) The cephalosporins. *Mayo Clin Proc* 74: 187-95.

Melancon, P., W. E. Tapprich, and L. Brakier-Gingras. (1992) Single-base mutations at position 2661 of *Escherichia coli* 23S rRNA increase efficiency of translational proofreading. *J Bacteriol* 174: 7896-901.

Miller, G. H., F. J. Sabatelli, R. S. Hare, Y. Glupczynski, P. Mackey, D. Shlaes, K. Shimizu, and K. J. Shaw. (1997) The most frequent aminoglycoside resistance mechanisms--changes with time and geographic area: A reflection of aminoglycoside usage patterns? Aminoglycoside resistance study groups. *Clin Infect Dis* 24 Suppl 1: S46-62.

Miller, L. A., K. Ratnam, and D. J. Payne. (2001) Beta-lactamase-inhibitor combinations in the 21st century: Current agents and new developments. *Curr Opin Pharmacol* 1: 451-8.

Miller, M. H., S. C. Edberg, L. J. Mandel, C. F. Behar, and N. H. Steigbigel. (1980) Gentamicin uptake in wild-type and aminoglycoside-resistant small-colony mutants of *Staphylococcus aureus*. *Antimicrob Agents Chemother* 18: 722-9.

Mingeot-Leclercq, M. P., Y. Glupczynski, and P. M. Tulkens. (1999) Aminoglycosides: Activity and resistance. *Antimicrob Agents Chemother* 43: 727-37.

Miyaguchi, H., H. Narita, K. Sakamoto, and S. Yokoyama. (1996) An antibiotic-binding motif of an RNA fragment derived from the A-site-related region of *Escherichia coli* 16S rRNA. *Nucleic Acids Res* 24: 3700-6.

Moazed, D. & H. F. Noller. (1987) Interaction of antibiotics with functional sites in 16S ribosomal RNA. *Nature* 327: 389-94.

Moellering, R. C. (2003) Linezolid: The first oxazolidinone antimicrobial. *Ann Intern Med* 138: 135-42.

Moore, R. A., D. DeShazer, S. Reckseidler, A. Weissman, and D. E. Woods. (1999) Efflux-mediated aminoglycoside and macrolide resistance in *Burkholderia pseudomallei*. *Antimicrob Agents Chemother* 43: 465-70.

Moore, R. A. & R. E. Hancock. (1986) Involvement of outer membrane of *Pseudomonas cepacia* in aminoglycoside and polymyxin resistance. *Antimicrob Agents Chemother* 30: 923-6.

Muir, M. E., M. Ballesteros, and B. J. Wallace. (1985) Respiration rate, growth rate and the accumulation of streptomycin in *Escherichia coli*. *J Gen Microbiol* 131 (Pt 10): 2573-9.

Muir, M. E., D. R. Hanwell, and B. J. Wallace. (1981) Characterization of a respiratory mutant of *Escherichia coli* with reduced uptake of aminoglycoside antibiotics. *Biochim Biophys Acta* 638: 234-41.

Muir, M. E. & B. J. Wallace. (1979) Isolation of mutants of *Escherichia coli* uncoupled in oxidative phosphorylation using hypersensitivity to streptomycin. *Biochim Biophys Acta* 547: 218-29.

Neu, H. C. (1992) The crisis in antibiotic resistance. *Science* 257: 1064-73.

Neuwald, A. F. & D. Landsman. (1997) GCN5-related histone *N*-acetyltransferases belong to a diverse superfamily that includes the yeast spt10 protein. *Trends Biochem. Sci.* 22: 154-155.

Normark, B. H. & S. Normark. (2002) Evolution and spread of antibiotic resistance. *J Intern Med* 252: 91-106.

Nyirjesy, P., J. D. Sobel, M. V. Weitz, D. J. Leaman, and S. P. Gelone. (1998) Difficult-to-treat trichomoniasis: Results with paromomycin cream. *Clin Infect Dis* 26: 986-8.

Ohmiya, K., T. Tanaka, N. Noguchi, K. O'Hara, and M. Kono. (1989) Nucleotide sequence of the chromosomal gene coding for the aminoglycoside 6-adenylyltransferase from *Bacillus subtilis* marburg 168. *Gene* 78: 377-8.

Page, R.D.M. (1996) Treeview: An application to display phylogenetic trees on personal computers. *Computer Applications in the Biosciences* 12: 357-358.

Pasteur, L. & J. Lister. (1996) The germ theory and its application to medicine and surgery. In *Germ theory and its applications to medicine & on the antiseptic principle of the practice of surgery*. H. C. (translator) Ernst,eds. Prometheus Books, New York. 110-117.

Payie, K. G.&A. J. Clarke. (1997) Characterization of gentamicin 2'-*N*-acetyltransferase from *Providencia stuartii*: Its use of peptidoglycan metabolites for acetylation of both aminoglycosides and peptidoglycan. *J Bacteriol* 179: 4106-14.

Payie, K. G., P. N. Rather, and A. J. Clarke. (1995) Contribution of gentamicin 2'-*N*-acetyltransferase to the O-acetylation of peptidoglycan in providencia stuartii. *J Bacteriol* 177: 4303-10.

Pedersen, L. C., M. M. Benning, and H. M. Holden. (1995) Structural investigation of the antibiotic and ATP-binding sites in kanamycin nucleotidyltransferase. *Biochemistry* 34: 13305-11.

Poirel, L., T. Lambert, S. Turkoglu, E. Ronco, J. Gaillard, and P. Nordmann. (2001) Characterization of class 1 integrons from *Pseudomonas aeruginosa* that contain the *bla(vim-2)* carbapenem-hydrolyzing beta-lactamase gene and of two novel aminoglycoside resistance gene cassettes. *Antimicrob Agents Chemother* 45: 546-52.

Rahim, S., S. K. Pillai, H. S. Gold, L. Venkataraman, K. Inglima, and R. A. Press. (2003) Linezolid-resistant, vancomycin-resistant *Enterococcus faecium* infection in patients without prior exposure to linezolid. *Clin Infect Dis* 36: E146-8.

Rather, P. N., P. A. Mann, R. Mierzwa, R. S. Hare, G. H. Miller, and K. J. Shaw. (1993a) Analysis of the *aac(3)-VIa* gene encoding a novel 3-*N*-acetyltransferase. *Antimicrob Agents Chemother* 37: 2074-9.

Rather, P. N., R. Mierzwa, R. S. Hare, G. H. Miller, and K. J. Shaw. (1992) Cloning and DNA sequence analysis of an *aac(3)-Vb* gene from *Serratia marcescens*. *Antimicrob Agents Chemother* 36: 2222-7.

Rather, P. N., E. Orosz, K. J. Shaw, R. Hare, and G. Miller. (1993b) Characterization and transcriptional regulation of the 2'-*N*-acetyltransferase gene from *Providencia stuartii*. *J Bacteriol* 175: 6492-8.

Recht, M. I., S. Douthwaite, and J. D. Puglisi. (1999) Basis for prokaryotic specificity of action of aminoglycoside antibiotics. *EMBO J* 18: 3133-8.

Recht, M. I., D. Fourmy, S. C. Blanchard, K. D. Dahlquist, and J. D. Puglisi. (1996) RNA sequence determinants for aminoglycoside binding to an A-site rRNA model oligonucleotide. *J Mol Biol* 262: 421-36.

Riccio, M. L., J. D. Docquier, E. Dell'Amico, F. Luzzaro, G. Amicosante, and G. M. Rossolini. (2003) Novel 3-N-aminoglycoside acetyltransferase gene, *aac(3)-Ic*, from a *Pseudomonas aeruginosa* integron. *Antimicrob Agents Chemother* 47: 1746-8.

Rudant, E., P. Bourlioux, P. Courvalin, and T. Lambert. (1994) Characterization of the *aac(6')-Ik* gene of Acinetobacter sp. 6. *FEMS Microbiol Lett* 124: 49-54.

Rudant, E., P. Bouvet, P. Courvalin, and T. Lambert. (1999) Phylogenetic analysis of proteolytic Acinetobacter strains based on the sequence of genes encoding aminoglycoside 6'-*N*-acetyltransferases. *Syst Appl Microbiol* 22: 59-67.

Sakon, J., H. H. Liao, A. M. Kanikula, M. M. Benning, I. Rayment, and H. M. Holden. (1993) Molecular structure of kanamycin nucleotidyltransferase determined to 3.0-Å resolution. *Biochemistry* 32: 11977-84.

Salauze, D., J. A. Perez-Gonzalez, W. Piepersberg, and J. Davies. (1991) Characterisation of aminoglycoside acetyltransferase-encoding genes of neomycin-producing *Micromonospora chalcea* and *Streptomyces fradiae*. *Gene* 101: 143-8.

Schatz, A., E. Bugie, and S. A. Waksman. (1944) Streptomycin, a substance exhibiting antibiotic activity against Gram-positive and Gram-negative bacteria. *Proc Soc Exp Biol Med* 55: 66-69.

Schmidt, F. R., E. J. Nucken, and R. B. Henschke. (1988) Nucleotide sequence analysis of 2"-aminoglycoside nucleotidyl-transferase *ant(2")* from Tn4000: Its relationship with *aad(3")* and impact on Tn21 evolution. *Mol Microbiol* 2: 709-17.

Schmitz, F. J., P. G. Higgins, S. Mayer, A. C. Fluit, and A. Dalhoff. (2002) Activity of quinolones against Gram-positive cocci: Mechanisms of drug action and bacterial resistance. *Eur J Clin Microbiol Infect Dis* 21: 647-59.

Schwocho, L. R., C. P. Schaffner, G. H. Miller, R. S. Hare, and K. J. Shaw. (1995) Cloning and characterization of a 3-*N*-aminoglycoside acetyltransferase gene, *aac(3)-Ib*, from *Pseudomonas aeruginosa*. *Antimicrob Agents Chemother* 39: 1790-6.

Sefton, A. M. (2002) Mechanisms of antimicrobial resistance: Their clinical relevance in the new millennium. *Drugs* 62: 557-66.

Shaw, K. J., P. N. Rather, F. J. Sabatelli, P. Mann, H. Munayyer, R. Mierzwa, G. L. Petrikkos, R. S. Hare, G. H. Miller, P. Bennett, and P. Downey (1992) Characterization of the chromosomal *aac(6')-Ic* gene from *Serratia marcescens*. *Antimicrob Agents Chemother* 36: 1447-55.

Shaw, K.J., P.N. Rather, R.S. Hare, and G.H. Miller. (1993) Molecular genetics of aminoglycoside resistance genes and familial relationships of the aminoglycoside-modifying enzymes. *Microbiol. Rev.* 57: 138-163.

Skeggs, P. A., D. J. Holmes, and E. Cundliffe. (1987) Cloning of aminoglycoside-resistance determinants from *Streptomyces tenebrarius* and comparison with related genes from other actinomycetes. *J Gen Microbiol* 133 (Pt 4): 915-23.

Smith, C. A. & E. N. Baker. (2002) Aminoglycoside antibiotic resistance by enzymatic deactivation. *Curr Drug Targets Infect Disord* 2: 143-60.

Smith, C. L. & K. R. Powell. (2000) Review of the sulfonamides and trimethoprim. *Pediatr Rev* 21: 368-71.

Sreevatsan, S., X. Pan, K. E. Stockbauer, D. L. Williams, B. N. Kreiswirth, and J. M. Musser. (1996) Characterization of *rpsL* and *rrs* mutations in streptomycin-resistant *Mycobacterium tuberculosis* isolates from diverse geographic localities. *Antimicrob Agents Chemother* 40: 1024-6.

Sucheck, S.J., A.L. Wong, K.M. Koeller, D.D. Boehr, K.a. Draker, P. Sears, G.D. Wright, and C.H. Wong. (2000) Design of bifunctional antibiotics that target bacterial rRNA and inhibit resistance-causing enzymes. *J. Am. Chem. Soc.* 122: 5230-5231.

Sunada, A., M. Nakajima, Y. Ikeda, S. Kondo, and K. Hotta. (1999) Enzymatic 1-N-acetylation of paromomycin by an Actinomycete strain #8 with multiple aminoglycoside resistance and paromomycin sensitivity. *J Antibiot (Tokyo)* 52: 809-14.

Taber, H. W., J. P. Mueller, P. F. Miller, and A. S. Arrow. (1987) Bacterial uptake of aminoglycoside antibiotics. *Microbiol Rev* 51: 439-57.

Taber, H. W., B. J. Sugarman, and G. M. Halfenger. (1981) Involvement of menaquinone in the active accumulation of aminoglycosides by *Bacillus subtilis*. *J Gen Microbiol* 123: 143-9.

Tenover, F. C., D. Filpula, K. L. Phillips, and J. J. Plorde. (1988) Cloning and sequencing of a gene encoding an aminoglycoside 6'-*N*-acetyltransferase from an R factor of *Citrobacter diversus*. *J Bacteriol* 170: 471-3.

Teran, F. J., J. E. Suarez, and M. C. Mendoza. (1991) Cloning, sequencing, and use as a molecular probe of a gene encoding an aminoglycoside 6'-*N*-acetyltransferase of broad substrate profile. *Antimicrob Agents Chemother* 35: 714-9.

Thompson, J. D., D. G. Higgins, and T. J. Gibson. (1994) Clustal W: Improving the sensitivity of progressive multiple sequence alignment through sequence weighting, position-specific gap penalties and weight matrix choice. *Nucleic Acids Res* 22: 4673-80.

Thompson, J., P. A. Skeggs, and E. Cundliffe. (1985) Methylation of 16S ribosomal RNA and resistance to the aminoglycoside antibiotics gentamicin and kanamycin determined by DNA from the gentamicin-producer, *Micromonospora purpurea*. *Mol Gen Genet* 201: 168-73.

Tran van Nhieu, G. & E. Collatz. (1987) Primary structure of an aminoglycoside 6'-*N*-acetyltransferase aac(6')-4, fused in vivo with the signal peptide of the Tn3-encoded beta-lactamase. *J Bacteriol* 169: 5708-14.

Tsiodras, S., H. S. Gold, G. Sakoulas, G. M. Eliopoulos, C. Wennersten, L. Venkataraman, R. C. Moellering, and M. J. Ferraro. (2001) Linezolid resistance in a clinical isolate of *Staphylococcus aureus*. *Lancet* 358: 207-8.

Van Bambeke, F., E. Balzi, and P. M. Tulkens. (2000) Antibiotic efflux pumps. *Biochem Pharmacol* 60: 457-70.

Vetting, M. W., S. S. Hegde, F. Javid-Majd, J. S. Blanchard, and S. L. Roderick. (2002) Aminoglycoside 2'-*N*-acetyltransferase from *Mycobacterium tuberculosis* in complex with coenzyme A and aminoglycoside substrates. *Nat Struct Biol* 9: 653-8.

Vicens, Q. & E. Westhof. (2002) Crystal structure of a complex between the aminoglycoside tobramycin and an oligonucleotide containing the ribosomal decoding A site. *Chem Biol* 9: 747-55.

Virk, A.&J. M. Steckelberg. (2000) Clinical aspects of antimicrobial resistance. *Mayo Clin Proc* 75: 200-14.

Vliegenthart, J. S., P. A. Ketelaar-van Gaalen, and J. A. van de Klundert. (1991) Nucleotide sequence of the *aac3* gene, a gentamicin resistance determinant encoding aminoglycoside-(3)-*N*-acetyltransferase iii expressed in *Pseudomonas aeruginosa* but not in *Escherichia coli*. *Antimicrob Agents Chemother* 35: 892-7.

Williams, J. W. & D. B. Northrop. (1976) Purification and properties of gentamicin acetyltransferase I. *Biochemistry* 15: 125-31.

Williams, J. W. & D. B. Northrop. (1978a) Kinetic mechanisms of gentamicin acetyltransferase I. Antibiotic-dependent shift from rapid to nonrapid equilibrium random mechanisms. *J Biol Chem* 253: 5902-7.

Williams, J. W. & D. B. Northrop. (1978b) Substrate specificity and structure-activity relationships of gentamicin acetyltransferase I. The dependence of antibiotic resistance upon substrate Vmax/Km values. *J Biol Chem* 253: 5908-14.

Williams, J. W. & D. B. Northrop. (1979) Synthesis of a tight-binding, multisubstrate analog inhibitor of gentamicin acetyltransferase I. *J Antibiot (Tokyo)* 32: 1147-54.

Wolf, E., A. Vassilev, Y. Makino, A. Sali, Y. Nakatani, and S. K. Burley. (1998) Crystal structure of a GCN5-related *N*-acetyltransferase: *Serratia marcescens* aminoglycoside 3-*N*-acetyltransferase. *Cell* 94: 439-49.

Wright, A. J. (1999a) The penicillins. *Mayo Clin Proc* 74: 290-307.

Wright, G. D. (1999b) Aminoglycoside-modifying enzymes. *Curr Opin Microbiol* 2: 499-503.

Wright, G. D. & P. R. Thompson. (1999) Aminoglycoside phosphotransferases: Proteins, structure, and mechanism. *Front Biosci* 4: D9-21.

Wright, G.D. (2002) Mechanisms of aminoglycoside antibiotic resistance. In *Bacterial resistance to antimicrobials*. K. Lewis, H.W. Taber and A.A. Salyers,eds. Marcel Dekker Inc., New York. 91-121.

Wright, G.D. & P. Ladak. (1997) Overexpression and characterization of the chromosomal aminoglycoside 6'-*N*-acetyltransferase from E*nterococcus faecium*. *Antimicrob. Agents Chemother.* 41: 956-960.

Wu, H. Y., G. H. Miller, M. G. Blanco, R. S. Hare, and K. J. Shaw. (1997) Cloning and characterization of an aminoglycoside 6'-*N*-acetyltransferase gene from *Citrobacter freundii* which confers an altered resistance profile. *Antimicrob Agents Chemother* 41: 2439-47.

Wybenga-Groot, L. E., K. Draker, G. D. Wright, and A. M. Berghuis. (1999) Crystal structure of an aminoglycoside 6'-N-acetyltransferase: Defining the GCN5-related *N*-acetyltransferase superfamily fold. *Structure Fold Des* 7: 497-507.

Young, M. L., M. Bains, A. Bell, and R. E. Hancock. (1992) Role of *Pseudomonas aeruginosa* outer membrane protein OprH in polymyxin and gentamicin resistance: Isolation of an OprH-deficient mutant by gene replacement techniques. *Antimicrob Agents Chemother* 36: 2566-8.

Chapter 2

Ligand-Induced Conformational Changes in AAC(6')-Ii

2.0 Summary

The research described in this chapter characterizes the conformational changes observed for AAC(6')-Ii in response to the binding of both AcCoA and AG substrates. Through a series of studies including partial proteolysis, tryptophan fluorescence, circular dichroism, and ^{15}N-^{1}H NMR, we have demonstrated that this enzyme undergoes a significant structural rearrangement upon the binding of AcCoA, with changes also noted in response to AG binding. Our results have established that AAC(6')-Ii is in a flexible, open conformation in its ligand-free form and assumes a closed conformation upon substrate binding, thereby generating a catalytically competent enzyme. The elucidation of the AAC(6')-Ii·AcCoA crystal structure that succeeded these studies (Wybenga-Groot *et al.*, 1999) allowed us to further interpret our results in the context of the proteins' tertiary structure, as well as to identify the correct dimer interface from numerous alternatives presented by the crystal structure data.

We gratefully acknowledge the ^{15}N-^{1}H NMR work done by Dr. Kevin Gardner at the University of Toronto, Department of Medical Genetics and Microbiology. We also thank Dr. Kirk Green, who performed the mass spectrometry analysis of AAC(6')-Ii proteolytic fragments at the McMaster Regional Center for Mass Spectrometry. Lastly, we thank Leanne Wybenga-Groot, who solved the AAC(6')-Ii·AcCoA binary complex structure at McMaster and provided valuable crystallographic data that aided in the identification of the AAC(6')-Ii physiological dimer.

2.1 Introduction

Protein conformational changes in response to ligand binding are a well documented phenomenon and the subject of many comprehensive reviews (Gerstein *et al.*, 1994; Hammes, 2002; Yon *et al.*, 1998). The motions of structural domains within proteins have been repeatedly demonstrated to be essential for a wide range of protein functions, including efficient catalysis by several classes of enzymes such as dehydrogenases, kinases, synthases, proteases, and many others (Gerstein *et al.*, 1994). The idea that substrate-induced conformational changes are a requirement for catalysis was first proposed in Koshland's induced-fit theory of enzyme specificity, which consists of a set of postulates outlining the importance of structural rearrangements upon ligand binding in order to generate enzyme specificity and the proper orientation of substrates in the active site (Koshland, 1958). The extent of a substrate-induced conformational change can vary greatly depending on the protein, with only subtle changes localized to the active site in some instances and much larger movements, sometimes distant from the active site, observed for other enzymes. A classic example of the latter case is ligand-induced domain closure, in which a substrate binds in a cleft-like region between two domains and induces a "closed" protein conformation (Gerstein *et al.*, 1994). X-ray crystallography in particular has provided a wealth of information regarding enzyme conformational changes, largely based on structural comparisons of an enzyme in uncomplexed *versus* complexed forms (Gerstein *et al.*, 1994; Yon *et al.*, 1998). Additional methods such as fluorescence spectroscopy and NMR can also aid in

characterizing the nature and extent of ligand-induced protein movements (Yon *et al.*, 1998), and often complement crystallographic studies.

Recent work on several different GNAT enzymes has revealed that substrate-induced conformational changes are common for this superfamily. In particular, yeast histone acetyltransferase (HAT) has been shown to become refractory to protease digestion upon formation of the HAT·AcCoA complex, suggesting a change in protein conformation upon association with cofactor (Dutnall *et al.*, 1998). As well, crystal structures of the tetrahymena GCN5 enzyme with bound AcCoA as well as the ternary complex indicate that cofactor binding of essential in orienting the protein for proper histone binding and *N*-acetyltransfer (Rojas *et al.*, 1999). Similarly, the structure of serotonin *N*-acetyltransferase (AANAT) in complex with a bisubstrate analog shows that cofactor binding is accompanied by both changes in secondary structure and conformation in order to form the serotonin binding site (Hickman *et al.*, 1999a; Hickman *et al.*, 1999b).

This chapter focuses on the conformational changes in AAC(6')-Ii in response to both AcCoA and AG binding. In the absence of a three-dimensional structure of AAC(6')-Ii in unliganded or ternary complex forms, we turned to a series of experiments including protease susceptibility and Trp fluorescence to probe local conformational and general structural changes in response to ligand binding. Our results complement the structural determinations for this enzyme (Wybenga-Groot *et al.*, 1999; Burk *et al.*, 2003) and also contribute important protein structural information relevant to AAC(6')-Ii catalysis.

2.2 Materials and Methods

2.2.1 Reagents

Kanamycin A, paromomycin, neomycin, 4,4'-dithiodipyridine, subtilisin, 2-[N-morpholino]ethansulfonic acid (MES), and phenylmethylsulfonyl fluoride (PMSF) were from Sigma. AcCoA was from Boehringer Mannheim.

2.2.2 AAC(6')-Ii Purification and Steady-State Kinetic Assays

Wild type and mutant AAC(6')-Ii proteins were purified by anion exchange, gel filtration and affinity column chromatography as previously described (Wright & Ladak, 1997). AG-dependent acetyltransferase activity was monitored during purification and steady-state kinetic studies by *in situ* titration of free coenzyme A with 4,4'-dithiodipyridine as described previously (Williams & Northrop, 1978; Wright & Ladak, 1997). Assay conditions for kinetic analysis of mutant AAC(6')-Ii enzymes were similar to those described for the wild type protein (Wright & Ladak, 1997).

2.2.3 Proteolysis Studies and Mass Spectrometry

The susceptibility of AAC(6')-Ii to the serine protease subtilisin was assessed by sodium dodecyl sulfate polyacrylamide gel electrophoresis (SDS-PAGE) analysis. Reaction mixtures typically contained 20 ng subtilisin per 1 μg of purified AAC(6')-Ii in 50 mM HEPES, pH 7.5, 40 mM KCl, 10 mM $MgCl_2$, and 2 mM $CaCl_2$. AAC(6')-Ii was treated with protease for varying times from 0 to 75 min. Reactions were quenched with 100 mM PMSF, applied onto 20% SDS polyacrylamide gels, and protein fragments separated by electrophoresis at a constant voltage of 200 V. The gels were stained with

Coomassie blue for visualization of intact protein and proteolytic fragments. Susceptibility of AAC(6')-Ii to subtilisin digestion was further determined in the presence of various combinations of AcCoA and/or AG. Reactions were prepared as described above with the addition of either 100 μM paromomycin, 250 μM AcCoA, or 100 μM paromomycin + 250 μM AcCoA. Proteolysis was allowed to proceed for a maximum of 75 min. All digestions were performed at room temperature with appropriate controls that contained no protecting agent.

N-terminal sequence determinations were performed on proteolytic fragments produced from digestion of free AAC(6')-Ii with subtilisin. Peptide fragments were electroblotted onto polyvinylidene difluoride membranes as previously described (Xu & Shively, 1988). N-terminal sequencing was performed at the HSC/Pharmacia Biotechnology Service Center, University of Toronto (Toronto, Ontario) using a Proton Gas-Phase Microsequencer with in-line 3-phenyl-2-thiohydantoin amino acid analysis. Electrospray mass spectrometric analysis was also performed on AAC(6')-Ii proteolytic fragments to aid in identifying the precise sites of cleavage. Digestion reactions were prepared as described above and separated over a Superdex 75 gel filtration column (Pharmacia) to isolate full length AAC(6')-Ii and *ca.* 17 and 15 kDa fragments. Electrospray mass spectrometry was performed at the McMaster Regional Center for Mass Spectrometry using a Micromass Quatro LC triple quadropole mass spectrometer in positive ion mode and a 15 μM sample in H_20 + 0.2% formic acid in acetonitrile/H_20.

2.2.4 Protein ^{15}N-^{1}H NMR

To further characterize the protein conformational changes suggested from partial proteolysis data, several ^{15}N-^{1}H NMR experiments were performed. ^{15}N-labeled AAC(6')-Ii was obtained by purification of the protein from cells grown in M9 minimal medium (Ausubel *et al.*, 1994) supplemented with $^{15}NH_4Cl$ (0.5g/500 mL). Sensitivity-enhanced ^{15}N-^{1}H HSQC spectra (Kay *et al.*, 1992) were recorded on samples of uniformly ^{15}N-labeled AAC(6')-Ii containing either 100 μM or 200 μM protein in 0.5 mL of 100 mM sodium phosphate buffer pH 6.0, 0.25 mM EDTA and 90% H_2O:10% D_2O. All spectra were obtained using a 500 MHz Varian Unity Inova spectrometer, using a sample temperature of 40 °C. Each spectrum was collected as a 64*(^{15}N)x512*(^{1}H) point matrix and used 16 (32) scans per transient for the 200 μM (100 μM) samples.

2.2.5 Spectroscopic Studies

2.2.5.1 Circular Dichroism (CD) Spectroscopy

We employed CD spectroscopy to investigate whether ligand binding to AAC(6')-Ii induces observable changes in protein secondary structure. CD spectra of AAC(6')-Ii were recorded using a Jasco J600A spectropolarimeter. Samples were scanned from 250 to 190 nm at room temperature using 0.1 cm path length quartz cells. Samples contained 10 mM phosphate buffer, pH 6.0 with 5 μM wild type AAC(6')-Ii and various combinations of 100 μM paromomycin and/or 125 μM AcCoA. All samples were baseline corrected using baseline spectra for buffer alone, paromomycin, and/or AcCoA as appropriate.

2.2.5.2 Fluorescence Spectroscopy Measurements

The intrinsic fluorescence of tryptophan residues in AAC(6')-Ii was utilized to probe changes in enzyme conformation in response to ligand binding. Fluorescence measurements were performed at 37 ° C using an SLM-Aminco Series 2 luminescence spectrometer with a temperature-regulated cuvette block and 1 cm path length quartz cuvettes. Tryptophan fluorescence was selected by excitation at 295 nm and emission spectra obtained by scanning between 310 and 430 nm. Excitation and emission slit widths were set at 4 nm. Samples contained 5 μM AAC(6')-Ii protein (wild type or Trp site mutants, see below) in 25 mM MES, pH 6 and 1 mM EDTA, with the addition of various combinations of 100 μM paromomycin and/or 125 μM AcCoA. All fluorescence spectra were baseline and instrument corrected.

2.2.6 Site-Directed Mutagenesis of AAC(6')-Ii Trp Residues

In an effort to investigate the contribution of individual Trp residues to the fluorescence changes observed in response to ligand, four AAC(6')-Ii site-mutants were created for subsequent fluorescence and steady-state kinetic analysis. Each mutant replaced one of the four Trp residues in the enzyme with Ala. The Trp25Ala and Trp71Ala mutations were generated by amplifying the full-length mutant *aac(6')-Ii* gene from pPLaac-1 (Wright & Ladak, 1997) using the oligonucleotide primers 5' GAATTCCATATGATAATCAGTGAATTTGACCGTAAAATCCAGTATTGAAAGA CCAGCTTTCTGATTTACTGAGACTGACTGCGCCGGAAGAATATGG 3' and 5' GC CCAAGCTTTATTGAGAATCTGGTCGAGG 3' for Trp25Ala, and 5' GGAATTCCA

TATGA TAATCAGTGAATTTGAC 3' and 5' GCCCAAGCTTTATTGAGAATCTGG TCGAGGAATAATCGTTTTTGCCATCGCAATATCC 3' for Trp170Ala. Polymerase chain reaction (PCR) amplifications were performed using Vent DNA polymerase (New England Biolabs) and consisted of 30 cycles of 1 min at 94 °C, 1 min at 50 °C, and 2 min at 72 °C. The mutated genes were subcloned into pET22-b (+) (Novagen, Madison, WI) using the restriction enzymes *Nde*I and *Hind*III to generate the expression constructs p*aac*-W25A and p*aac*-W170A. The Trp71Ala and Trp164Ala mutants were generated using the QuikChange site-directed mutagenesis protocol (Stratagene) and the mutagenic oligonucleotide primers 5' CTCAATACGGTATCACAGGTGCGGAATTGCATCC 3' (Trp71Ala) and 5' CCAAATGCAAATGGTGCGGACAAACCG 3' (Trp164Ala) in addition to their respective reverse complementary sequence. The wild type *aac(6')-Ii* gene was subcloned from pPLaac-1 into the pET22-b (+) vector (Novagen, Madison, WI) to create p*aac*-WT for use as template DNA. PCR amplifications were performed with *Pfu* DNA polymerase by 16 cycles consisting of 12 min at 68 °C, 1 min at 55 °C, and 1 min at 94 °C. PCR products were treated with *Dpn* I and the nicked vector DNA used to transform *E. coli* XL1-Blue competent cells to generate the plasmids p*aac*-W71A and p*aac*-W164A. The presence of the desired mutation in all mutant *aac(6')-Ii* genes and the absence of adventitious mutations was confirmed by complete gene sequencing at the Central Facility of the Institute for Molecular Biology and Biotechnology, McMaster University. All constructs were used to transform *E. coli* BL21(DE3) competent cells for subsequent enzyme overexpression and purification.

2.3 Results and Discussion

2.3.1 Partial Proteolysis Studies

Incubation of purified AAC(6')-Ii with the Ser protease subtilisin results in cleavage of the 20.7 kDa protein first into a fragment of ~ 17 kDa followed by the appearance of a ~ 15 kDa peptide as assessed by SDS-PAGE (Figure 2.1A). N-terminal sequencing of both proteolytic fragments yielded the sequence MIISEFD which corresponds to the N-terminal sequence of AAC(6')-Ii, indicating that proteolytic cleavage occurs successively in the C-terminus. Further analysis by electrospray mass spectrometry gave accurate masses of the proteolytic fragments to be 15 427 and 13 463 Da, with an additional smaller fragment of 5301.6 Da identified. These results indicate, within 1 Da, that free AAC(6')-Ii is first cleaved in a loop region C-terminal to Gln137 to generate fragments 1-137 (15.4 kDa) and 138-182 (5.3 kDa), with subsequent cleavage of the larger peptide fragment C-terminal to Leu120, also within a loop region, to generate an additional 13.5 kDa fragment 120 amino acids in length (Figure 2.2).

AAC(6')-Ii was shown to have a decreased protease susceptibility in the presence of both AcCoA and AG, revealing that the binding of these ligands induces a conformational change in the enzyme to a form which is resistant to proteolysis. Based on the identified sites of proteolysis for the free enzyme, the conformational changes can be somewhat localized to the C-terminal loop region (Figure 2.2). More specifically, the enzyme is almost completely protected upon formation of the AAC(6')-Ii·AcCoA and ternary complex, with less protection offered by the binding of AG (Figure 2.1B).

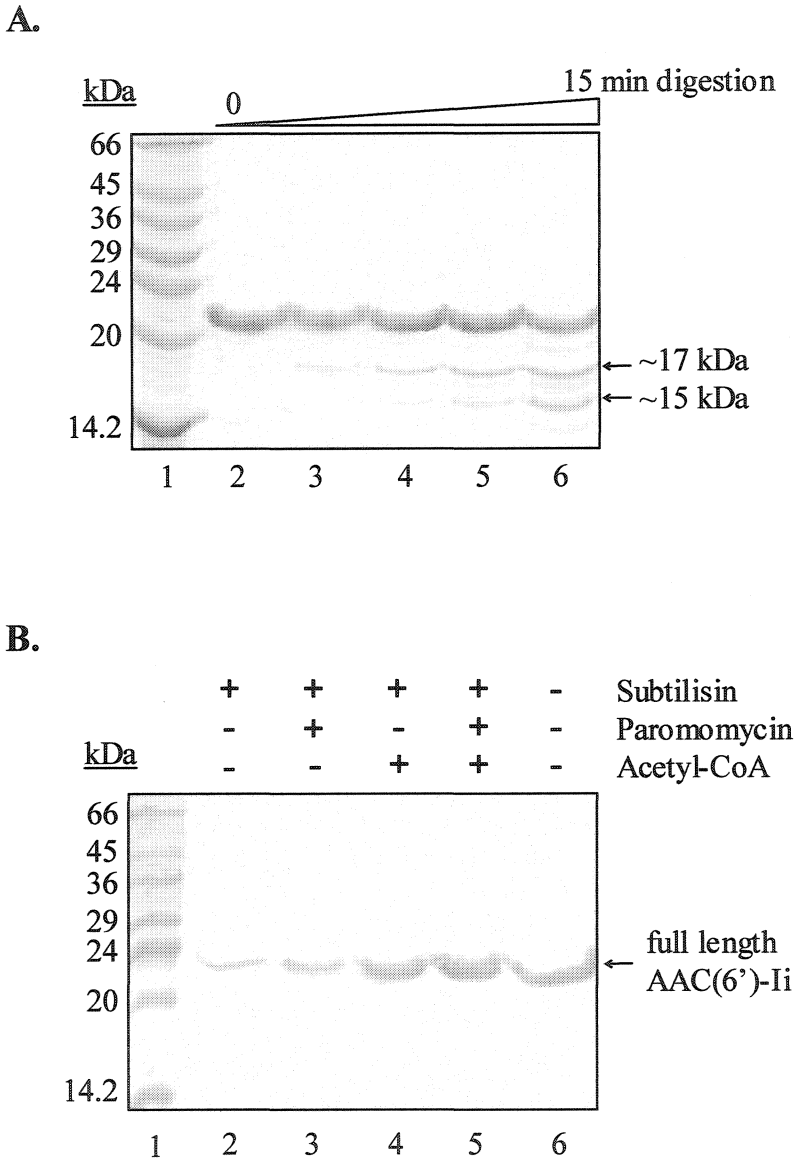

Figure 2.1: Partial proteolysis of AAC(6')-Ii in the presence and absence of ligands. The SDS-20% polyacrylamide gels were stained with Coomassie blue. All samples were prepared as described in materials and methods. **A.** Susceptibility of free AAC(6')-Ii to subtilisin digestion when incubated for: lane 2, 0 min; lane 3, 2 min; lane 4, 5 min; lane 5, 10 min; lane 6, 15 min. Lane 1, molecular mass standards. **B.** Proteolysis of AAC(6')-Ii in the presence of: lane 2, no ligands; lane 3, paromomycin; lane 4, AcCoA; lane 5, paromomycin + AcCoA. Lane 6, untreated AAC(6')-Ii; and lane 1, molecular mass standards.

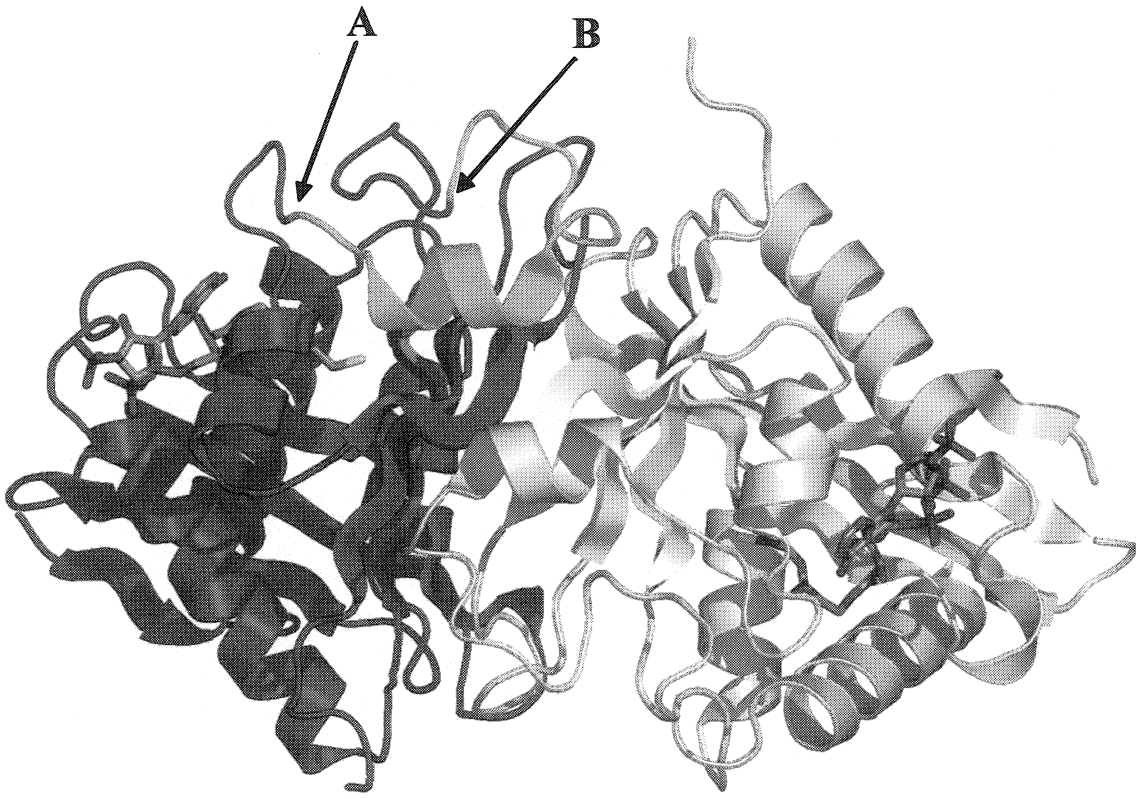

Figure 2.2: Sites of AAC(6')-Ii cleavage by subtilisin. Digestion of free enzyme with the Ser protease subtilisin gives two main sites of hydrolysis per monomer, shown as sites A and B. The first site of cleavage (site A) occurs C-terminal to Gln137 to generate 15.4 kDa (blue & green) and 5.3 kDa (red) fragments. The 15.4 kDa fragment is then successively cleaved C-terminal to Leu120 (site B) to produce a 13.5 kDa fragment (blue). The dimeric AAC(6')-Ii·CoA complex is shown (pdb code 1N71, Burk *et al.*, 2003) to illustrate the sites of cleavage in the context of the physiological dimer. Note that the indicated sites A and B are no longer accessible to protease upon formation of the AAC(6')-Ii·AcCoA binary complex. This figure was generated using the molecular graphics software PyMOL (DeLano, 2002).

The fact that the AcCoA·AAC(6')-Ii binary complex is more stable to hydrolysis than the paromomycin·AAC(6')-Ii complex indicates that the binding of cofactor induces a more significant change in AAC(6')-Ii conformation compared to the that induced by AG. Although only the AAC(6')-Ii·AcCoA/CoA structures have been elucidated, substantial alterations in protein movement and flexibility can be envisioned upon the binding of AcCoA, which is within the cleft-like region between the N and C-terminal domains of the AAC(6')-Ii monomer (Wybenga-Groot *et al.*, 1999). Our protease susceptibility experiments also reveal that AAC(6')-Ii is almost completely protected from digestion in the ternary complex form, consistent with a more "closed" tertiary structure when both substrates are bound in the active site.

The changes in AAC(6')-Ii conformation noted in response to paromomycin binding are interesting in several respects. First, we know from mechanistic studies that AAC(6')-Ii follows an ordered bi-bi kinetic mechanism in which AcCoA binds first followed by AG to form a productive ternary complex (discussed in chapter 3). This indicates that AcCoA must bind prior to AG in order for catalysis to occur. The work presented here in addition to isothermal titration calorimetry (ITC) studies discussed in the next chapter shows that AG can bind in the absence of AcCoA, even though this interaction is unproductive in a catalytic sense. It is therefore unknown whether the changes observed upon association of free AAC(6')-Ii with AG is relevant to catalysis, although the structural rearrangements seen upon formation of the ternary complex do support the importance of AG-induced conformational changes.

2.3.2 Protein ^{15}N-^{1}H NMR

AAC(6')-Ii was enriched in ^{15}N by expressing the enzyme in cells grown in minimal medium with $^{15}NH_4Cl$ as the nitrogen source. The ^{15}N-^{1}H heteronuclear correlation experiments demonstrated a significant change upon binding of both AcCoA and paromomycin, as shown in Figure 2.3;

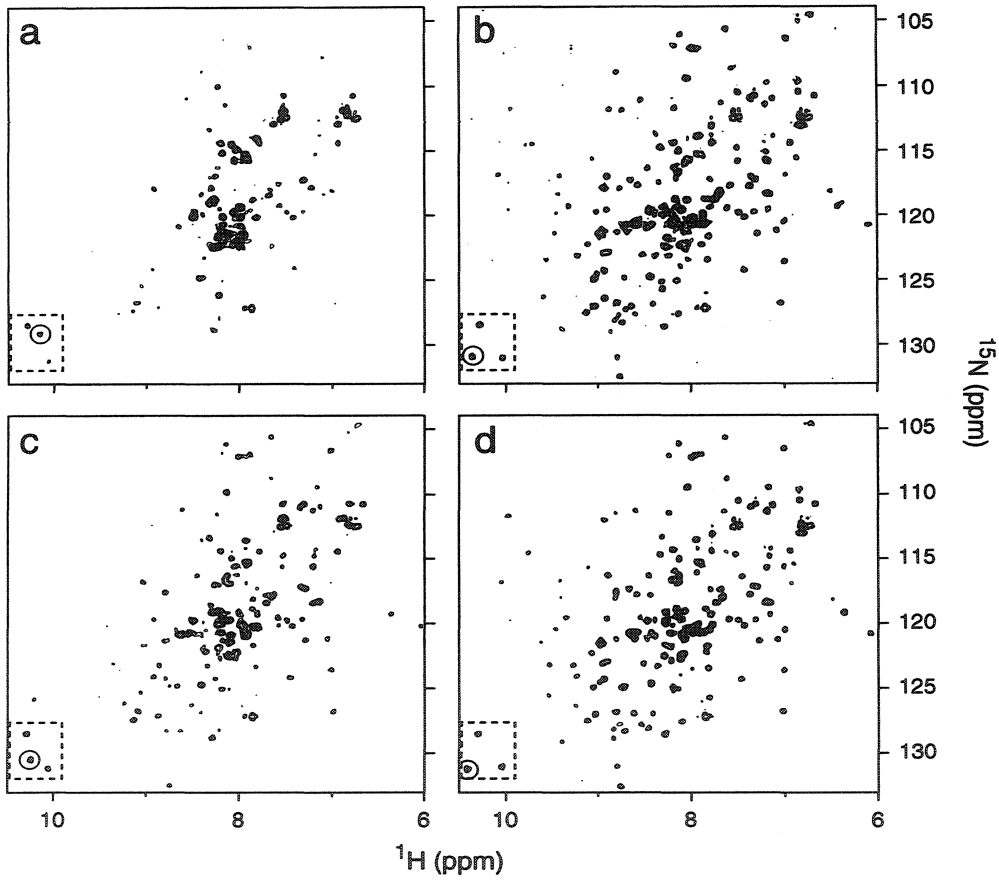

Figure 2.3: NMR-based evidence for ligand-induced conformational changes in AAC(6')-Ii. ^{15}N-^{1}H HSQC spectra are shown for (a) free AAC(6')-Ii; (b) AAC(6')-Ii with AcCoA (c) AAC(6')-Ii with paromomycin, and (d) the ternary complex of AAC(6')-Ii·AcCoA·paromomycin. Ligands were present in 3-fold (b) or 6-fold (c,d) molar excess over the AAC(6')-Ii monomer concentration. Trp indoles are boxed in the bottom left-hand corner of each spectra. The observable movement of one Trp residue is circled.

There are 205 expected amide peaks derived from AAC(6')-Ii including Trp, Asn and Gln side chains. In the non-complexed enzyme, 91 are clearly resolved (Figure 2.3a). Upon binding of AcCoA (Figure 2.3b) or paromomycin (Figure 2.3c), the number of resolvable peaks increases dramatically to 154 and 135 respectively, indicative of conformational changes accompanying the formation of these binary complexes. In the ternary complex, the number of resolved peaks increases further to 175 peaks and the ^{15}N-^{1}H correlation spectrum is qualitatively similar to the AcCoA bound spectrum (Figure 2.3d). Also interesting to note is the Trp indole resonances that were observed and the ligand-induced movement of one of these residues (see boxed residues in Figure 2.3). Overall, the increased ^{15}N and ^{1}H chemical shift dispersion upon ligand binding clearly demonstrates changes in the flexibility of the enzyme on the msec time scale, with significant amide reorganization in AAC(6')-Ii upon formation of the AAC(6')-Ii·AcCoA and ternary complex, and less of a change noted upon formation of the AAC(6')-Ii·paromomycin complex. In addition, these results correlate well with the observations made from our proteolysis studies.

2.3.3 CD and Trp Fluorescence

The CD spectrum of uncomplexed AAC(6')-Ii demonstrates significant negative ellipticity at approximately 208 nm indicative of the α-helical component of the enzyme (Figure 2.4). Addition of the AG paromomycin and/or AcCoA had no observable effect on the resulting spectra (Figure 2.4), indicating that no large secondary structural rearrangements are induced in AAC(6')-Ii by the binding of AcCoA, AG, or with

formation of the ternary complex. This observation suggests that the changes noted from partial proteolysis and protein ^{15}N-^{1}H NMR studies are due to local tertiary conformational changes in AAC(6')-Ii in response to cofactor/substrate, and are not due to large-scale changes in enzyme secondary structure.

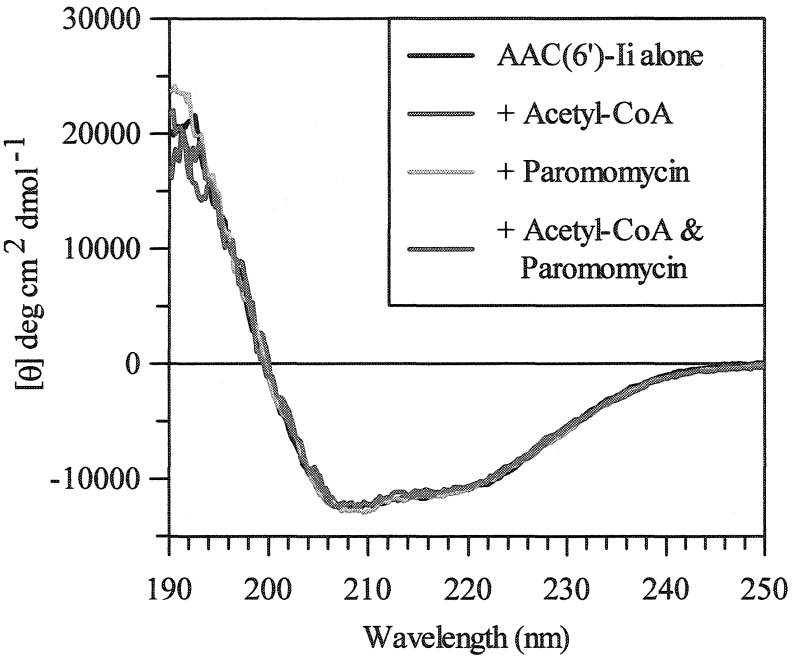

Figure 2.4: Influence of ligands on the CD spectra of AAC(6')-Ii. Shown are the spectra for free and complexed forms of the enzyme according to the legend above.

There are four Trp residues within AAC(6')-Ii, one in the N-terminus at position 25, one in the central portion of the enzyme at position 71, and two in the immediate C-terminal region at positions 164 and 170. Trp25 is located just outside of α1; Trp71 is the second residue of β4; Trp164 is in the loop region between β6 and β7; and Trp170 is the third residue of β7 (Figure 2.5).

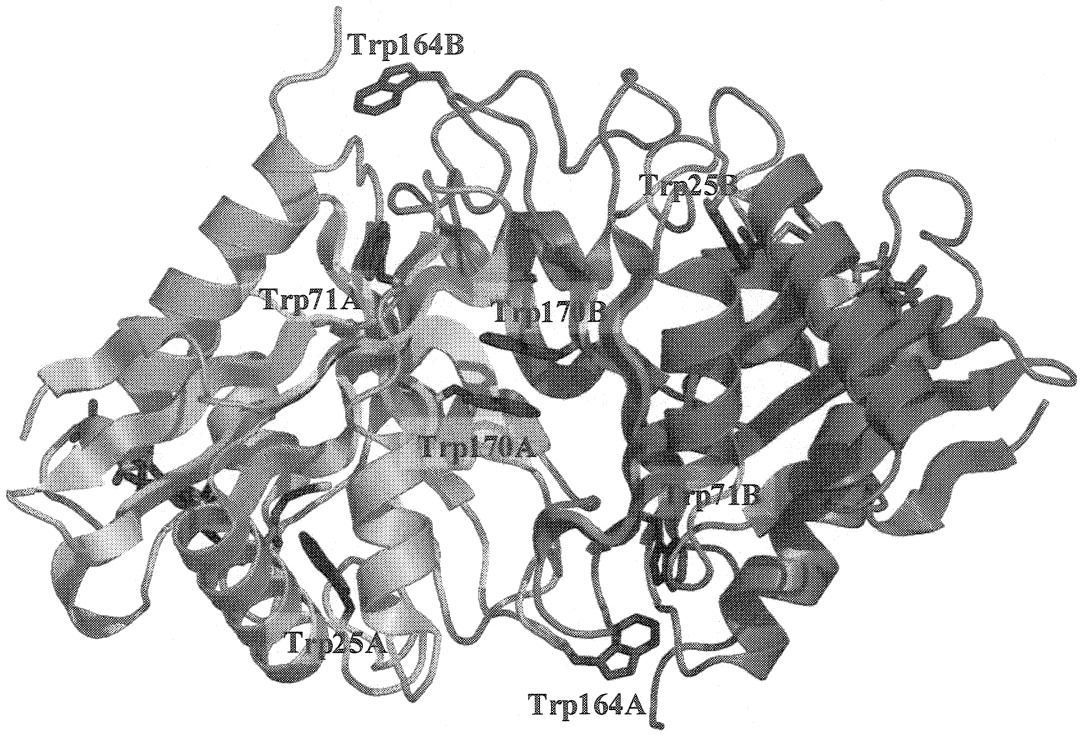

Figure 2.5: Structure of the AAC(6')-Ii·CoA dimer indicating the positions of the four Trp residues per monomer. Trp25 is located in the active site cleft and makes hydrophobic contacts with AcCoA (Wybenga-Groot *et al.*, 1999). Trp71 is located on β-strand 4 and in close proximity to the AcCoA binding site. The C-terminal residues Trp164 and Trp170 participate in monomer-monomer interactions. See text for additional details. This figure was generated using PyMOL (DeLano, 2002).

Trp fluorescence studies with the wild type enzyme revealed a complex pattern of λ_{em} blue shift, as well as changes in relative intensity upon AG binding. The free enzyme displays a typical Trp fluorescence spectrum with λ_{em} of 337 nm (Figure 2.6, Table 2.1). Formation of either binary or ternary complexes results in a significant blue shift of λ_{em}, indicative of a shift of Trp residues from a polar to a non-polar environment, consistent with a structural rearrangement and formation of less flexible enzyme·ligand complexes. Specifically, the addition of paromomycin causes a 5 nm blue shift in λ_{em} to 332 nm, indicative of transfer of one or more Trp residues to a more non-polar environment. In

addition, a significant increase in overall quantum yield as indicated by the increase in relative fluorescence intensity was also observed. Binding of AcCoA also results in a blue shift in λ_{em} (3 nm) with no significant increase in quantum yield observed. Addition of both AcCoA and paromomycin results in a 9 nm blue shift in λ_{em}, with a relative intensity comparable to the native enzyme and compatible with an additive effect between the two binary complexes. These changes in Trp fluorescence are open to two possible interpretations. The first is that only a subset of the Trps in AAC(6')-Ii are perturbed by ligand binding and thus a local conformational change in the protein may account for the observed changes. The second possibility is that the enzyme undergoes a more global change in conformation and/or flexibility, resulting in alterations in the mobility and packing of numerous Trp residues. Knowledge of the AAC(6')-Ii·AcCoA structure (Wybenga-Groot *et al.*, 1999) and the lack of any nearby Trps in the region protected from proteolysis upon ligand binding appears to support the latter hypothesis.

^{15}N-^{1}H NMR correlation spectrum of AAC(6')-Ii shows at least three downfield peaks (^{1}H >10 ppm, ^{15}N > 130 ppm) with chemical shifts that are consistent with three of four Trp indole nitrogen resonances (Figure 2.4). The chemical shifts of two of these are relatively invariant in position in the uncomplexed and ligand-bound forms (see boxed region in Figure 2.4), one of which may correspond to the C-terminal Trp170 involved in AAC(6')-Ii monomer-monomer interactions. It can be speculated that Trp164, which appears to be quite flexible in the protein dimer and distant from the active site, may account for the unobserved Trp indole nitrogen resonance. In addition, one of the Trps

undergoes a major change upon formation of the paromomycin and AcCoA binary complexes (circled in Figure 2.3) and thus the environment of at least one of the Trp residues is sensitive to the nature of the protein-bound ligand(s). We speculate that this residue is Trp25, since it is one of the hydrophobic residues making van der Waal's contacts with the β-mercaptoeythylamine moiety of AcCoA in the active site cleft (Wybenga-Groot *et al.*, 1999). Thus its mobility would be restricted somewhat in both binary complexes and the ternary complex, accounting for the chemical shift observed upon AAC(6')-Ii association with AG and cofactor.

2.3.4 Site-Directed Mutagenesis of AAC(6')-Ii Trps

In order to better understand the contribution of individual Trp residues to the fluorescence changes observed in response to ligand, we generated four AAC(6')-Ii Trp mutants, each having one of the four Trp residues replaced with Ala. Proteolysis experiments performed on purified mutant enzymes indicated, with the exception of W164A, that these proteins retained the structural integrity of the wild type protein. The W164A variant was subsequently shown to be a monomer in solution in contrast to the wild type AAC(6')-Ii dimer and is discussed later. Steady-state kinetic analyses of the Trp mutants were interesting in that they revealed a significant degree of change from the wild type enzyme (Table 2.2).

The W25A mutant, while displaying minimal changes in fluorescence upon ligand binding as compared to the wild type enzyme, did however show significant effects on enzyme activity and substrate recognition (Table 2.2). Most dramatic were the decreases

in the apparent affinity for AGs, noted by a 54- to 320-fold increase in K_m values which was paralleled by a 164-fold increase in the K_i for paromomycin relative to wild type. The location of Trp25 in the AAC(6')-Ii active site and its interaction with AcCoA most likely accounts for the changes observed, particularly the 8-fold increase in the K_m for AcCoA. Trp fluorescence studies for this mutant demonstrated a large 8 nm blue shift in response to paromomycin binding but an attenuated increase in relative fluorescence. A 1 nm blue shift was also noted upon formation of the AAC·AcCoA binary complex (Table 2.1, Figure 2.6).

Kinetic analysis of the W71A mutant revealed that this variant was also somewhat impaired in catalytically competent AG recognition, with a 58-fold increase in the K_m for kanamycin and smaller changes noted for neomycin and the binding of the inhibitor paromomycin (Table 2.2). This substitution also had a large effect on the apparent affinity for AcCoA, a greater than 31-fold increase in K_m over the wild type enzyme. Trp71 appears to be relevant to the blue shifts observed upon ligand binding for the wild type enzyme, as only a small 1 nm blue-shifted spectrum was observed in response to paromomycin binding and no blue shifts noted for the AAC(6')-Ii·AcCoA or ternary complex for this mutant (Table 2.1, Figure 2.6). Furthermore, the significant increase in relative fluorescence observed upon binding of paromomycin to the wild type enzyme was completely abolished.

The C-terminal W164A mutant demonstrated a significant drop in specificity for kanamycin with approximately 10-fold changes in both K_m and k_{cat} (Table 2.2).

Similarly, neomycin specificity decreased by a factor of ~ 7-fold with most of the change due to an increase in K_m, a change that was paralleled in the 5-fold increase in the K_i for paromomycin. The kinetic parameters for AcCoA, however, were only marginally affected with a 2-fold decrease in k_{cat}/K_m. This mutant was found to be more susceptible to subtilisin cleavage than wild type AAC(6')-Ii and neither AcCoA nor AG afforded significant protection, although the ternary complex was marginally protected. This prompted us to perform analytical gel filtration experiments on this mutant, which revealed that it exists as a monomer in solution, in contrast with the dimeric form of the wild type enzyme. This change most likely accounts for the increased susceptibility of this variant to protease and also suggests that Trp164 participates in critical monomer-monomer interactions in the native dimer. These results complemented initial crystallographic evidence and allowed us to identify the physiological AAC(6')-Ii dimer from several candidates. The recent structural determination of the AAC(6')-Ii·CoA complex as a dimer (see Figures 2.2 and 2.5) has since confirmed our previous identification (Burk *et al.*, 2003). Trp fluorescence studies were also interesting for the W164A mutant in that there was no blue shift observed upon formation of the paromomycin·AAC(6')-Ii complex (Figure 2.6, Table 2.1), suggesting that Trp164 may be buried as a result of AG binding. This appears to be unlikely, however, given its relatively solvent accessible surface in the binary complex (Figure 2.5). Close contact with bound substrate is also unlikely as it is somewhat removed from the active site, and

thus the blue shift observed upon formation of the wild type AAC(6')-Ii·paromomycin complex may be characteristic of the dimeric form of the enzyme.

The W170A mutant demonstrated a major increase in the K_m for kanamycin (114-fold) but much less so with neomycin (6.5 fold increase) and no change with AcCoA (Table 2.2). Trp fluorescence spectra largely mirrored the blue shifts seen upon ligand binding in the wild type enzyme, with a 2.2-fold increase in the relative fluorescence intensity observed upon AAC(6')-Ii association with paromomycin (Table 2.1 and Figure 2.6). Interestingly, the AAC(6')-Ii dimer reveals that this C-terminal Trp makes contact with Trp170 of the opposing monomer at the dimer interface (Figure 2.5).

Taken together, these results indicate that the environments of all four Trp residues are perturbed in some manner by the binding of AcCoA and AG. Trp71 in particular appears to account for the blue shifts observed upon the formation of AAC(6')-Ii binary and ternary complexes, with the two N-terminal Trps (25 and 71) largely responsible for the increase in relative fluorescence intensity noted upon AG binding. The C-terminal Trps (164 and 170) involved in dimer interface interactions also appear to undergo changes in response to ligand, although analysis is complicated by the monomeric form of the W164A mutant and the hydrophobic interactions observed between Trp170 residues (Figure 2.5). The Trp fluorescence studies therefore suggest changes in the mobility and packing of several Trp residues in response to ligand binding, and thus supports a more global change in conformation and AAC(6')-Ii flexibility upon association with AcCoA and/or AG.

Table 2.1: Fluorescence changes of wild type and mutant AAC(6')-Ii proteins in response to ligand binding.

Protein alone		AG/AcCoA binding					
		Paromomycin		AcCoA		Paromomycin + AcCoA	
Protein	Emission λ_{max} (nm)	% Change [a]	Emission λ_{max} (nm)	% Change	Emission λ_{max} (nm)	% Change	Emission λ_{max} (nm)
Wild Type	337	+26.7	332	+3.5	334	+25.6	328
Trp25Ala	333	+9.7	325	-1.6	334	+8.2	324
Trp71Ala	333	-1.9	332	-3.1	334	-8.0	334
Trp164Ala	340	+13.3	340	+0.82	338	+2.7	331
Trp170Ala	337	+59.0	331	-2.7	339	+52.6	326

[a] Enhancement (+) or quenching (-) of fluorescence intensities are given as the percent change at the indicated wavelength maxima in response to ligand binding relative to the initial fluorescence of the specified protein alone.

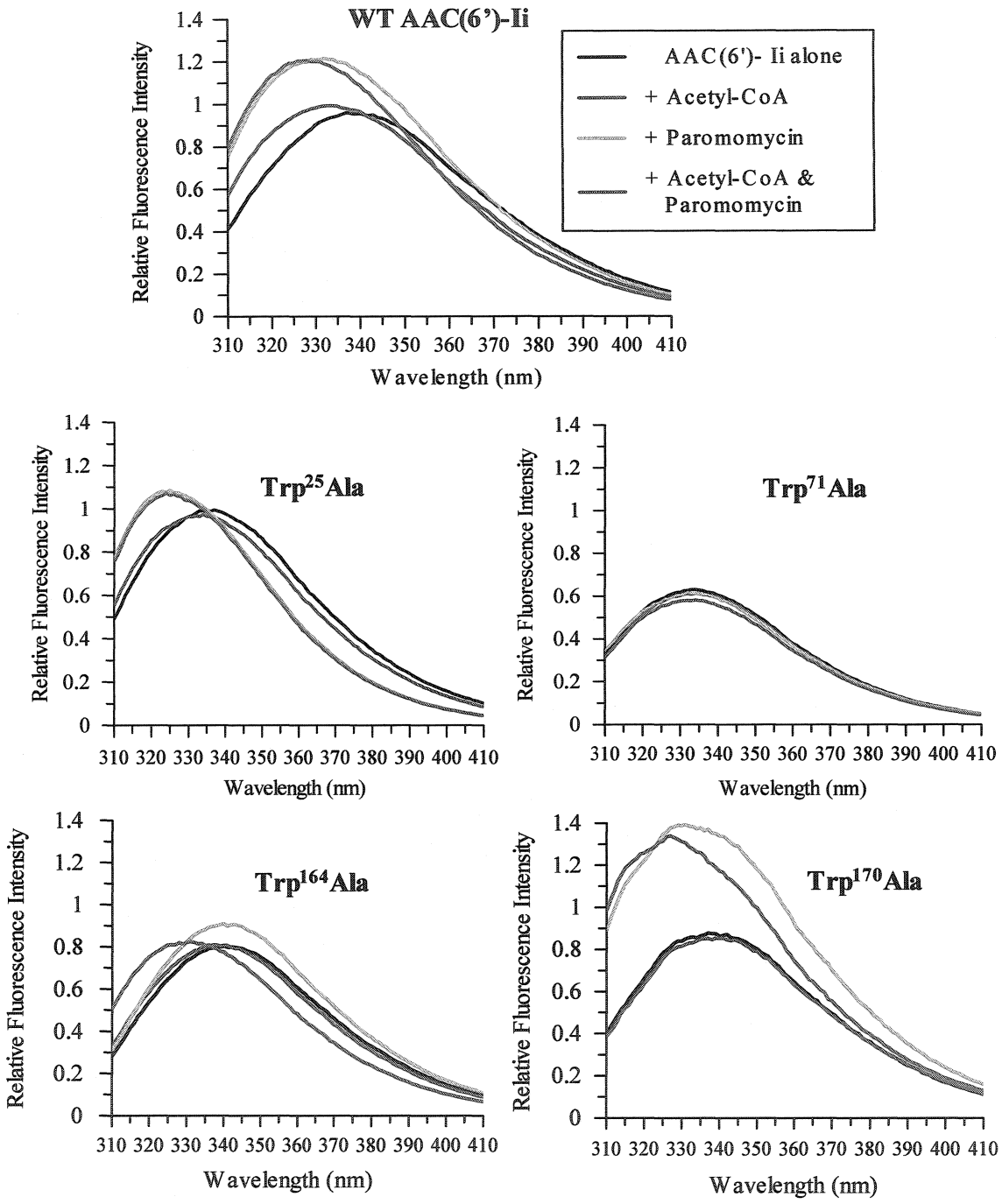

Figure 2.6: Influence of ligands on the fluorescence spectra of wild type AAC(6')-Ii and the Trp site mutants. The spectra for uncomplexed AAC(6')-Ii (—), binary complexes of AAC(6')-Ii·AcCoA (—) and AAC(6')-Ii·paromomycin (—), and the AAC(6')-Ii·AcCoA·paromomycin ternary complex (—) is shown for each protein above. See Table 2.1 for additional details.

Table 2.2: Steady-state kinetic parameters for wild type and mutant AAC(6')-Ii proteins.[a]

Substrate	K_m (μM)	k_{cat} (s^{-1})	K_i (μM)	k_{cat}/K_m ($M^{-1}s^{-1}$)
		Wild Type[b]		
Kanamycin A	19.9 ± 8.8	0.82 ± 0.21	196 ± 153	4.6×10^4
Neomycin	5.3 ± 0.6	0.21 ± 0.00		3.9×10^4
Acetyl-CoA	23.5 ± 3.7	0.40 ± 0.02		1.7×10^4
Paromomycin			1.1 ± 0.2	
		Trp25Ala[c]		
Kanamycin A	6390 ± 610	0.70 ± 0.02		1.1×10^2
Neomycin	287 ± 26	1.61 ± 0.03		5.6×10^3
Acetyl-CoA	196 ± 41	0.05 ± 0.00		2.6×10^2
Paromomycin			174 ± 32	
		Trp71Ala[c]		
Kanamycin A	1160 ± 278	0.33 ± 0.01	3131 ± 1018	2.8×10^2
Neomycin	20.9 ± 3.26	0.04 ± 0.00		2.2×10^3
Acetyl-CoA	661 ± 207	0.16 ± 0.00		2.5×10^2
Paromomycin			2.3 ± 0.7	
		Trp164Ala		
Kanamycin A	280 ± 26	0.08 ± 0.00		2.8×10^2
Neomycin	23.7 ± 3.1	0.13 ± 0.00		5.7×10^3
Acetyl-CoA	20.6 ± 2.3	0.17 ± 0.00		8.4×10^3
Paromomycin			5.3 ± 1.7	
		Trp170Ala		
Kanamycin A	2270 ± 489	0.82 ± 0.00	1730 ± 513	3.6×10^2
Neomycin	34.4 ± 4.6	0.57 ± 0.00		1.7×10^4
Acetyl-CoA	17.9 ± 3.1	0.35 ± 0.00	503 ± 117	1.9×10^4
Paromomycin			7.2 ± 2.2	

[a] Reactions were carried out at 37 °C in 25 mM MES, pH 6.0 and 1 mM EDTA.
[b] Kinetic parameters for wild type AAC(6')-Ii are reproduced from Wright & Ladak (1997).
[c] Kinetic parameters for AGs were determined using subsaturating concentrations of AcCoA (250 μM per reaction).

2.4 Conclusions

AG resistance conferred by the action of modifying enzymes poses intriguing questions regarding protein structure, specificity, and function. In particular, the means by which resistance proteins such as AAC(6')-Ii can recognize, in a catalytically competent fashion, such a broad spectrum of AG substrates is of particular importance from the point of view of the introduction of new AGs into the clinic and the design of specific inhibitors of the enzyme. The results presented here using a variety of biophysical methods cumulatively demonstrate a significant rearrangement in overall structure of AAC(6')-Ii upon interaction with AcCoA in particular and also with AG substrates. The crystal structures of AAC(6')-Ii with bound AcCoA and CoA (Wybenga-Groot *et al.*, 1999; Burk *et al.*, 2003) are consistent with our interpretations, as the two domains of the enzyme appear to "close" around this first substrate, requiring significant protein rearrangement. Since this enzyme also has great tolerance in acyl-acceptor substrates, with the capacity to modify a broad range of AGs as well as proteins and peptides (Wright & Ladak, 1997; Wybenga-Groot *et al.*, 1999), we propose that the AG-induced changes upon formation of the ternary complex play an important role in this regard. The ligand binding strategy of flexibility in the uncomplexed form of AAC(6')-Ii and a more closed structure upon substrate binding likely contributes to the broad substrate specificity observed. The conformational changes described here are therefore a requirement for AAC(6')-Ii catalysis, a point that is further supported by the mechanistic studies described in the following chapter.

2.5 References

Ausubel, F. M., R. Brent, R. E. Kingston, D. D. Moore, J. G. Seidman, J. A. Smith, and K. Struhl. (1994) *Current protocols in molecular biology*. John Wiley & Sons, Inc., New York.

Burk, D. L., N. Ghuman, L. E. Wybenga-Groot, and A. M. Berghuis. (2003) X-ray structure of the AAC(6')-Ii antibiotic resistance enzyme at 1.8 Å resolution; examination of oligomeric arrangements in GNAT superfamily members. *Protein Sci* 12: 426-37.

DeLano, W. L. The pymol molecular graphics system 0.82. DeLano Scientific, San Carlos, CA. USA.

Dutnall, R. N., S. T. Tafrov, R. Sternglanz, and V. Ramakrishnan. (1998) Structure of the histone acetyltransferase Hat1: A paradigm for the GCN5-related N-acetyltransferase superfamily. *Cell* 94: 427-438.

Gerstein, M., A. M. Lesk, and C. Chothia. (1994) Structural mechanisms for domain movements in proteins. *Biochemistry* 33: 6739-49.

Hammes, G. G. (2002) Multiple conformational changes in enzyme catalysis. *Biochemistry* 41: 8221-8.

Hickman, A. B., D. C. Klein, and F. Dyda. (1999a) Melatonin biosynthesis: The structure of serotonin N-acetyltransferase at 2.5 Å resolution suggests a catalytic mechanism. *Mol Cell* 3: 23-32.

Hickman, A. B., M. A. Namboodiri, D. C. Klein, and F. Dyda. (1999b) The structural basis of ordered substrate binding by serotonin N- acetyltransferase: Enzyme complex at 1.8 Å resolution with a bisubstrate analog. *Cell* 97: 361-369.

Kay, L.E., P. Keifer, and T. Saarinen. (1992) Pure absorption gradient enhanced heteronuclear single quantum correlation spectroscopy with improved sensitivity. *J Am Chem Soc* 114: 10663-10665.

Koshland, D. E. Jr. (1958) Application of the theory of enzyme specificity to protein synthesis. *Proc Natl Acad Sci U S A* 44: 98-104.

Rojas, J. R., R. C. Trievel, J. Zhou, Y. Mo, X. Li, S. L. Berger, C. D. Allis, and R. Marmorstein. (1999) Structure of tetrahymena GCN5 bound to coenzyme A and a histone H3 peptide. *Nature* 401: 93-98.

Williams, J. W. & D. B. Northrop. (1978) Kinetic mechanisms of gentamicin acetyltransferase I. Antibiotic- dependent shift from rapid to nonrapid equilibrium random mechanisms. *J Biol Chem* 253: 5902-5907.

Wright, G. D. & P. Ladak. (1997) Overexpression and characterization of the chromosomal aminoglycoside 6'-*N*-acetyltransferase from *Enterococcus faecium*. *Antimicrob Agents Chemother* 41: 956-960.

Wybenga-Groot, L. E., K. Draker, G. D. Wright, and A. M. Berghuis. (1999) Crystal structure of an aminoglycoside 6'-*N*-acetyltransferase: Defining the GCN5-related *N*-acetyltransferase superfamily fold. *Structure Fold Des* 7: 497-507.

Xu, Q. Y. & J. E. Shively. (1988) Microsequence analysis of peptides and proteins. Viii. Improved electroblotting of proteins onto membranes and derivatized glass-fiber sheets. *Anal Biochem* 170: 19-30.

Yon, J. M., D. Perahia, and C. Ghelis. (1998) Conformational dynamics and enzyme activity. *Biochimie* 80: 33-42.

Chapter 3

Kinetic Mechanism of AAC(6')-Ii

Published as

Draker, K. A., D. B. Northrop, and G. D. Wright. (2003) Kinetic Mechanism of the GCN5-Related Chromosomal Aminoglycoside Acetyltransferase AAC(6')-Ii from *Enterococcus faecium*: Evidence of Dimer Subunit Cooperativity. *Biochemistry.* 42: 6565-6574.

3.0 Preface

This chapter describes numerous studies that were performed to decipher the kinetic mechanism of AAC(6')-Ii. As this research has recently been published in the journal *Biochemistry* (Draker *et al.*, 2003), it is presented here in a sandwich style format. Only changes to the layout of the document have been made in order to conform to the overall format of the thesis. I performed all of the experiments described in the following sections and was also responsible for the writing of the original manuscript and any revisions requested by reviewers prior to publication.

As detailed here, AAC(6')-Ii follows an ordered bi-bi ternary complex mechanism, with the rate-contributing steps in catalysis identified as diffusion-controlled events. Additional studies helped to characterize the binding of AGs by this enzyme as well as the subunit cooperativity observed for the protein dimer. Although some background information included in this chapter overlaps with that covered in the introduction (chapter 1), the document as a whole conveys the relevance of this work in further characterizing this enzyme, both as a resistance determinant and as a member of the GNAT superfamily.

We sincerely thank Dr. Dexter Northrop, who made a significant intellectual contribution to this work by suggesting additional experiments to strengthen our analysis and in addressing reviewers' comments during the revision process. He therefore appears as second author on the journal article describing this research. We also acknowledge Dr. Kalinka Koteva for her technical assistance in the synthesis of acetylated AG and Dr. Raquel Epand for useful discussions concerning isothermal titration calorimetry.

3.1 Summary

The AG 6'-*N*-acetyltransferase AAC(6')-Ii from *Enterococcus faecium* is an important microbial resistance determinant and a member of the GCN5-related *N*-acetyltransferase (GNAT) superfamily. We report here the further characterization of this enzyme in terms of the kinetic mechanism of acetyl transfer and identification of rate-contributing step(s) in catalysis, as well as investigations into the binding of both AcCoA and AG substrates to the AAC(6')-Ii dimer. Product and dead-end inhibition studies revealed that AAC(6')-Ii follows an ordered bi-bi ternary complex mechanism with AcCoA binding first followed by antibiotic. Solvent viscosity studies demonstrated that AG binding and product release govern the rate of acetyl transfer, as evidenced by changes in both the k_{cat}/K_b for AG and k_{cat}, respectively, with increasing solvent viscosity. Solvent isotope effects were consistent with our viscosity studies that diffusion-controlled processes and not the chemical step were rate-limiting in drug modification. The patterns of partial and mixed inhibition observed during our mechanistic studies were followed up by investigating the possibility of subunit cooperativity in the AAC(6')-Ii dimer. Through the use of Trp164Ala, an active mutant which exists as a monomer in solution, the partial nature of the competitive inhibition observed in wild type dead-end inhibition studies was alleviated. Isothermal titration calorimetry studies also indicated two nonequivalent antibiotic binding sites for the AAC(6')-Ii dimer but only one binding site for the Trp164Ala mutant. Taken together, these results demonstrate subunit cooperativity in the AAC(6')-Ii dimer, with possible relevance to other oligomeric members of the GNAT superfamily.

3.2 Introduction

Aminocyclitol-AG antibiotics are a class of bactericidal drugs used in the treatment of infections caused by various Gram positive and Gram negative bacteria. Clinically relevant resistance to the AGs is mediated by the action of enzymes that modify the drugs and decrease their affinity for the 30S ribosomal subunit target (Davies & Wright, 1997; Llano-Sotelo *et al.*, 2002). AG-inactivating enzymes include the phosphotransferase (APH),[1] nucleotidylyltransferase (ANT), and acetyltransferase (AAC) proteins, which are responsible for *O*-phosphorylation, *O*-adenylation, and *N*- or *O*-acetylation of the drugs, respectively (reviewed in Miller *et al.*, 1997 and Wright, 1999).

N-Acetylation at the 6' position of AGs is one of the most prevalent forms of modification in Gram negative bacteria (Miller *et al.*, 1997). To date, only two AAC(6') enzymes from Gram positive pathogens have been identified and characterized: the bifunctional AAC(6')-APH(2") protein from enterococci and staphylococci (Daigle *et al.*, 1999) and AAC(6')-Ii from *E. faecium* (Wright & Ladak, 1997). The presence of these resistance determinants in enterococci complicates the use of β-lactam/AG combination therapy in clinical treatment (Moellering *et al.*, 1973; Moellering *et al.*, 1979; Wennersten & Moellering, 1980; Costa *et al.*, 1993) and thus increases the reliance on other antimicrobials such as glycopeptides. As such, these proteins are worthy of study to both better understand the resistance they confer and to apply this knowledge to the identification and/or design of enzyme inhibitors. The focus of this report is the further kinetic characterization of the AG 6'-*N*-acetyltransferase, AAC(6')-Ii.

The *aac(6')-Ii* gene from *E. faecium* is chromosomal in origin and has been shown to confer low-level AG resistance *in vivo* (Costa *et al.*, 1993). Initial characterization of purified AAC(6)-Ii by Wright and Ladak (Wright & Ladak, 1997) revealed that the protein is a homodimer in solution with a broad substrate specificity for several AGs of the 4,5- and 4,6-disubstituted deoxystreptamine class (see Figure 3.1) and specificity constants (k_{cat}/K_m) on the order of 10^4 $M^{-1}s^{-1}$.

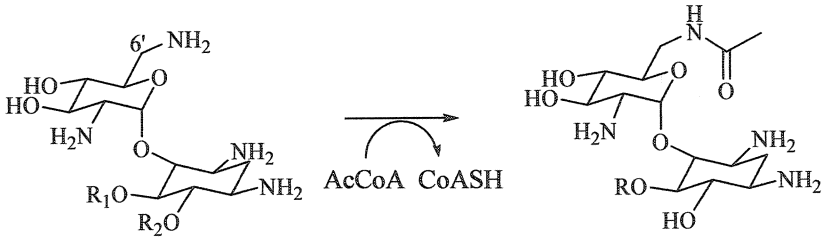

Neamine, R_1 and R_2 = H

Ribostamycin, R_1 = 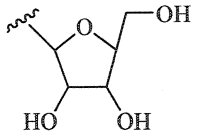 R_2 = H

Paromomycin, R_1 = 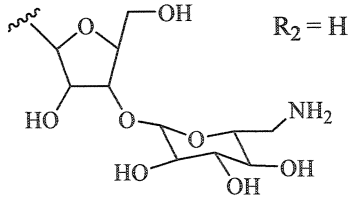 R_2 = H and 6'-NH_2 is replaced by 6'-OH

Kanamycin A, R_1= H R_2 = 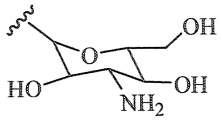

Figure 3.1: Regiospecific acetyl transfer reaction catalyzed by AAC(6')-Ii and structures of AGs used in this study.

The crystal structure of the AAC(6')-Ii monomer in complex with AcCoA was solved by Berghuis and co-workers in 1999 (Wybenga-Groot *et al.*, 1999), who identified it as a member of the GNAT superfamily (Neuwald & Landsman, 1997). This family of diverse enzymes is defined by several conserved sequence motifs involved in the binding of the common acyl-CoA substrate. Several recent crystal structures of various GNAT enzymes such as transcription factor/histone acetyltransferases (Dutnall *et al.*, 1998; Angus-Hill *et al.*, 1999; Clements *et al.*, 1999; Rojas *et al.*, 1999; Trievel *et al.*, 1999), arylamine/arylalkylamine acetyltransferases (Hickman *et al.*, 1999a; Hickman *et al.*, 1999b; Sinclair *et al.*, 2000; Obsil *et al.*, 2001), and *N*-myristoyltransferases (Bhatnagar *et al.*, 1999; Hickman *et al.*, 1999a), as well as sugar (Peneff *et al.*, 2001) and AG acetyltransferases (Wolf *et al.*, 1998; Wybenga-Groot *et al.*, 1999; Vetting *et al.*, 2002), reveal the striking structural homology shared among the superfamily members (reviewed in Dyda *et al.*, 2000). In addition to structural homology, AAC(6')-Ii has also been shown to be a functional homologue of histone acetyltransferases, revealed by its capacity to modify histones as well as other small basic proteins (Wybenga-Groot *et al.*, 1999).

Several detailed kinetic analyses have been done to better characterize the mechanism of group transfer by many GNAT superfamily members (Rudnick *et al.*, 1991; De Angelis *et al.*, 1998; Lau *et al.*, 2000; Tanner *et al.*, 2000), as well as a limited number of studies on bacterial AG acetyltransferases (Radika & Northrop, 1984c, 1984b; Magnet *et al.*, 2001; Hegde *et al.*, 2002). Our level of understanding of the molecular mechanism of AAC(6')-Ii, however, is superficial, and we therefore report here a series

of mechanistic studies on this enzyme to determine the kinetic mechanism of catalysis and to identify the rate-determining steps of acetyl transfer. Additional studies with a monomeric form of the enzyme and isothermal titration calorimetry (ITC) experiments further defined the mechanism of acetyl transfer by AAC(6')-Ii and provide insight into the physiological homodimeric form of AAC(6')-Ii. Our results allow us to compare the mechanism of acetylation by this resistance determinant with other bacterial AACs as well as with other members of the GNAT superfamily.

3.3 Materials and Methods

3.3.1 General

AGs, desulfo-CoA, and 4,4-dithiodipyridine (DTDP) were from Sigma-Aldrich Chemical Co. (St. Louis, MO). The *aac(6')-Ii* gene was subcloned from the pPLaac vector (Wright & Ladak, 1997) into pET22b(+) (Novagen, Madison, WI) using the flanking *Nde*I and *Hin*dIII restriction sites. AAC(6')Ii was subsequently overexpressed in *E. coli* BL21(DE3) cells and purified to homogeneity following the procedures outlined previously (Wright & Ladak, 1997).

3.3.2 AAC(6')-Ii Kinetic Assays

Protein acetyltransferase activity was monitored with a continuous assay by the *in situ* titration of coenzyme A product with DTDP at 324 nm, as previously described (Williams & Northrop, 1978; Wright & Ladak, 1997).

3.3.3 Initial Velocity Experiments

Initial rate data for AAC(6')-Ii acetylation of ribostamycin were collected at various concentrations of both AcCoA and AG. The data were fit by nonlinear least-squares fit to global eq 1 using Grafit software (Leatherbarrow, 2000). The equation describes a sequential, ternary complex mechanism, where [A] and [B] are the concentrations of substrates, K_a and K_b are the respective Michaelis-Menten constants, and K_{ia} is the dissociation constant for A;

$$v = V_{max}[A][B]/(K_{ia}K_b + K_b[A] + K_a[B] + [A][B]) \quad (1)$$

3.3.4 AAC(6')-Ii Inhibition Studies

AAC(6')-Ii acetyltransferase activity was monitored in the presence of the dead-end inhibitors desulfo-CoA and paromomycin or the product inhibitor 6'-N-acetylated ribostamycin. Individual rate data generated at various concentrations of inhibitor were first fit to eq 2 describing Michaelis-Menten kinetics using Grafit 4.0 software (Leatherbarrow, 2000):

$$v = V_{max}[S]/(K_m + [S]) \quad (2)$$

Reciprocal plots of each data set were then generated and are presented in Figures 3.3, 3.4, and 3.5. Kinetic constants included in Table I are derived from the fit of the data to global equations of best fit describing either partially competitive inhibition (eq 3), uncompetitive inhibition (eq 4), or noncompetitive/mixed inhibition (eq 5), by non-linear least squares using the Enzyme Kinetics Module of Sigma Plot (Brannan *et al.*, 2000) ;

$$v = V_{max}[S]/(K_m(1 + I/K_{ii})/(1 + I/K_{is}) + [S]) \quad (3)$$

$$v = V_{max}[S]/(K_m + [S](1 + I/K_{ii})) \quad (4)$$

$$v = V_{max}[S]/(K_m(1 + I/K_{is}) + [S](1 + I/K_{ii})) \quad (5)$$

3.3.5 Alternative Substrate Method

To verify the kinetic mechanism of AAC(6')-Ii determined by our inhibitor studies, alternative substrate studies described by Radika & Northrop (1984a) were performed. Briefly, initial rate data were collected at varying concentrations of AcCoA (5-250 μM) using saturating concentrations (>10x K_m) of neomycin, ribostamycin, butirosin, neamine, or amikacin. Data were fit to eq 2 and reciprocal plots of $1/v$ vs 1/[AcCoA] for each alternate AG used in the diagnostic were generated.

3.3.6 Enzymatic Synthesis of 6'-N-Acetylated Ribostamycin

6'-*N*-Acetylated ribostamycin (AcRibo) was enzymatically synthesized by AAC(6')-Ii using AcCoA and ribostamycin as AG substrate. Synthesis of AcRibo was conducted using a 1:5 molar ratio of ribostamycin to AcCoA and ca. 2 μmoles of AAC(6')-Ii enzyme. Reactions were carried out in water and incubated for 1 h at room temperature. AcRibo was separated from other components by applying the reaction mixture to a 2 mL column of Dowex analytical grade cation-exchanger resin AG 50W (BioRad) equilibrated with H_20, followed by elution at 2 M NH_2OH using a 1 M stepwise gradient from 1 to 5 M NH_2OH. The progress of AcRibo formation and separation from other reaction components was monitored by thin layer chromatography (TLC), using 250 μm silica G plates and a 5:2 ratio of MeOH:NH_4OH as the solvent system. Distinct spots for AcRibo (R_f = 0.30) and ribostamycin controls (R_f = 0.12) were visualized by ninhydrin

spray and CoA product (R_f = 0.53) was visualized under UV light. The identity of the isolated product as 6'-N-acetylated ribostamycin was confirmed by electrospray mass spectrometry as well as proton and ^{13}C NMR.

3.3.7 Viscosity Studies

AAC(6')-Ii kinetic assays were performed with the macroviscosogen PEG 8000 (6.7%) and the microviscosogen sucrose (0-30%). The viscosity of solutions was determined in quadruplicate at 22 °C using an Ostwald viscometer, relative to the standard AAC(6')-Ii kinetics buffer consisting of 25 mM MES; pH 6.0, and 1 mM EDTA. K_i determinations for the competitive inhibitor paromomycin were made in the presence of 30% microviscosogen to ensure that the reagents were not binding to the enzyme active site. Enzyme assays were performed in duplicate in a final volume of 800 µL. Initial rate data were fit by nonlinear least-squares regression to eq 2 using Grafit 4.0 software (Leatherbarrow, 2000). The values reported in Table 3.2 are the slopes of plots from either k_{cat}^0/k_{cat} or $((k_{cat}/K_m^0)/k_{cat}/K_m)$ versus the relative viscosity of the solution.

3.3.8 Trp164Ala Monomer Mutant

The replacement of tryptophan at position 164 with alanine was performed using the QuikChange site-directed mutagenesis protocol (Stratagene) and the mutagenic oligonucleotide primers 5' CTCAATACGGTATCACAGGTGCGGAATTGCATCC 3' and 5' GGATGCAATTCCGCACCTGTGATACCGTATTGAG 3'. The presence of the desired mutation in the *aac(6')-Ii* gene as well as the absence of adventitious mutations was confirmed by complete gene sequencing at the Central Facility of the Institute for

Molecular Biology and Biotechnology, McMaster University. Subsequent overexpression and purification of the Trp164Ala mutant, as well as the determination of kinetics of acetyltransfer to various AGs for this mutant, were the same as those described for the wild type enzyme (Wright & Ladak, 1997).

Analytical gel filtration experiments on Trp164Ala were used to confirm initial evidence that this mutant was a monomer in solution. Trp164Ala at ~ 2.10 mg/mL was analyzed on an analytical Superdex 200 HR 10/30 column (BioRad). A molecular mass calibration curve was generated using α-lactalbumin (14.2 kDa), carbonic anhydrase (29 kDa), chicken egg albumin (45 kDa), and BSA (66 kDa monomer, 132 kDa dimer) as well as Blue Dextran to determine the column void volume. The molecular masses of wild type AAC(6')-Ii and the Trp164Ala mutant were estimated using the formula $K_{av} = (V_e - V_0)/(V_t - V_0)$, where V_e is the protein elution volume from the column, V_t is the total column volume, and V_0 is the column void volume. From these analytical gel filtration experiments, the estimated molecular mass of wild type AAC(6')-Ii was ~ 45 900 Da and Trp164Ala ~ 22 900 Da, confirming the monomeric form of this mutant in solution.

3.3.9 Isothermal Titration Calorimetry Experiments

All ITC measurements were made using a MicroCal VP-ITC isothermal titration calorimeter from MicroCal, Inc. (Northampton, MA). A buffer solution of 25 mM HEPES, pH 7.5 and 2 mM EDTA was used to dialyze purified AAC(6')-Ii wild type or the Trp164Ala enzyme and the resulting dialyzate used to make AG and/or CoA solutions. In general, a 100 μM solution of AAC(6')-Ii in 25 mM HEPES, pH 7.5, and 2

mM EDTA was added to the sample cell (ca. 1.4 mL) and a 0.5-2.0 mM solution of neamine, kanamycin A, or ribostamycin as titrant was loaded into the injection syringe. For each titration experiment, a 60 s delay at the start was followed by 29 injections of 10 μL of the titrant solution, spaced apart by 240 s. The sample cell was stirred at 300 rpm throughout and maintained at a temperature of 37 °C. Additional experiments were performed as described above in the presence of 2 mM coenzyme A in both the sample cell and injection syringe. Several control titrations were performed, and included baseline titrations of buffer into enzyme, titrant solutions into buffer, and CoA titrated into an enzyme and CoA solution. Titration data were analyzed using Origin 5.0 software supplied by Microcal. Briefly, data sets were corrected for baseline heats of dilutions from blank or control runs as appropriate. Corrected data were then fit to a theoretical titration curve describing two independent sets of binding sites for titrant. Calculated K_a values with the smallest standard error gave an acceptable c value between 1 and 1000 (Wiseman *et al.*, 1989). Free energies of association (ΔG) were calculated using the equation:

$$\Delta G = - RT \ln K_a \qquad (6)$$

ITC experiments performed with the Trp164Ala monomer were as described for the wild type enzyme and the data best fit to a theoretical titration curve describing one binding site for the AG titrant.

3.4 Results

3.4.1 Initial Velocity Studies

Initial velocity patterns obtained when the ribostamycin concentration was varied at various fixed concentrations of AcCoA displayed intersecting lines in the double reciprocal plot (Figure 3.2), indicative of a ternary complex, sequential mechanism.

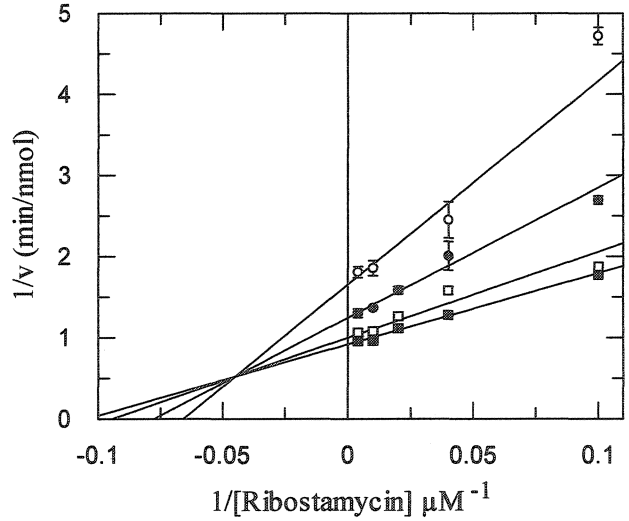

Figure 3.2: AAC(6')-Ii initial velocity patterns. Double reciprocal plot of initial rate data at varying ribostamycin concentrations and fixed concentrations of AcCoA at 5 μM (○), 10 μM (●), 25 μM (□), and 50 μM (■). The pattern of intersecting lines is indicative of a sequential kinetic mechanism. The best fit of the data to eq 1 gave kinetic constants of K_a = 8.3 ± 1.4 μM, K_b = 4.9 + 0.58 μM, and K_{ia} = 22 ± 6.3 μM.

3.4.2 Inhibition Studies

To gain further insight into the mechanism of AAC(6')-Ii acetyl transfer, desulfo-CoA and paromomycin were used as dead-end inhibitors to investigate the order of substrate binding and product release by the enzyme. Desulfo-CoA was chosen as the dead-end inhibitor as it does not interfere with the thiol titration assay, and the AG

paromomycin, which lacks a 6' amino group, has already been shown to be a competitive inhibitor of AAC(6')-Ii activity (Wright & Ladak, 1997).

AAC(6')-Ii acetyl transfer kinetics in the presence of increasing concentrations of desulfo-CoA resulted in partial competitive inhibition of enzyme activity when AcCoA was the varied substrate, with K_{is} = 6.6 μM and K_{ii} = 24 μM for the dead-end inhibitor (Figure 3.3 and Table 3.1). Noncompetitive/mixed-type inhibition was observed when the AG ribostamycin was the variable substrate in desulfo-CoA inhibition studies. In the presence of a fixed subsaturating concentration of AcCoA (50 μM), K_{is} = 81 μM and K_{ii} = 99 μM (Table 3.1).

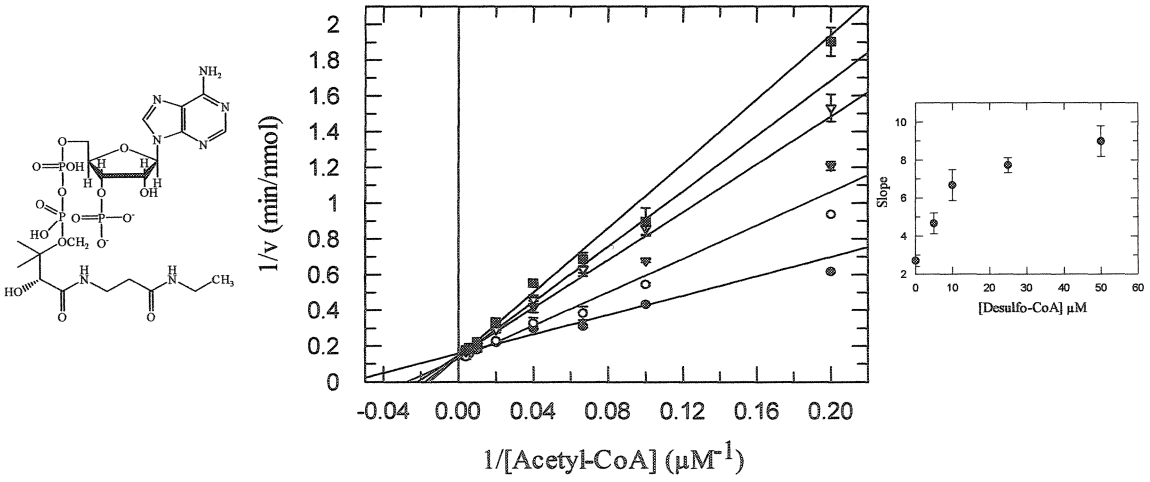

Figure 3.3: Partial competitive inhibition of AAC(6')-Ii activity through the use of desulfo-CoA as a dead-end inhibitor. The structure of desulfo-CoA is shown at left. Shown is a plot of 1/*v* versus 1/[AcCoA] at fixed concentrations of 0 μM (●), 5 μM (○), 10 μM (▼), 25 μM (▽), and 50 μM (■) desulfo-CoA. Ribostamycin was present in the assays at a saturating concentration of 200 μM. Inset: Hyperbolic-shaped replot for AcCoA versus [desulfo-CoA], indicating partial inhibition.

We used the 6'-hydroxy AG paromomycin as a dead-end inhibitor of AAC(6')-Ii activity to further elucidate the kinetic mechanism. From the double reciprocal plot of $1/v$ versus 1/[AcCoA] shown in Figure 3.4, paromomycin exhibits uncompetitive inhibition of AAC(6')-Ii activity versus AcCoA (Table 3.1). This pattern of inhibition indicates that paromomycin can bind to either the AAC(6')-Ii·AcCoA binary complex or the AAC(6')-Ii·CoA product complex, with paromomycin binding to the latter preventing the release of CoA and suggesting partial rate limitation by the dissociation of CoA from the enzyme. Our results are therefore consistent with ordered substrate addition and product release.

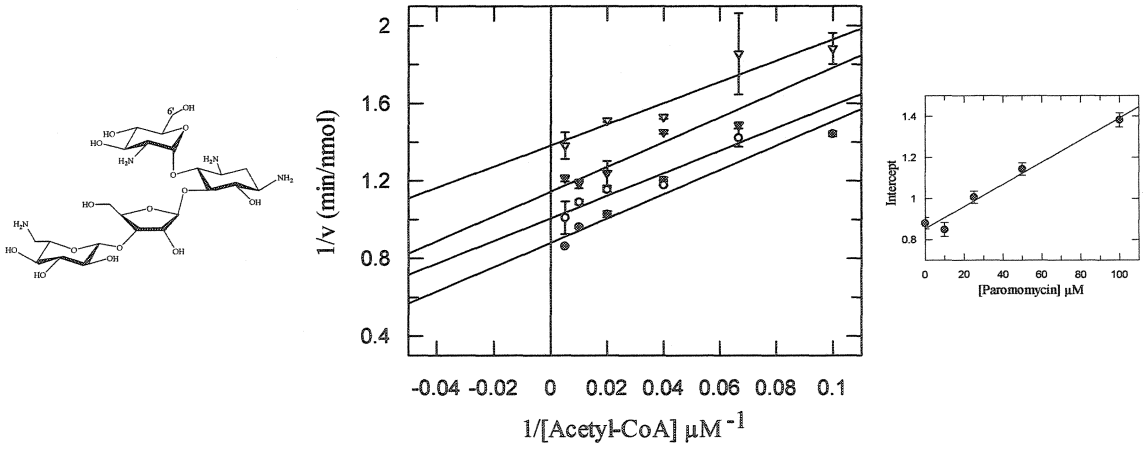

Figure 3.4: Uncompetitive inhibition of AAC(6')-Ii activity through the use of paromomycin as a dead-end inhibitor. The structure of paromomycin is shown at left. Plot of $1/v$ versus 1/[AcCoA] at fixed concentrations of 0 μM (●), 25 μM (○), 50 μM (▼), and 100 μM (▽) paromomycin. Ribostamycin was present at a saturating concentration of 100 μM. Inset: Intercept replot for AcCoA versus [paromomycin].

6'-*N*-Acetylated ribostamycin (AcRibo) used in product inhibition studies was found to be a noncompetitive/mixed-type inhibitor versus AG substrate with K_{is} and K_{ii} values of 46 and 363 μM, respectively (Figure 3.5 and Table 3.1), indicative of AcRibo binding to the AAC(6')-Ii·CoA complex. In addition, AcRibo did not behave as an inhibitor versus AcCoA in the presence of either fixed subsaturating (20 μM) or fixed saturating (100 μM) concentrations of AG. This lack of inhibition was evident even when AcRibo concentrations exceeded the fixed concentration of ribostamycin substrate by up to 50-fold.

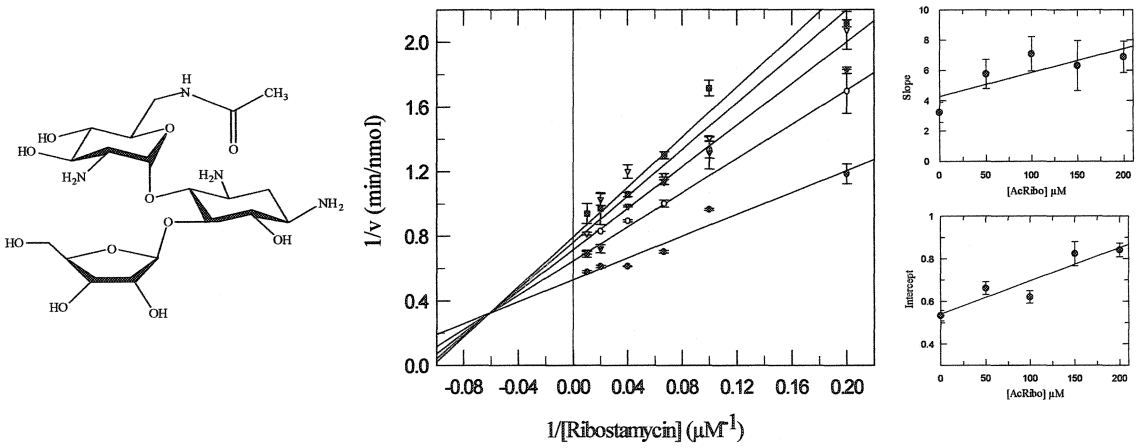

Figure 3.5: Mixed inhibition of AAC(6')-Ii through the use of 6' *N*-acetylated ribostamycin (AcRibo) as a product inhibitor. The structure of AcRibo is shown at left. Double-reciprocal plot of initial rate data at varying ribostamycin concentrations and fixed concentrations of AcRibo at 0 μM (●), 50μM (○), 100 μM (▼), 150 μM (▽) and 200μM (■). AcCoA was present at a saturating concentration of 100 μM. Inset: Intercept and slope replots for ribostamycin versus [AcRibo].

We hypothesize that AcRibo could behave as a noncompetitive inhibitor of AcCoA at significantly higher concentrations that we could not achieve experimentally, which would be consistent with our dead-end inhibition. Our AcRibo inhibition results as a whole, however, supports the kinetic mechanism and are consistent with the release of acetylated AG first, followed by the slower release of the CoA product.

Taken together, the results of product and dead-end inhibition studies (summarized in Table 3.1) indicate that AAC(6')-Ii follows an ordered bi-bi reaction mechanism, as outlined in Scheme 1.

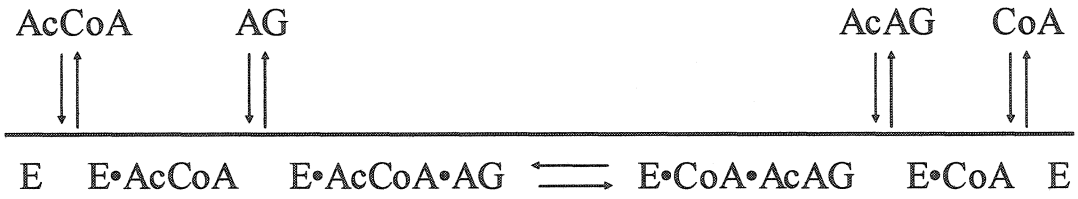

Scheme 1: AAC(6')-Ii follows an ordered bi-bi kinetic mechanism. AcCoA, acetyl-CoA; AG, aminoglycoside substrate; AcAG, acetylated aminoglycoside product.

Table 3.1: Summary of AAC(6')-Ii Dead-End and Product Inhibition Studies.

Inhibitor	Varied Substrate	Fixed Substrate	Pattern of Inhibition	K_{is} (μM) [a]	K_{ii} (μM) [b]
desulfo-CoA	AcCoA	ribostamycin (200 μM)	partially competitive	6.58 ± 2.18	24.3 ± 8.9
desulfo-CoA	ribostamycin	AcCoA (50 μM)	noncompetitive/mixed	81.3 ± 42.1	99.0 ± 34
paromomycin	AcCoA	ribostamycin (100 μM)	uncompetitive	------	180 ± 13
AcRibo	ribostamycin	AcCoA (100 μM)	noncompetitive/mixed	45.9 ± 14.1	363 ± 190
AcRibo	AcCoA	ribostamycin (20 μM)	no inhibition [c]	------	------

[a] K_{is}, $K_{i\,(slope)} = \alpha K_i$, where α is the factor by which K_m changes when I is bound to the ES complex.
[b] K_{ii}, $K_{i\,(intercept)} = K_i$.
[c] See text for details.

3.4.3 Alternative Substrate Diagnostic

Parallel patterns were obtained from double reciprocal plots of $1/v$ versus 1/[AcCoA] at saturating concentrations of numerous alternative AG substrates (Figure 3.6). Thus, k_{cat}/K_a values determined for AcCoA are independent of the AG substrate, consistent with an ordered bi-bi mechanism (Radika & Northrop, 1984a) and our product and dead-end inhibition results.

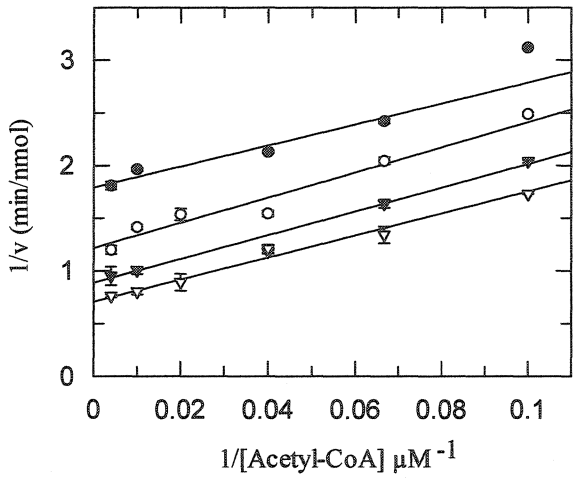

Figure 3.6: Alternate substrate diagnostic with AcCoA as the variable substrate and fixed concentrations of AG. Shown is a double reciprocal plot of $1/v$ versus 1/[AcCoA] at fixed, saturating concentrations of neomycin (●), isepamicin (○), ribostamycin (▼), and butirosin (▽). Parallel lines are diagnostic of an ordered bi-bi kinetic mechanism.

3.4.4 Solvent Viscosity Effects

We also explored the rate-determining step(s) in AAC(6')-Ii acetyl transfer using several approaches. Solvent viscosity effects on enzyme activity were first investigated to assess whether diffusion-controlled events such as product release may be rate-limiting. Using the microviscosogen sucrose, it was shown that there were significant solvent

viscosity effects on AAC(6')-Ii activity (Table 3.2). As a control, the macroviscosogen PEG 8000 was shown to have no effect on enzyme activity, revealing that the rate changes observed in the presence of sucrose are effects on diffusion-controlled phenomenon and not the result of changes in global viscosity (Blacklow *et al.*, 1988; McKay & Wright, 1996). In general, solvent viscosity effects describing k_{cat} changes ranged from 0.52 to 0.79 (Table 3.2), consistent with the suggestion that product release contributes significantly to the rate-determining step(s). In turn, the productive formation of the AAC·AcCoA complex does not appear to be rate-limiting at all since virtually no viscosity effect was observed on k_{cat}/K_a values for AcCoA (Table 3.2). The large k_{cat}/K_b changes observed when AG is the varied substrate, however, do suggest that the productive formation of an enzyme complex with AG may contribute to the rate-determining step(s). These results as a whole therefore indicate that diffusion-controlled events and not chemistry contribute to the rate-limiting step(s) in AAC(6')-Ii acetyl transfer.

Table 3.2: Solvent viscosity effects on AAC(6')-Ii activity

Viscosogen	Varied substrate	Fixed Substrate	$(k_{cat}^{0}/k_{cat})^{\eta\,a}$	$((k_{cat}/K_m^{0})/k_{cat}/K_m)^{\eta}$
PEG 8000	AcCoA	Kan A (200 μM)	0.02	-0.01
	Kanamycin A	AcCoA (100 μM)	0.00	-0.03
Sucrose	AcCoA	Ribo (100 μM)	0.79	-0.01
	Kanamycin A	AcCoA (100 μM)	0.42	1.09
	Ribostamycin	AcCoA (100 μM)	0.52	0.72

[a]The values reported are the slopes of plots for k_{cat}^{o}/k_{cat} or $[(k_{cat}/K_m^{o})/(k_{cat}/K_m)]$ versus the relative viscosity of the solution.

3.4.5 Solvent Isotope Effects

To confirm our solvent viscosity effects that chemistry is not rate-limiting in AAC(6')-Ii acetyl transfer, we performed D_2O solvent isotope experiments to investigate the dependence of k_{cat} on proton abstraction at the 6'-amino group of an AG substrate. Kinetic assays were performed in either 100% H_2O or ~ 94% D_2O and a solvent isotope effect ($k_{cat}^{H/D}$ or $k_{cat}/K_m^{H/D}$) was determined. No significant solvent isotope effect was observed for ribostamycin or kanamycin, with $k_{cat}^{H/D}$ ranging from 1.1 to 1.3 and $k_{cat}/K_m^{H/D}$ from 1.1 to 1.4. In contrast, Benke-Marti (Benke-Marti, 1987) observed a solvent isotope effect on k_{cat}/K_m of 10 for the acetylation of tobramycin by AAC(3)-I, an enzyme that also follows an ordered bi-bi kinetic mechanism. The small effect that was observed for AAC(6')-Ii may be attributed to the higher relative viscosity of D_2O compared to H_2O (Schowen, 1978), supporting our argument for a diffusion-controlled process limiting AAC(6')-Ii reaction rates.

3.4.6 Studies on Monomeric Trp164Ala

Mutation of Trp164 to Ala resulted in an active enzyme with the characteristics of a monomer rather than a dimer, which is the native state of the enzyme. Trp164 is located in the C-terminal region of AAC(6')-Ii and is relatively solvent exposed in the published crystal structure (Wybenga-Groot *et al.*, 1999). Given that mutation of this residue blocks homodimer formation, we propose that this residue is involved in critical monomer-monomer interactions that are essential for dimer formation.

3.4.7 Activity of Trp164Ala

Steady-state kinetic analysis revealed that the Trp164Ala monomer retained the capacity to modify various AGs, including the minimal substrate neamine (Wright & Ladak, 1997) as well as both the 4,5- and 4,6- classes of antibiotics acetylated by the wild type enzyme (Table 3.3). Specificity constants ranged from ~ 10^2 to 10^3 $M^{-1}s^{-1}$ for this mutant due to both K_m and k_{cat} changes, compared to k_{cat}/K_m values on the order of 10^4 $M^{-1}s^{-1}$ for wild type AAC(6')-Ii (Table 3.3).

Table 3.3: Steady-state kinetic parameters for wild type and Trp164Ala proteins [a]

		Wild Type [b]	
Substrate	K_m (μM)	k_{cat} (s^{-1})	k_{cat}/K_m ($M^{-1}s^{-1}$)
Neamine	5.8 ± 1.0	0.42 ± 0.02	7.2 x 10^4
Kanamycin A	19.9 ± 8.8	0.82 ± 0.21	4.6 x 10^4
Rbostamycin	9.1 ± 2.0	0.34 ± 0.22	3.7 x 10^4
Neomycin C	5.3 ± 0.6	0.20 ± 0.00	3.9 x 10^4
AcCoA	23.5 ± 3.7	0.40 ± 0.02	1.7 x 10^4
		Trp164Ala	
Substrate	K_m (μM)	k_{cat} (s^{-1})	k_{cat}/K_m ($M^{-1}s^{-1}$)
Neamine	206 ± 32	0.05 ± 0.00	2.3 x 10^2
Kanamycin A	280 ± 26	0.08 ± 0.00	2.8 x 10^2
Ribostamycin	217 ± 22	0.05 ± 0.00	2.1 x 10^2
Neomycin C	23.7 ± 3.1	0.14 ± 0.00	5.7 x 10^3
AcCoA	20.6 ± 2.3	0.17 ± 0.00	8.4 x 10^3

[a] Reactions were carried out at 37 °C in 25 mM MES, pH 6.0 and 1 mM EDTA.
[b] Kinetic parameters for wild type AAC(6')-Ii are reproduced from Wright & Ladak (1997).

Our kinetic results suggest that although the Trp164Ala mutant is somewhat impaired in the recognition and acetylation of AGs, its catalytic ability nonetheless indicates that there is one functional active site per monomer subunit, as initially evidenced by the well-defined AcCoA binding pocket in the AAC(6')-Ii binary complex structure (Wybenga-Groot *et al.*, 1999). We therefore proceeded to dead-end inhibition studies with Trp164Ala to investigate whether the same partial inhibition observed for the AAC(6')Ii homodimer would be evident for this monomeric mutant.

3.4.8 Desulfo-CoA Inhibition Studies with Trp164Ala

Desulfo-CoA was found to be a full competitive inhibitor of the AAC(6')-Ii reaction versus AcCoA, in contrast to the partial competitive inhibition observed for the wild type homodimer (Figure 3.3, Table 3.1). As can be seen from the slope replot comparisons in Figure 3.7, the hyberbolic nature of the wild type replot is completely alleviated when monomeric Trp164Ala is used in the inhibition studies. A K_{is} value of 39 ± 11 μM for desulfo-CoA inhibition of the Trp164Ala mutant was determined, revealing an ca. 6-fold increase in the K_{is} as compared to that determined for the wild type enzyme (Table 3.1). Desulfo-CoA is therefore a more potent inhibitor of acetyltransferase activity when AAC(6')-Ii is in dimeric form, perhaps through perturbation of AcCoA binding to one monomer subunit when the second monomer subunit contains bound desulfo-CoA. This idea is also consistent with one possible explanation for the partial competitive inhibition observed for the wild type dimer, which is that desulfo-CoA can bind to different sites on the homodimer (i.e., either AcCoA binding site per monomer), with AcCoA having a

decreased affinity for enzyme if inhibitor is bound to one subunit. The result is that both free and desulfo-CoA-bound enzymes retain the ability to turnover product, if one looks at the homodimer as an "enzyme form" with two functional active sites per dimer.

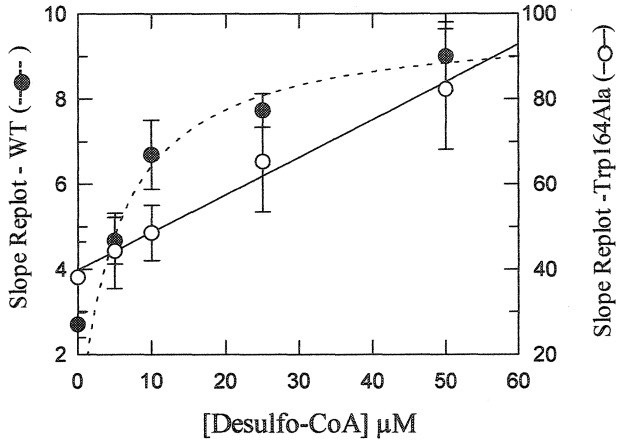

Figure 3.7: Slope replot comparisons of desulfo-CoA inhibition of wild type and mutant AAC(6')-Ii activity. The partial competitive inhibition revealed by the hyberbolic shape of the replot for wild type enzyme (●) is not evident when the monomeric form of Trp164Ala (o) is used in dead-end inhibition studies.

3.4.9 Isothermal Titration Calorimetry Studies

We employed ITC studies to further investigate the binding of AGs to both wild type AAC(6')-Ii and the Trp164Ala monomer. These experiments were initiated to better understand the noncompetitive/mixed inhibition that was observed with acetylated ribostamycin, since a possible explanation was, similar to the desulfo-CoA inhibitor results, that there were unequivalent binding sites for AG substrate per dimer. The results of our ITC experiments are summarized in Table 3.4 and representative ITC profiles for ribostamycin binding to wild type and Trp164Ala proteins are included in Figures 8 and 9, respectively.

Table 3.4: Thermodynamic parameters of the binding of aminoglycosides to AAC(6')-Ii [a]

	No. of sites [b]	K_{d1} (μM)	K_{d2} (μM)	$\Delta G°_1$ (kcal/mol)	$\Delta G°_2$ (kcal/mol)	ΔH_1 (kcal/mol)	ΔH_2 (kcal/mol)	$T\Delta S_1$ (kcal/mol)	$T\Delta S_2$ (kcal/mol)
Wild Type AAC(6')-Ii									
Neamine	2	13.0 ± 0.34	0.03 ± 0.02	-6.9	-10.7	-38.3 ± 0.8	-33.5 ± 0.1	-31.3	-22.8
Kanamycin A	2	3.4 ± 0.14	0.20 ± 0.01	-7.8	-9.5	-30.1 ± 0.5	-93.6 ± 2.0	-22.3	-84.0
Ribostamycin	2	1.3 ± 0.07	0.06 ± 0.01	-8.4	-10.2	-44.8 ± 0.5	-81.1 ± 2.0	-36.4	-70.9
Neamine + CoA	2	0.10 ± 0.01	5.8 ± 0.47	-9.9	-7.4	-21.0 ± 0.1	-11.8 ± 0.6	-11.1	-4.34
Kanamycin + CoA	2	0.62 ± 0.40	65 ± 15	-8.8	-5.9	-15.8 ± 0.2	NR[c]	-7.0	NR
Ribostamycin + CoA	2	0.87 ± 0.14	0.02 ± 0.00	-8.6	-10.9	-9.1 ± 0.4	-24.8 ± 0.4	-36.3	-71.0
Trp164Ala									
Neamine	1	486 ± 38	-------	-4.7	-------	-72.5 ± 3.7	-------	-67.8	-------
Kanamycin A	1	833 ± 17	-------	-4.4	-------	-25.3 ± 0.3	-------	-20.9	-------
Ribostamycin	1	250 ± 5.4	-------	-5.1	-------	-17.3 ± 0.2	-------	-12.1	-------

[a] All titrations were determined at 37 °C (310 K).
[b] Refers to the number of independent binding sites for titrant as determined by the theoretical curve of best fit.
[c] NR, not reported due to large error associated with the value obtained.

It was immediately apparent that our titration data using wild type AAC(6')-Ii and various AG substrates fit best to a theoretical model describing two independent binding sites for the AG titrant (Table 3.4 and Figure 3.8), a phenomenon which was consistent for all three representative antibiotics tested.

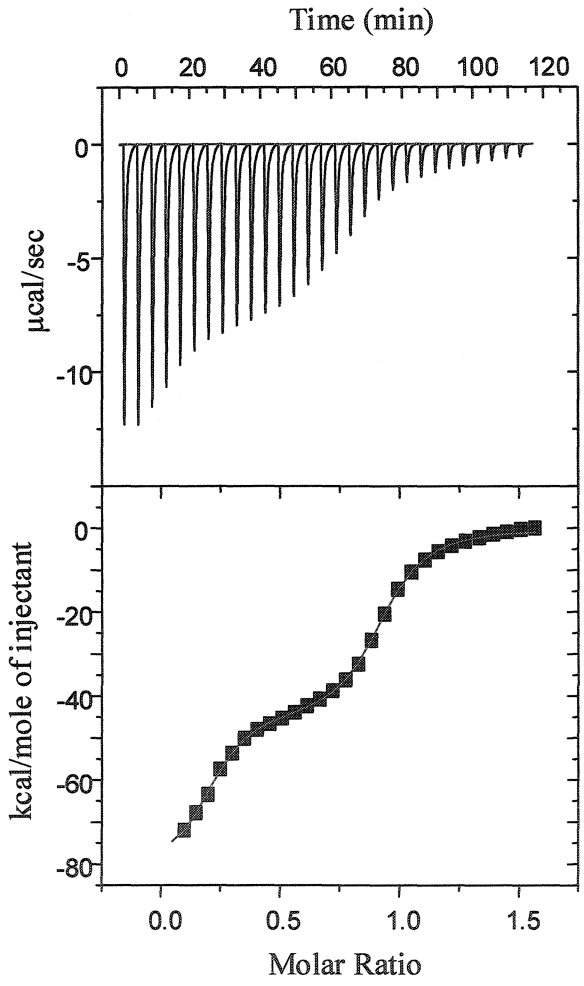

Figure 3.8: ITC profile of wild type AAC(6')-Ii with ribostamycin as the AG titrant. Top: raw experimental data from 29 automatic injections of 10 µL each of 0.7 mM ribostamycin. Bottom: integrated titration curve showing data points (■) and the line of best fit (——) to a model describing two independent AG binding sites per AAC(6')-Ii dimer. ITC experimental conditions are described in section *3.3.9.*

Although a complete titration curve for wild type enzyme was difficult to obtain due to the titration of multiple binding sites (see Figure 3.8), the K_d values with the lowest standard error (Table 3.4) were in the low micromolar range, in relative agreement with K_m values reported previously for AAC(6')-Ii (Wright & Ladak, 1997; Table 3.3). As expected from the nature of the antibiotic binding site in AAC(6')-Ii and other AMEs (Wolf *et al.*, 1998; Wright *et al.*, 1999; Wybenga-Groot *et al.*, 1999; Vetting *et al.*, 2002), our results also indicate that free enzyme can bind AG in the absence of AcCoA, generating an unproductive complex. Consistent with the numerous electrostatic interactions hypothesized to occur between protein and antibiotic based on our knowledge of the 3D structure, binding enthalpies ranged from $-\Delta H$ values of ~ 30 kcal mol $^{-1}$ to ~ 94 kcal mol $^{-1}$ for AG binding to free AAC(6')-Ii (Table 3.4), indicating that this process is largely enthalpy driven. The AG binding sites present per monomer are therefore not thermodynamically equivalent in the wild type AAC(6')-Ii dimer. Additional AG titrations were performed in the presence of CoA to investigate whether the binary AAC(6')-Ii·CoA complex would impact the thermodynamics of antibiotic binding. Again, the titration of two independent AG sites (Table 3.4) made any interpretation as to whether AG has a higher affinity for the AAC(6')-Ii binary complex difficult.

In contrast to the results obtained for the AAC(6')-Ii dimer, binding of AG substrates to the Trp164Ala monomer fit best to theoretical titration curves describing only one binding site (Table 3.4), also seen by the representative ITC profile in Figure 3.9. The

single K_d values reported for neamine, kanamycin, and ribostamycin for Trp164Ala were comparable to the K_m values determined for this mutant (see Tables 3.3 and 3.4), the largest discrepancy being only a 3-fold difference for kanamycin. The binding enthalpies varied from –17.3 to –72.5 kcal mol^{-1}, comparable to the range observed for the wild type AAC(6')-Ii dimer, with only slightly higher ΔG values reported (Table 3.4).

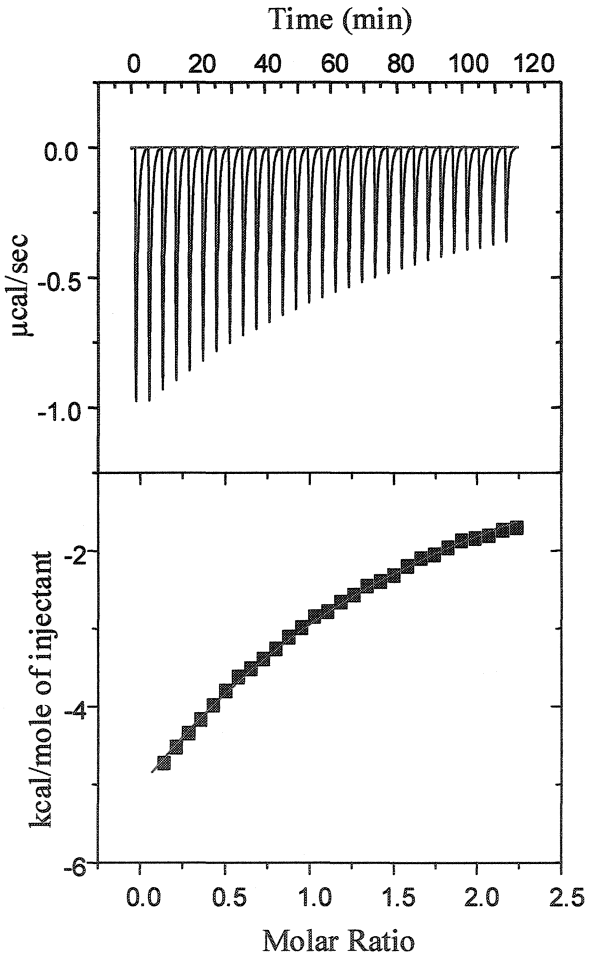

Figure 3.9: ITC profile of the Trp164Ala monomer with 2 mM ribostamycin as the titrant. Experimental conditions were the same as that described in Figure 3.8 and in Materials and Methods. Top: raw experimental data. Bottom: integrated titration curve showing data points (■) and the line of best fit (——) to a model describing one binding site for the AG titrant.

Taken together, the ITC data for AG binding to both wild type and mutant proteins are consistent with our inhibition results and our hypothesis that the monomer subunits of the AAC(6')-Ii dimer may "cooperate" with one another. We speculate, on the basis of the results presented here, that substrate(s) bound to one monomer subunit may affect the binding and perhaps activity of the adjacent monomer in the AAC(6')-Ii dimer.

3.5 Discussion

The inhibition and alternative substrate diagnostic studies detailed here have shown that AAC(6')-Ii follows an ordered bi-bi ternary complex mechanism. As represented in Scheme 1, AcCoA binds first followed by the AG substrate to form a productive ternary complex. Acetylated AG is then the first product to be released after acetyl transfer, followed by coenzyme A. The sequential ternary complex mechanism described for this acetyltransferase appears to be common for all GNAT members studied to date (Williams & Northrop, 1978; Radika & Northrop, 1984b; Benke-Marti, 1987; Rudnick *et al.*, 1991; Hickman *et al.*, 1999b; Trievel *et al.*, 1999; Dyda *et al.*, 2000; Tanner *et al.*, 2000; Magnet *et al.*, 2001), and thus appears to be a universal property of this superfamily. The fact that all GCN5-related *N*-acetyltransferases share the striking structural homology centered on critical interactions with an acyl-CoA molecule suggests that these enzymes serve as catalytic scaffolds in their capacity to bind acyl-CoAs and a diverse array of other substrates to form a productive ternary complex. The ordered binding of acyl-CoA as a first substrate for many enzymes, including serotonin acetyltransferase (Hickman *et al.*, 1999b), and histone acetyltransferases (Rojas *et al.*, 1999; Trievel *et al.*, 1999), has

been complemented by observations of a protein conformational change in response to the binding of AcCoA. We have also noted such changes for AAC(6')-Ii through proteolysis studies and intrinsic protein fluorescence (results not shown), with the solvent viscosity and alternate substrate data presented here indicating that this change is a requirement for catalysis.

Product release appears to be partially rate-limiting in AAC(6')-Ii catalysis, as evidenced by k_{cat} changes from solvent viscosity studies and solvent isotope effects. The release of the final CoA product in particular appears to account for the rate limitation in this regard, as evidenced by our inhibition studies and previous observations of substrate inhibition with numerous AGs (Wright & Ladak, 1997). Of note are the significant changes in k_{cat}/K_b for AGs with increasing solvent viscosity. These results imply that the productive formation of an enzyme complex with AG is partly limited by diffusion, in which case one would expect significantly higher specificity constants on the order of 10^7 $M^{-1}s^{-1}$. Since AGs have several possible conformations in solution with only one conformer optimal as a substrate, a much lower diffusion-controlled k_{cat}/K_b is possible and has been shown for an alternate AG acetyltransferase (Benke-Marti, 1987). In contrast, solvent viscosity appeared to have no effect on the productive formation of the AAC·AcCoA complex, reflected in the lack of k_{cat}/K_a changes for AcCoA. A slow conformational change in the enzyme after AcCoA binding is consistent with our mechanism and may also explain why no viscosity effects were observed in this case.

Last, the lack of an observable solvent isotope effect confirms our viscosity results that diffusion-controlled events, and not the chemical step, largely govern k_{cat}.

The partial and mixed forms of inhibition observed during our investigation of the AAC(6')-Ii kinetic mechanism complicated initial interpretations of our dead-end and product inhibition results. In general, the hyberbolic partial competitive inhibition observed for desulfo-CoA versus AcCoA could be the result of randomness in substrate binding or could indicate that this inhibitor has more than one binding site on AAC(6')-Ii, resulting in a catalytically active ESI complex. This latter hypothesis can also be applied to the observed mixed-type inhibition by 6'-*N*-acetyl ribostamycin versus AG. We have definitively ruled out the former hypothesis of randomness in the enzyme mechanism through the alternative substrate diagnostic approach, which clearly shows that AAC(6')-Ii follows an ordered bi-bi kinetic mechanism. The implication of our observations of partial and mixed inhibitions is that multiple binding sites exist on the enzyme for both AcCoA and AG substrates. Several pieces of evidence suggest that the physiological dimer form of AAC(6')-Ii may act as a "functional unit" and account for the multiple binding sites hypothesized. First, the crystal structure of the AAC(6')-Ii·AcCoA binary complex (Wybenga-Groot *et al.*, 1999) and recent structural determination for the homodimer with bound coenzyme A (Burk *et al.*, 2003) reveal that there is one distinct cofactor binding site per monomer and two distinct sites per dimer. Kinetic analysis of the Trp164Ala monomer described here also indicates that each monomer subunit appears to be functional on its own, signifying single binding sites for the AG substrate

per monomer. We therefore hypothesized that the binding of substrates to one subunit may affect the binding and activity of the other subunit in the dimer, resulting in a form of cooperation between monomers and attributing to the inhibition kinetics we observed.

Consistent with our proposal of subunit cooperation in the AAC(6')-Ii dimer, the partial nature of the competitive inhibition observed for desulfo-CoA versus AcCoA was completely alleviated when the Trp164Ala monomer was used. The binding of desulfo-CoA to one active site may therefore change the affinity of the second active site for AcCoA substrate, a phenomenom which may occur through a slight conformational or structural change in the dimer upon ligand binding. In addition, subsequent ITC analysis of antibiotic binding to wild type AAC(6')-Ii revealed that two nonequivalent AG binding sites exist for the homodimer, in contrast to the one binding site characterized for the Trp164Ala monomer. Again, these results are consistent with subunit cooperation in the physiological dimer. Our ITC data also rule out the possibility of half-site reactivity of the AAC(6')-Ii homodimer, in contrast to that observed for the AG acetyltransferase AAC(6')-Iy from *Salmonella enterica* (Magnet *et al.*, 2001; Hegde *et al.*, 2002). As well, previous NMR spectroscopy evidence which identified two enzyme-bound conformers for the same AG substrate on AAC(6')-Ii (DiGiammarino *et al.*, 1998) is not inconsistent with our results. The likelihood of certain antibiotics having multiple binding modes per monomer active site, however, cannot be dismissed, given the multiple conformations possible for AG substrates in solution.

The implications of our observations of subunit cooperativity for the AAC(6')-Ii physiological dimer are severalfold. First, the fairly low specificity constants observed

for AG modification by AAC(6')-Ii (~ 10^{4} $M^{-1}s^{-1}$) can be partially attributed to this phenomenon if the reversible binding of ligands to each subunit effectively decreases the acetylation activity of the dimer as a whole. Second, the possibility of subunit cooperativity in other oligomeric members of the GNAT superfamily may implicate this phenomenon in the function and regulation of several enzymes, although this remains to be determined.

3.6 References

Angus-Hill, M. L., R. N. Dutnall, S. T. Tafrov, R. Sternglanz, and V. Ramakrishnan. (1999) Crystal structure of the histone acetyltransferase Hpa2: A tetrameric member of the GCN5-related *N*-acetyltransferase superfamily. *J Mol Biol* 294: 1311-25.

Benke-Marti, K. M. (1987) Ph.D. Thesis. Kinetic characterization of aminoglycoside acetyltransferase 3-I, University of Wiscosin-Madison.

Bhatnagar, R. S., K. Futterer, G. Waksman, and J. I. Gordon. (1999) The structure of myristoyl-CoA:Protein *N*-myristoyltransferase. *Biochim Biophys Acta* 1441: 162-72.

Blacklow, S. C., R. T. Raines, W. A. Lim, P. D. Zamore, and J. R. Knowles. (1988) Triosephosphate isomerase catalysis is diffusion controlled. Appendix: Analysis of triose phosphate equilibria in aqueous solution by 31P NMR. *Biochemistry* 27: 1158-67.

Brannan, T., B. Althoff, L. Jacobs, J. Norby, and Rubenstein S. Enzyme kinetics module 1.0 for SigmaPlot 2000 Version 6.10. SSPS Inc., Chicago, IL.

Burk, D. L., N. Ghuman, L. E. Wybenga-Groot, and A. M. Berghuis. (2003) X-ray structure of the aac(6')-Ii antibiotic resistance enzyme at 1.8 Å resolution; examination of oligomeric arrangements in GNAT superfamily members. *Protein Sci* 12: 426-37.

Clements, A., J. R. Rojas, R. C. Trievel, L. Wang, S. L. Berger, and R. Marmorstein. (1999) Crystal structure of the histone acetyltransferase domain of the human PCAF transcriptional regulator bound to coenzyme aA *Embo J* 18: 3521-32.

Costa, Y., M. Galimand, R. Leclercq, J. Duval, and P. Courvalin. (1993) Characterization of the chromosomal *aac(6')-Ii* gene specific for *Enterococcus faecium*. *Antimicrob. Agents Chemother.* 37: 1896-1903.

Daigle, D. M., D. W. Hughes, and G. D. Wright. (1999) Prodigious substrate specificity of AAC(6')-APH(2"), an aminoglycoside antibiotic resistance determinant in enterococci and staphylococci. *Chem Biol* 6: 99-110.

Davies, J. & G. D. Wright. (1997) Bacterial resistance to aminoglycoside antibiotics. *Trends Microbiol* 5: 234-40.

De Angelis, J., J. Gastel, D. C. Klein, and P. A. Cole. (1998) Kinetic analysis of the catalytic mechanism of serotonin *N*-acetyltransferase (EC 2.3.1.87). *J Biol Chem* 273: 3045-50.

DiGiammarino, E.L., K.a. Draker, G.D. Wright, and E.H. Serpesu. (1998) Solution studies of isepamicin and conformational comparisons between isepamicin and butirosin a when bound to an aminoglycoside 6'-*N*-acetyltransferase determined by NMR spectroscopy. *Biochemistry* 37: 3638-3644.

Dutnall, R. N., S. T. Tafrov, R. Sternglanz, and V. Ramakrishnan. (1998) Structure of the histone acetyltransferase hat1: A paradigm for the GCN5-related *N*-acetyltransferase superfamily. *Cell* 94: 427-438.

Dyda, F., D. C. Klein, and A. B. Hickman. (2000) GCN5-related *N*-acetyltransferases: A structural overview. *Annu Rev Biophys Biomol Struct* 29: 81-103.

Hegde, S. S., T. K. Dam, C. F. Brewer, and J. S. Blanchard. (2002) Thermodynamics of aminoglycoside and acyl-coenzyme A binding to the *Salmonella enterica* AAC(6')-Iy aminoglycoside *N*-acetyltransferase. *Biochemistry* 41: 7519-27.

Hickman, A. B., D. C. Klein, and F. Dyda. (1999a) Melatonin biosynthesis: The structure of serotonin *N*-acetyltransferase at 2.5 Å resolution suggests a catalytic mechanism. *Mol Cell* 3: 23-32.

Hickman, A. B., M. A. Namboodiri, D. C. Klein, and F. Dyda. (1999b) The structural basis of ordered substrate binding by serotonin N-acetyltransferase: Enzyme complex at 1.8 Å resolution with a bisubstrate analog. *Cell* 97: 361-9.

Lau, O. D., A. D. Courtney, A. Vassilev, L. A. Marzilli, R. J. Cotter, Y. Nakatani, and P. A. Cole. (2000) P300/CBP-associated factor histone acetyltransferase processing of a peptide substrate. Kinetic analysis of the catalytic mechanism. *J Biol Chem* 275: 21953-9.

Leatherbarrow, RJ. Grafit 4.0. Erithacus Software, Staines, UK.

Llano-Sotelo, B., E. F. Azucena, L. P. Kotra, S. Mobashery, and C. S. Chow. (2002) Aminoglycosides modified by resistance enzymes display diminished binding to the bacterial ribosomal aminoacyl-tRNA site. *Chem Biol* 9: 455-63.

Magnet, S., T. Lambert, P. Courvalin, and J. S. Blanchard. (2001) Kinetic and mutagenic characterization of the chromosomally encoded *Salmonella enterica* AAC(6')-Iy aminoglycoside *N*-acetyltransferase. *Biochemistry* 40: 3700-9.

McKay, G. A. & G. D. Wright. (1996) Catalytic mechanism of enterococcal kanamycin kinase (APH(3')-IIIa): Viscosity, thio, and solvent isotope effects support a theorell-chance mechanism. *Biochemistry* 35: 8680-5.

Miller, G. H., F. J. Sabatelli, R. S. Hare, Y. Glupczynski, P. Mackey, D. Shlaes, K. Shimizu, and K. J. Shaw. (1997) The most frequent aminoglycoside resistance mechanisms-changes with time and geographic area: A reflection of aminoglycoside usage patterns? Aminoglycoside resistance study groups. *Clin Infect Dis* 24 Suppl 1: S46-62.

Moellering, R. C., Jr., O. M. Korzeniowski, M. A. Sande, and C. B. Wennersten. (1979) Species-specific resistance to antimocrobial synergism in *Streptococcus faecium* and *Streptococcus faecalis*. *J Infect Dis* 140: 203-8.

Moellering, R. C., Jr., C. Wennersten, and A. J. Weinstein. (1973) Penicillin-tobramycin synergism against enterococci: A comparison with penicillin and gentamicin. *Antimicrob Agents Chemother* 3: 526-9.

Neuwald, A. F. & D. Landsman. (1997) GCN5-related histone N-acetyltransferases belong to a diverse superfamily that includes the yeast SPT10 protein. *Trends Biochem. Sci.* 22: 154-155.

Obsil, T., R. Ghirlando, D. C. Klein, S. Ganguly, and F. Dyda. (2001) Crystal structure of the 14-3-3zeta:Serotonin *N*-acetyltransferase complex. A role for scaffolding in enzyme regulation. *Cell* 105: 257-67.

Peneff, C., D. Mengin-Lecreulx, and Y. Bourne. (2001) The crystal structures of apo and complexed *Saccharomyces cerevisiae* GNA1 shed light on the catalytic mechanism of an amino-sugar *N*-acetyltransferase. *J Biol Chem* 276: 16328-34.

Radika, K. & D. Northrop. (1984a) A new kinetic diagnostic for enzymatic mechanisms using alternative substrates. *Anal Biochem* 141: 413-7.

Radika, K. & D. B. Northrop. (1984b) The kinetic mechanism of kanamycin acetyltransferase derived from the use of alternative antibiotics and coenzymes. *J Biol Chem* 259: 12543-6.

Radika, K. & D. B. Northrop. (1984c) Substrate specificities and structure-activity relationships for acylation of antibiotics catalyzed by kanamycin acetyltransferase. *Biochemistry* 23: 5118-22.

Rojas, J. R., R. C. Trievel, J. Zhou, Y. Mo, X. Li, S. L. Berger, C. D. Allis, and R. Marmorstein. (1999) Structure of tetrahymena GCN5 bound to coenzyme A and a histone H3 peptide. *Nature* 401: 93-8.

Rudnick, D. A., C. A. McWherter, W. J. Rocque, P. J. Lennon, D. P. Getman, and J. I. Gordon. (1991) Kinetic and structural evidence for a sequential ordered bi bi mechanism of catalysis by *Saccharomyces cerevisiae* myristoyl-CoA:Protein *N*-myristoyltransferase. *J Biol Chem* 266: 9732-9.

Schowen, K.B.J. (1978). In *Transition states of biological processes*. R.D. Gandour & R.L. Schowen,eds. Plenum Press, New York. 225-283.

Sinclair, J. C., J. Sandy, R. Delgoda, E. Sim, and M. E. Noble. (2000) Structure of arylamine *N*-acetyltransferase reveals a catalytic triad. *Nat Struct Biol* 7: 560-4.

Tanner, K. G., M. R. Langer, and J. M. Denu. (2000) Kinetic mechanism of human histone acetyltransferase P/CAF. *Biochemistry* 39: 11961-9.

Trievel, R. C., J. R. Rojas, D. E. Sterner, R. N. Venkataramani, L. Wang, J. Zhou, C. D. Allis, S. L. Berger, and R. Marmorstein. (1999) Crystal structure and mechanism of histone acetylation of the yeast GCN5 transcriptional coactivator. *Proc Natl Acad Sci U S A* 96: 8931-6.

Vetting, M. W., S. S. Hegde, F. Javid-Majd, J. S. Blanchard, and S. L. Roderick. (2002) Aminoglycoside 2'-*N*-acetyltransferase from *Mycobacterium tuberculosis* in complex with coenzymeA and aminoglycoside substrates. *Nat Struct Biol* 9: 653-8.

Wennersten, C.B. & R. C. Moellering, Jr. (1980) Mechanism of resistence to penicillin-aminoglycoside synergism in *Streptococcus faecium*. In *Current chemotherapy and infectious disease*, I. J.D. Nelson&C. Grassi,eds. American Society for Microbiology, Washington, D.C. 710-712.

Williams, J. W. & D. B. Northrop. (1978) Kinetic mechanisms of gentamicin acetyltransferase I. Antibiotic-dependent shift from rapid to nonrapid equilibrium random mechanisms. *J Biol Chem* 253: 5902-7.

Wiseman, T., S. Williston, J. F. Brandts, and L. N. Lin. (1989) Rapid measurement of binding constants and heats of binding using a new titration calorimeter. *Anal Biochem* 179: 131-7.

Wolf, E., A. Vassilev, Y. Makino, A. Sali, Y. Nakatani, and S. K. Burley. (1998) Crystal structure of a GCN5-related *N*-acetyltransferase: *Serratia marcescens* aminoglycoside 3-*N*-acetyltransferase. *Cell* 94: 439-49.

Wright, G. D. (1999) Aminoglycoside-modifying enzymes. *Curr Opin Microbiol* 2: 499-503.

Wright, G.D., A. M. Berghuis, and S. Mobashery. (1999) Aminoglycoside antibiotics: Structures, function, and resistance. In *Resolving the antibiotic paradox: Progress in drug design and resistance*. B.P. Rosen & S. Mobashery, eds. Plenum Publishing Corporation, New York, NY. 27-69.

Wright, G.D. & P. Ladak. (1997) Overexpression and characterization of the chromosomal aminoglycoside 6'-*N*-acetyltransferase from *Enterococcus faecium*. *Antimicrob. Agents Chemother.* 41: 956-960.

Wybenga-Groot, L., K.A. Draker, G.D. Wright, and A.M. Berghuis. (1999) Crystal structure of an aminoglycoside 6'-*N*-acetyltrasnferase: Defining the GCN5-related *N*-acetyltransferase superfamily fold. *Structure* 7: 497-507.

Chapter 4

Studies on the Catalytic Mechanism of AAC(6')-Ii

The research described in this chapter was written as a manuscript entitled

Molecular Mechanism of the Enterococcal Aminoglycoside 6'-*N*-Acetyltransferase AAC(6')-Ii: Role of GNAT-Conserved Residues in the Chemistry of Antibiotic Inactivation

Draker, K. A. and G. D. Wright, authors

4.0 Preface

This chapter describes research on the catalytic mechanism of acetyl transfer by AAC(6')-Ii and represents the second and final sandwich style inclusion in this thesis. The original manuscript detailing this work has been reformatted to meet thesis style guidelines and is presented here. In addition, supplemental data submitted with the manuscript is included in section *4.3.6*, with omission of the AAC(6')-Ii partial proteolysis data that has already been described in chapter 2. It is important to note that I conducted all of the research described in this chapter, with an acknowledged contribution made by Stevo Radinovic, an undergraduate project student who helped in the initial mutagenesis and purification of the His74Ala and Glu72Ala site mutants. I am also responsible for writing the manuscript, which has been accepted for publication in the journal *Biochemistry*. I also sincerely thank Drs. Murray Junop and Quyan Hoang for technical assistance in generating Figure 4.4.

The studies described in this chapter convey the importance of investigating the catalytic mechanism of AAC(6')-Ii, which has resulted in a greater understanding of AG acetylation by this enzyme and also allows us to compare and contrast our results with other *N*-acetyltransferases. The introduction presented in section *4.2* also contains relevant background information on the GNAT superfamily that was not detailed in chapter 1. Furthermore, this work complements the research described in chapter 3 on the kinetic mechanism of AAC(6')-Ii, with several key findings from those studies applied to the characterization of several AAC(6')-Ii site mutants as detailed here.

4.1 Summary

The Gram positive pathogen *Enterococcus faecium* is intrinsically resistant to AG antibiotics due to the presence of a chromosomally encoded AG 6'-*N*-acetyltransferase, AAC(6')-Ii. This enzyme is a member of the GCN5-related *N*-acetyltransferase (GNAT) superfamily and is therefore structurally homologous to proteins that catalyze acetyl transfer to diverse acyl-accepting substrates. This study reports the investigation of several potential catalytic residues that are present in the AAC(6')-Ii active site and also conserved in many GNAT enzymes. Site-directed mutagenesis of Glu72, His74, Leu76, and Tyr147 with characterization of the purified site mutants gave valuable information on the roles of these amino acids in acetyl transfer chemistry. More specifically, steady-state kinetic analysis of protein activity, solvent viscosity effects, pH studies, as well as antibiotic resistance profiles were all used to assess the roles of Glu72 and His74 as potential active site bases, Tyr147 as a general acid, and the importance of the amide NH of Leu76 in transition state stabilization. Taken together, our results indicate that Glu72 is not involved in general base catalysis, but is instead critical for the proper positioning and orientation of AG substrates in the active site. Similarly, His74 is also not acting as the active site base, with pH studies revealing that this residue must be protonated for optimal AAC(6')-Ii activity. Mutation of Tyr147 was found not to affect the chemical step of catalysis and our results were not consistent with this residue acting as a general acid. Lastly, the amide NH of Leu76 is implicated in important interactions with AcCoA and transition state stabilization. In summary, the work described here provides important information regarding the molecular mechanism of AAC(6')-Ii catalysis that allows us to

contrast our findings with other GNAT proteins and to demonstrate that these enzymes use a variety of chemical mechanisms to accelerate acyl transfer.

4.2 Introduction

Bacterial resistance to the AG-aminocyclitol antibiotics is most commonly due to the action of *O*-phosphotransferases (APHs)[1], *O*-nucleotidylyltransferases (ANTs), and *N*-acetyltransferases (AACs), which modify various hydroxyl or amino functionalities on the drug (Davies & Wright, 1997; Wright *et al.*, 1998). Antibiotic modification by these AG modifying enzymes (AMEs) decreases the affinity of the antibiotic for its 30S ribosomal subunit target (Llano-Sotelo *et al.*, 2002), resulting in microbial resistance and complications in the clinical treatment of infections caused by both Gram positive and Gram negative bacteria. In particular, AG resistance in Gram positive enterococci renders routine β-lactam/AG therapy ineffective, due in many instances to high level gentamicin resistance in *Enterococcus faecalis* (Patterson & Zervos, 1990) or low-level resistance to numerous AGs in *E. faecium* (Wennersten & Moellering JR., 1980). This failure of commonplace treatments increases the reliance on other classes of drugs such as the glycopeptides, resulting in an additional clinical problem in the form of vancomycin resistant enterococci (VRE) and a disturbing trend of bacterial multi-drug resistance (Huycke *et al.*, 1998; Murray, 1998).

A prevalent form of modification conferring AG resistance in bacteria is 6'-N-acetylation, with two such enzymes responsible for antibiotic inactivation in Gram

positive enterococci (Davies & Wright, 1997; Shaw & Wright, 2000). In *E. faecalis*, high-level AG resistance is often due to the plasmid-mediated expression of the AAC(6')-APH(2") bifunctional enzyme, that both acetylates and phosphorylates various AGs (Daigle *et al.*, 1999). In *E. faecium,* intrinsic resistance is mediated by expression of the chromosomally encoded *aac(6')-Ii* gene, conferring low-level resistance to the 4,5- and 4,6-disubstituted deoxystreptamine classes of AGs (Costa *et al.*, 1993). *In vitro* characterization of purified AAC(6')-Ii revealed its broad substrate specificity and defined the kinetics of acetyl transfer to be sub-optimal for a detoxification enzyme, with fairly low specificity constants (k_{cat}/K_m values) on the order of 10^{4} $M^{-1}s^{-1}$ and poor correlation of this specificity with minimum inhibitory concentration (MIC) (Wright & Ladak, 1997). More recent studies have shown that AAC(6')-Ii follows an ordered bi-bi reaction mechanism similar to numerous other *N*-acetyltransferases, in which AcCoA binds first to the enzyme followed by AG to form a productive ternary complex (Draker *et al.*, 2003). Solvent viscosity and isotope effects also revealed that diffusion-controlled processes and not the chemical step govern the rate of AAC(6')-Ii acetyl transfer (Draker *et al.*, 2003).

The crystal structure of AAC(6')-Ii in complex with AcCoA (Wybenga-Groot *et al.*, 1999) identified this resistance enzyme as a member of the large GCN5-related *N*-acetyltransferase (GNAT) superfamily, which includes a diverse group of enzymes from both prokaryotes and eukaryotes. Originally based on primary sequence data which identified four sequence motifs common to *N*-acetyltransferases, early structural determinations of two GNAT members first revealed the remarkable structural homology

among superfamily members despite the lack of extensive primary sequence homology (Dutnall *et al.*, 1998; Wolf *et al.*, 1998). The subsequent structural determination of the AAC(6')-Ii·AcCoA binary complex helped to further define the four conserved structural motifs and their role in AcCoA binding, as well as to characterize AAC(6')-Ii as both a structural and functional homolog of eukaryotic histone acetyltransferases (HATs) (Wybenga-Groot *et al.*, 1999). Numerous GNAT crystal structures are now available that exemplify both the structural similarities among superfamily members and the diverse specificity of these enzymes for acyl-accepting substrates, such as AGs and other sugars (Wolf *et al.*, 1998; Wybenga-Groot *et al.*, 1999; Peneff *et al.*, 2001; Vetting *et al.*, 2002), small molecules such as serotonin (Hickman *et al.*, 1999a; Hickman *et al.*, 1999b), as well as histones and other proteins (Bhatnagar *et al.*, 1998; Dutnall *et al.*, 1998; Weston *et al.*, 1998; Angus-Hill *et al.*, 1999; Clements *et al.*, 1999; Rojas *et al.*, 1999; Poux *et al.*, 2002) (Figure 4.1).

To date, crystal structures of three AG *N*-acetyltransferases representing the 3, 2', and 6' regiospecificities of drug modification have been determined (Wolf *et al.*, 1998; Wybenga-Groot *et al.*, 1999; Vetting *et al.*, 2002). A structure-based sequence alignment of these AACs with other homologues in the GNAT superfamily provides information regarding the residues conserved within the structural motifs A-D (Figure 4.2). In addition to the numerous non-polar residues important for the GNAT structural fold (Dyda *et al.*, 2000), several active site amino acids that could play a catalytic role are also structurally aligned in the highly conserved motifs A and B (Figure 4.2).

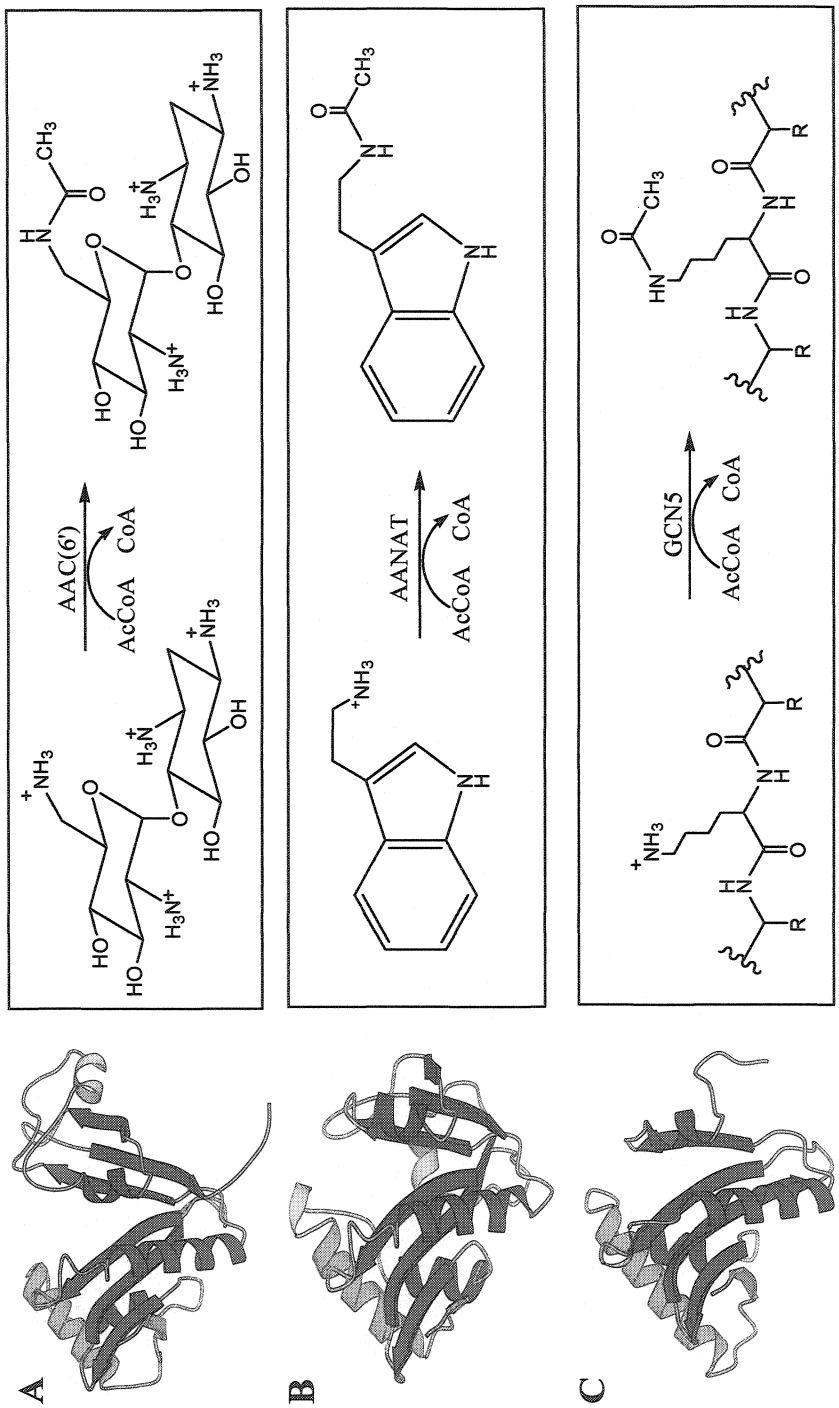

Figure 4.1: Structures of three representative classes of GNAT enzymes (left) and the diverse acetyltransferase reactions they catalyze (right). **A.** Typical kanamycin modification by a bacterial AG 6'-*N*-acetyltransferase, like AAC(6')-Ii (shown) (Wybenga-Groot *et al.*, 1999). **B.** Eukaryotic arylalkylamine *N*-acetyltransferases (AANATs) catalyze the acetylation of small molecules such as serotonin. Shown is AANAT from sheep (Hickman *et al.*, 1999). **C.** The N-acetylation of histones at specific lysine residues is accomplished by HAT enzymes, like the tetrahymena GCN5 protein shown (Rojas *et al.*, 1999). Structures of each of the represented proteins were generated using MOLSCRIPT (Kraulis, 1991) and Raster3D (Merritt & Murphy, 1994), with the GNAT sequence motifs A-D colored blue, purple, green, and red, respectively.

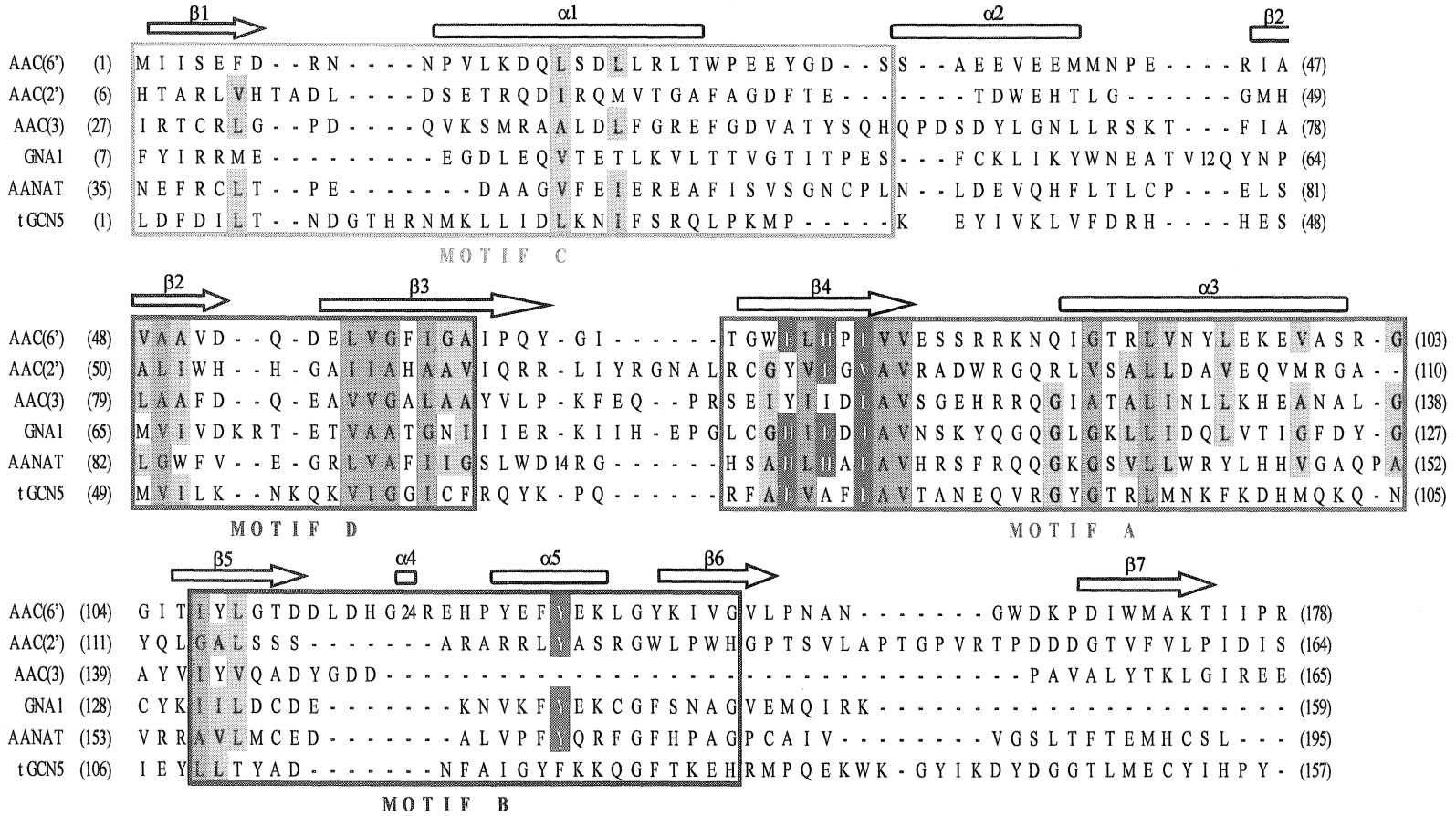

Figure 4.2: Structure-based sequence alignment of representative members of the GNAT superfamily. Included (from top) are primary sequences of the aminoglycoside acetyltransferases AAC(6')-Ii (Wybenga-Groot *et al.*, 1999), AAC(3)-Ia, (Wolf *et al.*, 1998), and AAC(2')-Ic (Vetting *et al.*, 2002), as well as the sugar transferase GNA1 (Peneff *et al.*, 2001), AANAT (Hickman *et al.*, 1999), and tGCN5 (Rojas *et al.*, 1999). The alignment was generated using the Vector Alignment Search Tool (VAST) algorithm (Madej *et al.*, 1995; Gibrat *et al.*, 1996). Non-polar residues important for the GNAT structural fold are boxed in dark grey (conserved) or light grey (semi-conserved). Boxed in blue are potential catalytic residues that are conserved among some members, including AAC(6')-Ii residues Glu72, His74, Leu76, and Tyr147. GNAT structural motifs A-D are indicated.

In particular, AAC(6')-Ii residues Glu72, His74, Leu76 and Tyr147 align well with chemically similar residues from several GNATs (Figure 4.2) and have the potential to play a role in general acid/base catalysis or transition state stabilization typical for an acetyl transfer reaction, as shown in Figure 4.3;

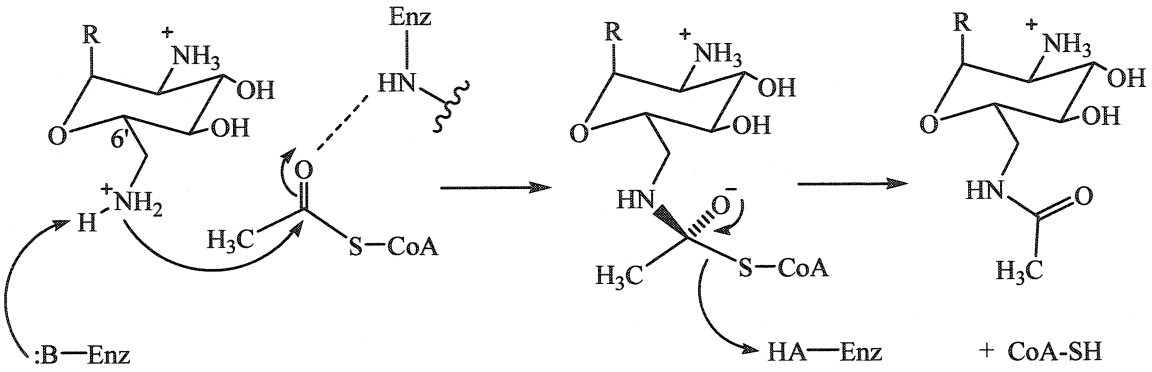

Figure 4.3: Proposed reaction pathway for AAC(6')-Ii-catalyzed acetyl transfer. The probable mechanism of AG acetylation by AAC(6')-Ii, showing nucleophilic attack of the carbonyl carbon of AcCoA by the deprotonated 6'-amino group of an AG (right) and formation of a tetrahedral-like transition state (middle). Possible general acid/base catalysis and transition state stabilization by the enzyme is also shown.

The current study concentrates on these potential catalytic residues that line the AAC(6')-Ii active site, represented in Figure 4.4. The amino acids Glu72, His74, and Leu76 are found on β-strand four (motif A), which contains the GNAT-conserved β-bulge and makes the majority of contacts with AcCoA (Wybenga-Groot *et al.*, 1999; Dyda *et al.*, 2000). Tyr147 is part of α-helix 5 (motif B), which also interacts with bound cofactor in the AAC(6')-Ii crystal structure. More specifically, Glu72 is in close proximity to the substrate acetyl moiety and may act as a general base by deprotonating

the incoming 6'-amino group of the AG. His74 could behave as either a general acid or base in drug modification. The backbone NH of Leu76 may also be critical for AAC(6')-Ii catalysis, as this main chain element is in close proximity to the carbonyl oxygen of AcCoA (Figure 4.4) and equivalent residues have been repeatedly implicated in transition state stabilization for several GNATs (Bhatnagar *et al.*, 1998; Hickman *et al.*, 1999b; Rojas *et al.*, 1999; Vetting *et al.*, 2002). Finally, the hydroxyl group of Tyr147 interacts with the sulfur atom of AcCoA (Figure 4.4) and thus has the potential to act as a general acid in acetyl transfer by reprotonating the CoA leaving group. Interestingly, several amino acids from various GNATs that structurally align with the aforementioned AAC(6')-Ii residues have already been shown to play critical roles in reaction chemistry. These include Glu173 of yeast GCN5 (aligns with AAC(6')-Ii Glu72), which has been characterized by mutagenesis and kinetic analysis to act as the general base in histone acetylation (Trievel *et al.*, 1999). Recent studies on AANAT have shown that His122 (aligns with AAC(6')-Ii His74, Figure 4.2) acts as a remote general base in serotonin acetylation, with Tyr168 (aligns with AAC(6')-Ii Tyr147, Figure 4.2) behaving as the general acid (Scheibner *et al.*, 2002).

This report describes the characterization of AAC(6')-Ii site mutants Glu72Ala, His74Ala, Leu76Ala, Leu76Pro, Tyr147Ala, and Tyr147Phe. Kinetic analysis of mutant enzyme activity was followed up with solvent viscosity studies to determine whether any of the amino acid substitutions resulted in a protein impaired at the chemical step of acetyl transfer. Additional studies on the pH dependence of wild type and His74Ala activity identified ionizable groups important for catalysis and further defined the

chemical mechanism of AAC(6')-Ii. Finally, the impact of each amino acid substitution on AAC(6')-Ii drug acetylation *in vivo* was assessed by MIC determinations of select AG antibiotics. The goal of this work is to elucidate the molecular mechanism of AG inactivation by this enzyme, which will no doubt be useful in both the identification and/or design of AAC(6')-Ii specific inhibitors in the future. In addition, an understanding of the chemical mechanisms of GNAT enzymes and how they differ may shed light on the broad specificities displayed for acyl-accepting substrates and on the evolution of these *N*-acyltransferases as a superfamily.

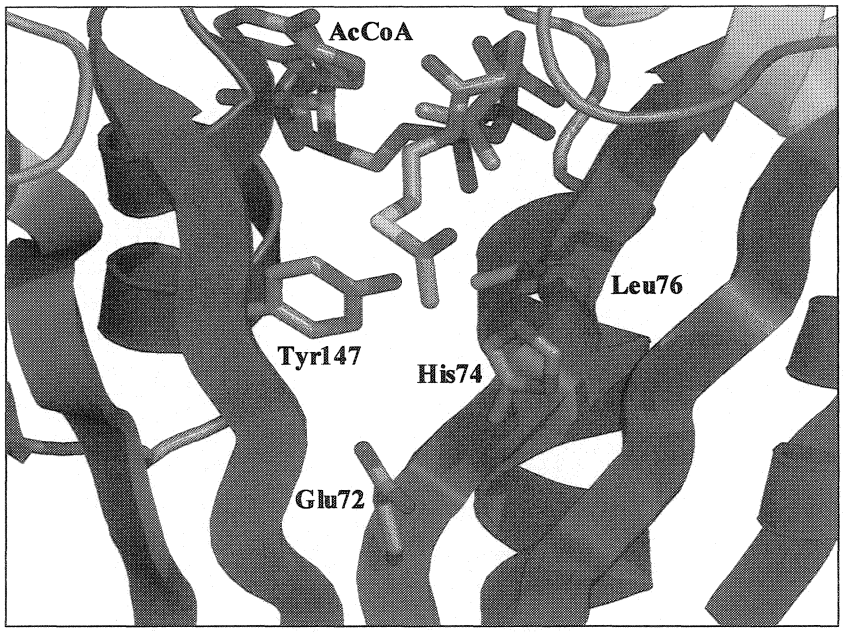

Figure 4.4: Potential catalytic residues lining the AAC(6')-Ii active site. Bound AcCoA and nearby amino acids Glu72, His74, Leu76, and Tyr147 are represented. The potential roles of these amino acids are discussed throughout the text. The sulfur atom of AcCoA is colored yellow and the amide N of Leu76 is represented as a blue sphere. Secondary structure that is part of a conserved motif is colored blue (motif A), purple (motif B), green (motif C) or red (motif D). This figure was generated using the pdb file 1B87 (Wybenga-Groot *et al.*, 1999) and PyMOL (DeLano, 2002).

4.3 Materials and Methods

4.3.1 General

AGs and DTDP were from Sigma Chemical Co. (St. Louis, MO, USA). Neamine was the kind gift of Dr. Shahriar Mobashery at the Institute for Drug Design, Departments of Chemistry, Pharmacology and Biochemistry and Molecular Biology, Wayne State University, Detroit, Michigan, USA. AcCoA was from Amersham Pharmacia and [1-^{14}C]-labelled AcCoA (specific activity = 65 mCi/mmol) was from ICN radiochemicals (Costa Mesa, CA, USA). Mutagenic oligonucleotide primers were synthesized at the Central Facility of the Institute for Molecular Biology and Biotechnology, McMaster University.

4.3.2 Site-Directed Mutagenesis of AAC(6')-Ii

To investigate the roles of Glu72, His74, Leu76, and Tyr147 in acetyl transfer, eight site mutants were generated by the QuikChange site-directed mutagenesis protocol (Stratagene, La Jolla, CA, USA) using the appropriate mutagenic oligonucleotide primer (Table 4.1) and its reverse complement. The wild type *aac(6')-Ii* gene cloned into pET22b(+) (Novagen, Madison, WI) (Draker *et al.*, 2003) was used as template DNA in all PCR amplifications. The presence of the desired mutation in all mutant *aac(6')-Ii* genes as well as the absence of adventitious mutations was confirmed by complete gene sequencing at the Central Facility of the Institute for Molecular Biology and Biotechnology, McMaster University. All expression constructs were used to transform *E. coli* BL21(DE3) competent cells for subsequent enzyme overexpression and purification.

Table 4.1: Mutagenic oligonucleotides used in this study

Mutation	Oligonucleotide Sequence [a]
Glu72Ala	5'- ggtatcacaggttgggcattgcatccattag - 3'
Glu72Gln	5'- ggtatcacaggttggcaattgcatccattag - 3'
Glu72Asp	5'- ggtatcacaggttgggatttgcatccattag - 3'
His74Ala	5' - ggttgggaattggctccattagttgtagaaagc - 3'
Leu76Ala	5' - gggaattgcatccagcagttgtagaaagctc - 3'
Leu76Pro	5' - gggaattgcatccaccagttgtagaaagctc - 3'
Tyr147Ala	5' - ggacatccgtatgagttcgctgaaaaattagg - 3'
Tyr147Phe	5' - ggacatccgtatgagttctttgaaaaattagg - 3'

[a] Underlined bases indicate the codon change used to generate the desired amino acid substitution

4.3.3 Purification of Site Mutants

Wild type and mutant AAC(6')-Ii proteins were overexpressed and purified by the three-step column chromatography procedure previously described (Wright & Ladak, 1997). Exceptions were the Glu72Gln and Glu72Asp mutants, which were overexpressed following induction with IPTG at 16 °C overnight. This was done to obtain a reasonable quantity of soluble protein after initial attempts using wild type procedures were unsuccessful.

4.3.4 Partial Proteolysis of Mutant AAC(6')-Ii Proteins

Incubation of wild type AAC(6')-Ii with subtilisin results in a reproducible pattern of proteolysis as visualized by SDS-PAGE. In addition, AAC(6')-Ii is almost completely protected from proteolysis in the presence of AcCoA, with bound AG offering less protection (see chapter 2). The susceptibility of mutant AAC(6')-Ii proteins to subtilisin

was therefore investigated for confirmation that the introduced mutations did not perturb the overall tertiary structure of the proteins, as assessed by visual comparison with wild type digestion patterns.

4.3.5 Steady-State Kinetic Analysis

AG-dependent acetyltransferase activity was monitored during protein purification and steady-state kinetic studies by *in situ* titration of free CoA with DTDP as described previously (Williams & Northrop, 1978; Wright & Ladak, 1997). Assay conditions for the kinetic analysis of mutant AAC(6')-Ii enzymes were similar to those described for the wild type protein (Wright & Ladak, 1997), but scaled down to a final volume of 250 µL to monitor reactions in microtiter plate format using a Molecular Devices SpectraMAX Plus spectrophotometer. Initial rates were fit to equation 1 describing Michaelis-Menten kinetics,

$$v = k_{cat}E_t[S]/(K_m + [S]) \qquad \text{(Eq. 1)}$$

or equation 2,

$$v = k_{cat}E_t[S]/(K_m + [S])(1 + [S]/K_i)) \qquad \text{(Eq. 2)}$$

when substrate inhibition was detected, using Grafit 4.0 software (Leatherbarrow, 2000). Peptide acetylation activities of wild type and Glu72Ala proteins were compared using the modified phosphocellulose binding assay and the model peptide substrate poly-L-Lys as described previously (Wybenga-Groot *et al.*, 1999). Reactions were allowed to proceed for 45 min and contained varying concentrations of poly-L-Lys, 0.1 µCi [1-^{14}C] AcCoA (160 µM), and ca. 25 pmoles enzyme in 25 mM HEPES pH 7.5, 2 mM EDTA.

4.3.6 Supplemental Data Relevant to Kinetic Analysis

Recent isothermal titration calorimetry (ITC) experiments have shown that the K_m values for AG binding to AAC(6')-Ii approximates the dissociation contants (K_d) for these substrates (Draker *et al.*, 2003). To assess whether the K_m for AcCoA also reflects the K_d, we turned to equilibrium dialysis and fluorescence anisotropy experiments to determine the dissociation constants for AcCoA and N^6 - ethenocoenzyme A (εCoA), respectively. Our results indicate that K_m does approximate K_d, allowing us to interpret changes in the kinetic parameter K_m for the AAC(6')-Ii site mutants as changes in binding affinity for both AcCoA and AG substrates.

4.3.6.1 Equilibrium Dialysis Experiments

K_d determinations for AcCoA binding to AAC(6')-Ii were made using disposable equilibrium dialyzers with a 10 kDa cut-off membrane separating two small volume chambers (~ 75 µL). AAC(6')-Ii enzyme at a 100 µM concentration was added to the sample chamber and 5-320 µM of [^{14}C]-AcCoA added to the other (buffer) chamber. Both chambers contained 25 mM Hepes, pH 7.5 and 1 mM EDTA as buffer. Following a 2 day equilibration on a level shaker, duplicate samples were recovered from each chamber and applied to filter paper. The dried filter paper was then counted by liquid scintillation to determine the amount of radioactivity in the buffer ($[AcCoA]_{free}$), and sample ($[AcCoA]_{free}$ + [AcCoA·AAC(6')-Ii]) chambers. The concentration of bound AcCoA was determined by subtracting the $[AcCoA]_{free}$ value from the $[AcCoA]_{free}$ + [AcCoA·AAC(6')-Ii] determination. A K_d value for AcCoA

binding was determined by nonlinear least squares fitting to equation 3 describing 1 site ligand binding, using Grafit 4.0 (Leatherbarrow, 2000).

$$[\text{AcCoA}\cdot\text{AAC(6')-Ii}] = ([\text{AAC(6')-Ii}]_{total} * [\text{AcCoA}]_{free})/K_d + [\text{AcCoA}]_{free} \quad \text{(Eq. 3)}$$

Fitting of the equilibrium dialysis data to the above equation describing 1 site ligand binding gave a K_d value of 16.8 ± 2.5 μM (Figure 4.5A). This is in good agreement with the published K_m value of 23.5 ± 3.7 μM for AcCoA (Wright & Ladak, 1997).

4.3.6.2 Fluorescence Anisotropy Experiments

The compound 1, N^6-ethenocoenzyme A (εCoA) was used in steady-state anisotropy experiments to approximate the K_d for CoA binding to AAC(6')-Ii. Triplicate measurements were made in which ~ 2 mLs of 0.5 μM εCoA was titrated with increasing concentrations of AAC(6')-Ii. Concentrated enzyme was added in 2-5 μL increments to the solution containing εCoA, and the anisotropy changes measured after 1 min of stirring. All titrations were done at 25 °C in 25 mM Hepes, pH 7.5 and 1 mM EDTA using quartz cuvettes and a steady-state fluorescence spectrophotometer. Excitation of ε CoA occurred at 305 nm (4-nm slits), and emission monitored at 405 nm with 16-nm slits for both parallel and perpendicular components. The anisotropy *r* of εCoA was calculated by instrument software using the parallel *Ivv* and perpendicular *Ivh* polarized fluorescence intensities measured upon εCoA excitation. Data were fit to equation 4 as described previously (Richards *et al.*, 1996) to determine K_d using Grafit 4.0 software

(Leatherbarrow, 2000).

$$A = ((A_{bound} - A_{free}) * [AAC(6')\text{-}Ii] / K_d + [AAC(6')\text{-}Ii]) + A_{free} \quad \text{(Eq. 4)}$$

Fitting of the fluorescence anisotropy data to equation 4 gave a K_d value of 6.3 ± 0.6 μM (Figure 4.5B). Again this value is in the low μM range, representing only a 3.7-fold change relative to the K_m for AcCoA and a 2.7-fold difference from the K_d determined using equilibrium dialysis. Taken together, our results therefore allow us to equate K_m with K_d for this substrate.

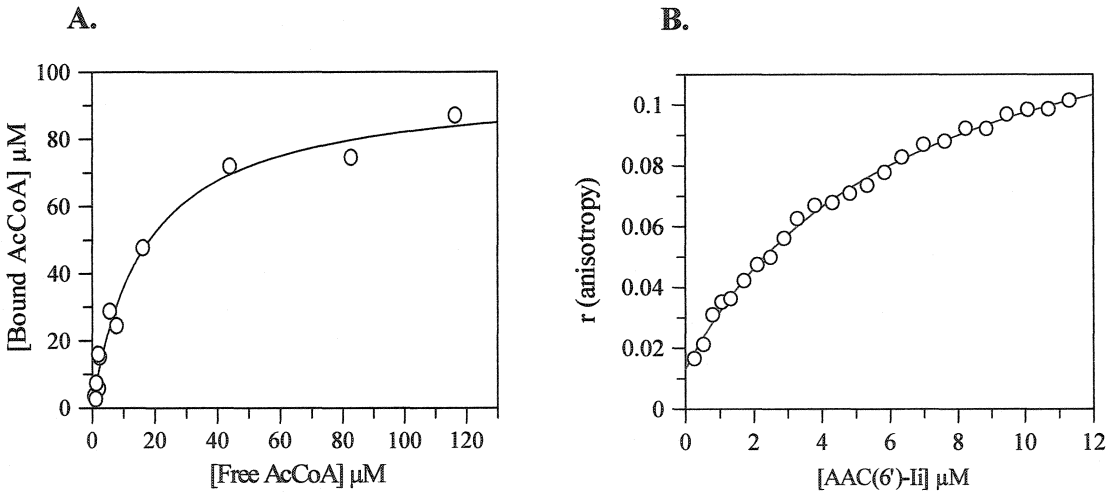

Figure 4.5: Non-linear fits of equilibrium dialysis (A) and fluorescence anisotropy (B) data used to determine dissociation constants (K_d). A K_d of 16.8 ± 2.5 μM was determined for AcCoA using equilibrium dialysis and a K_d of 6.3 ± 0.6 μM for ε*CoA* based on fluorescence anisotropy experiments.

4.3.7 Sucrose Viscosity Studies on AAC(6')-Ii Mutants

The rate of acetyl transfer for wild type AAC(6')-Ii is largely governed by CoA product release, as recently shown by solvent viscosity effects determined using the microviscosogen sucrose (Draker *et al.*, 2003). Viscosity studies were employed here to assess whether any of the amino acid substitutions under investigation affected the chemical step and therefore altered the rate limiting segment(s) of the reaction from product release to acetyl transfer chemistry. In such a case, we would not expect changes in enzymatic rates with increasing solvent viscosity. Viscosity studies with Glu72Ala, His74Ala, Leu76Ala, Leu76Pro, Tyr147Ala, and Tyr147Phe site mutants were done using the microviscosogen sucrose (0 – 30 %) and ribostamycin as the varied substrate as described previously (Draker *et al.*, 2003). Initial rate data were fit by non-linear least squares to equation 1 using Grafit 4.0 software (Leatherbarrow, 2000). Values reported in Table 4.3 are the slopes of plots from either k_{cat}^{0}/k_{cat} or $((k_{cat}/K_m^{0})/k_{cat}/K_m)$ *versus* the relative viscosity of the sucrose containing solution for each mutant.

4.3.8 pH Dependence on AAC(6')-Ii Activity

pH studies on the wild type enzyme were performed to generate a profile of enzyme activity as a function of pH. Acetyl transfer activity was monitored from pH 5.5 to 9.0 every 0.5 pH unit using overlapping 50 mM buffers of MES (pH 5.5-7.0), HEPES (pH 7.0-8.0), or TAPS (pH 8.0 - 9.0). The resulting kinetic data were fit to equation 1 to obtain the first- and second-order kinetic parameters k_{cat} and k_{cat}/K_m, respectively. Profiles were generated by plotting log k_{cat} or log k_{cat}/K_m as a function of pH and relevant pK values identified by a fit of the data to global equations of best fit using the Enzyme

Kinetics Module of Sigma Plot software (Brannan *et al.*, 2000). The wild type AAC(6')-Ii pH profile fit best to equation 3 describing a single pK_a value, where v is either the k_{cat} or k_{cat}/K_m rate constants, C represents the pH-independent value, K_a is the acid equilibrium constant, and H is the proton concentration;

$$\log v = \log [C/(1 + K_a/H)] \qquad \text{(Eq. 5)}$$

Similar studies on the His74Ala mutant were performed as described above for the wild type enzyme.

4.3.9 MIC Determinations

MICs of kanamycin A and neomycin were determined using the serial dilution method in liquid culture and microtiter plate format according to standard NCCLS guidelines (Standards, 2000). The MIC was defined in this study as the lowest concentration of AG antibiotic to completely inhibit growth of *E. coli* BL21(DE3) cells expressing wild type or mutant AAC(6')-Ii proteins. *E. coli* BL21(DE3) cells containing pET22b(+) or no plasmid DNA served as MIC controls. Western blot analysis of AAC(6')-Ii protein from bacterial lysates confirmed that expression levels of wild type and the various site mutants were comparable.

4.4 Results and Discussion

4.4.1 Purification and Stability of AAC(6')-Ii Site Mutants

The AAC(6')-Ii mutants Glu72Ala, His74Ala, Leu76Ala, Leu76Pro, Tyr147Ala, and Tyr147Phe were successfully overexpressed and purified using wild type procedures, indicating that these proteins maintained the general properties of the native protein.

In addition, partial proteolysis patterns for these mutants were identical to native AAC(6')-Ii, providing good evidence that the site mutations did not perturb the overall fold of the enzymes. The Glu72Gln and Glu72Asp mutants, which required lower overexpression temperatures to obtain soluble protein, were found to have an increased protease susceptibility and different proteolytic pattern compared to wild type, revealing that these proteins did not have the same protein fold as the native enzyme. As a result, only the substitution of Glu72 to Ala was characterized in this study.

4.4.2 Steady-State Kinetic Analysis of AAC(6')-Ii Site Mutants

Recent work on wild type AAC(6')-Ii has shown that the apparent affinity (K_m) of both AcCoA and AG for the enzyme approximates the dissociation constant (K_d) for these substrates (see section *4.3.6* and Draker *et al.*, 2003). This allows us to directly correlate changes in substrate K_ms for the site mutants as changes in binding affinity. Since we also know that the rate of acetyl transfer by AAC(6')-Ii is largely governed by product (CoA) release and is reflected in k_{cat} values, changes in catalytic efficiency (k_{cat}/K_m) as well as solvent viscosity effects were used to assess changes in the chemical steps for the various site mutants. The sucrose viscosity studies in particular were found to complement our steady-state kinetic analysis of each site mutant, as we could now assess whether each protein was catalytically impaired at the chemical steps as a result of the introduced mutation. Our results are discussed below for each site mutant with steady-state kinetic results included in Table 4.2 and solvent viscosity effects presented in Table 4.3.

Table 4.2: Steady-state kinetic parameters for wild type & mutant AAC(6')-Ii proteins [a]

Wild Type [b]

Substrate	K_m (μM)	k_{cat} (s^{-1})	k_{cat}/K_m ($M^{-1}s^{-1}$)
Acetyl-CoA	23.5 ± 3.7	0.40 ± 0.02	1.7×10^4
Neamine	5.8 ± 1.0	0.42 ± 0.02	7.2×10^4
Kanamycin A	19.9 ± 8.8	0.82 ± 0.21	4.6×10^4
Tobramycin	22.0 ± 5.6	1.1 ± 0.20	5.1×10^4
Amikacin	13.1 ± 2.1	0.11 ± 0.01	8.1×10^3
Neomycin	5.3 ± 0.6	0.20 ± 0.00	3.9×10^4
Ribostamycin	9.1 ± 2.0	0.34 ± 0.22	3.7×10^4

Glu72Ala

Substrate	K_m (μM)	k_{cat} (s^{-1})	k_{cat}/K_m ($M^{-1}s^{-1}$)
Acetyl-CoA	154 ± 39	0.99 ± 0.15	6.4×10^3
Neamine	482 ± 49	0.44 ± 0.01	9.1×10^2
Kanamycin A	3490 ± 512	0.55 ± 0.03	1.6×10^2
Tobramycin	1150 ± 304	1.1 ± 0.20	9.6×10^2
Amikacin	380 ± 51	0.05 ± 0.00	1.3×10^2
Neomycin	29.0 ± 4.2	1.1 ± 0.07	3.8×10^4
Ribostamycin	301 ± 43	0.35 ± 0.02	1.2×10^3

His74Ala

Substrate	K_m (μM)	k_{cat} (s^{-1})	k_{cat}/K_m ($M^{-1}s^{-1}$)
Acetyl-CoA	7.3 ± 0.8	0.18 ± 0.00	2.5×10^4
Neamine	43.2 ± 9.0	0.15 ± 0.02	3.5×10^3
Kanamycin A	14.4 ± 2.9	0.05 ± 0.00	3.3×10^3
Tobramycin	36.9 ± 3.6	0.30 ± 0.01	8.2×10^3
Amikacin	58.2 ± 4.8	0.04 ± 0.00	7.1×10^2
Neomycin	18.2 ± 3.2	0.19 ± 0.01	1.0×10^4
Ribostamycin	38.1 ± 3.9	0.23 ± 0.01	6.0×10^3

Leu76Ala

Substrate	K_m (μM)	k_{cat} (s^{-1})	k_{cat}/K_m ($M^{-1}s^{-1}$)
Acetyl-CoA	3.3 ± 0.6	0.23 ± 0.01	6.9×10^4
Neamine	22.4 ± 5.6	0.38 ± 0.01	1.7×10^4
Kanamycin A	25.7 ± 2.6	0.27 ± 0.01	1.1×10^4
Tobramycin	62 ± 12	0.89 ± 0.14	1.4×10^4
Amikacin	11.4 ± 2.1	0.03 ± 0.00	2.5×10^3
Neomycin	19.0 ± 3.0	0.16 ± 0.01	8.4×10^3
Ribostamycin	21.4 ± 1.0	0.15 ± 0.00	7.0×10^3

Table 4.2: *continued*

Leu76Pro

Substrate	K_m (μM)	k_{cat} (s^{-1})	k_{cat}/K_m ($M^{-1}s^{-1}$)
Acetyl-CoA	48.9 ± 9.9	0.06 ± 0.00	1.2×10^{3}
Neamine	68.2 ± 8.8	0.002 ± 0.000	3.1×10^{1}
Kanamycin A	No activity [c]		
Tobramycin	146 ± 23	0.01 ± 0.00	3.8×10^{1}
Amikacin	No activity		
Neomycin	57.3 ± 5.4	0.04 ± 0.00	6.5×10^{2}
Ribostamycin	107 ± 16	0.01 ± 0.00	7.7×10^{1}

Tyr147Ala

Substrate	K_m (μM)	k_{cat} (s^{-1})	k_{cat}/K_m ($M^{-1}s^{-1}$)
Acetyl-CoA	4.68 ± 0.81	0.01 ± 0.00	1.6×10^{3}
Neamine	169 ± 20	0.004 ± 0.000	2.2×10^{1}
Kanamycin A	110 ± 41	0.01 ± 0.00	5.6×10^{1}
Tobramycin	147 ± 22	0.004 ± 0.001	2.6×10^{1}
Amikacin	No activity		
Neomycin	38.6 ± 8.8	0.001 ± 0.000	3.6×10^{1}
Ribostamycin	109 ± 16	0.02 ± 0.00	1.5×10^{2}

Tyr147Phe

Substrate	K_m (μM)	k_{cat} (s^{-1})	k_{cat}/K_m ($M^{-1}s^{-1}$)
Acetyl-CoA	4.07 ± 0.79	0.07 ± 0.00	1.8×10^{4}
Neamine	150 ± 24	0.05 ± 0.00	3.2×10^{2}
Kanamycin A	340 ± 14	0.03 ± 0.01	1.0×10^{2}
Tobramycin	136 ± 19	0.10 ± 0.00	7.1×10^{2}
Amikacin	2190 ± 600	0.003 ± 0.000	1.2×10^{0}
Neomycin	55.3 ± 20.8	0.07 ± 0.01	1.3×10^{3}
Ribostamycin	306 ± 89	0.12 ± 0.01	4.0×10^{2}

[a] Reactions were carried out at 37°C in 25 mM MES, pH 6.0 and 1 mM EDTA.
[b] Kinetic parameters for wild type AAC(6')-Ii are reproduced from Wright & Ladak (1997)
[c] No measurable activity observed for up to 3 nmoles of protein added per reaction.

Table 4.3: Solvent viscosity effects on wild type and mutant AAC(6')-Ii activities [a]

Protein	$(k_{cat}^0/k_{cat})^{\eta}$ [b]	$((k_{cat}/K_b^0)/k_{cat}/K_b)^{\eta}$	Catalytic Mutant [c]
Wild Type [d]	0.52	0.72	No
Glu72Ala	0.04	0.02	Yes
His74Ala	0.21	- 0.03	Yes
Leu76Ala	0.61	0.70	No
Leu76Pro	0.35	0.07	Yes
Tyr147Ala	0.28	0.45	No
Tyr147Phe	0.54	0.60	No

[a] Reported sucrose viscosity effects are for k_{cat} and k_{cat}/K_b with ribostamycin as varied AG and saturating concentrations of AcCoA.
[b] The values reported are the slopes of plots for k_{cat}^0/k_{cat} or $((k_{cat}/K_b^0)/k_{cat}/K_b)$ *versus* the relative viscosity of the solution.
[c] AAC(6')-Ii proteins with an amino acid substitution that caused the chemical step of acetyl transfer to become rate-limiting was considered a catalytic mutant.
[d] Reproduced from Draker *et al.* (2003)

4.4.3 Role of Glu72

The mutation of Glu72 to Ala caused a notable reduction in affinity for both the 4,5- and 4,6-disubstituted classes of AGs, with the largest changes being an 83-fold decrease in the affinity for the minimal substrate neamine and a 175-fold reduction in K_m for kanamycin A (Table 4.2). Little change in the rate of substrate turnover was observed for any of the AGs tested, with the exception of a 5-fold increase in k_{cat} for neomycin acetylation. Reductions in specificity constants (k_{cat}/K_m) for this mutant were largely a result of the decrease in protein affinity for AG substrates, with the efficiency of neamine acetylation reduced by almost 80-fold and the specificity for kanamycin A decreased by 290-fold (Table 4.2). Sucrose viscosity studies revealed that this mutant was likely

impaired at the chemical step of acetyl transfer, as evidenced by the lack of an effect on both k_{cat} and k_{cat}/K_b in response to increasing solvent viscosity (Table 4.3). Since AAC(6')-Ii can also modify the model substrate poly-L-lysine (Wybenga-Groot *et al.*, 1999), kinetic parameters were determined for the Glu72Ala mutant using this peptide and revealed no significant change in this activity compared to wild type (1.25-fold change in k_{cat}/K_m).

Taken together, these kinetic results support a role for Glu72 in AG recognition and are not consistent with this residue acting as a general base in antibiotic or peptide acetylation. Our results instead suggest that the carboxylate moiety of Glu72 may be interacting, either directly or indirectly, with a common AG functional group on the 6-aminohexose or the aminocyclitol ring. The fact that the apparent affinity of AAC(6')-Ii for the peptide substrate poly-L-Lys was not affected by this mutation provides additional support that this residue interacts specifically with AG. Our sucrose viscosity results also imply that Glu72, in addition to its role in AG recognition, may be critical for the proper positioning and orientation of this substrate in the AAC(6')-Ii active site in order for efficient acetyl transfer to occur.

4.4.4 pH Dependence of AAC(6')-Ii Activity and the Role of His74

pH studies on the wild type enzyme were performed to identify enzyme ionizable groups that are relevant to the acetyl transfer mechanism. As we now know through viscosity studies and solvent isotope effects that substrate turnover, or $k_{cat,}$, is largely governed by a diffusion-controlled process and not the chemical step (Draker *et al.*, 2003), we have concentrated on catalytic efficiency, or k_{cat}/K_m values, in our analysis. In

addition, since AAC(6')-Ii follows an ordered bi-bi kinetic mechanism with AG being the second substrate to add in the formation of a productive ternary complex, changes in k_{cat}/K_b were analyzed in order to identify ionizable groups and protonation states relevant to both substrate binding and catalysis (Cleland, 1986). The results of our pH studies with wild type AAC(6')-Ii indicate that an ionizable group with a pK of 6.9 ± 0.1 is important for optimal acetyltransferase activity, determined from the best fit of the data to eq. 3. As can be seen from the plateau shaped pH profile in Figure 4.6A, the descending nature of the plot indicates that the ionizable group identified must be protonated for optimal catalytic efficiency. Since the determined pK value of 6.9 is consistent with the ionizable group of a histidine imidazole, pH studies were repeated with the His74Ala site mutant to investigate whether this residue was responsible for the observed pH dependence of wild type AAC(6')-Ii, the results of which are discussed below.

Steady-state kinetic parameters determined for the His74Ala mutant revealed only a small effect on enzyme activity. K_m values for AcCoA and the 4,5-and 4,6 disubstituted AGs only differed by a range of 2 to 7.5-fold compared to wild type, indicating no significant change in apparent affinity (Table 4.2). Similarly, rates of acetyl transfer to the AGs tested were almost identical to those obtained for the wild type protein. k_{cat}/K_m values were only slightly lower than wild type, ranging from a 6-fold reduction in tobramycin acetylation efficiency to a 20-fold decrease observed for neamine (Table 4.2). Surprisingly, solvent viscosity effects indicated that this substitution altered the rate-determining step of acetyl transfer from a diffusion-controlled process to the chemical

step. As can be seen from Table 4.3, no viscosity effect was observed for k_{cat}/K_b when AG was the varied substrate, in contrast to the significant effect observed for the wild type enzyme. Also supporting the importance of this residue are the results from pH studies with the His74Ala site mutant. Figure 4.6B clearly shows that the pH profile of His74Ala activity lacks the descending limb evident in the wild type plot (Figure 4a), revealing that the ionizable group of this residue was identified from the wild type pH profile. Most importantly, these findings support the identification of the ionization of the His74 imidazole, with a pK_a of 6.9 and in its protonated form, as essential for optimal AAC(6')-Ii activity, which effectively rules out the possibility that this residue functions as an active site base.

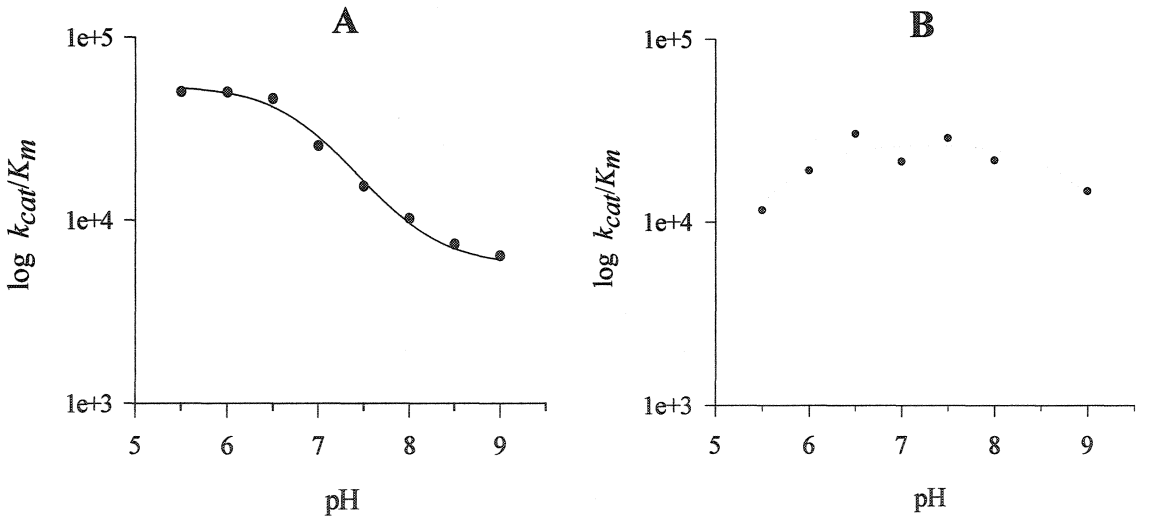

Figure 4.6: pH profiles of wild type AAC(6')-Ii (A) and His74Ala (B) activity as a function of pH. Shown are plots of log (k_{cat}/K_b) versus pH, which ranged from 5.5 to 9.0 using 50 mM buffers of MES, HEPES, or TAPS as described in materials and methods. Enzyme activity was measured with ribostamycin AG as the variable substrate and saturating concentrations of AcCoA. A single pK_a of 6.9 ± 0.1 was identified for the wild type protein based on the best fit of the generated data to equation 3. No relevant pK value was determined from the His74Ala pH profile based on the collected data.

The relatively close proximity of His74 NE2 to the carbonyl oxygen of AcCoA (~ 5 Å) in the crystal structure (Figure 4.4) raises an interesting possibility that it may serve to polarize this oxygen for greater electrophilicity at the carbonyl carbon and also stabilize the negative charge which forms on the carbonyl oxygen in the transition state. His74 may therefore contribute to the formation of an oxyanion hole in the AAC(6')-Ii active site.

4.4.5 Leu76

The potential role of the main chain NH of Leu76 in catalysis was investigated by mutating this residue to Ala or Pro, with the latter substitution eliminating the hydrogen bonding capacity of the backbone NH. The Leu76Ala mutant demonstrated virtually wild type activity as expected, with the biggest changes being a 3.6-fold reduction in the apparent affinity for neomycin and a 3.7-fold decrease in k_{cat} for amikacin (Table 4.2). Sucrose viscosity effects for this mutant were identical to the wild type enzyme, indicating that diffusion controlled processes still governed the rate of acetyl transfer (Table 4.3). In contrast, the Leu76Pro mutant was found to be dramatically impaired in both AG recognition and catalysis. Specificity constants in particular revealed a large decrease in AAC(6')-Ii catalytic efficiency, including a 2300-fold decrease in k_{cat}/K_b for neamine modification, a 1300-fold reduction in k_{cat}/K_b for tobramycin, and no detectable acetyl transfer activity towards several AGs (Table 4.2). Consistent with the kinetic analysis is the lack of a solvent viscosity effect on k_{cat}/K_b (Table 4.3), revealing that the substitution of Leu76 with Pro generates a catalytic mutant impaired at the chemical step.

These results and the obvious differences in Leu76Ala and Leu76Pro protein activities lend support to a role for the backbone NH of Leu76 in catalysis.

As Leu76 is adjacent to the GNAT-conserved β-bulge in AAC(6')-Ii, mutation of this residue to Pro would result in two adjacent prolines along β-strand 4. We are confident, however, that the kinetic changes for this mutant are a result of functional alterations in AAC(6')-Ii chemistry, as opposed to structural changes in the active site as a consequence of the introduced mutation. First, wild type proteolysis patterns were observed for the Leu76Pro mutant, indicating no gross changes in AAC(6')-Ii tertiary structure. Also, the mutation to Pro is not expected to alter the hydrogen bonding patterns between β-strands 3 and 4, since the amide NH of Leu76 does not participate in these interactions. Finally, the Leu76Pro site mutant displays only a marginal decrease (2-fold) in the affinity for acetyl CoA, suggesting that this mutation does not affect the enzyme's interactions with this substrate. Taken together, the evidence presented here does implicate the amide NH of Leu76 in transition state or intermediate stabilization and reveals that this backbone interaction is a requirement for efficient AAC(6')-Ii catalysis.

4.4.6 Tyr147

Replacement of Tyr147 with Ala caused significant reductions in AAC(6')-Ii affinity for all the AGs tested in addition to reductions in k_{cat} (Table 4.2). As a result, specificity constants (k_{cat}/K_m) were dramatically lower than for the wild type protein, with changes ranging from 250-fold for ribostamycin acetylation to over a 3000-fold reduction for neamine modification. Characterization of the Tyr147Phe was more informative, as the

substitution to Phe maintains the aromatic ring of the side chain but removes the hydrogen bonding potential and general acid capabilities of the Tyr phenolic hydroxyl. As can be seen from Table 4.2, this mutant also demonstrated significant reductions in both apparent affinity (K_m) and catalytic turnover (k_{cat}), resulting in lower specificity constants compared to the wild type enzyme. In particular, decreases in AG affinity ranged from a 6-fold decrease for tobramycin to a large 170-fold change in K_m for amikacin (Table 4.2). In general, the significant reductions in catalytic efficiency observed for the Tyr147Phe mutant suggests that the side chain hydroxyl plays a critical role in AAC(6')-Ii catalysis. Solvent viscosity studies on both Tyr147Ala and Tyr147Phe proteins, however, demonstrated that rate-limiting segments in catalysis remained diffusion-controlled, with only slightly smaller effects observed for the Tyr147Ala mutant compared to the wild type enzyme (Table 4.3). As well, pH studies did not identify an ionizable group consistent with a Tyr to be important for protein activity, suggesting that Tyr147 is not acting as an active site acid. The results presented here are consistent with the hydroxyl group of Tyr147 acting in some capacity to orient the acetyl moiety of AcCoA for optimal interaction with AG. It is possible that without this interaction the position of the acetyl-group may be altered slightly and actually perturb the productive binding of AG, likely explaining the reductions in Tyr147Phe affinity noted for this second substrate. Our results therefore suggest that Tyr147 does not act as the general acid in catalysis, but instead plays a major role in orienting the acetyl group for efficient transfer to the 6'-amino group of AGs.

4.4.7 MIC Determinations

To complement our *in vitro* analysis, we investigated the effects of each amino acid substitution on protein activity *in vivo* by MIC determinations of kanamycin A and neomycin for *E. coli* BL21(DE3) cells expressing either wild type AAC(6')-Ii or one of the site mutants. As can be seen from Table 4.4, all of the mutants conferred a lower level of resistance to kanamycin A compared to the wild type protein. Increased susceptibility to this AG was most notable with Leu76Pro, Tyr147Ala, and Tyr147Phe proteins, revealed by a 16-fold change in MIC (Table 4.4). Similarly, the substitution of Glu72 with Ala caused an 8-fold change in MIC with kanamycin A, likely due to the large decreases in protein affinity for AGs as determined from our kinetic studies.

Table 4.4: MICs of select AGs for AAC(6')-Ii site mutants

Site Mutant	***MIC in µg/mL***	
	Kanamycin A	**Neomycin**
BL21(DE3) [a]	4	1
Wild Type	128	8
Glu72Ala	16	4
His74Ala	32	4
Leu76Ala	32	8
Leu76Pro	8	1
Tyr147Ala	8	4
Tyr147Phe	8	4

[a] Negative control using *E.coli* BL21(DE3) and *E.coli* BL21(DE3)/pET22b(+).

In contrast to that observed for kanamycin A, changes in MICs in the presence of neomycin were for the most part small, with no change observed for the Leu76Ala mutant, and only a 2-fold decrease in the MIC due to Glu72Ala, His74Ala, Tyr147Ala, and Tyr147Phe activities. The Leu76Pro protein, on the other hand, conferred no resistance to neomycin, with *E. coli cells* expressing this mutant becoming completely susceptible to this AG (Table 4.4). Overall, the increase in drug susceptibility observed by a decrease in MIC for *E. coli* expressing the mutant enzymes correlated well with changes in protein activity demonstrated *in vitro*.

4.4.8 Implications for the GNAT Superfamily

Characterization of the AAC(6')-Ii site mutants described here has convincingly shown the importance of Glu72, His74, Tyr147 and the amide NH of Leu76 in catalysis. Since the structural fold and active site geometry of GNAT enzymes are very similar, our results also allow us to compare the functions of these residues with equivalent amino acids from other GNAT enzymes. Our finding that Glu72 is not behaving as the active site base in AAC(6')-Ii catalysis contrasts what was shown for Glu173 from tGCN5, an equivalent residue acting as the general base in histone modification (Tanner *et al.*, 1999). Similarly, His122 from AANAT (Scheibner *et al.*, 2002) and Asp99 from AAC(6')-Ie (Boehr *et al.*, 2003) are geometrically equivalent to His74 from AAC(6')-Ii, and have both been shown to function as an active site base. Our results indicate that His74 is instead critical for optimal enzyme activity in its protonated form, and may contribute to the formation of an oxyanion hole in the active site. Additional differences

were also observed for the role of the GNAT conserved Tyr in acetyl transfer. Tyr168 from AANAT has been characterized as the general acid in serotonin acetylation by AANAT (Scheibner *et al.*, 2002), with a similar function for AAC(6')-Ii Tyr147 not supported based on our current results. Interestingly, mutation of an equivalent Tyr in AAC(6')-Ib (Tyr166) and *in vivo* analysis of protein activity implicated this residue in the recognition of AG substrates (Shmara *et al.*, 2001), which is consistent with the changes in AG affinity that we observed with the mutation of Tyr147 in AAC(6')-Ii. Lastly, we have shown the importance of the amide NH of Leu76 in AAC(6')-Ii activity, a finding that supports its involvement in transition state or intermediate stabilization and confirms previous speculation that this main chain element is critical for catalysis.

Our results and the growing body of information available on the catalytic mechanisms of several other GNAT enzymes clearly reveal differences in catalysis among these proteins, particularly in the function of geometrically equivalent, active site residues. As members of this superfamily are structural homologs and bind AcCoA in a similar manner, we propose that the observed differences are a consequence of the acyl-accepting substrate. Since all GNAT enzymes to our knowledge follow a ternary complex mechanism, the requirement to bind both substrates in the active site would generate obvious differences in acetyl transfer chemistry, especially given the diverse group of acyl-accepting substrates. The unique ability of AAC(6')-Ii to acetylate both AGs and basic proteins, for example, could be attributed to the different roles of active site residues as discussed, compared to other AACs and HAT enzymes. Furthermore, with the exception of the Leu76Pro mutation, mutagenesis of amino acid residues, while impeding

optimal catalysis, did not result in catastrophic loss of activity either *in vivo* or *in vitro*. This parallels several studies with other GNAT family members. The primary role of the GNAT protein scaffold may then simply be to bind and orient acyl-CoAs and their cognate substrates in a geometry appropriate to acyl group transfer, rather than to provide a framework for setting a constellation of amino acids residues essential for group transfer chemistry.

4.5 References

Angus-Hill, M. L., R. N. Dutnall, S. T. Tafrov, R. Sternglanz, and V. Ramakrishnan. (1999) Crystal structure of the histone acetyltransferase Hpa2: A tetrameric member of the GCN5-related *N*-acetyltransferase superfamily. *J Mol Biol* 294: 1311-25.

Bhatnagar, R. S., K. Futterer, T. A. Farazi, S. Korolev, C. L. Murray, E. Jackson-Machelski, G. W. Gokel, J. I. Gordon, and G. Waksman. (1998) Structure of *N*-myristoyltransferase with bound myristoyl CoA and peptide substrate analogs. *Nat Struct Biol* 5: 1091-7.

Boehr, D. D., S. I. Jenkins, and G. D. Wright. (2003) The molecular basis of the expansive substrate specificity of the antibiotic resistance enzyme aminoglycoside acetyltransferase-6'-aminoglycoside phosphotransferase-2". The role of Asp-99 as an active site base important for acetyl transfer. *J Biol Chem* 278: 12873-80.

Brannan, T., B. Althoff, L. Jacobs, J. Norby, and Rubenstein S. Enzyme Kinetics Module 1.0 of Sigmaplot 2000 for Windows. Version 6.10, SSPS Inc., Chicago, IL.

Cleland, W. W. (1986) Enzyme kinetics as a tool for determination of enzyme mechanisms. In *Investigation of rates and mechanisms of reactions, part 1: General considerations and reactions at conventional rates.* C. F. Bernasconi & A. Weisberger,eds. John Wiley & Sons, New York. 854-870.

Clements, A., J. R. Rojas, R. C. Trievel, L. Wang, S. L. Berger, and R. Marmorstein. (1999) Crystal structure of the histone acetyltransferase domain of the human PCAF transcriptional regulator bound to coenzyme A. *Embo J* 18: 3521-32.

Costa, Y., M. Galimand, R. Leclercq, J. Duval, and P. Courvalin. (1993) Characterization of the chromosomal *aac(6')-Ii* gene specific for *Enterococcus faecium*. *Antimicrob. Agents Chemother.* 37: 1896-1903.

Daigle, D. M., D. W. Hughes, and G. D. Wright. (1999) Prodigious substrate specificity of AAC(6')-APH(2"), an aminoglycoside antibiotic resistance determinant in enterococci and staphylococci. *Chem Biol* 6: 99-110.

Davies, J. & G. D. Wright. (1997) Bacterial resistance to aminoglycoside antibiotics. *Trends Microbiol* 5: 234-40.

DeLano, W. L. The PyMOL molecular graphics system 0.82. DeLano Scientific, San Carlos, CA. USA.

Draker, K. A., D. B. Northrop, and G. D. Wright. (2003) Kinetic mechanism of the GCN5-related chromosomal aminoglycoside acetyltransferase AAC(6')-Ii from *Enterococcus faecium*: Evidence of dimer subunit cooperativity. *Biochemistry* 42: 6565-6574.

Dutnall, R. N., S. T. Tafrov, R. Sternglanz, and V. Ramakrishnan. (1998) Structure of the histone acetyltransferase Hat1: A paradigm for the GCN5-related *N*-acetyltransferase superfamily. *Cell* 94: 427-438.

Dyda, F., D. C. Klein, and A. B. Hickman. (2000) GCN5-related *N*-acetyltransferases: A structural overview. *Annu Rev Biophys Biomol Struct* 29: 81-103.

Hickman, A. B., D. C. Klein, and F. Dyda. (1999a) Melatonin biosynthesis: The structure of serotonin *N*-acetyltransferase at 2.5 Å resolution suggests a catalytic mechanism. *Mol Cell* 3: 23-32.

Hickman, A. B., M. A. Namboodiri, D. C. Klein, and F. Dyda. (1999b) The structural basis of ordered substrate binding by serotonin *N*-acetyltransferase: Enzyme complex at 1.8 Å resolution with a bisubstrate analog. *Cell* 97: 361-9.

Huycke, M. M., D. F. Sahm, and M. S. Gilmore. (1998) Multiple-drug resistant enterococci: The nature of the problem and an agenda for the future. *Emerg Infect Dis* 4: 239-49.

Leatherbarrow, R. J. Grafit 4.0. Erithacus Software. Staines, UK.

Llano-Sotelo, B., E. F. Azucena, L. P. Kotra, S. Mobashery, and C. S. Chow. (2002) Aminoglycosides modified by resistance enzymes display diminished binding to the bacterial ribosomal aminoacyl-tRNA site. *Chem Biol* 9: 455-63.

Murray, B. E. (1998) Diversity among multidrug-resistant enterococci. *Emerg Infect Dis* 4: 37-47.

Patterson, J. E.&M. J. Zervos. (1990) High-level gentamicin resistance in enterococcus: Microbiology, genetic basis, and epidemiology. *Rev Infect Dis* 12: 644-52.

Peneff, C., D. Mengin-Lecreulx, and Y. Bourne. (2001) The crystal structures of apo and complexed *Saccharomyces cerevisiae* GNA1 shed light on the catalytic mechanism of an amino-sugar *N*-acetyltransferase. *J Biol Chem* 276: 16328-34.

Poux, A. N., M. Cebrat, C. M. Kim, P. A. Cole, and R. Marmorstein. (2002) Structure of the GCN5 histone acetyltransferase bound to a bisubstrate inhibitor. *Proc Natl Acad Sci U S A* 99: 14065-70.

Richards, J. P., H. P. Bachinger, R. H. Goodman, and R. G. Brennan. (1996) Analysis of the structural properties of camp-responsive element-binding protein (CREB) and phosphorylated CREB. *J Biol Chem* 271: 13716-23.

Rojas, J. R., R. C. Trievel, J. Zhou, Y. Mo, X. Li, S. L. Berger, C. D. Allis, and R. Marmorstein. (1999) Structure of tetrahymena GCN5 bound to coenzyme A and a histone H3 peptide. *Nature* 401: 93-8.

Scheibner, K. A., J. De Angelis, S. K. Burley, and P. A. Cole. (2002) Investigation of the roles of catalytic residues in serotonin *N*-acetyltransferase. *J Biol Chem* 277: 18118-26.

Shaw, K.J. & G. D. Wright. (2000) Aminoglycoside resistance in gram-positive bacteria. In *Gram-positive pathogens*. V.A. Fischetti, R.P. Novick, J.J. Ferretti, D.A. Portnoy and J.I. Rood,eds. ASM press, Washington, D.C. 635-646.

Shmara, A., N. Weinsetel, K. J. Dery, R. Chavideh, and M. E. Tolmasky. (2001) Systematic analysis of a conserved region of the aminoglycoside 6'-*N*-acetyltransferase type Ib. *Antimicrob Agents Chemother* 45: 3287-92.

Standards, National Committee for Clinical Laboratory. (2000) Methods for dilution antimicrobial susceptibility tests for bacteria that grow aerobically; approved standard - fifth edition. Document M7 - A5.

Tanner, K. G., R. C. Trievel, M. H. Kuo, R. M. Howard, S. L. Berger, C. D. Allis, R. Marmorstein, and J. M. Denu. (1999) Catalytic mechanism and function of invariant glutamic acid 173 from the histone acetyltransferase GCN5 transcriptional coactivator. *J Biol Chem* 274: 18157-60.

Trievel, R. C., J. R. Rojas, D. E. Sterner, R. N. Venkataramani, L. Wang, J. Zhou, C. D. Allis, S. L. Berger, and R. Marmorstein. (1999) Crystal structure and mechanism of histone acetylation of the yeast GCN5 transcriptional coactivator. *Proc Natl Acad Sci U S A* 96: 8931-6.

Vetting, M. W., S. S. Hegde, F. Javid-Majd, J. S. Blanchard, and S. L. Roderick. (2002) Aminoglycoside 2'-N-acetyltransferase from *Mycobacterium tuberculosis* in complex with coenzyme A and aminoglycoside substrates. *Nat Struct Biol* 9: 653-8.

Wennersten, C.B. & R.C. Moellering JR. (1980) Mechanism of resistance to penicillin-aminoglycoside synergism in *Streptococcus faecium*. In *Current chemotherapy and infectious disease*, 1. J.D. Nelson & C. Grassi, eds. American Society for Microbiology, Washington, D.C. 710-712.

Weston, S. A., R. Camble, J. Colls, G. Rosenbrock, I. Taylor, M. Egerton, A. D. Tucker, A. Tunnicliffe, A. Mistry, F. Mancia, E. de la Fortelle, J. Irwin, G. Bricogne, and R. A. Pauptit. (1998) Crystal structure of the anti-fungal target *N*-myristoyl transferase. *Nat Struct Biol* 5: 213-21.

Williams, J. W. & D. B. Northrop. (1978) Kinetic mechanisms of gentamicin acetyltransferase I. Antibiotic-dependent shift from rapid to nonrapid equilibrium random mechanisms. *J Biol Chem* 253: 5902-7.

Wolf, E., A. Vassilev, Y. Makino, A. Sali, Y. Nakatani, and S. K. Burley. (1998) Crystal structure of a GCN5-related *N*-acetyltransferase: *Serratia marcescens* aminoglycoside 3-*N*-acetyltransferase. *Cell* 94: 439-49.

Wright, G. D., A. M. Berghuis, and S. Mobashery. (1998) Aminoglycoside antibiotics. Structures, functions, and resistance. *Adv Exp Med Biol* 456: 27-69.

Wright, G.D. & P. Ladak. (1997) Overexpression and characterization of the chromosomal aminoglycoside 6'-*N*-acetyltransferase from *Enterococcus faecium*. *Antimicrob. Agents Chemother.* 41: 956-960.

Wybenga-Groot, L. E., K. Draker, G. D. Wright, and A. M. Berghuis. (1999) Crystal structure of an aminoglycoside 6'-*N*-acetyltransferase: Defining the GCN5-related *N*-acetyltransferase superfamily fold. *Structure Fold Des* 7: 497-507.

Chapter 5

Studies on the Putative Aminoglycoside Binding Site of AAC(6')-Ii

5.0 Summary

This chapter briefly describes site-directed mutagenesis studies that were performed in an attempt to better characterize the AG binding site of AAC(6')-Ii. Using structural information obtained from the AAC(6')-Ii·AcCoA binary complex (Wybenga-Groot *et al.*, 1999), we mutated several Glu and Asp residues that form a negatively charged surface patch localized at the enzyme active site. Mutation of Glu28 revealed that this residue is critical to the proper tertiary fold of the enzyme and may participate in important hydrogen bonding interactions, possibly with AG substrates. Mutation of Glu39 to Ala had virtually no impact on AG acetylation and is most likely not involved in direct interactions with AG functional groups. Glu72, previously characterized in chapter 4, was shown to be important in the proper binding and orientation of AG substrates in the active site. Similarly, residues Asp112 and Asp168 both appear to play an important role in AG binding, with interactions of the Asp168 side chain at the dimer interface implicated in the formation of a proper AG binding site. In general, this mutagenesis work awaits structural elucidation of AAC(6')-Ii in complex with bound AG and/or molecular modeling studies in order to complement the analysis presented here.

The research described in this chapter was performed in collaboration with Christina Capone, a summer student who generated a number of the site mutants described here. She was also responsible for purification of the Glu28Gln, Glu39Ala, Asp112Ala, and Asp168Ala mutants in addition to assessing the structural integrity of these proteins by partial proteolysis. We thank Christina for her contribution to this work.

5.1 Introduction

The available crystal structures of all three representative classes of AMEs has provided valuable information regarding both substrate binding and catalysis by these resistance proteins (reviewed in Wright, 1999 and Smith & Baker, 2002). In particular, the presence of a negatively charged surface patch hypothesized to be the AG binding site has been noted in all AME structures, including the kanamycin nucleotidylyltransferase ANT(4') (Sakon *et al.*, 1993; Pedersen *et al.*, 1995), the phosphotransferase APH (3')-IIIa (Hon *et al.*, 1997; Fong & Berghuis, 2002), as well as the AAC(3)-I, AAC(6')-Ii, and AAC(2')-Ic acetyltransferases (Wolf *et al.*, 1998; Wybenga-Groot *et al.*, 1999; Vetting *et al.*, 2002). Made up of several negatively charged Glu and Asp residues, this region is believed to draw in the cationic AG substrates to the enzyme active site by electrostatic interactions (Wright *et al.*, 1998). A greater understanding of the specific interactions between inactivating enzymes and AGs has also come from crystallographic studies, in which several AME structures in complex with bound AG have been reported. These include ANT(4') in complex with an ATP analog and kanamycin (Pedersen *et al.*, 1995), APH(3')-IIIa with bound ADP and kanamycin or neomycin (Fong & Berghuis, 2002), and AAC(2')-Ic in complex with CoA and kanamycin, tobramycin, or ribostamycin (Vetting *et al.*, 2002). In the case of APH(3')-IIIa, additional studies involving site-directed mutagenesis and molecular docking experiments have aiding in characterizing the AG binding site for this enzyme (Thompson *et al.*, 1999), in addition to complementing the subsequent structural determination of this AME with bound AG (Fong & Berghuis, 2002). More importantly, this work also reveals the utility in studying

AG binding by protein mutagenesis and other studies, providing a rationale for the AAC(6')-Ii studies described here.

Similar to other AMEs, the structure of AAC(6')-Ii in complex with AcCoA reveals an obvious surface patch of negative charge, localized between the two domains of the protein monomer (Figure 5.1). This anionic depression consists of several negatively charged amino acids in close proximity to the acetyl moiety of AcCoA (see Figure 5.2), including the residues Glu28, Glu39, Glu72, Asp112, and Asp168, all hypothesized to be involved in AG binding (Wybenga-Groot *et al.*, 1999).

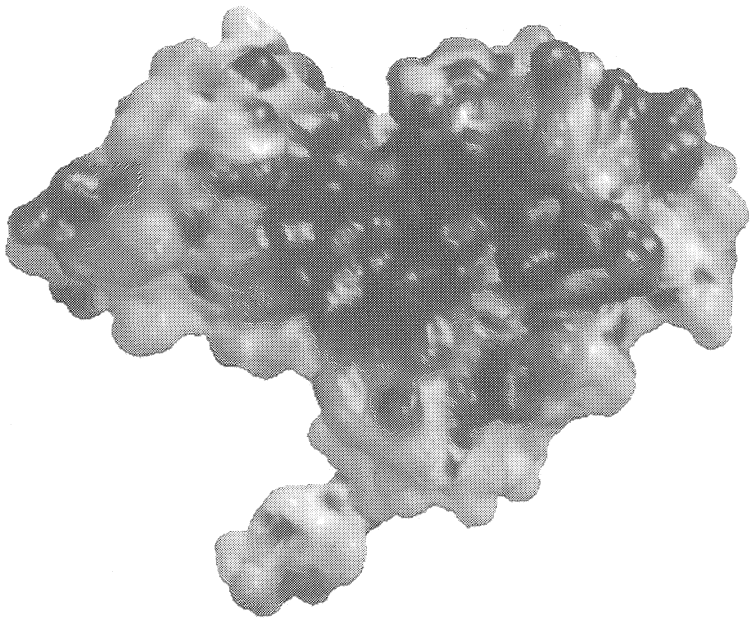

Figure 5.1: Electrostatic surface potential of the AAC(6')-Ii monomer in complex with AcCoA. The molecular surface potential is colored red (electronegative) to blue (electropositive) using the range -10 to +10 k_BT and was calculated using the program GRASP (Nicholls *et al.*, 1991). Present in the region of the active site cleft between the N-terminal (right) and C-terminal (left) domains of the monomer is the negatively charged surface patch, hypothesized to be the AG binding site. This figure was adapted from Wybenga-Groot *et al.* (1993) with permission from Elsevier.

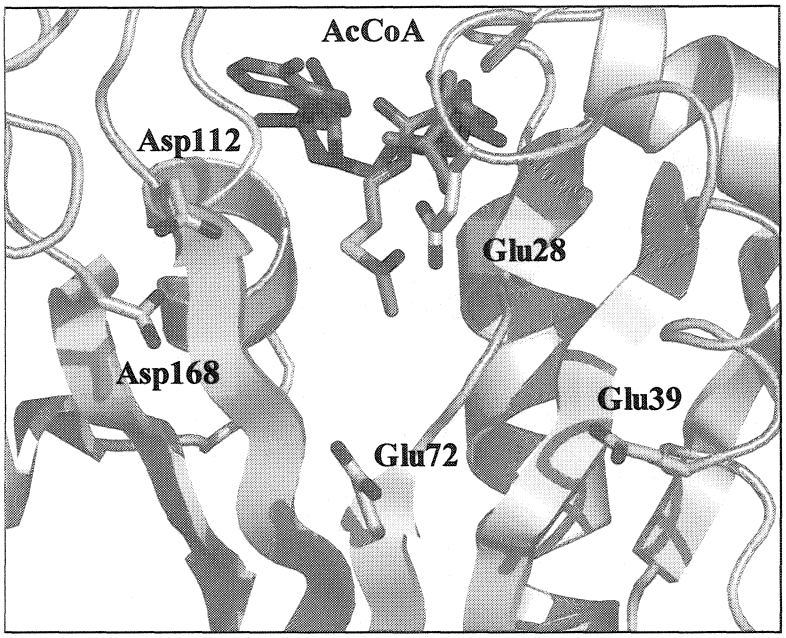

Figure 5.2: Several negatively charged residues make up the putative AG binding site of AAC(6')-Ii. Indicated above are the residues Glu28, Glu39, Glu72, Asp112, and Asp168. The active site view of the AAC(6')-Ii·AcCoA complex is shown with the same protein orientation as that represented in Figure 5.1. This figure was generated using PyMOL molecular graphics software (DeLano, 2002).

Also of interest is the arrangement of these Glu and Asp residues in the AAC(6')-Ii dimer, recently solved in complex with CoA by Burk *et al.* (2003). As shown in Figure 5.3, the putative AG binding sites from each monomer are in close proximity to one another, which essentially creates a larger region of electronegativity to draw in AG substrates. In addition, this configuration may help to explain the subunit cooperativity observed for the AAC(6')-Ii dimer during our kinetic mechanism studies, which are described in detailed in chapter 3.

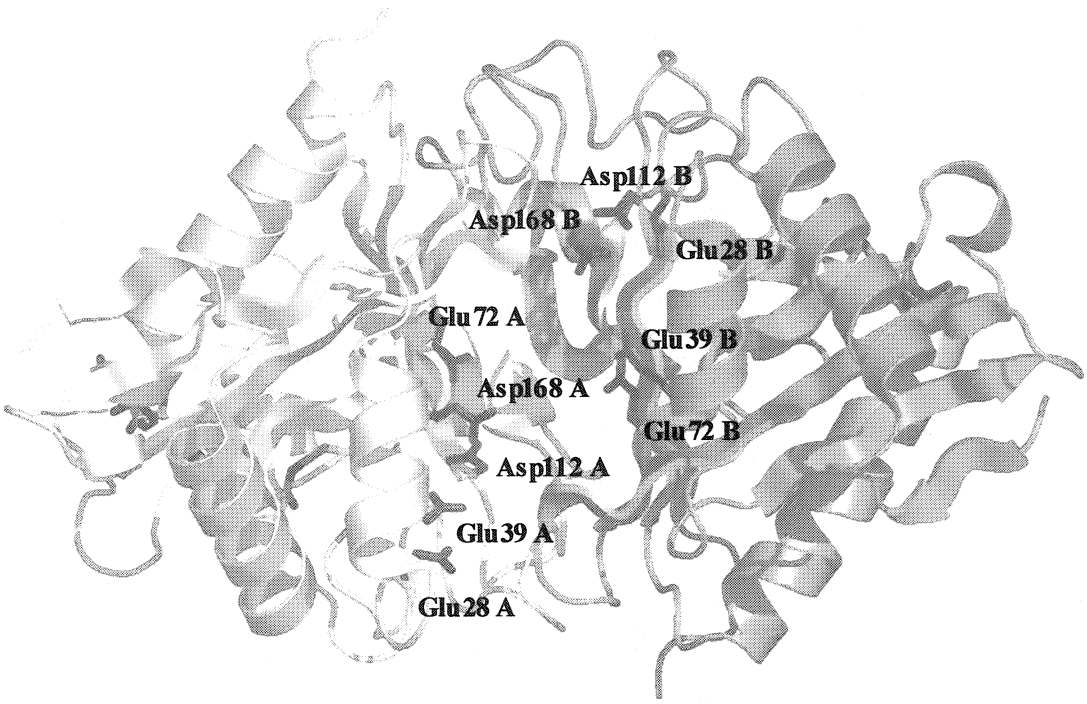

Figure 5.3: The close proximity of putative AG binding sites in the AAC(6')-Ii dimer. The entire side chain of each Glu or Asp residue under investigation is colored red for clarity, with monomer A shown as light grey and monomer B as dark grey. Bound CoA in each monomer is also represented, with the sulfur of CoA in yellow. This figure was generated with PyMOL (DeLano, 2002), using the pdb code 1N71 (Burk *et al.*, 2003).

With the exception of Asp168 (discussed below), none of the residues mutated in this study make any contacts with the opposing subunit in the AAC(6')-Ii dimer. Several pieces of evidence also indicate that there is one functional active site per monomer, including initial steady-state kinetic analysis of the wild type enzyme (Wright & Ladak, 1997) and recent studies on a monomeric mutant of AAC(6')-Ii (Draker *et al.*, 2003).

Based on information from the crystal structure of ACC(6')-Ii in complex with AcCoA (Wybenga-Groot *et al.*, 1999), Glu28 is found in the loop region between

α-helices 1 and 2 and hydrogen bonds with one of many water molecules ordered in the enzyme active site. Glu39 is the last residue of α2 and is the fourth negatively charged amino acid along this helix. Glu72 is part of β-strand 4, which makes the majority of protein contacts with the AcCoA substrate. Similar to Glu28, Asp112 also interacts with ordered water molecules in the active site when AcCoA is bound. Finally, Asp168 is the first residue of β-strand 7 in the C-terminal region of AAC(6')-Ii. Based on structural data from the AAC(6')-Ii dimer (Burk *et al.,* 2003 & pdb code 1N71), the side chain of this amino acid makes up part of the dimer interface, hydrogen bonding with the phenolic hydroxyl of Tyr66 from the opposing monomer.

In the absence of a crystal structure of AAC(6')-Ii in complex with both cofactor and antibiotic, we turned to site-directed mutagenesis of Glu28, Glu39, Glu72, Asp112, and Asp168 in hopes of defining the antibiotic binding site of AAC(6')-Ii. Steady-state kinetic analysis of AAC(6')-Ii site mutants and *in vivo* analysis of their AG inactivation activity in *E. coli* were used to assess the importance and possible role of each residue in binding AGs.

5.2 Materials and Methods

Only a brief description of experimental procedures is given here since many of the same methods are described in the previous chapter. Details regarding mutation of Glu72 can also be found in chapter 4. Refer to section *4.3*, pages 119-126 for additional details.

5.2.1 General

AGs, AcCoA, DTDP, and mutagenic oligonucleotide primers were from the same sources as indicated in chapter 4, section *4.3.1.*

5.2.2 Site-Directed Mutagenesis of AAC(6')-Ii

Glu28, Glu39, Asp112, and Asp168 mutants of AAC(6')-Ii were generated by the QuikChange mutagenesis procedure as described in section *4.3.2*, page 119. The mutagenic oligonucleotide primers used are included in Table 5.1 with the reverse complement of each primer not shown. Confirmation of the desired mutation and subsequent overexpression were also as described in section *4.3.2.*

Table 5.1: Mutagenic oligonucleotides used in this study

Mutation	Oligonucleotide Sequence [a]
Glu28Gln	5'- ctgacttggccggaacaatatggagacagc - 3'
Glu39Ala	5'- cggcagaagaagtagaagctatgatgaatcc - 3'
Asp112Ala	5'- cgatttatttaggtacggctgatttagaccatgg - 3'
Asp112Asn	5'- cgatttatttaggtacgaatgatttagaccatgg - 3'
Asp168Ala	5'- ggctgggacaaaccggctatttggatggc - 3'
Asp168Asn	5'- ggctgggacaaaccgaatatttggatggc - 3'

[a] Underlined bases indicate the codon change used to generate the desired amino acid substitution.

5.2.3 Purification of Site Mutants and Steady-State Kinetic Analysis

Overexpressed wild type and mutant AAC(6')-Ii proteins were purified by the three-step procedure described previously (Wright & Ladak, 1997). Soluble Glu28Ala and Glu28Asp proteins could not be obtained and thus only the purified Glu28Gln site mutant is discussed here. The structural integrity of purified site mutants was assessed by partial proteolysis relative to wild type digestion patterns, as described in section *4.3.4.*

Steady-state kinetic analysis of mutant AAC(6')-Ii activities were performed as described in section *4.3.5* using the same spectrophotometric assay and microtiter plate format. Initial rates were fit to equation 1 describing Michaelis-Menton kinetics using Grafit 4.0 (Leatherbarrow, 2000);

$$v = k_{cat}E_t[S]/(K_m + [S]) \qquad \text{(Eq. 1)}$$

5.2.4 Sucrose Viscosity Effects on AAC(6')-Ii Site Mutants

As described in chapter 3, solvent viscosity studies were used to determine that diffusion-controlled processes govern the rate of AAC(6')-Ii catalysis. The effects of increasing solvent viscosity on the activity of Glu28Gln, Glu39Ala, Asp112Ala, Asp112Asn, Asp168Ala, and Asp168Asn site mutants were assessed by determining the kinetic parameters k_{cat} and k_{cat}/K_m at 0 % and 30 % sucrose using ribostamycin as the varied substrate (see section *4.3.7* for additional details). The ratio of k_{cat}^0/k_{cat} and $(k_{cat}/K_m^0)/(k_{cat}/K_m)$ obtained for each mutant were similar to wild type ratios, indicating that none of the above proteins became impaired at the chemical step of acetyl transfer as a result of the introduced mutation. Note that substitution of Glu72 to Ala did result in the generation of a catalytic mutant, with significant changes in solvent viscosity effects compared to the wild type enzyme, as described in chapter 4.

5.2.5 MIC Determinations

MICs of kanamycin A and neomycin were determined using the serial dilution method in liquid culture and microtiter plate format according to standard NCCLS guidelines (Standards, 2000), with the same MIC and protein level controls as described in section *4.3.9*, page 126.

5.3 Results and Discussion

The AAC(6')-Ii site mutants Glu28Gln, Glu39Ala, Glu72Ala, Asp112Ala, Asp112Asn, Asp168Ala, and Asp168Asn were all successfully purified using wild type procedures and shown to have the same partial proteolysis patterns as the native enzyme, providing good evidence that the amino acid substitutions did not perturb the overall fold and tertiary structure of the proteins. Steady-state kinetic parameters for these site mutants are presented in Table 5.2 with the exception of Glu72Ala, which is detailed in section *4.4.3* and Table 4.2 of the previous chapter.

5.3.1 Glu28Gln

As mentioned in section *5.2.3*, attempts to obtain soluble Glu28Ala and Glu28Asp proteins were unsuccessful using wild type procedures and variations in growth and protein overexpression conditions. This suggests that this residue is in some way critical for wild type protein stability and structural integrity. The fact that the most conservative substitution of Glu28 to Gln was tolerated suggests that side chain length and hydrogen bonding capabilities are essential at this position. Based on steady-state kinetic analysis, the mutation of Glu28 to Gln appeared to have little effect on AG binding or acetyl transfer. Only slight increases in K_ms were observed, ranging from a 2.5-fold change in apparent affinity for neamine to a 4.8-fold change observed for amikacin. (Table 5.2). In addition, no significant changes in catalytic efficiency of AG modification, reflected in k_{cat}/K_m values, were observed relative to the wild type enzyme. As a whole, these results suggest that Glu28 participates in important hydrogen bonding interactions, although our current data does not specifically identify a role for this residue in AG binding.

Table 5.2: Steady-state kinetic parameters for wild type & mutant AAC(6')-Ii proteins [a]

Wild Type [b]			
Substrate	K_m (μM)	k_{cat} (s^{-1})	k_{cat}/K_m ($M^{-1}s^{-1}$)
Acetyl-CoA	23.5 ± 3.7	0.40 ± 0.02	1.7×10^4
Neamine	5.8 ± 1.0	0.42 ± 0.02	7.2×10^4
Kanamycin A	19.9 ± 8.8	0.82 ± 0.21	4.6×10^4
Tobramycin	22.0 ± 5.6	1.1 ± 0.20	5.1×10^4
Amikacin	13.1 ± 2.1	0.11 ± 0.01	8.1×10^3
Neomycin	5.3 ± 0.6	0.20 ± 0.00	3.9×10^4
Ribostamycin	9.1 ± 2.0	0.34 ± 0.22	3.7×10^4
Glu28Gln			
Substrate	K_m (μM)	k_{cat} (s^{-1})	k_{cat}/K_m ($M^{-1}s^{-1}$)
Acetyl-CoA	9.8 ± 2.8	0.41 ± 0.03	4.2×10^4
Neamine	14.5 ± 4.3	0.56 ± 0.05	3.9×10^4
Kanamycin A	75.3 ± 15.3	0.38 ± 0.02	5.0×10^3
Tobramycin	61.7 ± 17.3	0.50 ± 0.05	8.1×10^3
Amikacin	62.6 ± 15.3	0.09 ± 0.01	1.4×10^3
Neomycin	14.1 ± 3.3	0.25 ± 0.02	1.8×10^4
Ribostamycin	29.9 ± 7.3	0.44 ± 0.04	1.5×10^4
Glu39Ala			
Substrate	K_m (μM)	k_{cat} (s^{-1})	k_{cat}/K_m ($M^{-1}s^{-1}$)
Acetyl-CoA	2.7 ± 0.3	0.17 ± 0.00	6.4×10^4
Neamine	20.7 ± 3.1	0.68 ± 0.04	3.3×10^4
Kanamycin A	9.1 ± 0.4	0.47 ± 0.00	5.2×10^4
Tobramycin	19.2 ± 3.4	1.1 ± 0.04	5.6×10^4
Amikacin	33.8 ± 6.2	0.13 ± 0.01	3.8×10^3
Neomycin	7.7 ± 1.7	0.18 ± 0.01	2.3×10^4
Ribostamycin	11.4 ± 2.9	0.34 ± 0.02	3.0×10^4
Asp112Ala			
Substrate	K_m (μM)	k_{cat} (s^{-1})	k_{cat}/K_m ($M^{-1}s^{-1}$)
Acetyl-CoA	6.6 ± 0.1	0.04 ± 0.00	6.5×10^3
Neamine	355 ± 20	0.16 ± 0.01	4.5×10^2
Kanamycin A	55 ± 12	0.04 ± 0.00	7.7×10^2
Tobramycin	21.5 ± 3.4	0.04 ± 0.00	1.9×10^3
Amikacin	32.4 ± 9.6	0.01 ± 0.00	1.5×10^2
Neomycin	17.9 ± 1.6	0.10 ± 0.00	5.4×10^3
Ribostamycin	46.3 ± 4.3	0.01 ± 0.00	3.0×10^2

Table 5.2: *continued*

Asp112Asn

Substrate	K_m (μM)	k_{cat} (s^{-1})	k_{cat}/K_m ($M^{-1}s^{-1}$)
Acetyl-CoA	4.8 ± 1.0	0.05 ± 0.00	1.1×10^{4}
Neamine	296 ± 75	0.10 ± 0.02	3.4×10^{2}
Kanamycin A	44.2 ± 6.0	0.08 ± 0.00	1.8×10^{3}
Tobramycin	98 ± 11	0.02 ± 0.00	2.0×10^{2}
Amikacin	18.9 ± 3.2	0.01 ± 0.00	2.6×10^{2}
Neomycin	11.8 ± 1.7	0.05 ± 0.00	4.4×10^{3}
Ribostamycin	70.5 ± 6.2	0.03 ± 0.00	4.0×10^{2}

Asp168Ala

Substrate	K_m (μM)	k_{cat} (s^{-1})	k_{cat}/K_m ($M^{-1}s^{-1}$)
Acetyl-CoA	4.2 ± 0.9	0.22 ± 0.01	5.3×10^{4}
Neamine	8580 ± 200	0.21 ± 0.00	2.4×10^{1}
Kanamycin A	5520 ± 880	0.05 ± 0.01	8.9×10^{0}
Tobramycin	2210 ± 520	0.04 ± 0.00	1.8×10^{1}
Amikacin	524 ± 51	0.01 ± 0.00	2.1×10^{1}
Neomycin	431 ± 95	0.27 ± 0.02	6.3×10^{2}
Ribostamycin	730 ± 71	0.004 ± 0.001	5.5×10^{0}

Asp168Asn

Substrate	K_m (μM)	k_{cat} (s^{-1})	k_{cat}/K_m ($M^{-1}s^{-1}$)
Acetyl-CoA	7.7 ± 1.0	0.16 ± 0.01	2.0×10^{4}
Neamine	4290 ± 760	0.20 ± 0.02	4.8×10^{1}
Kanamycin A	3910 ± 1170	0.09 ± 0.01	2.2×10^{1}
Tobramycin	2570 ± 650	0.05 ± 0.00	1.9×10^{1}
Amikacin	N.D.		
Neomycin	1100 ± 210	0.14 ± 0.01	1.3×10^{2}
Ribostamycin	2220 ± 330	0.01 ± 0.00	4.1×10^{0}

[a] Reactions were carried out at 37°C in 25 mM MES, pH 6.0 and 1 mM EDTA.
[b] Kinetic parameters for wild type AAC(6')-Ii are reproduced from Wright & Ladak (1997).

5.3.2 Glu39Ala

The mutation of Glu39 to Ala had only minimal effects on substrate recognition and catalytic turnover by this variant. K_m values for all AGs tested were similar to those reported for the wild type protein, with the largest change in apparent affinity being a 3.6-fold reduction noted for neamine (Table 5.2). Surprisingly, a 9-fold decrease in the K_m for AcCoA was also observed, although it is currently not known why this mutation would cause an increase in AAC(6')-Ii affinity for this substrate. Analyses of the Glu39Gln and Glu39Asp site mutants were not pursued due to the virtually wild type kinetics obtained for the Glu to Ala substitution. In general, our results do not indicate that Glu39 makes any important interactions with AG substrates.

5.3.3 Glu72Ala

Glu72 was originally mutated to Ala to investigate the potential role of this amino acid as a general base. As detailed in chapter 4, this residue was shown not to act in this capacity, but is instead essential for the productive binding of AG substrates. Most notable were the large decreases in the affinity for neamine (83-fold) and kanamycin (175-fold), with significant changes in AG affinity accounting for the large reductions in specificity constants (k_{cat}/K_ms) for this mutant (see Table 4.2, page 128). Previous sucrose viscosity studies also revealed that this mutant was likely impaired at the chemical step of acetyl transfer, suggesting that in addition to AG recognition, Glu72 may be critical in the proper positioning and orientation of AGs in the AAC(6')-Ii active site in order for efficient acetyl transfer.

5.3.4 Mutation of Asp112

Initial steady-state kinetic analysis of the Asp112Ala site mutant revealed a large reduction in the apparent affinity for neamine compared to the wild type enzyme, shown by a 60-fold increase in K_m (Table 5.2). Since we have good evidence that K_m values approximate the dissociation constants (K_d) for AG substrates, the change likely reflects a decreased protein affinity for this minimal substrate. Significant changes were also noted in k_{cat} values for numerous AGs, including a 24-fold decrease in the k_{cat} for ribostamycin and a 27-fold reduction in tobramycin turnover (Table 5.2). Specificity constants largely reflected the differences noted above, with the most significant reduction observed as a 160-fold decrease in the catalytic efficiency of neamine modification by this variant. Similar changes were also observed for the Asp112 to Asn mutant, including the relevant decrease in AAC(6')-Ii affinity for neamine (~ 50-fold) and the numerous reductions in k_{cat} (Table 5.2). These results indicate that removal of the negative charge at this position by substitution of Asp112 with Ala or Asn may account for the kinetic changes observed. The observation that only the affinity for neamine appears to be affected by these mutations suggests that Asp112 may interact with a functional group that is unique to this substrate, although only the 5- or 6-hydroxyl groups on the 2-deoxystreptamine ring are unique when compared to 4,5- and 4,6-disubstituted AGs, respectively. Although purely speculative, alterations in the binding of this minimal substrate by Asp112Ala/Asn may be reflected almost exclusively in K_m values, while changes in the binding of AGs with additional sugars may be revealed in other kinetic parameters. Since our sucrose viscosity studies indicated that diffusion-controlled events still govern the overall rate (k_{cat}) of

Asp112Ala and Asp112Asn mutant activity, we can speculate that the decreases in k_{cat} may reflect significant changes in the productive binding of AG substrates, which has been shown to contribute to the rate-determining steps for wild type AAC(6')-Ii (Draker *et al.*, 2003) Again this is highly speculative, and additional, more in-depth analysis is certainly required to properly account for these changes. Based on the results presented here, however, we can conclude that Asp112 does play some role in AG binding in the wild type enzyme.

5.3.5 Role of Asp168

Mutation of Asp168 had significant effects on AG modification by the Asp168Ala and Asp168Asn variants, particularly at the level of K_m. Large changes were observed for the apparent affinity of several AGs, including a 740-fold increase in the K_m for neamine with Asp168Asn (Table 5.2). Other K_m increases ranged from 40 to 280-fold for both 4,5- and 4,6 disubstituted AGs relative to the wild type enzyme. Changes in substrate turnover (k_{cat}) were also significant for several substrates, including kanamycin, tobramycin, amikacin and ribostamycin. The importance of this residue was also suggested by the changes in catalytic efficiency of AG modification by the Asp168Asn mutant specifically, which ranged from a 300-fold decrease for neomycin acetylation to a huge ~ 9000 fold reduction in k_{cat}/K_m for ribostamycin (Table 5.2).

Since we know that Asp168 makes intermolecular contacts with Tyr66 of the opposing subunit in the AAC(6)-Ii dimer, we hypothesize that mutation of this residue likely disrupts this interaction and causes alterations to both AG binding sites. In addition, both Asp168Ala and Asp168Asn proteins still appear to be dimeric based on gel

filtration results during purification, which also suggests that mutation of Asp168 disrupts AG binding in the AAC(6')-Ii dimer. A change in orientation or geometry of several residues in the region where AG substrates bind could very well account for the large changes in substrate affinity observed. We therefore speculate that Asp168 plays an indirect but important role in the efficient modification of AGs by AAC(6')-Ii.

5.3.6 MIC Determinations

To complement our steady-state kinetic analysis, we investigated the effects of each amino acid substitution on mutant protein activity *in vivo.* This was done by MIC determinations of kanamycin A and neomycin for *E. coli* expressing either wild type AAC(6')-Ii or one of the site mutants (Table 5.3). Consistent with our *in vitro* results were the near wild type AG resistance conferred by the Glu28Gln and Glu39Ala proteins, which displayed no significant changes in acetylation activity *in vitro* compared to the native enzyme. The 2-fold change observed in kanamycin MIC as a result of Glu39Ala activity represents an acceptable MIC range according to NCCLS guidelines (Standards 2000), and likely reflects little change in conferred resistance relative to the wild type enzyme. Increased susceptibility to kanamycin was noted for *E. coli* expressing the Asp112Ala and Asp112Asn mutants, seen by a 4-fold reduction in MIC with kanamycin A (Table 5.3). An 8-fold decrease in MIC for kanamycin A was noted for cells expressing each Asp168 variant, correlating well with the large decreases in AG affinity observed for these mutants *in vitro,* in addition to revealing similarities with the Glu72Ala protein described in chapter 4. Only a 2-fold increase in neomycin

susceptibility was observed for both Asp112 and Asp168 site mutants. In summary, AG susceptibility observed by MIC changes for *E. coli* expressing the AAC(6')-Ii variants were consistent with the *in vitro* analyses of mutant protein activity.

Table 5.3: MICs of select AGs for AAC(6')-Ii site mutants

Site Mutant	*MIC in µg/mL*	
	Kanamycin A	**Neomycin**
BL21(DE3) [a]	4	1
Wild Type	128	8
Glu28Gln	128	8
Glu39Ala	64	8
Asp112Ala	32	4
Asp112Asn	32	4
Asp168Ala	16	4
Asp168Asn	16	4

[a] Negative control using *E. coli* BL21(DE3) and *E. coli* BL21(DE3)/pET22b(+).

5.4 Conclusions

The site-directed mutagenesis studies described in this chapter have revealed the importance of Glu72Ala, Asp112Ala and Asp168 in AG binding by AAC(6')-Ii, shown by steady-state kinetic analysis of mutant proteins and *in vivo* analysis of AG resistance conferred by these variants. As this body of work represents only the initial stages of characterizing this protein's AG binding site, our understanding of this phenomenon remains superficial. It is also important to note that many other types of interactions probably occur between AAC(6')-Ii and AG in addition to direct contacts with acidic

residues, including other polar or even hydrophobic interactions. Also of interest is the number of main chain contacts and intervening water molecules involved in AG binding for the AAC(2')-Ic enzyme, revealed by the structural determination of this acetyltransferase with bound CoA and various AG substrates (Vetting *et al.*, 2002). A comparison between the mode of AG binding by AAC(2')-Ic and our enzyme awaits the structural elucidation of AAC(6')-Ii with bound AG. Additional crystallographic studies of AAC(6')-Ii in complex with different 4,5- and 4,6-disubstituted AGs may also shed light on the multiple AG binding modes suggested from steady-state kinetic analysis of AAC(6')-Ii and NMR studies (Wright & Ladak, 1997; DiGiammarino *et al.*, 1998).

5.5 References

Burk, D. L., N. Ghuman, L. E. Wybenga-Groot, and A. M. Berghuis. (2003) X-ray structure of the AAC(6')-Ii antibiotic resistance enzyme at 1.8 Å resolution; examination of oligomeric arrangements in GNAT superfamily members. *Protein Sci* 12: 426-37.

DeLano, W. L. The PyMOL molecular graphics system 0.82. DeLano Scientific, San Carlos, CA. USA.

DiGiammarino, E. L., K. A. Draker, G. D. Wright, and E. H. Serpersu. (1998) Solution studies of isepamicin and conformational comparisons between isepamicin and butirosin a when bound to an aminoglycoside 6'-*N*-acetyltransferase determined by NMR spectroscopy. *Biochemistry* 37: 3638-44.

Draker, K. A., D. B. Northrop, and G. D. Wright. (2003) Kinetic mechanism of the GCN5-related chromosomal aminoglycoside acetyltransferase AAC(6')-Ii from *Enterococcus faecium*: Evidence of dimer subunit cooperativity. *Biochemistry* 42: 6565-6574.

Fong, D. H. & A. M. Berghuis. (2002) Substrate promiscuity of an aminoglycoside antibiotic resistance enzyme via target mimicry. *Embo J* 21: 2323-31.

Hon, W. C., G. A. McKay, P. R. Thompson, R. M. Sweet, D. S. Yang, G. D. Wright, and A. M. Berghuis. (1997) Structure of an enzyme required for aminoglycoside antibiotic resistance reveals homology to eukaryotic protein kinases. *Cell* 89: 887-95.

Leatherbarrow, R. J. Grafit 4.0. Erithacus Software. Staines, UK.

Nicholls, A., K. A. Sharp, and B. Honig. (1991) Protein folding and association: Insights from the interfacial and thermodynamic properties of hydrocarbons. *Proteins* 11: 281-96.

Pedersen, L. C., M. M. Benning, and H. M. Holden. (1995) Structural investigation of the antibiotic and ATP-binding sites in kanamycin nucleotidyltransferase. *Biochemistry* 34: 13305-11.

Sakon, J., H. H. Liao, A. M. Kanikula, M. M. Benning, I. Rayment, and H. M. Holden. (1993) Molecular structure of kanamycin nucleotidyltransferase determined to 3.0-Å resolution. *Biochemistry* 32: 11977-84.

Smith, C. A. & E. N. Baker. (2002) Aminoglycoside antibiotic resistance by enzymatic deactivation. *Curr Drug Targets Infect Disord* 2: 143-60.

Standards, National Committee for Clinical Laboratory. (2000) Methods for dilution antimicrobial susceptibility tests for bacteria that grow aerobically; approved standard - fifth edition. Document M7 - A5.

Thompson, P. R., J. Schwartzenhauer, D. W. Hughes, A. M. Berghuis, and G. D. Wright. (1999) The COOH terminus of aminoglycoside phosphotransferase (3')-IIIa is critical for antibiotic recognition and resistance. *J Biol Chem* 274: 30697-706.

Vetting, M. W., S. S. Hegde, F. Javid-Majd, J. S. Blanchard, and S. L. Roderick. (2002) Aminoglycoside 2'-*N*-acetyltransferase from *Mycobacterium tuberculosis* in complex with coenzyme A and aminoglycoside substrates. *Nat Struct Biol* 9: 653-8.

Wolf, E., A. Vassilev, Y. Makino, A. Sali, Y. Nakatani, and S. K. Burley. (1998) Crystal structure of a GCN5-related N-acetyltransferase: *Serratia marcescens* aminoglycoside 3-*N*-acetyltransferase. *Cell* 94: 439-49.

Wright, G. D. (1999) Aminoglycoside modifying enzymes. *Curr Opin Microbiol* 2: 499-503.

Wright, G. D., A. M. Berghuis, and S. Mobashery. (1998) Aminoglycoside antibiotics. Structures, functions, and resistance. *Adv Exp Med Biol* 456: 27-69.

Wright, G.D. & P. Ladak. (1997) Overexpression and characterization of the chromosomal aminoglycoside 6'-*N*-acetyltransferase from *Enterococcus faecium*. *Antimicrob. Agents Chemother.* 41: 956-960.

Wybenga-Groot, L. E., K. Draker, G. D. Wright, and A. M. Berghuis. (1999) Crystal structure of an aminoglycoside 6'-*N*-acetyltransferase: Defining the GCN5-related *N*-acetyltransferase superfamily fold. *Structure Fold Des* 7: 497-507.

Chapter 6

AAC(6')-Ii Inhibitor Studies

6.1 Introduction

A thorough characterization of any enzyme, particularly for those that confer bacterial drug resistance, requires an investigation of protein inhibition. The identification of compounds that behave as inhibitors can complement mechanistic analysis of an enzyme, and in the case of AMEs, could lead to the development of clinically relevant molecules that reverse AG resistance *in vivo*. Drug potentiation by the co-administration of AGs with AME inhibitors remains a real possibility, especially given the successful use of β-lactam/β-lactamase combinations in the clinic (Miller *et al.*, 2001). Compounds that could inhibit all classes of AMEs, perhaps by disrupting the binding of AGs, would represent an ideal broad specificity inhibitor for these resistance enzymes. Targeting the drug binding site may also prevent inhibitor cross reactivity with the numerous eukaryotic proteins that are structurally homologous to AMEs, and which share many similarities in the binding of ATP and AcCoA (Smith & Baker, 2002; Wright, 1999). An alternate approach to overcome AG resistance is the development of new or modified AG antimicrobials that are not inactivated by AMEs but still exhibit bactericidal activity (Mingeot-Leclercq *et al.*, 1999). The design of bifunctional AGs that exhibit antibiotic activity plus inhibit AMEs has also been recently explored and shown to be a promising avenue of research (Sucheck *et al.*, 2000).

These approaches have all been applied to the AAC(6')-Ii inhibitor studies described in the sections that follow, with emphasis on classes of compounds that may inhibit enzyme activity in addition to the characterization of numerous AG derivatives.

6.1.1 Survey of Potential AAC(6)-Ii Inhibitors

Steady-state kinetic studies on AAC(6')-Ii have shown that this enzyme follows an ordered bi-bi ternary complex mechanism, indicating that both AcCoA and AG must be bound in the active site prior to acetyl transfer (Draker *et al.*, 2003). Based on this knowledge and the classical reaction mechanism involving nucleophilic substitution at a carbonyl carbon, we propose a tetrahedral transition state for the reaction catalysed by AAC(6')-Ii (Figure 6.1).

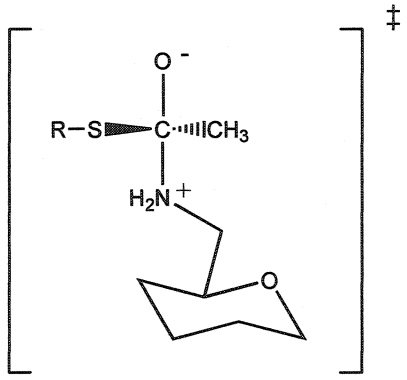

Figure 6.1: Tetrahedral transition state proposed for the acetyl transfer reaction catalyzed by AAC(6')-Ii.

As compounds which mimic the transition state or intermediate of a reaction commonly behave as excellent inhibitors of enzyme activity (Radzicka & Wolfenden, 1996), we tested a number of in-house and commercially available compounds that may mimic the tetrahedral geometry of the proposed transition state. This small survey of thiazolidine and oxazoline-containing compounds tested as potential inhibitors of AAC(6')-Ii acetyl transfer is described in section *6.3.1*.

6.1.2 AG Derivatives as Potential Bifunctional Antimicrobials

In collaboration with Dr. Chi-Huey Wong at the Skaggs Institute for Chemical Biology, Scripps Research Institute, several neamine derivatives generated in Dr. Wong's lab were tested as both AAC(6')-Ii substrates and inhibitors. Many of these derivatives, consisting of modified neamine monomers (Figure 6.2) or dimers attached by linkers of variable structure and length (Figure 6.3), have been shown to target bacterial rRNA and act as antibiotics *in vivo* (Greenberg *et al.*, 1999; Sucheck *et al.*, 2000). A number of derivatives were subsequently tested in our lab as potential bifunctional compounds that may also inhibit the activity of AMEs. The results obtained for the AAC(6')-Ii enzyme are described in section *6.3.2.*

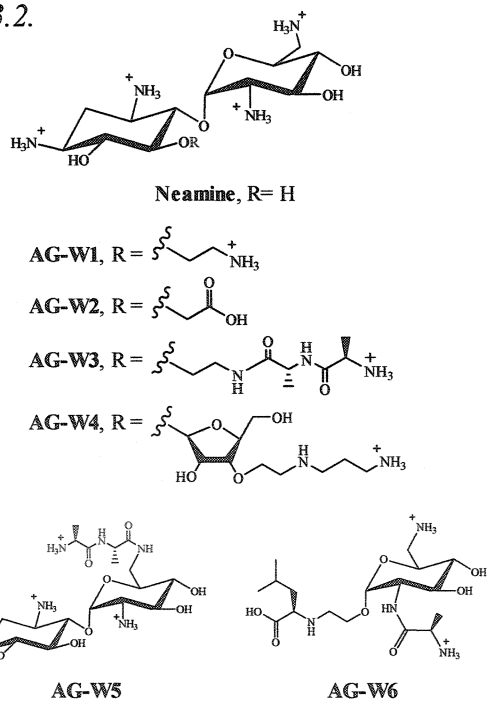

Figure 6.2: Structures of the monomeric neamine derivatives tested as potential AAC(6')-Ii substrates and inhibitors. Derivatives AG-W1 through AG-W4 differ in their functionality at position 5 on the aminocyclitol ring, as shown. AG-W5 is altered at the 6' position on the aminohexose ring, indicated in red. AG-W6 lacks the aminocyclitol ring but has various substituents at the 1' and 2' positions of the aminohexose.

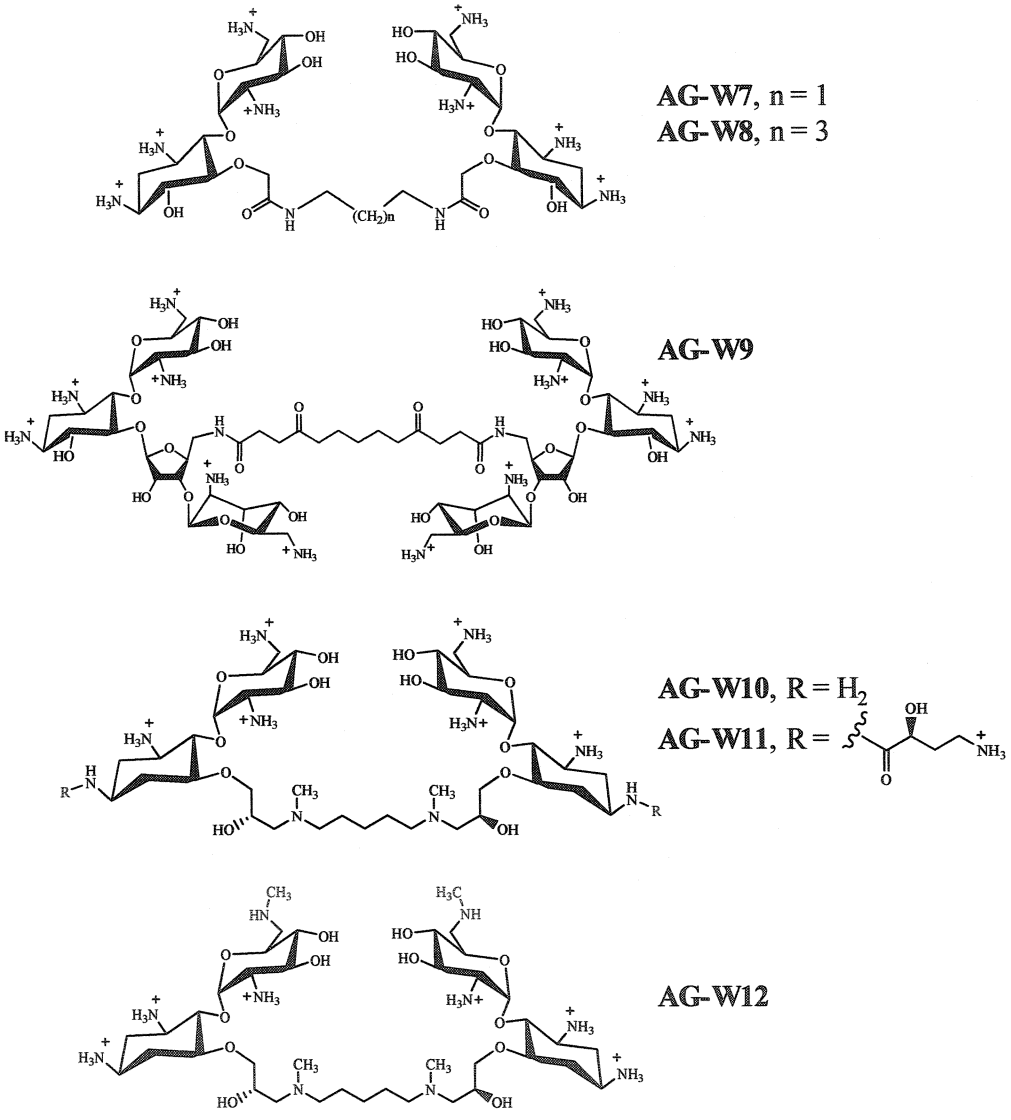

Figure 6.3: Structures of the neamine-based dimers investigated as substrates and inhibitors for AAC(6')-Ii. Two molecules of neamine are attached at position 5 of the aminocyclitol rings through the various linkers shown for AG-W7 through AG-W12. AG-W11 is additionally modified on the aminocyclitol ring as shown. AG-W12 represents the only 6' N-methyl derivative (in red) investigated in this study.

6.1.3 Cationic Peptides as Potential AAC(6')-Ii Inhibitors

The three dimensional structures representing all classes of AMEs have provided a great deal of useful information regarding both substrate binding and catalysis (Wright, 1999). Relevent to this chapter is the negatively charged surface patch that is evident for AAC(6')-Ii and other AG resistance enzymes, which is believed to draw in the positively charged AG substrate to the active site (Vetting *et al.*, 2002; Wolf *et al.*, 1998; Wright *et al.*, 1998; Wybenga-Groot *et al.*, 1999). It is therefore possible that positively charged species could bind at or near this antibiotic binding site and inhibit group transfer by AAC(6')-Ii. The fact that AAC(6')-Ii also has the capacity to bind and acetylate protein and peptide substrates (Wybenga-Groot *et al.*, 1999), similar to that shown for two AG phosphotransferases as well (Daigle *et al.*, 1999), lends support to our choice to investigate cationic peptides as potential inhibitors. In collaboration with Dr. Bob Hancock at the University of British Columbia, Department of Microbiology and Immunology, our lab obtained several antimicrobial cationic peptides (see Table 6.3) to screen against the AAC(6')-Ii enzyme as well as other AMEs studied in our lab by David D. Boehr. Although only the AAC(6')-Ii inhibition results conducted by myself are discussed in detail here, studies performed with the APH(3')-IIIa and bifunctional AAC(6')-APH(2") enzymes are included in Boehr *et al.* (2003). This publication describes the inhibition of several AMEs (including AAC(6')-Ii) by cationic peptides and also addresses the mode of inhibition and structure-activity relationships for representative peptides.

6.2 Materials and Methods

6.2.1 Chemicals

Kanamycin A and 4,4'-dithiodipyridine were from Sigma-Aldrich Chemical Co. (St. Louis, MO). AcCoA was from Amersham Pharmacia (Baie d'Urfe, PQ). Using Table 6.1 numbering, compounds 1-9 were also from Sigma-Aldrich Chemical Co. (St. Louis, MO) and compounds 10-18 were from Maybridge Chemical Company, Ltd. (Cornwall, U.K.). The 12 neamine derivatives tested as AAC(6')-Ii substrates and inhibitors (section *6.3.2*) were the kind gift of Dr. Chi-Huey Wong at The Scripps Research Institute in La Jolla, CA. The numerous cationic peptides discussed in section *6.3.3* were graciously supplied by Dr. Robert E. Hancock at the University of British Columbia, Department of Microbiology and Immunology.

6.2.2 Survey of Potential AAC(6')-Ii Inhibitors

AAC(6')-Ii activity was measured in the presence of each of the compounds listed in Table 6.1 to identify any inhibitors of enzymatic acetyl transfer. The compounds were dissolved in DMSO and added to a final concentration of 5 to 100 μM to standard AAC(6')-Ii assay mixtures consisting of 50 μM AcCoA, 50 μM kanamycin A, and 2.0 mM DTDP in 25mM HEPES, pH 7.5, and 1 mM EDTA. Final volumes were approximately 1 mL and the mixtures were incubated at 37EC for 3-5 min before the addition of *ca.* 0.5 nmoles AAC(6')-Ii. Acetyl transfer activity was monitored by *in situ* titration of free CoA with DTDP as previously described (Williams & Northrop, 1978; Wright & Ladak, 1997). All reactions were performed in duplicate with the mean

percentage activity and standard error reported in Table 6.1 relative to control activity measured with no potential inhibitor present. The compounds were also tested as slow-binding inhibitors by assessing the time dependence of any possible inhibition over a time course of one hour.

6.2.3 Survey of Neamine Derivatives

The twelve neamine derivatives represented in figures 6.2 and 6.3 were tested as both AAC(6')-Ii substrates and inhibitors. Note that all of the derivatives screened were first tested in the Wong lab for antimicrobial activity using the methods described previously (Greenberg *et al.*, 1999; Sucheck *et al.*, 2000). All derivatives exhibited antibiotic behaviour with the exception of AG-W5 and AG-W6, which were not active.

For the initial substrate screen, 100 μM and 250 μM final concentrations of derivatives were added to a standard assay mixture consisting of 50 μM Ac-CoA, 1.3 μM AAC(6')-Ii and 2 mM DTDP in 25 mM MES, pH 6.0, 1 mM EDTA. Acetyl transfer activity was measured by the *in situ* titration of free CoA with DTDP as described in section *6.2.2*. Kinetic parameters for those analogs behaving as substrates were then determined in duplicate and initial rates fit to equation 1 describing Michaelis-Menten kinetics or equation 2 when substrate inhibition was detected, using Grafit 4.0 software (Leatherbarrow, 2000).

$$v = k_{cat}E_t[S]/(K_m + [S]) \qquad \text{(Eq. 1)}$$

$$v = k_{cat}E_t[S]/(K_m + [S])(1 + [S]/K_i)) \qquad \text{(Eq. 2)}$$

The neamine derivatives were screened as potential inhibitors by using the same concentrations and assay procedure described above but with the addition of 50 μM (2x

K_m) kanamycin A. Control reactions monitored the acetylation of kanamycin A in the absence of potential inhibitors with the initial rates compared to the rates obtained from those reactions containing the various derivatives. All reactions were performed in duplicate. An IC_{50} (inhibitory concentration 50 %) determination for the lone AG-W12 inhibitor was determined using the kinetic assay described and by collecting initial velocity data in the presence of increasing concentrations of AG-W12 and subsaturating 50 μM concentrations of AcCoA and kanamycin A. The data were fit to equation 3 using Grafit 4.0 software (Leatherbarrow, 2000), where x is the inhibitor concentration, y is the enzymatic rate, and *range* is the uninhibited rates minus background values.

$$y = \frac{Range}{1 + \left(\frac{x}{IC_{50}}\right)^{s}} + \text{Background} \qquad \text{(Eq. 3)}$$

6.2.4 Survey of Cationic Peptides

The twelve cationic peptides listed in Table 6.3 were first dissolved in 20 % ethanol and initially screened at a 50 μM final concentration. Standard assay mixtures included 2.0 μM AAC(6')-Ii, 50 μM AcCoA, and 2 mM DTDP in 25 mM MES, pH 6.0 and 1 mM EDTA. AAC(6')-Ii was preincubated with the peptides for 10 min at 37 ° C before the addition of 50-75 μM kanamycin A to initiate the reaction. Control reactions contained no cationic peptide. Acetyl transfer activity was measured by the kinetic assay described in the previous sections. IC_{50} determinations for CM3, indolicidin, CP11CN, CP10A, and

gramicidin peptides were made as described in section *6.2.3*. K_i estimations for indolicin and CP10A peptides were made by determining the steady-state kinetic parameters for AAC(6')-Ii kanamycin acetylation in the presence of increasing concentrations of peptide. The data were fit to the appropriate equation of best fit describing either competitive (equation 4), or noncompetitive/mixed-type inhibition (equation 5) using Grafit 4.0 (Leatherbarrow, 2000):

$$v = V_{max}[S]/(K_m((1 + I/K_i) + [S]) \quad \text{(Eq. 4)}$$

$$v = V_{max}[S]/(K_m(1 + I/K_{is}) + [S](1 + I/K_{ii})) \quad \text{(Eq. 5)}$$

Kinetic parameters for those cationic peptides behaving as substrates were determined using a phosphocellulose binding assay and [1-^{14}C]AcCoA as described previously (Wybenga-Groot *et al.*, 1999). Reactions were allowed to proceed for 45 min prior to placement on the phosphocellulose.

6.3 Results and Discussion

6.3.1 Survey of Potential AAC(6')-Ii inhibitors

As can be seen from Table 6.1, the majority of compounds had little to no effect on AAC(6')-Ii activity at the concentrations tested. Note that thiostrepton (# 8) did give 30 % inhibition of AAC(6')-Ii at 100 μM but no inhibition was detected at lower concentrations (Table 6.1). In addition, no slow-binding inhibition was noted for any of the compounds surveyed.

Table 6.1: Survey of potential AAC(6')-Ii inhibitors

Potential Inhibitor		Structure	% Activity[a]
	Control, no potential inhibitor added	----------	100
1	Thiazolidine	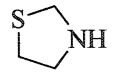	100 ± 1
2	3,4-Dimethyl-5-(2-hydroxyethyl) thiazolium iodide	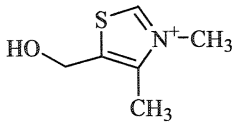	100 ± 2
3	2,4,4-Trimethyl-2-oxazoline	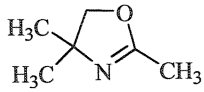	100 ± 3
4	4-Phenyl-2-oxazolidinone	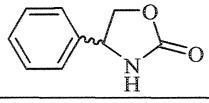	100 ± 6
5	Cefotaxime	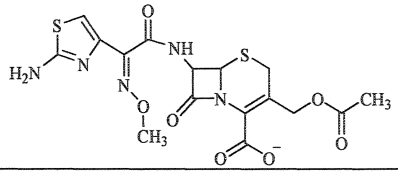	100 ± 5
6	Ceftriaxone	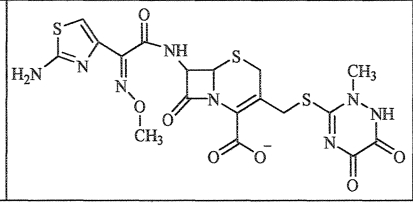	100 ± 2

Table 6.1: *continued*

Potential Inhibitor		Structure	% Activity [a]
7	Cefoxitin	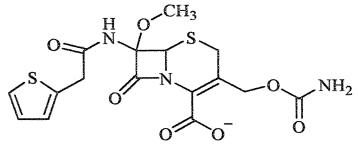	100 ± 7
8	Thiostrepton	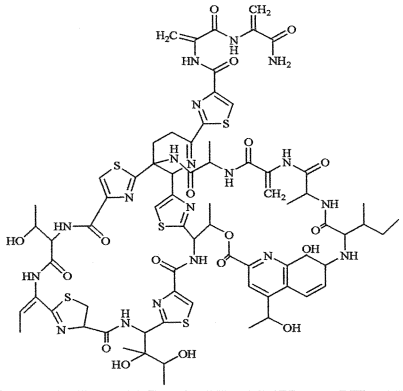	70 ± 3 @ 100 μM 100 ± 5 @ 10 μM 100 ± 2 @ 5 μM
9	4-methoxy-8-phenyl-octahydro-5,7,9-trioxa-1-thia3-az	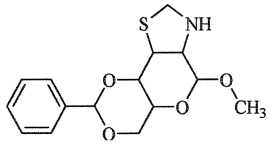	100 ± 3
10	2-(1,2,4,5-tetrahydroxy-3-{[3,4,5-trihydroxy-6-(hydroxymethyl) tetrahydro-2H-pyran-2-yl]oxy} pentyl)-1,3-thiazolane-4-carboxylic acid	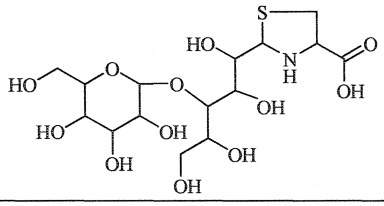	90 ± 4
11	3,5-di(acetyloxy)-2-[(acetyloxy)methyl]-6-(2-methoxy-4-{3-[(methylamino)carbonyl]-1,3-thiazolan-2-ylphenoxy)tetrahydro-2H-pyran-4-yl acetate	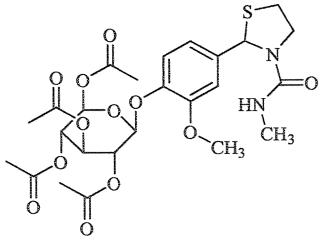	100 ± 2
12	2,3-di(acetyloxy)-1-[acetyloxy) methyl]-3-{1-oxo-3-[1,2,3,4-tetra(acetyloxy)butyl]perhydrol[1,3] thiazolo[3,4-c][1,3]oxazol-5-yl} propyl acetate	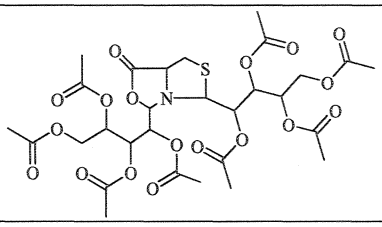	100 ± 5

Table 6.1: *continued*

Potential Inhibitor		Structure	% Activity [a]
13	2-(8-acetyl-7,7-dimethyl-2-oxo-3-oxa-6-thia-8-azabicyclo[3,2,1]oct-4-yl)-2-(acetyloxy)-1-[acetyoxy) methyl]ethyl acetate	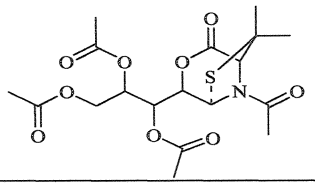	100 ± 1
14	N1-tetrahydrofuran-2-ylmethyl-2-[(5-oxo-2,3-dihydro-5H-pyrimido [2,1-b][1,3]thiazol-6-yl)carbonyl] hydrazine-1-carbothioamide	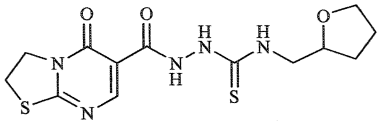	100 ± 4
15	4-[3-(5-oxo-2,3-dihydro-5H-pyrimido[2,1-b][1,3]thiazol-6-yl)-1,2,4-oxadiazol-5-yl] butanoic acid	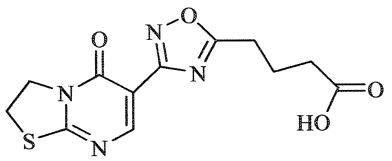	100 ± 3
16	6-{3-[4-(trifluoromethyl)phenyl]-1,2,4-oxadiazol-5-yl}-2,3-dihydro-5H-pyrimido[2,1-b] [1,3]thiazol-5-one	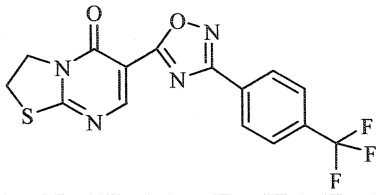	100 ± 9 @ 25 μM
17	O1-[(5-oxo-2,3-dihydro-5H-pyrimido[2,1-b][1,3]thiazol-6-yl) carbonyl]-4-(trifluoromethyl) benzene-1-carbohydroximamide	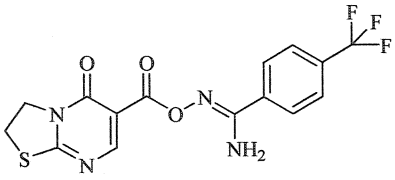	100 ± 6 @ 25 μM
18	3-[3-(4-chlorophenyl)-1,2,4-oxadiazol-5-yl]-1-(4,4-dimethyl-5-methyene-2-{[3-trifluoromethyl) phenyl]imino}-1,3-thiazolan-3-yl) propan-1-one	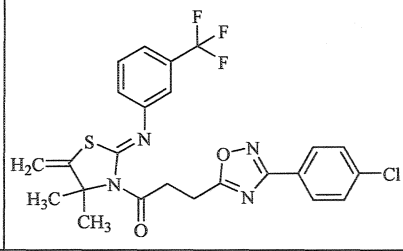	90 ± 3 @ 25 μM

There are several explanations as to why no significant enzyme inhibition was observed with any of the compounds tested. One simple reason is that the small number of potential inhibitors in our survey may not mimic the transition state of the reaction

enough to have an effect on acetyltransferase activity. More interesting is the possibility that the substrate-induced conformational changes in AAC(6')-Ii described in chapter 2 may account for the lack of inhibition observed. Since there is evidence that these structural rearrangments are a requirement for acetyl transfer and are essential in forming a catalytically productive active site, we can speculate that transition state analogs will not induce the same conformational changes in AAC(6')-Ii as AcCoA and AG substrates. As a result, the compounds would have no significant affinity for the enzyme.

6.3.2 AG Analogs as Potential Inhibitors

Of the 12 neamine derivatives tested as AAC(6') substrates and inhibitors (see Figures 6.2 and 6.3), nine of these compounds were found to behave as fairly good substrates for the enzyme (Table 6.2):

Table 6.2: AAC(6')-Ii steady-state kinetic parameters for neamine derivatives [a]

Substrate [b]	K_m (μM)	k_{cat} (s^{-1})	K_i (μM)	k_{cat}/K_m ($M^{-1}s^{-1}$)
Neamine [c]	5.8 ± 1.0	0.42 ± 0.02		7.2×10^4
AG-W1	19.6 ± 7.4	0.35 ± 0.07	286 ± 149	1.8×10^4
AG-W2	320 ± 65	0.31 ± 0.02		9.7×10^2
AG-W3	10.8 ± 1.7	0.26 ± 0.01		2.4×10^4
AG-W4	40.7 ± 4.4	0.55 ± 0.02		1.3×10^4
AG-W7	53.4 ± 23.8	0.86 ± 0.23	311 ± 177	1.6×10^4
AG-W8	83.6 ± 33.4	1.9 ± 0.53		2.3×10^4
AG-W9	143 ± 57	0.27 ± 0.03		1.9×10^3
AG-W10	28.7 ± 4.9	0.27 ± 0.10		9.3×10^3
AG-W11	34.1 ± 5.3	0.60 ± 0.02		1.8×10^4

[a] Reactions were carried out at 37°C in 25 mM MES, pH 6.0 and 1 mM EDTA.
[b] Note that derivatives AG-W5, AG-W6, and AG-W12 did not behave as substrates.
[c] Kinetic parameters for neamine are reproduced from Wright & Ladak (1997).

For the monomeric derivatives AG-W1, AG-W3, and AG-W4, K_m values only differed from ~ 2 to 7-fold relative to neamine, with AG-W2 having the least apparent affinity for AAC(6')-Ii noted from a 55-fold increase in K_m (Table 6.2). Turnover rates were similar to that determined for neamine, resulting in essentially wild type catalytic efficiencies for AG-W1, AG-W3, and AG-W4. A 75-fold decrease in k_{cat}/K_m was observed for AG-W2, largely due to the changes in K_m. As expected, AG-W5 did not behave as a substrate for AAC(6')-Ii due to the lack of a free 6'-amino group (Figure 2.2). Similarly, AG-W6 was also not a substrate, consistent with the finding that neamine, made up of an aminocyclitol and 6-aminohexose ring, is the minimal substrate for this enzyme (Wright & Ladak, 1997). In addition, both AG-W5 and AG-W6 did not behave as inhibitors of AAC(6')-Ii activity.

Five of the six AG dimers tested were also shown to be good AAC(6')-Ii substrates. In addition, both AG-W7 and AG-W8 had higher k_{cat} values compared to neamine as well as all the other derivatives tested (Table 6.2). Since two free 6'-amino groups may be accessible to AAC(6')-Ii in these cases, it is possible that both are acetylated, accounting for the observed increases in k_{cat}. The flexible amide linkers between these neamine dimers (Figure 6.3) may very well allow each monomer to be separately bound to AAC(6')-Ii and acetylated. Additional differences in the linker regions between neamine monomers was also shown to effect the efficiency of AAC(6')-Ii acetylation. As can be seen from the kinetic parameters determined for AG-W9, the addition of two sugar moieties per monomer to generate a neomycin dimer resulted in the second poorest catalytic efficiency observed (Table 6.2).

AG-W12 was the only derivative out of the twelve screened that inhibited AAC(6')-Ii activity. The 6' N-methylated derivative of neamine attached through a diaminobutyl linker (Figure 6.3) was found to be a potent inhibitor of kanamycin A acetylation, with a IC_{50} of 1.03 ± 0.11 μM. Unfortunately, a K_i determination that would identify the type of inhibition could not be made due to the limited quantity of the derivative we received.

In summary, it is evident that although the majority of the analogs were acetylated by AAC(6')-Ii, variations between derivatives did have an effect on the efficiency of modification, with methylation of the 6' amino group generating an inhibitor of AAC(6')-Ii acetyl transfer. In addition, the neamine dimers AG-W7, AG-W8, and AG-W10 (designated dimers 4, 6, and 27, respectively in Sucheck *et al.* (2000)) were shown by David Boehr in our lab to behave as potent inhibitors towards the phosphotransferase domain of the bifunctional enzyme AAC(6')-APH(2") (Sucheck *et al.*, 2000), illustrating that this type of approach can indeed identify inhibitors for AG inactivating enzymes. More importantly, those derivatives that behave as antibiotics *in vivo* and that also can inhibit resistance enzymes have the potential to act as efficient bifunctional drugs in a clinical setting.

6.3.3 Cationic Peptides as Inhibitors of AAC(6')-Ii Activity

The initial screen for AAC(6')-Ii inhibition at 50 μM cationic peptide revealed that seven out of the twelve peptides tested behaved as inhibitors, as seen in Table 6.3. Note that the cyclic peptide gramicidin, which is not cationic, was used as a control in the initial screen.

Table 6.3: Properties of cationic peptides and inhibition of AAC(6')-Ii activity

Peptide	Sequence	Charge at pH 7	Inhibition Observed [a]	IC_{50} (μM)
CP26	KWKSFIKKLTSAAKKVVTTAKPLISS	7	+	N.D.[b]
CP27	KWKLFKKIGIGAVLKVLTTGLPALIS	5	-	-
CP28	KWKLFKKIGIGAVLKVLTTGLPALKLTK	7	-	-
CP29	KWKSFIKKLTTAVKKVLTTGLPALIS	6	-	-
CP2600	KWKSFIKKLTSAAKKVLTTAKPLISS	7	-	-
Cpα1	KWKSFIKKLTSAAKKVTTAAKPLTK	8	-	-
Cpα2	KWKKFIKKIGIGAVLKVLTTGLPALKLTKK	9	-	-
CM3	KWKKFIKSLTKAAKTVVKTAKKPLIV(NH_2)	9	+	24 ± 0.6
Indolicidin	ILPWKWPWWPWRR(NH_2)	1	+	13 ± 1.3
CP11CN	ILKKWPWWPWRRK(NH_2)	3	+	23 ± 4.3
CP10A	ILAWKWAWWAWRR(NH_2)	1	+	4.4 ± 0.2
MS178	GIGKFLKKAKKFGKATVKILKK(NH_2)	9	+	N.D.
Gramicidin	L(dF)PVOL(dF)PVO (cyclic)	-	+	148 ± 13.8

[a] + indicates detectable inhibition of AAC(6')-Ii using 50 μM cationic peptide as described in section *6.2.3.*
[b] N.D., not determined.

IC_{50}s were determined to be in the low μM range for almost all of the inhibitory peptides evaluated except the control peptide gramicidin S, which exhibited significantly less inhibition. The indolicidin analog CP10A was found to have the greatest effect on AAC(6')-Ii activity with an IC_{50} of ~ 4 μM. Based on the results presented in Table 6.3,

the generalization can be made that the shorter peptides appear to be more consistently inhibitory than the longer peptides for AAC(6')-Ii. Strangely, the peptides behaving as inhibitors do not share a similar structure, as CM3 and CP10A are α-helical, indolicidin and CP11CN adopt extended structures, and Gramicidin S is a β-sheet (Scott *et al.*, 1999; Zhang *et al.*, 2001). To further characterize the inhibition observed, indolicidin and CP10A were selected for K_i determinations and structure-activity relationships. Both peptides were found to be competitive inhibitors *versus* AG substrate (K_{is} = 4.2 ± 1.0 for indolicidin and 2.4 μM ± 0.6 for CP10A), indicating that they compete for the AG binding site on the enzyme. Noncompetitive/mixed-type inhibition was observed *versus* AcCoA (K_{is} = 38 ± 2 for indolicidin, and K_{is} = 4.7 ± 1.3 μM & K_{ii} = 32 ± 8 μM for CP10A), consistent with the peptides having no little to no effect on AcCoA binding. The inhibition patterns observed for CP10A are included as an example in Figure 6.4:

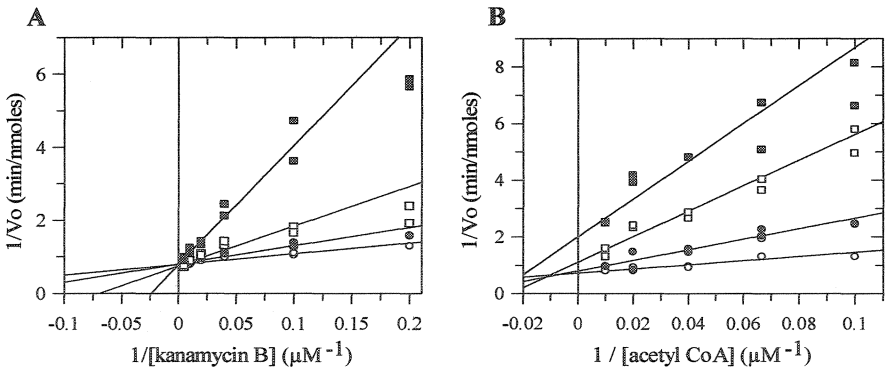

Figure 6.4: Patterns of AAC(6')-Ii inhibition by the cationic peptide CP10A. Shown are double-reciprocal plots indicative of competitive inhibition *vs.* AG **(A)** and noncompetitive/mixed inhibition *vs.* AcCoA **(B)**. The varying concentrations of CP10A shown in A are 0 μM (○), 5 μM (●), 10 μM (□), & 20 μM (■) and in B, 0 μM (○), 10 μM (●), 20 μM (□), & 40 μM (■). A K_{is} of 2.4 ± 0.6 μM was determined for CP10A *vs.* AG and a K_{is} = 4.7 ± 1.3 μM & K_{ii} = 32 ± 8 μM for CP10A *vs.* AcCoA. This figure was reproduced from Boehr *et al.*, 2003, with permission from Elsevier.

Also interesting to note is the fact that various cationic peptides behaved differently toward other AMEs that were tested by David Boehr in our lab, suggesting that the mode of inhibition by these peptides may be enzyme specific (Boehr *et al.*, 2003).

Information on the structure-function relationships of the CP10A peptide was gained by additional studies with AAC(6')-Ii as well as with other AMEs investigated by David Boehr. Specifically, increasing the salt concentrations of kinetic assay mixtures was shown to increase IC_{50} values for CP10A (and therefore decrease the inhibition), consistent with these peptides making electrostatic interactions with the acetyltransferase and phophostransferase enzymes tested (Boehr *et al.*, 2003). Activity screens of truncated versions of CP10A made by Dr. Kalinka Koteva in our lab also revealed that hydrophobic interactions and Van der Waals forces are important in enzyme-peptide interactions and the inhibition observed (Boehr *et al.*, 2003).

Finally, since it is known that AAC(6')-Ii can modify a number of small basic proteins as well as poly-L-lysine (Wybenga-Groot *et al.*, 1999), it was investigated whether some of the cationic peptides were also being acetylated. As can be seen from Table 6.4, three peptides that were inhibitory also behaved as AAC(6')-Ii substrates. The kinetic parameters determined for CM3, CP11CN and MS178 were comparable to those determined for poly-L-lysine, suggesting that one or more lysine residues are being modified. Most importantly, the acetylation of these peptides was found not to effect their antimicrobial activity, demonstrating that the presence of AAC(6')-Ii does not confer resistance to these cationic peptides *in vivo* (Boehr *et al.*, 2003).

Table 6.4: Acetylation of cationic peptides by AAC(6')-Ii [a]

Substrate	K_m (μM)	k_{cat} (sec^{-1})	k_{cat}/K_m ($M^{-1}sec^{-1}$)
Kanamycin A[b]	19.9 ± 8.8	0.816 ± 0.207	4.60×10^4
Poly-L-Lysine[c]	17.1 ± 1.4	0.004 ± 0.001	2.23×10^2
CM3	27 ± 12	0.03 ± 0.01	1.1×10^3
CP11CN	25 ± 14	0.04 ± 0.01	1.7×10^3
MS178	16 ± 7	0.01 ± 0.00	2.7×10^2

[a] This table was reproduced from Boehr *et al.* (2003), with permission from Elsevier.
[b] Kinetic parameters for kanamycin A are reproduced from Wright & Ladak (1997).
[c] Kinetic parameters for poly-L-lysine are reproduced from Wybenga-Groot *et al.* (1999).

In summary, the results presented here convincingly show that cationic peptides can act as inhibitors of AAC(6')-Ii activity by interfering with the binding of AG substrates to the enzyme. These studies, in conjunction with the inhibition also observed for other acetyltransferase and phosphotransferase enzymes, reveals the potential for cationic peptides to be used as broad-spectrum inhibitors of AG inactivating enzymes.

6.4 References

Boehr, D. D., K. Draker, K. Koteva, M. Bains, R. E. Hancock, and G. D. Wright. (2003) Broad-spectrum peptide inhibitors of aminoglycoside antibiotic resistance enzymes. *Chem Biol* 10: 189-96.

Daigle, D. M., G. A. McKay, P. R. Thompson, and G. D. Wright. (1999) Aminoglycoside antibiotic phosphotransferases are also serine protein kinases. *Chem Biol* 6: 11-8.

Draker, K. A., D. B. Northrop, and G. D. Wright. (2003) Kinetic mechanism of the GCN5-related chromosomal aminoglycoside acetyltransferase AAC(6')-Ii from *Enterococcus faecium*: Evidence of dimer subunit cooperativity. *Biochemistry* 42: 6565-6574.

Greenberg, W. A., E. S. Priestley, P. S. Sears, P. B. Alper, C. Rosenbohm, M. Hendrix, S.-C. Hung, and C.-H. Wong. (1999) Design and synthesis of new aminoglycoside antibiotics containing neamine as an optimal core structure: Correlation of antibiotic activity with *in vitro* inhibition of translation. *J. Am. Chem. Soc* 121: 6527-6541.

Leatherbarrow, R. J. Grafit 4.0. Erithacus Software. Staines, UK.

Miller, L. A., K. Ratnam, and D. J. Payne. (2001) Beta-lactamase-inhibitor combinations in the 21st century: Current agents and new developments. *Curr Opin Pharmacol* 1: 451-8.

Mingeot-Leclercq, M. P., Y. Glupczynski, and P. M. Tulkens. (1999) Aminoglycosides: Activity and resistance. *Antimicrob Agents Chemother* 43: 727-37.

Radzicka, A . & R. Wolfenden. (1996) Transition state and multisubstrate analog inhibitors. In *Contemporary enzyme kinetics and mechanism*. D. L. Purich, eds. Academic Press, San Diego, CA. 229-257.

Scott, M. G., H. Yan, and R. E. Hancock. (1999) Biological properties of structurally related alpha-helical cationic antimicrobial peptides. *Infect Immun* 67: 2005-9.

Smith, C. A. & E. N. Baker. (2002) AG antibiotic resistance by enzymatic deactivation. *Curr Drug Targets Infect Disord* 2: 143-60.

Sucheck, S.J., A. L. Wong, K. M. Koeller, D. D. Boehr, K.-a. Draker, P. Sears, G. D. Wright, and C.-H. Wong. (2000) Design of bifunctional antibiotics that target bacterial rRNA and inhibit resistance-causing enzymes. *J. Am. Chem. Soc.* 122: 5230-5231.

Vetting, M. W., S. S. Hegde, F. Javid-Majd, J. S. Blanchard, and S. L. Roderick. (2002) AG 2'-*N*-acetyltransferase from *Mycobacterium tuberculosis* in complex with coenzyme A and aminoglycoside substrates. *Nat Struct Biol* 9: 653-8.

Williams, J. W. & D. B. Northrop. (1978) Kinetic mechanisms of gentamicin acetyltransferase I. Antibiotic-dependent shift from rapid to nonrapid equilibrium random mechanisms. *J Biol Chem* 253: 5902-7.

Wolf, E., A. Vassilev, Y. Makino, A. Sali, Y. Nakatani, and S. K. Burley. (1998) Crystal structure of a GCN5-related N-acetyltransferase: *Serratia marcescens* aminoglycoside 3-N-acetyltransferase. *Cell* 94: 439-49.

Wright, G. D. (1999) AG-modifying enzymes. *Curr Opin Microbiol* 2: 499-503.

Wright, G. D., A. M. Berghuis, and S. Mobashery. (1998) Aminoglycoside antibiotics. Structures, functions, and resistance. *Adv Exp Med Biol* 456: 27-69.

Wright, G.D. & P. Ladak. (1997) Overexpression and characterization of the chromosomal aminoglycoside 6'-*N*-acetyltransferase from *Enterococcus faecium*. *Antimicrob. Agents Chemother.* 41: 956-960.

Wybenga-Groot, L. E., K. Draker, G. D. Wright, and A. M. Berghuis. (1999) Crystal structure of an aminoglycoside 6'-*N*-acetyltransferase: Defining the GCN5-related *N*-acetyltransferase superfamily fold. *Structure Fold Des* 7: 497-507.

Zhang, L., A. Rozek, and R. E. Hancock. (2001) Interaction of cationic antimicrobial peptides with model membranes. *J Biol Chem* 276: 35714-22.

Chapter 7

Studies on the Protein Acetylation Activity of AAC(6')-Ii

7.0 Summary

This chapter investigates the protein acetylation activity of AAC(6')-Ii as a possible alternate function for this modifying enzyme *in vivo*. An enrichment of small basic proteins from *E. faecium* has revealed that several proteins are acetylated *in vitro* by AAC(6')-Ii. Three of these proteins were further characterized by N-terminal sequencing analysis and putatively identified based on BLAST sequence analysis. Of particular interest was the identification of an AAC(6')-Ii substrate with N-terminal sequence homology to the *Bacillus subtilis* ribosomal protein S9, prompting us to initiate studies to investigate whether AAC(6')-Ii may be acetylating a similar ribosomal protein in *E. faecium*. In addition, we also have compelling evidence that AAC(6')-Ii is responsible for the modification of several unidentified proteins *in vivo*, shown by acetylation comparisons of crude protein extracts from wild type *E. faecium* and a knockout strain that has the *aac(6')-Ii* gene insertionally inactivated. Taken together, these results support the hypothesis that AAC(6')-Ii may have an alternate function *in vivo* as a protein acetyltransferase, a proposal that also suggests an evolutionary origin for this chromosomal AME in *E. faecium*.

7.1 Introduction

The proposal that AG resistance genes originate from antibiotic-producing bacteria was first made in the early 1970's, when it was reported that AMEs present in AG resistant clinical isolates were similar to enzymes found in AG-producing species of *Streptomyces* and *Micromonospora* (Benveniste & Davies, 1973). Another widely accepted theory based on an analysis by Piepersberg *et al.* (1988) suggests that duplication and mutation of bacterial genes involved in basic cellular processes also accounts for the derivation of AG resistance determinants, in both AG-producing and non-producing bacteria. Specifically, analyses of phylogenetic relationships among the APH and AAC classes of enzymes led to the proposal that these proteins may have evolved from protein kinases and acetyltransferases, respectively (Piepersberg *et al.*, 1988). Recent biochemical and structural studies on two AMEs have supported this hypothesis, shown by the structural and functional homology observed for APH(3')-IIIa and proteins kinases (Hon *et al.*, 1997; Daigle *et al.*, 1999), with similar homologies observed for AAC(6')-Ii and histone acetyltransferases (Wybenga-Groot *et al.*, 1999).

Relevant to this study is the characterization of several chromosomally encoded AAC enzymes, the results of which have suggested or identified alternate, *in vivo* functions for these AMEs. The AAC(2')-Ia from *Providencia stuartii*, for example, has been shown to play a role in peptidoglycan O-acetylation as well as in 2'-N-acetylation of AGs (Payie *et al.*, 1995; Payie & Clarke, 1997). Similarly, recent structural evidence from the *M. tuberculosis* AAC(2')-Ic protein solved with bound AG supports a possible role for this AAC in mycothiol biosynthesis (Vetting *et al.*, 2002; Vetting *et al.*, 2003).

Studies on the chromosomally encoded AAC(6')-Ii protein from *E. faecium* have also suggested that this enzyme may have a alternate function *in vivo* besides AG modification. The chromosomal origin of the *aac(6')-Ii* gene first suggested a possible physiological role, with studies by Costa *et al.* showing that insertional inactivation of *aac(6')-Ii* caused AG resistance to be reversed, but with no other biochemical or morphological changes observed in the knockout strain (Costa *et al.*, 1993). The genome sequencing project underway for *E. faecium* has so far not provided any clues as to an alternate role, since the genomic environment of *aac(6')-Ii* has yet to be rigorously determined.

As described in chapter 1, initial steady-state kinetic analysis of AAC(6')-Ii activity revealed a sub-optimal level of AG detoxification compared to other AMEs, seen by fairly low specificity constants (k_{cat} /K_m) on the order of 10^4 M^{-1} s^{-1} and a positive correlation of MIC values with k_{cat}, the rate at saturating AG concentrations (Wright & Ladak, 1997). In addition, AAC(6')-Ii has the capacity to acetylate eukaryotic histones as well as other small basic proteins and the model substrate poly-L-Lys (Figure 7.1), demonstrating a novel AAC(6')-Ii substrate specifity for protein lysine residues (Wybenga-Groot *et al.*, 1999). This biochemical evidence was also complemented by the structural similarity observed for AAC(6')-Ii and the yeast histone acetyltransferase yHAT 1, with both enzymes being members of the large GNAT superfamily (Dutnall *et al.*, 1998; Wybenga-Groot *et al.*, 1999). Based on these finding in particular, we initiated the research described here to further investigate the possibility that AAC(6')-Ii may behave as a protein acetyltransferase *in vivo* in *E. faecium.*

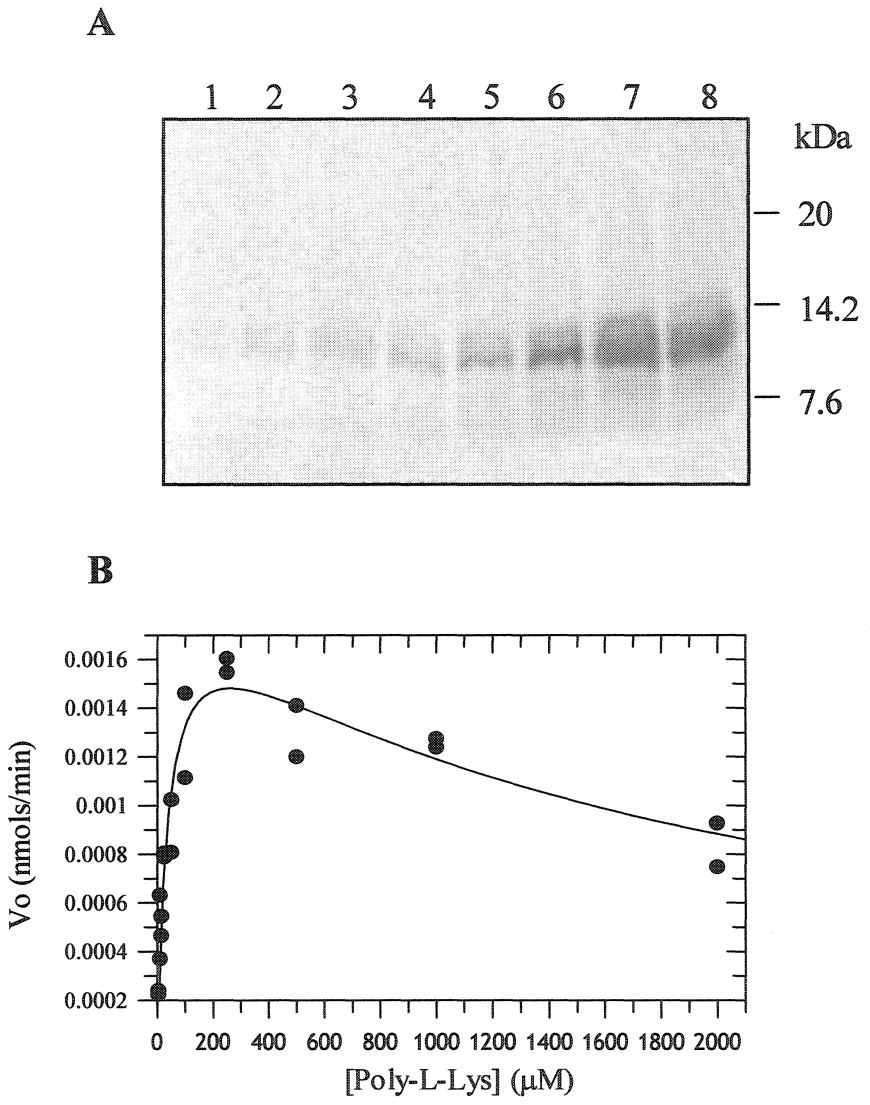

Figure 7.1: Protein and peptide acetylation activity of AAC(6')-Ii. Shown in **A** is an autoradiogram of eukaryotic histone acetylation by AAC(6')-Ii, analyzed by SDS-PAGE. Enzymatic modification of this protein substrate is observed over a range of histone concentrations: lane 1, 5 μM; lane 2, 10 μM; lane 3, 15 μM; lane 4, 25 μM; lane 5, 50 μM; lane 6, 100 μM; lane 7, 250 μM; lane 8, 500 μM. Experimental details are given in Wybenga-Groot *et al.* (1999). Shown in **B** is the steady-state kinetic analysis of poly-L-Lys acetylation by AAC(6')-Ii. A K_m of 38.5 ± 7.8 μM, a K_i of 1.78 mM and a k_{cat} = 0.0019 s^{-1} was determined from a fit of initial rate data to the equation $v = V_{max}[S]/(K_m + [S](1 + [S]/K_i))$ describing substrate inhibition. This figure was reproduced from Wybenga-Groot *et al.* (1999) with permission from Elsevier.

7.2 Materials and Methods

7.2.1 General

Calf thymus H3/H4 histones, type VIII-S were from Sigma-Aldrich Chemical Co. (St. Louis, MO, USA). AcCoA was from Amersham Pharmacia and [1-^{14}C]-labelled AcCoA (specific activity = 65 mCi/mmol) was from ICN radiochemicals (Costa Mesa, CA, USA). Wild type *E. faecium* strain C238 was obtained from J. Gunn-Munroe at the Chedoke-McMaster microbiology laboratory in Hamilton, ON, Canada (Wright & Ladak, 1997). Additional *E. faecium* strains CIP 54-32 (wild type) and BM4229 (*aac(6')-Ii* gene insertionally inactivated) described in Costa *et al.* (1993) were provided by Dr. Patrice Courvalin at the Institut Pasteur, National Centre for Scientific Research, Paris, France.

7.2.2 Enrichment of AAC (6')-Ii Protein Substrates from E. faecium

To identify any potential protein substrates for this enzyme in *E. faecium,* the following purification scheme was used to isolate small basic proteins, similar to the procedures previously described for the isolation of histone–like proteins of bacteria (Salti *et al.*, 1985). Briefly, 16 L of *E. faecium* C238 were grown to mid-log phase (OD_{600} ~ 0.5-06) at 37 °C and 250 rpm in brain heart infusion (BHI) media supplemented with 25 μg of kanamycin per ml. The 18 g of cells obtained were harvested by centrifugation at 10,000 x *g* for 15 min, washed with 0.85% NaCl, and resuspended in lysis buffer consisting of 25 mM HEPES, pH 7.5, 2 mM EDTA (buffer A) plus 0.15 M NaCl, 0.1 mM DTT, and 1 mM PMSF. Cells were subjected to bead-beater lysis by 3, 30-45 sec. intervals of disruption using 0.1 mm glass beads. Cell debris was removed by two 20 min centrifugations at 10 000 x *g*. The crude lysate (S1) was treated with 6 M HCl to a pH of

2 and incubated on ice for 15 min. Precipitated proteins were removed by centrifugation at 10000 x *g* for 30 min. The recovered supernatant was neutralised to pH 7 by the addition of 250 mM HEPES, pH 7.5 and 10 mM EDTA. The acid-soluble protein sample (S2) was loaded onto a 1.5 mL Mono S cation exchange column and basic proteins eluted by a 0-1 M linear NaCl gradient in buffer A. Peak A_{280} fractions were pooled and dialysed against buffer A at 4 °C overnight. Each pooled fraction (S3) was then separately reapplied to the Mono S column for greater separation of proteins in each sample. Peak A_{280} fractions were again pooled (S4), dialysed and then tested as potential substrates for AAC(6')-Ii. Reactions contained 10-20 μg of S4 protein sample, 50 μM AAC(6')-Ii, and 160 μM [^{14}C]-AcCoA in 25 mM HEPES, pH 7.5, and 1 mM EDTA. Similar to the histone acetylation experiments previously described (Wybenga-Groot *et al.*, 1999), SDS-PAGE and autoradiography were then used to visualise any acetylated proteins. Modification of eukaryotic histones by AAC(6')-Ii served as a positive control in these experiments.

7.2.3 N-terminal Sequencing of AAC(6')-Ii Protein Substrates

Two protein substrates (A and B) were selected for N-terminal sequencing based on the protein enrichment described above and the autoradiogram results shown (Figure 7.3, lanes 1-8). A third *E. faecium* protein was also chosen for sequencing (see lane 9, Figure 7.3) following a second protein enrichment of small basic proteins using the same procedure and 21 grams of *E. faecium* cells as starting material from 18 L of bacterial culture. N-terminal sequencing of proteins blotted onto polyvinyldifluoride (PVDF)

membranes was performed by a standard automated Edman degradation procedure at the Peptide Sequence Analysis Facility at the University of Toronto (Toronto, ON) for proteins A and B, using a Porton Gas-Phase Microsequencer with in-line 3-phenyl-2-thiohydantoin (PTH)-amino acid analysis. N-terminal sequencing of the third protein substrate was performed at the Harvard Microchemistry Facility (Cambridge, MA) using a PE/ABD Procise 494 HT Protein Sequencing System (VGR).

7.2.4 Preparation of E. faecium Ribosomes and Ribosomal Subunits

Based on the N-terminal sequencing results of protein substrate B (see section *7.3.1*), we wished to further investigate the possible physiological relevance of ribosomal protein acetylation by AAC(6')-Ii. To do this, we set out to perform comparative two-dimensional (2-D) gel electrophoretic analysis of ribosomal proteins from wild type and knockout strains of *E. faecium*. Although such an analysis has not been performed to date, the isolation of ribosomes and ribosomal subunits from *E. faecium* have been optimized and the protocol is therefore described here. 70S ribosomes were isolated in a similar manner as described in a protocol tailored for prokaryotic ribosomes (Spedding, 1990), which is a modification of methods previously described (Noll *et al.*, 1973; Jelenc, 1980). Steps to yield tight-coupled ribosomes were omitted as they were not required. Briefly, 2 L cultures of *E. faecium* BM4229 and CIP 54-32 were grown to mid-log phase in BHI media supplemented with 12.5 μg of kanamycin A per ml. Approximately 5 g of cells were obtained for each strain and lysed by several passages through a French press at 12000 p.s.i, with RNase-free DNase added to a final concentration of 2 μg/ml. The crude extracts were spun at 30 000 x *g* for 1 h and the top three-fourths of the supernatant

(S30) retained. Crude ribosomes were obtained by spinning the S30 fraction at 100 000 x *g* for 4 h at 4 ° C. The ribosomes were salt washed and dialysed several times against a typical ribosome storage buffer for proper storage @ -80 ° C. An A_{260}/A_{280} purity ratio of ≥ 1.8 was calculated for both preps, indicating the isolation of pure, "clean" ribosomes using the above protocol. After extensive dialysis of stored 70S ribosomes against a low Mg^{2+} buffer, ribosomal subunits were prepared by layering ~ 60 A_{260} units of sample onto 38 ml, 10 – 30 % (w/v) sucrose gradients made in low Mg^{2+} buffer. Samples were spun at 43 000 x *g* for 18 h at 4 ° C using a Beckman SW28 rotor. 30S and 50S peak fractions were pooled by monitoring absorbance at 260 nm of the fractionated gradients. Figure 7.2 shows the good separation of ribosomal subunits and reproducibility between the knock out and wild type preparations, which will be essential for any future comparisons of subunits or ribosomal proteins. Isolated subunits were pelleted at 200 000 x *g* for 18 h at 4 ° C, resuspended in storage buffer and then stored at - 80 ° C.

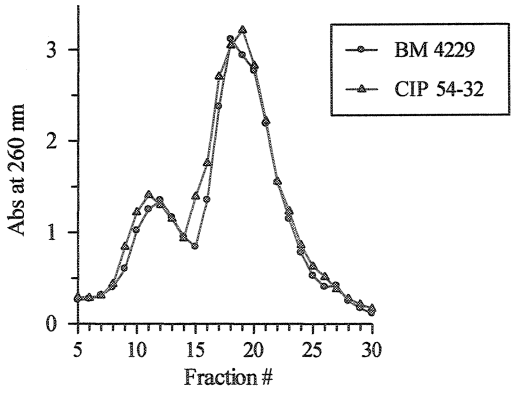

Figure 7.2: Separation of 30S and 50S ribosomal subunits by sucrose gradient density centrifugation. A 10% - 30% gradient was used. BM4229 (red) and CIP 54-32 (blue) denote the fractionation of the knockout and wild type ribosomal subunits, respectively. As expected, a 2:1 absorbance ratio was noted for 50S (larger peak) to 30S (smaller peak) subunits.

In addition, ribosomal proteins have also been successfully isolated from 30S and 50S ribosomal subunits based on an acetic acid extraction and acetone precipitation protocol previously described (Spedding, 1990).

7.2.5 In Vivo Protein Acetylation Comparisons

To investigate whether AAC(6')-Ii may be acetylating proteins *in vivo*, crude protein extracts of wild type and AAC(6')-Ii knockout strains of *E. faecium* were prepared. Briefly, 1L cultures of *E. faecium* CIP 54-32 (wild type) and BM4229 (knockout) strains were grown to mid-log phase at 37 °C and 250 rpm in BHI media supplemented with 12.5 μg of kanamycin per ml. The cells were harvested and lysed using the same lysis buffer and method described in section *7.2.2*. After cell debris was removed by two 20 min centrifugations at 10 000 x *g*, the crude lysate (S1) was DNase-treated and spun at 100 000 x *g* for 2 hrs @ 4 ° C. Samples of S1, supernatant from the high speed spin (S2), and resuspended pellet from the high speed spin (P2) were then used in the following incubations. 30 μg of crude protein extract (S1, S2, or P2) was incubated with 50 μM AAC(6')-Ii and 160 μM ^{14}C-AcCoA in 25 mM HEPES, pH 7.5, and 1 mM EDTA. Reactions were incubated at 37 ° C for 60 min before the addition of standard 2x loading buffer. Samples were boiled for 5 minutes, loaded onto a 20% SDS-PAGE gel and ran for 60 min at 200 V. The gel was dried and exposed to X-ray film for 10 days. The developed autoradiogram was used to assess whether any acetylation differences were apparent between the wild type and knockout *E. faecium* strains.

7.3 Results and Discussion

7.3.1 AAC(6')-Ii Protein Substrates from E. faecium

The purification of small basic proteins *from E. faecium* by acid treatment and cation exchange chromatography yielded less than 5% of the proteins present in S1. As seen in Figure 7.3, several of these proteins were acetylated by AAC(6')-Ii. The most intensely radiolabelled proteins, indicated as A, B, and C in Figure 7.3 were selected for N-terminal sequencing, the results of which are presented in Table 7.1.

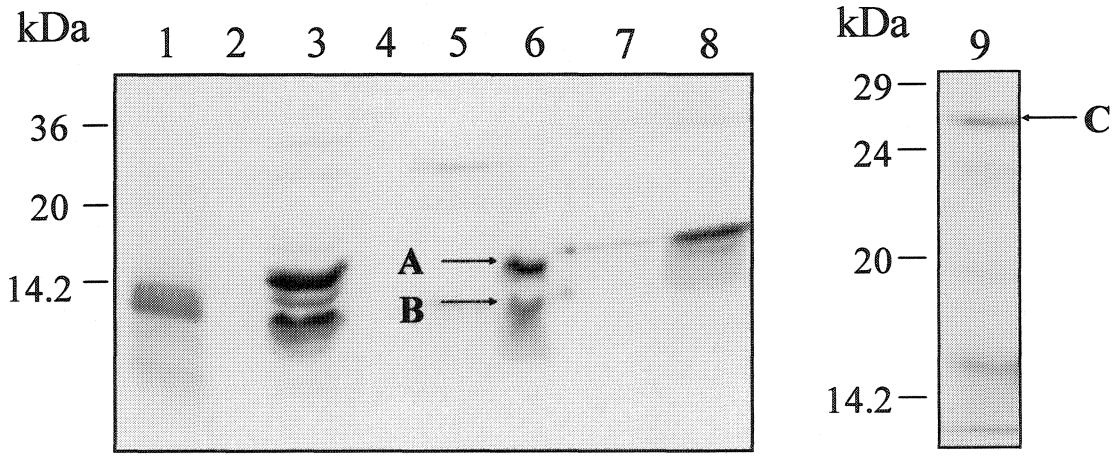

Figure 7.3: Autoradiograph of *E. faecium* proteins acetylated by AAC(6')-Ii. Potential protein substrates were incubated with AAC(6')-Ii and [1-^{14}C]-AcCoA as described in section *7.2.2*. Incubations contained 50 µM AAC(6')-Ii, 115 µM ^{14}C-AcCoA and 10 µg of the following; Lane 1, eukaryotic histones (+ve Co); lane 2, S1-crude lysate; lane 3, S2-acid soluble fraction; lane 4, blank; lanes 5-8, various S4 protein fractions from a second Mono S run. Lane 9 is from an additional autoradiogram revealing AAC(6')-Ii acetylation of a higher molecular weight protein from an enriched S4 sample. Proteins labelled A, B (left panel) and C (right panel) was sent for N-terminal sequencing as described.

Table 7.1: N-terminal sequencing results of AAC(6')-Ii protein substrates

Protein Substrate	N-Terminal Sequence	BLAST Search Results [a]	References
A	MEKKEFHVVAE	Phosphocarrier protein Hpr from *E. faecalis*	Deutscher *et al.*, 1986
B	AQVQYIGTGRR	Ribosomal protein S9 from *B. subtilis*	Higo *et al.*, 1982
C	MKKKQKQKLLNQFRPSLD	Hypothetical protein from *E. faecium*	Direct Submission (Accession No. ZP 00036196).

[a] based on protein-protein BLAST (Altschul *et al.*, 1990) using the option to search for short nearly exact matches in available protein sequence databases

7.3.1.1 AAC(6')-Ii Protein Substrate A

The N-terminal sequence of protein substrate A was identical to that of the HPr phosphocarrier protein from *E. faecalis*, suggesting that a homologous protein has been isolated from *E. faecium* in our study. Hpr is a lysine-rich, histidine-containing protein that functions in the phosphoenolpyruvate–sugar phosphotransferase system (PTS) as a phosphate carrier (Deutscher *et al.*, 1986). No follow-up studies have been conducted on this protein substrate for two reasons. First, this pathway has been well characterized in several species of bacteria and *in vivo* acetylation of Hpr has never been observed. Secondly, AAC(6')-Ii could be modifying certain residues simply because they are accessible to the enzyme or because the HPr protein is rich in lysine, as is the case for the eukaryotic histone substrates. The abundance of this substrate in our enriched protein samples may also be a factor in the extent of acetylation observed.

7.3.1.2 AAC(6')-Ii Protein Substrate B

We have focused more attention on protein substrate B, which shows N-terminal sequence homology to the 30S ribosomal protein S9 from *B. subtilis* (Higo *et al.*, 1982). The similarity in molecular mass of protein substrate B and the characterized S9 protein from *B. subtilis*, together with the BLAST search results, suggests that AAC(6')-Ii is acting on a homologous ribosomal protein from *E. faecium*. The possibility that AAC(6')-Ii may function as a ribosomal *N*-acetyltransferase *in vivo* is very interesting given the hypothesis set forth by Piepersberg *et al.* (1988) that AACs may have originated and evolved from ribosomal *N*-acetyltransferases. Although no significant primary amino acid sequence homology exists between AAC(6')-Ii and known bacterial ribosomal acetyltransferases, several residues known to be important for the GNAT structural fold are conserved (Figure 7.4), suggesting that these proteins, like AACs, are also members of the GNAT superfamily. Also of note is the absence of any positively charged lysines in the N-terminus of this protein, which is in contrast to other AAC(6')-Ii protein substrates characterized in this study and in previous investigations (Wybenga-Groot *et al.*, 1999). Our results with protein substrate B suggests that AAC(6')-Ii may also have the capacity to acetylate the free amino group on the terminal alanine residue, similar to ribosomal acetyltransferases. This is largely based on our hypothesis that AAC(6')-Ii is acetylating in the N-terminal region of protein substrates, due in part to the likely accessibility of this region to the enzyme active site, in addition to the identified sites of histone modification by the structurally homologous HAT enzymes (Marmorstein, 2001).

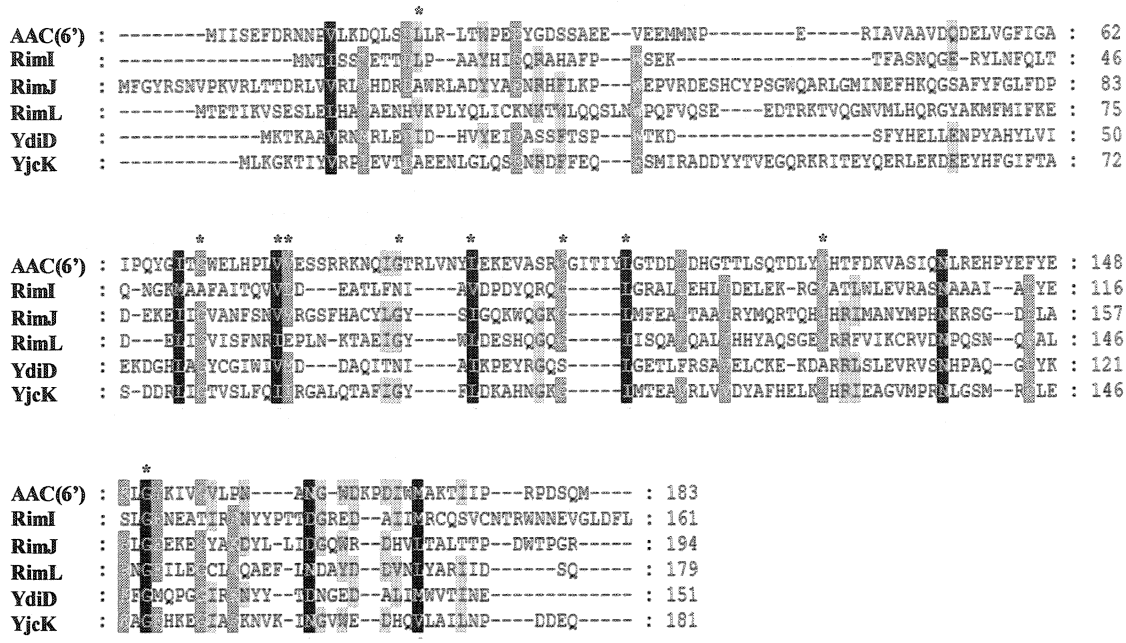

Figure 7.4: Primary sequence alignment of AAC(6')-Ii (top) with ribosomal *N*-acetyltransferases. RimI, RimJ and RimL are from *E. coli* (Yoshikawa *et al.*, 1987; Tanaka *et al.*, 1989). YdiD and YjcK are *B. subtilis* proteins deduced from the complete genome sequence (Kunst *et al.*, 1997). AAC(6')-Ii shares between 25-30 % amino acid sequence homology with the proteins included in the above alignment. Shaded residues are semi-conserved (grey) or conserved (black), with non-polar residues important for the GNAT structural fold indicated with a red asterisk. This alignment was generated using the program Clustal W (Thompson *et al.*, 1994).

The relevance of the observed *in vitro* ribosomal protein acetylation by AAC(6')-Ii is currently unknown. It is interesting to note that in *B. subtilis*, the characterization of 30S ribosomal proteins by 2-D electrophoresis revealed that the S9 protein was present in both non-acetylated and N-∝-acetylated forms (Higo *et al.*, 1982). The fact that S9 was the only 30S ribosomal protein shown to be acetylated in this study suggests that the acetylation of a homologous *E. faecium* protein by AAC(6')-Ii could be of physiological relevance. Steady state kinetic analysis of the semi-pure *E. faecium* "S9" protein gave a K_m of 35 μM, a k_{cat} of 3.7 x 10^{-3} s^{-1} and a k_{cat}/K_m on the order of 10^2 M^{-1} s^{-1},

comparable to values obtained with the model substrate poly-L-Lys and other cationic peptides (Boehr *et al.*, 2003). It must be noted that these are crude estimates only, considering both the sample purity and the possibility that a fraction of the protein may already be acetylated.

To investigate the possibility that AAC(6')-Ii may be acting as a ribosomal acetyltransferase *in vivo*, we focused on the isolation of 30S ribosomal proteins from wild type (CIP 54-32) and knockout (BM4229) strains of *E. faecium*. Our ultimate goal was to assess any differences in ribosomal protein acetylation in the two strains by comparative 2-D electrophoresis. This proposal was based on a previously reported study on *E. coli* ribosomal proteins in which a similar methodology was used to see acetylation differences between a wild type and mutant strain (Isono & Isono, 1980). Although such an analysis has not yet been successfully performed in our lab, a protocol has been optimized to isolate ribosomes and ribosomal subunits from *E. faecium*. As no published reports are available on ribosomal isolation from this bacterium, the methodology described in section *7.2.4* will be useful for the continuation of these studies and any future work that may involve enterococcal ribosomes. In summary, the *in vivo* relevance of the acetylation of protein substrate B by AAC(6')-Ii awaits the completion of the comparative 2-D gel electrophoresis analysis. If these experiments indicate that the ribosomal protein is acetylated in wild type but not in the knockout strain, it will convincingly show that AAC(6')-Ii is acting on this substrate *in vivo*.

7.3.1.3 AAC(6')-Ii Protein Substrate C

The third and final protein substrate analysed in this study was found to be identical in the first 18 amino acids to a hypothetical *E. faecium* protein, annotated as such based on data from the current genome sequencing project. In addition, the approximate molecular mass of 26 kDa for this protein substrate (see Figure 7.3) is in good agreement with the predicted size of the hypothetical protein, lending further support to our identification. Subsequent BLAST analysis using the entire amino acid sequence of protein substrate C revealed no significant homology with any other known proteins. We therefore know very little about this protein, except that its' N-terminus contains 5 lysine residues, many of which may be accessible for acetylation by AAC(6')-Ii. Similar to what was hypothesized for the HPr substrate (see section *7.3.1.1*), the abundance of this protein in our enriched fractions may account for its modification.

In general, the studies described so far have demonstrated that AAC(6')-Ii is capable of acetylating *E. faecium* proteins *in vitro*. Although these findings broaden the known protein substrate specificity of AAC(6)-Ii to include small basic proteins from the host organism, additional studies were performed to determine whether AAC(6')-Ii was acting as a protein acetyltransferase *in vivo*.

7.3.2 In Vivo Protein Acetylation Comparisons

To investigate whether AAC(6')-Ii may be acetylating proteins *in vivo* in *E. faecium*, crude protein extracts of wild type and AAC(6')-Ii knockout strains were prepared. We hypothesized that if endogenous AAC(6')-Ii was indeed acetylating proteins *in vivo* in the

wild type strain, then these proteins would not be radiolabelled (or radiolabelled as much) when exogenous ^{14}C-AcCoA was added, simply because these proteins would have already been acetylated. In contrast, the knockout strain of *E. faecium* would have no endogenous AAC(6')-Ii acting on these proteins and therefore these substrates would be more heavily radiolabelled by the addition of exogenous AAC(6')-Ii and ^{14}C-AcCoA. As can be seen from Figure 7.5, proteins from the P2 fraction of the knockout strain crude extracts were more strongly radiolabelled than the identical fraction from the wild type strain. This provides us with strong evidence that AAC(6')-Ii is acetylating proteins *in vivo*.

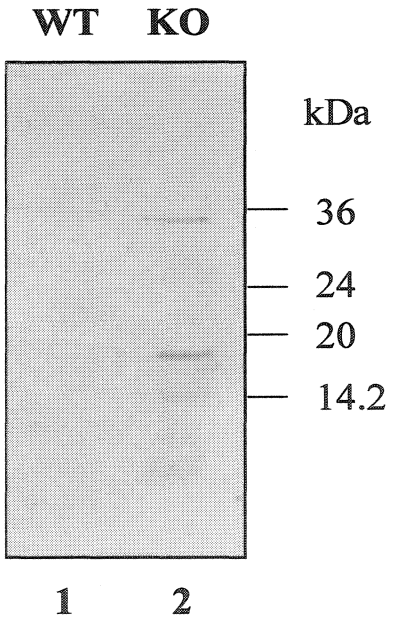

Figure 7.5: Acetylation comparisons of crude protein extracts from a wild type and AAC(6')-Ii-knockout strain of *E. faecium*. The more heavily labeled proteins in the knockout (KO) extract (lane 2) suggest that endogenous AAC(6')-Ii has previously acetylated these protein substrates *in vivo*.

Although we have not yet identified the *in vivo* protein substrates indicated in Figure 7.5, these results, together with the *in vitro* analysis of AAC(6')-Ii protein modification described in section *7.3.1*, convincingly show that this AAC has an alternate function in *E. faecium* as a protein acetyltransferase.

7.4 References

Altschul, S. F., W. Gish, W. Miller, E. W. Myers, and D. J. Lipman. (1990) Basic local alignment search tool. *J Mol Biol* 215: 403-10.

Benveniste, R. & J. Davies. (1973) Aminoglycoside antibiotic-inactivating enzymes in Actinomycetes similar to those present in clinical isolates of antibiotic-resistant bacteria. *Proc Natl Acad Sci U S A* 70: 2276-80.

Boehr, D. D., K. Draker, K. Koteva, M. Bains, R. E. Hancock, and G. D. Wright. (2003) Broad-spectrum peptide inhibitors of aminoglycoside antibiotic resistance enzymes. *Chem Biol* 10: 189-96.

Costa, Y., M. Galimand, R. Leclercq, J. Duval, and P. Courvalin. (1993) Characterization of the chromosomal *aac(6')-Ii* gene specific for *Enterococcus faecium*. *Antimicrob Agents Chemother* 37: 1896-903.

Daigle, D. M., G. A. McKay, P. R. Thompson, and G. D. Wright. (1999) Aminoglycoside antibiotic phosphotransferases are also serine protein kinases. *Chem Biol* 6: 11-8.

Deutscher, J., B. Pevec, K. Beyreuther, H. H. Kiltz, and W. Hengstenberg. (1986) Streptococcal phosphoenolpyruvate-sugar phosphotransferase system: Amino acid sequence and site of ATP-dependent phosphorylation of Hpr. *Biochemistry* 25: 6543-51.

Dutnall, R. N., S. T. Tafrov, R. Sternglanz, and V. Ramakrishnan. (1998) Structure of the histone acetyltransferase HAT1: A paradigm for the GCN5-related *N*-acetyltransferase superfamily. *Cell* 94: 427-438.

Higo, K., E. Otaka, and S. Osawa. (1982) Purification and characterization of 30S ribosomal proteins from *Bacillus subtilis*: Correlation to *Escherichia coli* 30S proteins. *Mol Gen Genet* 185: 239-44.

Hon, W. C., G. A. McKay, P. R. Thompson, R. M. Sweet, D. S. Yang, G. D. Wright, and A. M. Berghuis. (1997) Structure of an enzyme required for aminoglycoside antibiotic resistance reveals homology to eukaryotic protein kinases. *Cell* 89: 887-95.

Isono, K. & S. Isono. (1980) Ribosomal protein modification in *Escherichia coli.* II. Studies of a mutant lacking the N-terminal acetylation of protein S18. *Mol Gen Genet* 177: 645-51.

Jelenc, P. C. (1980) Rapid purification of highly active ribosomes from *Escherichia coli. Anal Biochem* 105: 369-74.

Kunst, F., N. Ogasawara, I. Moszer, A. M. Albertini, G. Alloni, V. Azevedo, M. G. Bertero, P. Bessieres, A. Bolotin, S. Borchert, R. Borriss, L. Boursier, A. Brans, M. Braun, S. C. Brignell, S. Bron, S. Brouillet, C. V. Bruschi, B. Caldwell, V. Capuano, N. M. Carter, S. K. Choi, J. J. Codani, I. F. Connerton, A. Danchin, and et al. (1997) The complete genome sequence of the Gram-positive bacterium *Bacillus subtilis. Nature* 390: 249-56.

Marmorstein, R. (2001) Structure and function of histone acetyltransferases. *Cell Mol Life Sci* 58: 693-703.

Noll, M., B. Hapke, M. H. Schreier, and H. Noll. (1973) Structural dynamics of bacterial ribosomes. I. Characterization of vacant couples and their relation to complexed ribosomes. *J Mol Biol* 75: 281-94.

Payie, K. G.&A. J. Clarke. (1997) Characterization of gentamicin 2'-*N*-acetyltransferase from *Providencia stuartii*: Its use of peptidoglycan metabolites for acetylation of both aminoglycosides and peptidoglycan. *J Bacteriol* 179: 4106-14.

Payie, K. G., P. N. Rather, and A. J. Clarke. (1995) Contribution of gentamicin 2'-*N*-acetyltransferase to the O acetylation of peptidoglycan in *Providencia stuartii. J Bacteriol* 177: 4303-10.

Piepersberg, W., J. Distler, P. Heinzel, and J.-A. Perez-Gonzalez. (1988) Antibiotic resistance by modification: Many resistance genes could be derived from cellular control genes inAactinomycetes - a hypothesis. *Actinomycetologica* 2: 83-98.

Salti, V., F. Le Hegarat, and L. Hirschbein. (1985) Isolation and characterization of small heat-stable acid-soluble DNA-binding proteins from *Bacillus subtilis* nucleoids. *J Gen Microbiol* 131 (Pt 3): 581-90.

Spedding, G. (1990) Isolation and analysis of ribosomes from prokaryotes, eukaryotes, and organelles. In *Ribosomes and protein synthesis: A practical approach.* G. Spedding,eds. Oxford University Press, New York, NY. 1-29 & appendix 1.

Tanaka, S., Y. Matsushita, A. Yoshikawa, and K. Isono. (1989) Cloning and molecular characterization of the gene *riml* which encodes an enzyme acetylating ribosomal protein L12 of *Escherichia coli* k12. *Mol Gen Genet* 217: 289-93.

Thompson, J. D., D. G. Higgins, and T. J. Gibson. (1994) Clustal W: Improving the sensitivity of progressive multiple sequence alignment through sequence weighting, position-specific gap penalties and weight matrix choice. *Nucleic Acids Res* 22: 4673-80.

Vetting, M., S. L. Roderick, S. Hegde, S. Magnet, and J. S. Blanchard. (2003) What can structure tell us about *in vivo* function? The case of aminoglycoside-resistance genes. *Biochem Soc Trans* 31: 520-2.

Vetting, M. W., S. S. Hegde, F. Javid-Majd, J. S. Blanchard, and S. L. Roderick. (2002) Aminoglycoside 2'-*N*-acetyltransferase from *Mycobacterium tuberculosis* in complex with coenzyme A and aminoglycoside substrates. *Nat Struct Biol* 9: 653-8.

Wright, G.D. & P. Ladak. (1997) Overexpression and characterization of the chromosomal aminoglycoside 6'-*N*-acetyltransferase from *Enterococcus faecium. Antimicrob. Agents Chemother.* 41: 956-960.

Wybenga-Groot, L. E., K. Draker, G. D. Wright, and A. M. Berghuis. (1999) Crystal structure of an aminoglycoside 6'-*N*-acetyltransferase: Defining the GCN5-related *N*-acetyltransferase superfamily fold. *Structure Fold Des* 7: 497-507.

Yoshikawa, A., S. Isono, A. Sheback, and K. Isono. (1987) Cloning and nucleotide sequencing of the genes *rimI* and *rimJ* which encode enzymes acetylating ribosomal proteins S18 and S5 of *Escherichia coli* K12. *Mol Gen Genet* 209: 481-8.

Chapter 8

Conclusions and Prospects for Future AAC(6')-Ii Research

8.1 Relevance of AAC(6')-Ii Research

Although the importance of the AAC(6')-Ii studies detailed here have been discussed in each individual chapter, the relevance of this research will be briefly reiterated in the following sections. Specifically, the broader significance of this work in terms of inhibitor studies and implications for the GNAT superfamily will be discussed.

8.1.1 Inhibition of AAC(6')-Ii Activity to Reverse AG Resistance

A prerequisite for any rationale-based drug design approach or inhibition study is a thorough understanding and characterization of the drug target. For the AMEs, this involves a working knowledge of the mechanism of aminoglycoside modification, including the mode of substrate binding and the underlying chemistry involved in drug inactivation. Although the characterization of AAC(6')-Ii is by no means complete, it complements the structural data available for AAC(6')-Ii, which together can be applied to relevant inhibitor studies. The investigation of cationic peptides as inhibitors of AAC(6')-Ii activity (chapter 6) is an example of a rationale and educated approach, as we set out to target the negatively charged surface patch present on this and other AMEs (Boehr *et al.*, 2003). The fact that this enzyme shares a similar AcCoA binding fold with that of eukaryotic protein acetyltransferases also validates the search for inhibitors specific to the AG binding site, in order to minimize potential cross reactivity with other GNAT enzymes.

8.1.2 Relevance to the GNAT superfamily

Our understanding of the kinetic and catalytic mechanism of AAC(6')-Ii (described in chapters 3 and 4) allows us to compare and contrast our results with other members of

the GNAT superfamily. Our dead-end and product inhibition studies have shown that AAC(6')-Ii follows a sequential ternary complex mechanism, similar to all other *N*-acetyltransferases characterized within the superfamily. These results therefore support the hypothesis that GNAT members share a similar kinetic mechanism. Our evidence of subunit cooperativity in the AAC(6')-Ii dimer may also be relevant to other oligomeric members of the GNAT superfamily, as this phenomenon may be important to the function and/or regulation of other acetyltransferase enzymes. Finally, our studies on the catalytic mechanism of AAC(6')-Ii (chapter 4) has revealed several differences compared to other GNAT superfamily members. This is in contrast to what was suggested by Dyda *et al.* (2000), and reveals that although the underlying chemistry is similar, the roles of geometrically equivalent residues in the active site of these enzymes are not.

8.2 Prospects for Future AAC(6')-Ii Studies

This section briefly describes various studies on AAC(6')-Ii that could be performed to complement the research described in the preceding chapters, in addition to several suggestions for new experiments.

8.2.1 Follow Up Studies

As described in chapter 3, sucrose viscosity studies demonstrated that both AG binding and product release govern the rate of AAC(6')-Ii acetyl transfer, revealed by changes in k_{cat}/K_b and k_{cat} with increasing solvent viscosity. To investigate the individual contributions of productive AG binding and product release to this rate-limitation, pre-steady state kinetic analysis could be done using both stopped flow and quenched flow

studies. It would also be interesting to investigate the binding of different AGs by AAC(6')-Ii using this technique. These experiments would be fairly straightforward since the equipment is available to us and a sensitive nonradioactive assay that detects CoA has previously been described for use in transient-state kinetic studies (Farazi *et al.*, 2000). The results from such experiments would complement previous kinetic mechanism studies and may also serve to better characterize the binding of AG substrates to AAC(6')-Ii. As no pre-steady state kinetic analysis on an AAC or other AME has been reported to date, this work may also have implications for other bacterial enzymes which bind and modify AG substrates.

Relevant to the research described in chapter 7, follow up studies on the protein acetylation activity of AAC(6')-Ii *in vivo* would further support our hypothesis that AAC(6')-Ii is behaving as a protein *N*-acetyltransferase in *E. faecium*. In order to identify the protein substrates that are evident from the autoradiograph shown in Figure 7.5 (Page 202), a semi-purification of these proteins would be needed to isolate them in sufficient quantity for subsequent N-terminal sequencing. Using ~ 15-20 grams of cells from both strains of *E. faecium* (wild type and knock out) as starting material, purification could begin by following the scheme in section *7.2.5* (page 195) to obtain P2, followed by cation exchange and/or size exclusion chromatography to further enrich our sample with the desired proteins. This work would be extremely important if we could eventually identify the proteins being acetylated by AAC(6')-Ii *in vivo*. Depending on whether we identify a ribosomal protein from our studies, we could follow up these findings with the comparative 2-D gel electrophoretic analysis proposed in section *7.3.1.2.*

8.2.2 Crystallographic Studies on AAC(6')-Ii

As mentioned numerous times throughout this thesis, a crystal structure of AAC(6')-Ii in ternary complex form would be very useful for a number of reasons. First, structural details on AAC(6')-Ii with bound CoA and AG would provide us with an approximate representation of the Michaelis complex, revealing important interactions between the enzyme and both substrates. In particular, it would give us additional information on the binding of AGs by AAC(6')-Ii, allowing us to further interpret the results included in chapter 5 and to compare the mode of binding to that observed for AAC(2')-Ic (Vetting *et al.*, 2002) and other AMEs (Pedersen *et al.*, 1995; Hon *et al.*, 1997). Furthermore, an AAC(6')-Ii·CoA·AG crystal structure would enable us to analyze the protein movements that we know to occur upon formation of the ternary complex, as described in chapter 2. Although the proposed work is currently underway in Dr. Albert Berghuis' Lab at McGill University, progress has not been made in crystallizing AAC(6')-Ii in complex with CoA and kanamycin or neomycin. Crystal trials with the minimal substrate neamine could alleviate some potential problems that may originate from the multiple conformations possible for AGs in solution.

8.2.3 AAC(6')-Ii Inhibitor Studies

Collaborations with other groups interested in bacterial AG resistance have proven very beneficial to past inhibitor studies on AAC(6')-Ii and other AMEs characterized in our lab (discussed in chapter 6), and this trend will no doubt continue. In addition, Dr. Ian Moore who is a post doc in our lab is currently characterizing several AAC(6')-Ii

inhibitory compounds, based on the results of a high throughput screen of this protein that he conducted in collaboration with the HTS facility at McMaster. Follow up research may include chemical derivatization of inhibitory compounds to investigate structure-activity relationships as well as crystal trials of AAC(6')-Ii with bound inhibitor.

8.3 Concluding Remarks

AAC(6')-Ii is a fascinating enzyme with the capacity to acetylate both aminoglycosides and a variety of small basic proteins and peptides. The research detailed in this thesis has characterized both activities, and reveals an enzyme with a molecular mechanism of acetylation that may contribute to the broad substrate specificity observed. The structural homology AAC(6')-Ii shares with histone and other protein acetyltransferases is also of great interest, and together with our biochemical evidence that suggests a role for this enzyme in protein acetylation *in vivo*, supports the hypothesis that AAC(6')-Ii may have evolved from a protein *N*-acetyltransferase.

8.4 References

Boehr, D. D., K. Draker, K. Koteva, M. Bains, R. E. Hancock, and G. D. Wright. (2003) Broad-spectrum peptide inhibitors of aminoglycoside antibiotic resistance enzymes. *Chem Biol* 10: 189-96.

Dyda, F., D. C. Klein, and A. B. Hickman. (2000) GCN5-related *N*-acetyltransferases: A structural overview. *Annu Rev Biophys Biomol Struct* 29: 81-103.

Farazi, T. A., J. K. Manchester, and J. I. Gordon. (2000) Transient-state kinetic analysis of *Saccharomyces cerevisiae* myristoyl CoA:Protein *N*-myristoyltransferase reveals that a step after chemical transformation is rate limiting. *Biochemistry* 39: 15807-16.

Hon, W. C., G. A. McKay, P. R. Thompson, R. M. Sweet, D. S. Yang, G. D. Wright, and A. M. Berghuis. (1997) Structure of an enzyme required for aminoglycoside antibiotic resistance reveals homology to eukaryotic protein kinases. *Cell* 89: 887-95.

Pedersen, L. C., M. M. Benning, and H. M. Holden. (1995) Structural investigation of the antibiotic and ATP-binding sites in kanamycin nucleotidyltransferase. *Biochemistry* 34: 13305-11.

Vetting, M. W., S. S. Hegde, F. Javid-Majd, J. S. Blanchard, and S. L. Roderick. (2002) Aminoglycoside 2'-*N*-acetyltransferase from *Mycobacterium tuberculosis* in complex with coenzyme A and aminoglycoside substrates. *Nat Struct Biol* 9: 653-8.